

Proceedings of the IRE



Poles and Zeros



WESCON. If one likes sun in his summer, then San Francisco during WESCON is not to be recommended. However, if

one is willing to accept continual air conditioning, the avoidance of showers, the inevitability of good San Francisco food, the hospitality and friendliness of the natives and recent immigrants, and a fine exhibit and technical program, then San Francisco during WESCON is the place to be. A product of fertile minds and expert management, this year's colossus of the West set high marks in every regard.

The technical program employed the experimental method with good results. The restriction of all sessions to three papers undoubtedly led to a low percentage of acceptances, and thus to higher quality in the technical program. This minimization of the acceptance/submission ratio as a criterion of quality, if it needed more than heuristic support, was amply proved by perusal of the abstracts and a sampling of the technical sessions. The limitation to three papers per two and one-half hour session also permitted ample coverage by the author as well as discussion from the floor. A novel feature of the discussion was the employment of the phenomenon of catalysis through a designated panel of discussers, these to present those first comments and questions which are so difficult to obtain unless planned in advance by an astute meeting chairman. Thus the audience was easily led into a form of bull session, and it was pointed out that this was indeed appropriate to the locale of the Cow Palace.

The exhibit areas were well arranged, even with aisles, although the configuration of the buildings tended to place the visitor in repetitive orbit—a device for precessing the orbit is needed. The breadth of the West Coast electronics industry, as well as of the whole field, was amply demonstrated once more; we were particularly impressed with the number of exhibits, not in themselves electronic, which represented products or processes being supplied to the industry.

Among our more useless conclusions from the show we find the following: vacuum tubes are still manufactured; do not develop a computer for an abstruse purpose—the high school boys already have it, as shown in the Future Engineers Show; modern equipment will not work without a projecting rim around the panel; stacking is important, be it component, molecular, or blonde; reliability is not optimum in the microphone-to-loud speaker link; electrons are still green.

SQ. These letters represent one of the less-well-known activi-

ties of the IRE, namely the *STUDENT QUARTERLY*, published for the benefit and edification of our Student Members in the colleges and the technical institutes. The fall issue, just available, is more than representative of the manner in which the electronic science story is carried to the students. The story of the discovery of the Van Allen radiation belts by Van Allen, the why of research by Terman, an analysis of the electronic field by McFarlan, are only a few of the papers presented during a typical year of this publication. The technical bits of information are sidebands on a carrier of cheery, informal, and sometimes surprising style—with cartoons, yet. Only the electronic profession could provide the bandwidth for this publication.

It has been stated that we must expand our knowledge by six per cent per year just to keep up with scientific inflation, and *SQ* is an attempt to bring up our potential engineers in the way they should go. Yes, you too, can subscribe; aren't you still a student?

Space ad Infinitum. We have always had some slight doubt over the manner in which nature will accept the infinity implied by Einstein in his various relations which employ the factor $(1 - v^2/c^2)^{-1/2}$. Noting that some of our classical ideas failed when we tackled micro-micro-space within the atom leads us to wonder if some of our other ideas may fall apart when we approach macro-macro-space among the stars. The publication in the June *PROCEEDINGS* of the paper "Relativity and Space Travel," by J. R. Pierce, has raised questions from many others if our correspondence is an indication. To present the arguments to all, we have selected four letters typical of the many, and they appear on pages 1778-1780, along with Dr. Pierce's reply.

With Mehta, Pioneer IV, and proposed satellite clock experiments, perhaps infinity is closer than we think.

Law of the Land. A set of By-Laws, by which our new Constitution is implemented, went into effect on August 19, by Board of Directors action of the preceding day. As we have previously pointed out, adoption of these new By-Laws is largely intended to continue present policies in IRE government. One change of import to all will soon be apparent, when you receive your annual ballot. This will call for a vote for two vice-presidents instead of the usual one. There will be a North-American Vice-President to actively aid the President, and a Vice-President not from North America, to emphasize that IRE is indeed an international organization.

Publication of the complete By-Laws will follow at an early date.—J.D.R.



Harry F. Olson

Director, 1959–1960

Harry F. Olson (A'37–VA'39–SM'48–F'49) was born on December 28, 1902 in Mt. Pleasant, Iowa. He received the degrees of B.E. in 1924, M.S. in 1925, Ph.D. in 1928, and Professional E.E. in 1932, all from the University of Iowa. In 1928 he joined the Radio Corporation of America, and worked in several of their divisions until 1941, when he joined the RCA Laboratories in Princeton, N. J. He is presently the Director of the Acoustical and Electro-mechanical Laboratory of the RCA Labs.

One of Dr. Olson's early contributions during his career with RCA was the velocity microphone, the first microphone with uniform directivity, which became standard for broadcasting use. Subsequently, he pioneered in several other directional types of microphones, including the uni-directional types now used in television broadcasting and sound motion picture filming. During World War II he developed underwater sound equipment, anti-noise microphones and high power announce systems. He also has made pioneering contributions to loudspeaker development, including the duocone speaker for high fidelity sound reproduction, and to the development and improvement of phonograph pickups and disc recording equipment, sound motion picture and public address systems. In addition, he has guided and contributed substantially to the development of electronic noise reducers, stereophonic sound systems, magnetic tape recorders for sound and television, the electronic music synthesizer, and the phonetic typewriter.

Dr. Olson holds over 80 U. S. Patents on devices and

systems in the acoustical field and is author of over 85 articles and papers published in professional journals as well as the books "Elements of Acoustical Engineering," "Acoustical Engineering," "Dynamical Analogies," and "Musical Engineering." From 1939–1943 he was a lecturer in acoustical engineering at Columbia University, New York, N. Y.

For his contributions to the field of audio engineering, Dr. Olson received the Modern Pioneer Award of the National Association of Manufacturers in 1940, the John H. Potts Medal of the Audio Engineering Society in 1952, the Samuel Warner Medal of the Society of Motion Picture and Television Engineers in 1955, the John Scott Medal of the City of Philadelphia in 1956, and the Achievement Award of the IRE Professional Group on Audio in 1956. In April of this year he was honored by election to the National Academy of Sciences.

Dr. Olson's affiliations include membership in Tau Beta Pi and Sigma Xi. He is a Fellow of the American Physical Society, the Acoustical Society of America, the Audio Engineering Society, and the Society of Motion Picture and Television Engineers. He was president of the Acoustical Society of America in 1952.

His IRE activities have included membership on several Institute committees including Annual Review, Board of Editors, Editorial Reviewers, Electroacoustics, Papers Procurement, and Standards. He has been IRE representative on several ASA committees. In 1957–1958 he served as chairman of the Professional Group on Audio.

Scanning the Issue

The Magnesium Oxide Cold Cathode and Its Application in Vacuum Tubes (Skellet, *et al.*, p. 1704)—Earlier this year a great deal of publicity appeared in the newspapers about a new type of cathode which would operate cold, without requiring the usual heater filament to induce electron emission. The absence of a heater in a tube eliminates one cause of power consumption; and by operating the cathode cold, the gradual depletion of cathode chemicals by evaporation is avoided, suggesting a long operating life. These features and the widespread publicity given them have aroused a great deal of interest in the tube industry. The technical details of this novel development are now reported. The cathode consists of a very thin layer of magnesium oxide on a nickel base. During operation, avalanche multiplication of electrons occurs within the magnesium oxide layer and a potential of about 150 volts, with respect to the base, develops on the outer surface of the layer, propelling the electrons with sufficient velocity to escape from the surface. This paper is most welcome: it is excellently written, it provides a clear description of both the capabilities and limitations (*e.g.*, noise) of a new device, and in so doing gives a more complete and accurate picture than was provided by the popular press.

The Quadrupole Amplifier, A Low-Noise Parametric Device (Adler, *et al.*, p. 1713)—Among the several kinds of parametric amplifying devices being talked about a great deal these days, one of the most interesting is a class that employs an electron beam. This class differs from conventional beam-type tubes, such as traveling-wave tubes, in that the fast electron wave of the beam, rather than the slow wave, is utilized for amplifying the signal. This distinction is important because noise present in the beam when it leaves the gun can never be completely removed from the slow wave, while it can, in theory, from the fast wave. The inherently noisier slow wave has been used in conventional devices because, until recently, no way had been found to amplify the fast wave. About two years ago, however, it was recognized that the fast wave could indeed be amplified by adding to the system an additional power source which operated on the fast wave at a pumping frequency higher than the signal frequency—in short, by applying the principle of parametric amplification. This idea was subsequently applied successfully to amplifying the fast space-charge wave of an electron beam. In this paper, it is applied to another type of fast wave, the cyclotron wave, *i.e.*, the spiralling motion of the electrons as they proceed along the beam path. The authors have devised a four-pole (quadrupole) structure which, when connected to the pump source, produces an alternating field which enhances this signal-induced spiralling motion, thus amplifying the signal. The resulting device shows a remarkably low noise figure for an electron device, as low as 1.4 db in certain applications. It also enjoys high stable gain over fairly wide bands. This development stands as an outstanding contribution to the art of low-noise amplification, one that will be referred to frequently in the future in a number of fields. The paper has the added blessing of being written in such a lucid and interesting style that all members will enjoy and benefit from reading it, regardless of their own field of interest.

Generation of Harmonics and Subharmonics at Microwave Frequencies with P-N Junction Diodes (Leenov and Uhler, p. 1724)—There is wide interest today in nonlinear devices that can be used as frequency converters to provide power sources or frequency standards in the microwave region. Resistive devices, ferrites and, most recently, a nonlinear capacitance junction diode have been employed in this role. In this paper, the author investigates the last-named item, compares it with a nonlinear resistance, and shows that the nonlinear capacitance is considerably more efficient. This higher efficiency plus the fact that a nonlinear capacitance, unlike a nonlinear resistance, can generate subharmonics as

well as harmonics, gives the one a clear advantage over the other.

Comparison and Evaluation of Cesium Atomic Beam Frequency Standards (Essen, *et al.*, p. 1730)—As the first comparison between two high-class frequency standards based on similar principles but of different construction, this paper will be of substantial interest to physicists, workers in frequency control and measurement, and those concerned with navigation and missile control problems. An American cesium atomic beam frequency standard known as the Atomichron® was shipped to the National Physical Laboratory in Teddington, England, where it was compared with the NPL cesium frequency standard. The unresolved discrepancy between the standards was found to be about 2 parts in 10^{10} . One important aspect of this comparison is that it provides information that will help in determining the accuracy with which such comparisons can be made on an intercontinental scale by means of transatlantic radio transmissions—a measurement program that is now in progress between NPL and Harvard.

Pattern Detection and Recognition (Unger, p. 1737)—Unfortunately, humans and data-processing machines do not speak the same language. It is usually necessary for a human operator first to translate the data into the digital language of the machine before the machine can be put to work. In some cases, the translation job would be so great as to defeat the purpose of using the machine at all. One of the most fascinating and potentially useful areas currently being investigated is in devising input devices which will do the translating automatically. This paper develops two interesting methods of automatic pattern processing, one of which was successfully used to detect L-shaped figures in the presence of other randomly drawn patterns. The other method made it possible to recognize hand-lettered numbers and letters. Identification of any character is uniquely established by asking from three to nine questions, in proper sequence, from a list of 36 questions concerning details of the shape of the pattern. It is estimated that within five years equipment could be available for performing character recognition operations at the rate of 2500 characters per second (which means this page would be gulped down in about 3 seconds).

A Unified Analysis of Range Performance of CW, Pulse, and Pulse Doppler Radar (Bussgang, *et al.*, p. 1753)—Volumes have been written on predicting the range performance of pulse radars, but relatively little regarding CW and pulse Doppler radars. This timely paper not only fills the gap but also provides a unified computational method which is especially useful in comparing two radars. It will be particularly helpful to radar engineers who do not have the inclination to wade through the more mathematical treatments of this subject.

Absorptive Filters for Microwave Harmonic Power (Met, p. 1762)—With transmitter powers in pulse radar systems rising tremendously and with increasing use of the microwave spectrum for communication purposes, the problem of harmonic interference has become very real and far reaching. This discussion of improved methods of suppressing the harmonic output transmitters should, therefore, interest a fairly wide circle of IRE readers.

Simple Methods for Computing Tropospheric and Ionospheric Refractive Effects on Radio Waves (Weisbrod and Anderson, p. 1770)—Simple, practical formulas are presented which greatly reduce the labor of computing the bending of radio waves that pass through the troposphere and ionosphere. Other refractive effects such as signal retardation, Doppler error, and Faraday rotation are also included, making this work of timely usefulness to a large group of people interested in accurately tracking radio stars, satellites, missiles, and other high-altitude objects.

Scanning the Transactions appears on page 1790.

The Magnesium Oxide Cold Cathode and Its Application in Vacuum Tubes*

A. M. SKELLETT†, FELLOW, IRE, B. G. FIRTH†, AND D. W. MAYER†

Summary—The MgO cold cathode is a new source of electrons with possible applications in various types of electron tubes. It consists of a thin layer of porous magnesium oxide on a nickel base. A strong electric field that exists across the layer while in operation is believed to produce the electron emission from the surface. Evidence supports the theory that avalanche multiplication occurs in the layer. This cathode glows with a pale blue luminescence during operation. The velocity distribution of the emitted electrons shows a peak at 13 electron volts. The outer surface potential has been measured and found to be of the order of 150 volts with respect to the nickel base. The emission is not self-starting, and starting means are discussed. Noise, life, emission density, and temperature range of operation are discussed in so far as present knowledge permits. An experimental design of an amplifier tube employing this cathode is described and the characteristics of the tube are given.

INTRODUCTION

THE magnesium oxide cold cathode was the result of studies of field dependent secondary emission¹⁻⁵ carried out at the Research and Development Laboratories of the U. S. Signal Corps, Evans Signal Laboratories, Fort Monmouth, N. J. Dobischek⁶ completely isolated the self-sustained emission component and produced it in tubes that had no provision for bombardment by primary electrons. These tubes were simple diodes, each consisting of a nickel cathode base covered with specially prepared magnesium oxide and a positive anode located a short distance away to draw the electron emission. He tried various methods of preparation of the MgO coatings, a number of which were successful, and determined that porosity of the layer was essential for good operation. His results encouraged the belief that this new type of cathode might be used in electron tubes.

On July 1, 1956 under a Signal Corps contract, Tung-Sol Electric Research Laboratories undertook the job of developing the MgO cathode toward this end. By further research and development and by applying vacuum-tube-production techniques, reproducible cathodes of good quality have been obtained.

PREPARATION OF THE CATHODE

In the early work carried out at the Signal Corps Laboratories, a number of methods were tried for producing the magnesium oxide coating. These included evaporation of magnesium through oxygen at a pressure of 80 microns, oxidation of vacuum-deposited MgO films, decomposition of MgCO₃ layers, and burning of magnesium in front of the cathode base metal to collect the MgO smoke. The best results were obtained with this last or "smoke" technique; the cathodes were much quieter and indicated that with further development they might be made to rival thermionic cathodes for some applications.

The original cathodes were made in the Tung-Sol Research Laboratories by two methods. The first was to spray magnesium oxide onto a magnesium or nickel base; the second was to coat the nickel sleeve by electrophoretic deposition of magnesium oxide. Both produced operative cathodes, but the sprayed cathodes showed the greater promise and the cataphoretic method was abandoned.

The cathodes are presently prepared by spraying a mixture of magnesium superoxol (MgO + 25% MgO₂) and magnesium carbonate in a vehicle of amyl acetate onto a nickel base. This base is usually a typical cathode nickel sleeve made of 499 alloy roughened by sand blasting and oxidized by heating in air. The coating is approximately 35 microns thick and appears rough textured.

The cathode is then assembled in the tube structure and processed in accordance with a typical exhaust procedure. It has been found necessary to heat the cathode to 800°C. in air or oxygen at reduced pressure as part of this procedure.

Fig. 1. shows the texture of the magnesium oxide surface of a processed cathode. During the processing the carbonate breaks down with the liberation of CO and CO₂. This evolution of gas enhances the porosity. It is believed that the final coating is magnesium oxide of a

* Original manuscript received by the IRE, May 4, 1959; revised manuscript received, June 15, 1959. This investigation was sponsored by the U. S. Army Signal Res. and Dev. Laboratory.

† Res. Div., Tung-Sol Electric, Inc., Bloomfield, N. J.

¹ L. Malter, *Phys. Rev.*, vol. 49, p. 478; 1936.

² L. Malter, *Phys. Rev.*, vol. 50, p. 48; 1936.

³ H. Jacobs, "Field dependent secondary emission," *Phys. Rev.*, vol. 84, pp. 877-884; December, 1951.

⁴ H. Jacobs, J. Freely, and F. A. Brand, "The mechanism of field dependent secondary emission," *Phys. Rev.*, vol. 88, pp. 492-499; November, 1952.

⁵ D. Dobischek, H. Jacobs, and J. Freely, "The mechanism of self-sustained electron emission from magnesium oxide," *Phys. Rev.*, vol. 91, pp. 804-812; August, 1953.

⁶ D. Dobischek, Abstract No. 78, Meeting of Electrochem. Soc., Wash. D. C.; May 12, 1957.

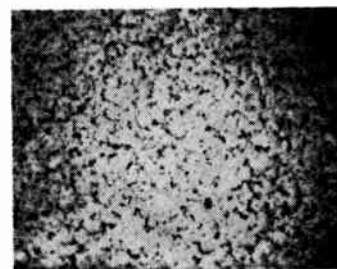


Fig. 1—Photograph of the surface of a processed magnesium oxide cathode; magnification about 100 times.

high degree of purity, but there is some evidence that small amounts of impurity may play a role in the operation.

In order to understand the mechanism of operation it is necessary to know the outer surface potential of the oxide layer and the energy distribution of the emitted electrons.

OUTER SURFACE POTENTIAL

A small cathode-ray tube was made, complete with electrostatic deflecting plates and fluorescent screen. The outer pair of deflecting plates served also as a magnesium oxide cold cathode diode. One plate was covered with the MgO porous coating prepared as de-

Fig. 3 shows the variation of the surface potential, curve *S*, determined in this way, as the current drawn from the cold cathode was increased. The anode potential for each value of current is also shown, as curve *P*. These curves show that the cathode surface potential, *S*, varied from 145 to 155 volts with respect to the cathode nickel base, as the current drawn varied from 0.1 to 0.6 ma. The anode potential, *P*, varied from 250 to 280 volts over this same current range. At 0.1 ma the difference of potential between *S* and *P* was 105 volts, and at 0.6 ma it was 125 volts. A number of such curves were taken with two tubes of this type, and although the currents were not as stable as might be desired, the curves all followed this general pattern.

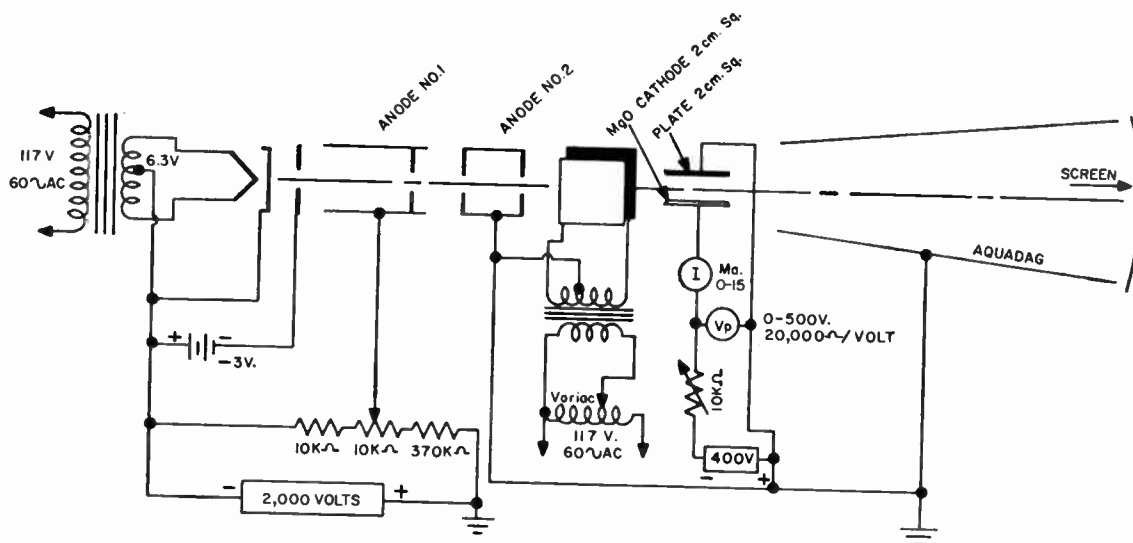


Fig. 2—Arrangement of elements and circuit for the experimental determination of surface potential.

scribed above, and the other plate served as the anode. Knowing the potential on the anode plate, the velocity of electrons in the beam, and the important distances involved, it was possible to determine the surface potential on the cathode plate from the deflection of the beam as measured on the fluorescent screen.

The tube used for this experiment consisted of a 5CP1 cathode ray electron gun sealed in a two inch OD bulb screened at one end. The last set of deflection plates was removed from the gun and replaced with 499-alloy plates 20 mm square and 4 mm apart. One plate was coated with MgO (about 1.9 mg/cm² and about 41 microns thick). The other plate was left uncoated. The distance from the center of these deflection plates to the screen was 60.8 mm (2 inches from the outer edge of the plate to the screen). The first set of deflection plates, 90 degrees from the second pair, was used to scan the electron beam vertically between the MgO cathode and plate at 60 cps. The image formed on the screen was a straight vertical line. Evidently any variations in surface potential were averaged out over the 2 cm length of the cathode. The arrangement of the electrodes and the circuit is shown in Fig. 2.

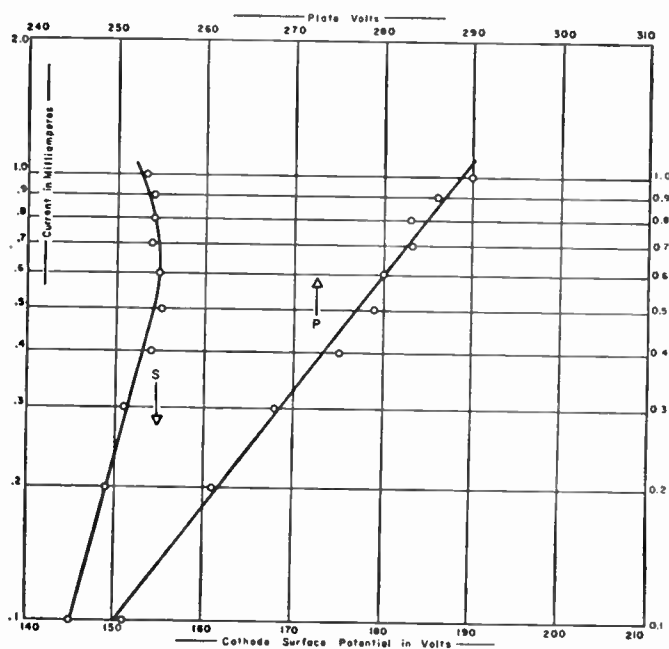


Fig. 3—Variation of surface and anode potentials with emission current.

Measurements of electron energy distribution give an indirect measurement of this surface potential as described below. For these studies the effective anode was closer to the cathode, and the difference between the surface and anode potentials was less.

ELECTRON ENERGY DISTRIBUTION

The energy distribution of the emitted electrons has been studied by the magnetic analyzer method. Fig. 4 shows the layout of the analyzer. All parts were made of non-magnetic material except for the nickel sleeve of the cathode. The main body of the analyzer was OFHC copper. As is well known, this type of magnetic analyzer allows a small angular spread of the electrons entering the first slit, because of the focus at 180°. The radius of the electron path was 8.9 cm. The entering and exit slits were 0.788 mm wide and the resolution varied from a fraction to several electron volts. The height of the slits was 1.65 cm.

The magnetic field was provided by a pair of Helmholtz coils, 40 cm in diameter. They were oriented with respect to the earth's field and tilted so that the resultant magnetic vector was parallel to the axis of the analyzer. The field strength was calibrated by standard magnetic measurements. In addition, the equipment was calibrated in electron volts by substituting a thermionic cathode (for which the velocity distribution of the electrons is known) and applying known accelerating voltages.

The thickness of the magnesium oxide cathode coating was 35 microns. The surrounding grid consisted of 4 mil wire, wound 42 turns per inch and spaced 0.0145 inch from the center of the wire to the cathode coating. Fig. 11 shows this grid spacing to scale. The cathode-grid structure was located one quarter of an inch behind the entrance slit of the analyzer.

The grid, analyzer structure, and Faraday cage collector were all operated at the same potential, which was 194 volts. A resistor of 45,000 ohms was in series with the power supply.

Data were taken by varying the strength of the magnetic field. For each value of the field, H , there is a corresponding value of kinetic energy that the electrons must have to arrive at the Faraday cage collector. This energy, E , expressed in electron volts, is related to H according to the formula

$$H = \frac{3.37\sqrt{E}}{R} \quad (1)$$

where R is the radius of curvature of the electron path. Fig. 5 shows how the distribution of electrons varied with this energy.

A galvanometer was used to measure the current to the Faraday cage collector. However, the galvanometer readings, G , for various values of the field, will not give

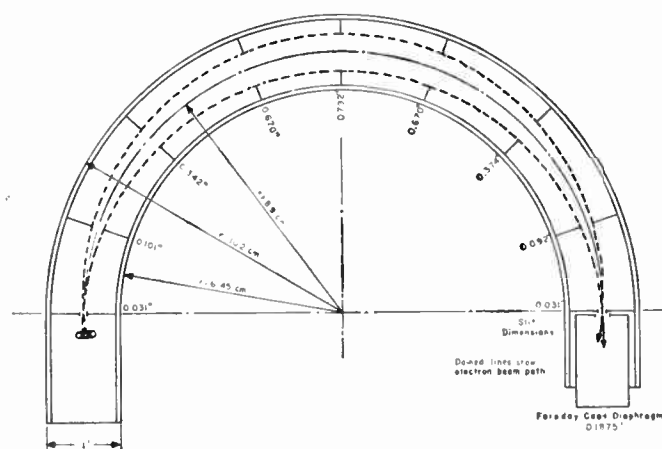


Fig. 4—Layout of magnetic analyzer. Cathode and sustaining grid are shown in left hand compartment.

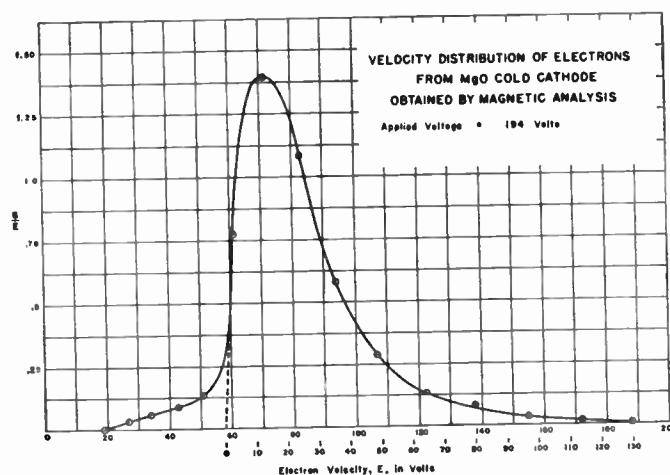


Fig. 5—Upper abscissa scale shows voltages referred to nickel base of cathode. Lower scale refers to the velocity of the electrons.

the correct velocity distribution, since the effective width of the slit system varies directly with the velocity of the electrons whose velocity is to be measured. Therefore, in plotting the curve, the galvanometer readings were reduced to the same effective slit width by dividing by the velocity, E , at each point. Thus the ordinates of the curve are in each case the galvanometer reading, G , divided by the electron velocity, E .

For the moment we will ignore the small initial rise between 19 and 58 volts.

The onset of the electrons was at approximately 58 volts; this was interpreted to be the voltage through which all electrons emitted by the cathode were accelerated. It was thus the potential difference between the outer surface and the grid and slit. Subtracting it from the applied voltage (194) gave 136 volts for the outer surface potential; *i.e.*, the voltage across the cathode coating. Contact potentials were not taken into account.

The peak of the curve was at 13 volts and 90 per cent of the electrons had velocities of less than 65 volts. There were some electrons, though relatively very few, that appear to have been accelerated by the full voltage applied. These probably were photo-electrons from the nickel sleeve that had emerged through a hole in the coating without collision, or with only elastic collisions.

The small initial rise between 19 and 58 volts is believed to be due to small areas or points on the cathode which were at higher voltages than the main body of the cathode surface. It seems certain that this initial rise does not represent secondaries from the slit edges, since it does not appear in the data obtained with electrons from a thermionic cathode.

This curve is believed to give a representation of the velocity or energy distribution that is accurate to a few volts.

The following equation fits the experimental curve reasonably well.

$$N_{dE} = \frac{2N\sqrt{E}}{\pi^{1/2}(KT)^{3/2}} e^{-E/KT} dE \quad (2)$$

where N_{dE} is the number out of N electrons that have an energy between E and dE ; K is Boltzmann's constant; and $KT = 13$ eV, giving an electron temperature T of 150,000°. This is the equation of a Maxwellian distribution.

EMISSION CHARACTERISTIC

A number of diodes were made, with the magnesium oxide approximately 35 microns thick and with a grid for the anode. The inner edge of this grid was located 0.0125 inch from the cathode surface and consisted of 0.004 inch diameter wire with a spacing of 42 turns per inch. The cathode area was 2.43 cm².

Fig. 6 is a typical plot of the anode current as a function of the anode voltage. Consider first the straight line portion from 1 microampere to 3 milliamperes. It shows that the current is exponentially dependent on the voltage and that the functional relationship may be expressed as

$$I = Ae^{BV} \quad (3)$$

where I is the current, V is the anode voltage, and A and B are constants.

This is also the relationship between current and voltage for the Townsend avalanche effect in a gas. Furthermore, the experiments described above show that a very high electric field exists across the magnesium oxide layer; this is a necessary condition for the avalanche effect. It is concluded, therefore, that the electrons, in passing through the oxide layer, are multiplied by the avalanche effect. The resistor shown in series with the anode in the circuit of Fig. 6 is necessary to assure that the emission be stable.

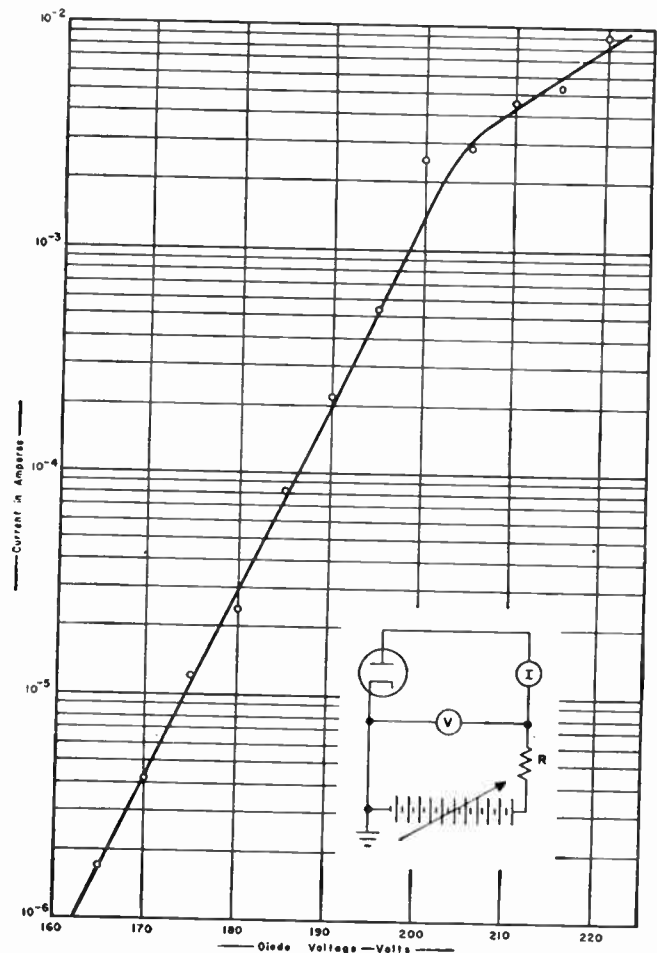


Fig. 6—Emission characteristic of a diode.

If the current is increased beyond about 3 milliamperes, the characteristic deviates from this straight line relationship. A thermocouple attached to the cathode sleeve of one of these diodes indicated a substantial rise in temperature at these higher current levels, and it appears that the curvature of the characteristic is due to a temperature effect. This increase in temperature is brought about by the dissipation of electron energy in the oxide layer. The curvature of the surface potential characteristic of Fig. 3, above 0.5 milliampere, is explained in the same way.

Although heavy emission has been drawn from these diodes while they were operating at a temperature of 700°C, devices using this cathode are normally designed so that the temperature rise in the cathode is small. In other words, tubes are designed to work over the linear portion of the emission characteristic of Fig. 6. Consideration should be given to cooling the cathode where heavy emission density is required.

Cathodes have also been operated satisfactorily at -195°C. These two temperatures (-195° and 700°) indicate the extremely wide operating-temperature range of the cathode.

The maximum emission density that has been drawn to date is 145 milliamperes per cm^2 . However, at this value cathode cooling must be provided.

BLUE LUMINESCENCE

A distinctive characteristic of this cathode is that it glows with a pale blue luminescence when operating. The brightness of this light varies with the emission intensity, thus providing a simple means of observing the uniformity of emission across the cathode surface.

The early cathodes were characterized by two types of luminescence. A general blue glow was distributed over the emitting areas, and brilliant points of light, also blue in color, were located at randomly spaced points on the cathode surface. These points were unstable and scintillated with a cycle of brightness variation that was often in the form of a saw-toothed wave. Much of the noise of the early cathodes was traced to these scintillating points, and effort was directed toward their elimination. This has been accomplished, and present cathodes have a uniform steady glow when viewed macroscopically.

THEORY OF OPERATION

In attempting to explain the mechanism of field-dependent secondary emission from porous magnesium oxide, Jacobs, Freely and Brand⁴ postulated an avalanche effect patterned after that in a Townsend discharge in gas. Dobischek, Jacobs and Freely⁵ carried this theory further and found that it applied to the emission from the magnesium oxide cold cathode. This cold cathode is of course identical with the porous MgO layers of the secondary emission studies.

The fundamental expression for the Townsend avalanche discharge is

$$I = I_0 e^{\alpha x} \quad (4)$$

where I is the total current, I_0 is the initial current, x is the distance through which the discharge takes place, and α is the number of new electrons created per unit length. Since the relationship between the distance and the voltage in the case of the MgO layer may be assumed to be linear, we may substitute BV for αx , where B is a constant and V is the voltage. Eq. (4) then becomes the same as (3), which was obtained from the experimental data, and I_0 is equal to A .

This equation fits the data whether V is the voltage on the anode or the surface potential (see Fig. 3), but for theoretical consideration, V should be the surface potential.

In the Townsend avalanche, I_0 is the initial current; *i.e.*, the electron current leaving the cathode. In the magnesium oxide cathode, I_0 may be defined as the current carried by those electrons leaving the nickel sleeve that cause the avalanches. This is a very small part of the total current. As determined from the experimental data, I_0 is some orders of magnitude less than I .

For every electron emitted there must be an electron transferred from the nickel sleeve to the oxide layer. Otherwise there would not be an equilibrium of charges.

These electrons may be explained in terms of hole conduction. For example, whenever there is an inelastic collision during the avalanche process that results in the freeing of additional electrons, a corresponding number of holes are created in the oxide. These holes are free to move at substantially slower speeds back toward the nickel base. They are equivalent to the positive ions in the Townsend discharge. Hole mobility in magnesium oxide has been measured by Yamaka and Sawamoto⁷ and found to be approximately 2 cm^2 per volt second.

Not much is known about the band-gap structure of magnesium oxide as used in this cathode, but it seems safe to assume that it is fairly complicated and contains a good many energy levels within the gap. Thus an electron need not traverse the whole band-gap of pure magnesium oxide, which is greater than 7.3 volts,⁸ in order to become available as a conduction electron. Traps, impurity levels, etc. may all be expected to play important roles.

The voids in the porous layer provide a longer path for accelerating the electrons than their mean free path in the solid magnesium oxide. Thus it may be in the voids that the electrons acquire enough energy to enable them to ionize and produce avalanche multiplication.

At the surface the electrons arrive with a wide distribution of velocities because of the different amounts of acceleration they have received from the field. Many of these electrons have velocities in excess of the 2.8 volts^{8,9} required to pass through the surface. Outside the surface there is another weaker electrostatic field caused by the anode potential, which serves to remove a sufficient number of electrons from the vicinity of the surface, to maintain the positive surface charge needed for equilibrium.

The blue glow is believed to be due to processes associated with electron-hole recombination within the layer. It extends into the ultraviolet region and undoubtedly plays a role in releasing electrons from the nickel base.

STARTING

Merely applying voltage (even high voltage) to the anode is not sufficient to start the emission. The following starting means have been successfully employed: ultraviolet light, intense visible light, radioactivity, electron bombardment, and the discharge from a Tesla coil. In each case there is a delay between the time of the application of starting means and the actual starting of the emission. The slowest starting means was radioactivity, requiring several minutes. With ultraviolet or visible light the starting time depends on the intensity of the radiation. Starting times of less than a second have been obtained with intense light. The discharge of a Tesla coil on the outside of the bulb will start the

⁷ E. Yamaka and K. Sawamoto, "Photo induced Hall effect in MgO," *Phys. Rev.*, vol. 101, pp. 565-566; January, 1956.

⁸ H. R. Day, "Irradiation-induced photoconductivity in magnesium oxide," *Phys. Rev.*, vol. 91, pp. 822-827; August, 1953.

⁹ J. B. Johnson and K. G. McKay, "Secondary electron emission in crystalline MgO," *Phys. Rev.*, vol. 91, pp. 582-587; August, 1953.

emission in a second or less. Electron bombardment can be even faster depending on its intensity as described below.

In all of these starting means, it is believed that either photo-electrons or secondary electrons are released from the surface by the starting operation, and that this loss of electrons charges the outer surface of the magnesium oxide layer positively to its operating potential.

One of the first "built in" starters tried employed field emission from a sharp tungsten point. Fig. 7 shows its position in a diode. The plate shield, which was grounded, was used in tubes with a collector grid to prevent wall charging. The tungsten point was one micron in diameter, and at a negative potential of 1000 volts the emission started in from 0.1 to 2 seconds with point emission of less than 0.01 microampere. This delay in starting was due primarily to the time required for the spread of the emission over the whole area of the cathode. The requirement of a high negative potential for the point was undesirable and this starting means was abandoned.

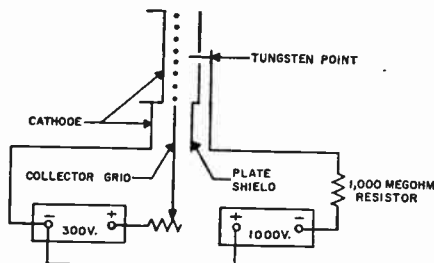


Fig. 7—Arrangement of tungsten point in diode for field emission starting.

The starter now employed in all tubes consists of a short length of 1 per cent thoriated tungsten filament that is brought up to electron-emitting temperature momentarily. It starts the emission in less than a second, the time required being partly that needed to bring the filament up to operating temperature. The filament dimensions are 0.50 inch long by 0.0022 inch in diameter. It is located behind the grid support wires (see Fig. 10) so that contaminants, which may be evaporated from it and which travel in straight lines in the vacuum, cannot reach the cathode surface. It is normally connected to the nickel cathode sleeve internally, and no extra voltage is needed except that required to bring it to 1600°C, which is its operating temperature. This is normally 1.9 volts and 0.58 amperes and may be ac or dc.

It is believed to operate as follows. Some of the light that it emits is reflected onto the cathode, causing the release of photo-electrons which start charging the cathode surface positively. When the surface potential reaches a value where the secondary to primary ratio is greater than unity, electrons from the filament, either directly over curved paths or reflected from the positive tube elements, bombard the cathode to start the emission.

In simple diodes it has been found that if a grid is

used as the anode the cathode will start more easily than if the anode is a solid plate.¹⁰

Fig. 8(a) shows a schematic representation of a MgO cold cathode with a plate rather close to the cathode. Fig. 8(b) represents a cold cathode with the plate replaced by a positive grid, beyond which lies a grounded shield. In Fig. 8(a) two factors tend to inhibit starting. 1) The plate acts as a shield against excitation of the cathode surface by whatever means may be used for starting. 2) Electrons are attracted to the plate without return.

In Fig. 8(b), on the other hand, excitation of the cathode is facilitated by spaces in the emission-sustaining grid. While some electrons reach the grid laterals, others miss them, and travel through the space in a parabolic path, returning to the cathode where they strike it with an energy that is equivalent to their initial velocity. Since magnesium oxide is a good secondary emitter, these returning electrons will generate secondaries with a ratio greater than unity at velocities well within the range of the returning electrons. Secondaries so produced aid in pulling the surface potential up to operating values. This is illustrated in the figure.

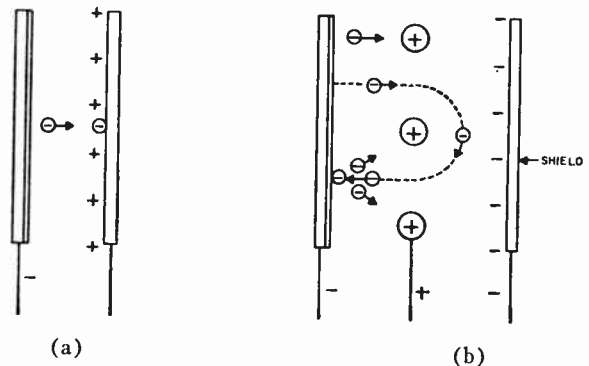


Fig. 8—Electron paths in diode with plate anode, A, and grid anode, B.

The ease in starting emission with a wire or mesh grid is reduced when the shield, or plate, beyond the grid is positively biased to the same or to a higher potential. In this case electrons do not return to the cathode. In accord with these observations, amplifier tubes provided with starter filaments are presently so connected in their operating circuits that the plate circuit is opened up momentarily while operating the starter.

KEEP-ALIVE OPERATION

It has been found that the emission is sustained at very low current densities. This provides a "keep-alive" feature. Furthermore, with the cathode sustaining emission at a low current, full emission may be restored in a very short time. For example, if the keep-alive current is a few microamperes/cm² the time required for full emis-

¹⁰ This should not be interpreted to mean that a grid is necessary. Diodes without grids and with simple plates for the anodes do start and operate satisfactorily.

sion restarting is approximately one millisecond. At higher keep-alive currents the restarting time is even less.

This high restarting speed suggests that the keep-alive current is not confined to any one spot of emission on the cathode, but must be at least fairly well distributed over its surface. Otherwise the time required for emission to spread over the cathode surface from one point, as in field emission point starting, would be much greater than that measured. The blue glow at keep-alive currents is too faint to be seen. Life tests of tubes at keep-alive current densities have shown no deterioration even after 2 years of continuous operation.

NOISE

Noise studies have been made on diodes similar to those used for obtaining the emission characteristics, but with a shield around the structure to prevent glass wall charging. It was found that the noise usually increased with decreasing frequency, that it had a crackling, rushing sound, and that for a frequency band from 3 to 200,000 cycles its magnitude was much greater than shot noise for the same current. Furthermore, microscopic examination of the emitting surface showed minute variations of intensity with time at various small areas on the cathode surface, similar in general to the localized variations in emission of the thermionic cathode. All of these facts indicated that the major component of noise was due to flicker effect.

For thermionic cathodes, the flicker-effect-noise level varies a great deal not only from type to type but from tube to tube of the same type.¹¹ It has been found that this is also true of the MgO cold cathode.

LIFE

In the operation of the barium-strontium-oxide cathode under ideal conditions there is a continual evaporation of barium oxide from the surface which gradually reduces the emissivity. When the depletion of these chemicals is nearly complete the end of life point is reached.

In contrast to this, no depletion of any kind has been detected during the operation of this magnesium-oxide cathode. The surface remains stable and chemically inert. Thus a long operating life may be expected. One of the early diodes was put on life test at a current drain of 4 ma (2.9 ma/cm²). No increase or decrease of emission occurred for 14,000 hours. Most cathodes have had shorter lives but this one example sets the objective of further development.

GRID CONTROL IN AMPLIFYING TUBES

A requirement for sustained emission is that the outer surface potential of the cathode coating be maintained at a high positive value. This in turn requires that there be a positive potential gradient between this sur-

face and the first element. The potential in the plane of the grid nearest the cathode, therefore, must be nearly 200 volts positive with respect to the nickel cathode sleeve. This requirement must be met whether this first grid is the emission sustaining element or the control grid.

If the first grid is the sustaining grid, it is followed by the control grid which operates at a lower potential, but is still positive with respect to the cathode nickel base. For this grid arrangement, a virtual cathode is apparently produced in front of the control grid. Successful amplifying tubes have been made experimentally in this design.

If the first grid is the control grid as in a conventional tube, then the second grid is the sustaining element, operating at a substantially higher potential than the first grid, so that the average potential in the plane of the first grid is always positive enough to sustain the emission. The pentode described below combines these two types of grid control

CHARACTERISTICS OF PENTODE

Fig. 9 shows the internal structure of the pentode. The plate is cut away in front so that the parts are visible. All parts are standard receiving-tube parts except for the cathode coating. There is a heater of the usual kind inside the cathode sleeve that is used during processing. It is never energized after the tube is sealed off of the pumps.

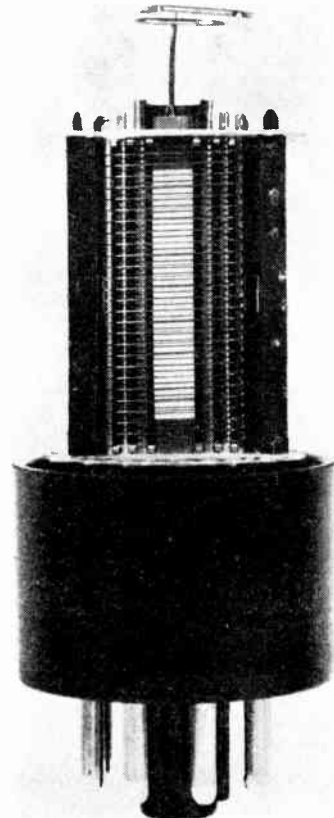


Fig. 9—Photograph of internal structure of pentode amplifier tube. Glass bulb has been removed and plate has been cut away.

¹¹ A. Van der Ziel, "Noise," Prentice-Hall, Inc., New York, N. Y., p. 225; 1954.

Fig. 10 shows a horizontal section through the tube. The second grid, G_2 , is the emission sustaining grid. The first grid, G_1 , and third grid, G_3 are tied together to give a double control as discussed above. Thus the tube has neither screen nor suppressor grid, and its action is more nearly like a triode than a conventional pentode.

The starter filament is outside the main structure, but in line with a window in the plate. Light and electrons that it gives off can find their way to the cathode, unlike contamination which travels in straight lines in a vacuum.

Fig. 11 is a vertical section through the tube structure drawn to scale showing the dimensions of the parts.

Fig. 12 is the grid characteristic, showing a transconductance of 600 micromhos. This has been confirmed by dynamic measurements.

Fig. 13 gives the plate family of curves. These were

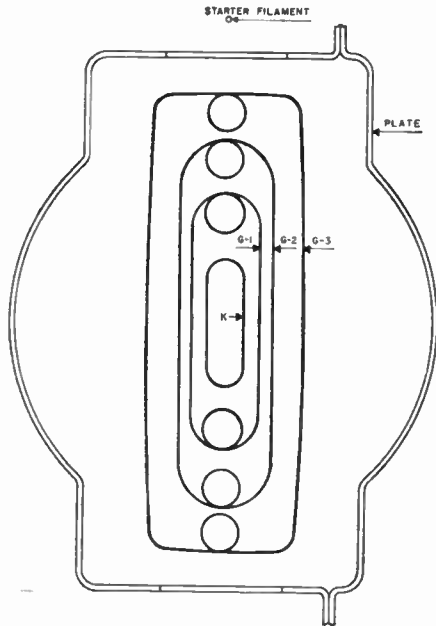


Fig. 10—Section through pentode taken perpendicular to axis and drawn to scale.

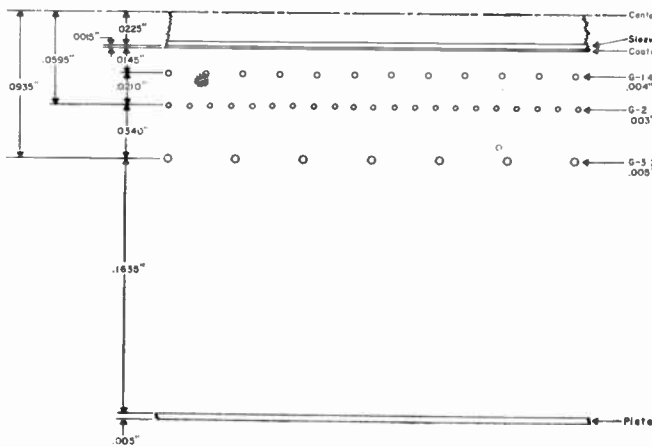


Fig. 11—Section through pentode taken parallel to axis and drawn to scale.

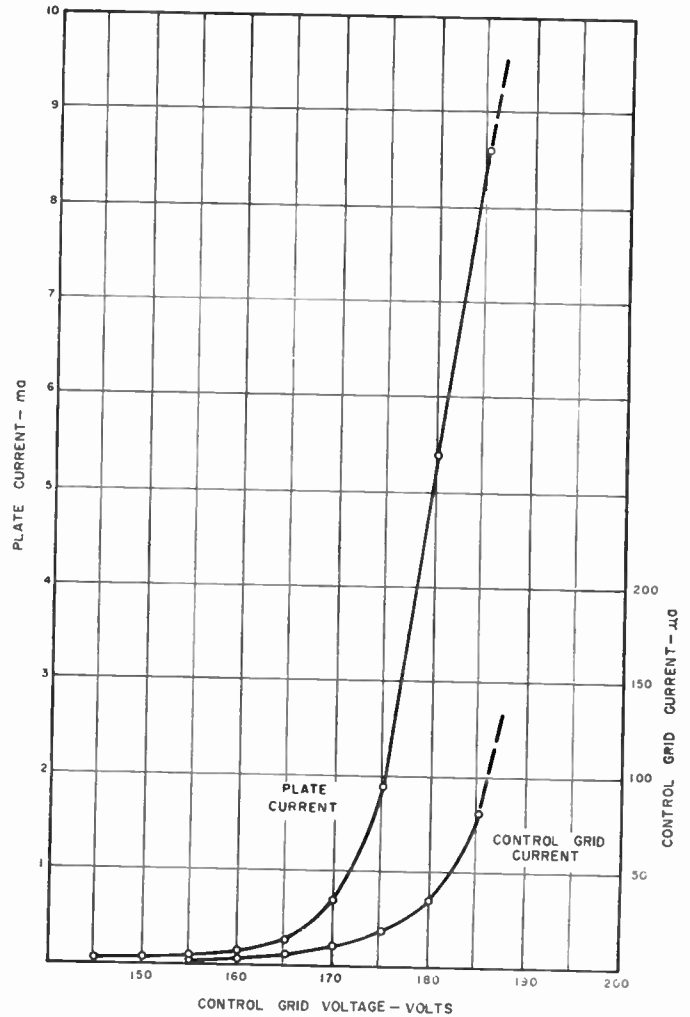


Fig. 12—Control grid characteristic of pentode. The control grid actually consists of G_1 and G_3 connected together. Plate voltage = 450, sustaining grid supply voltage = 450, sustaining grid resistor = 10,000 ohms.

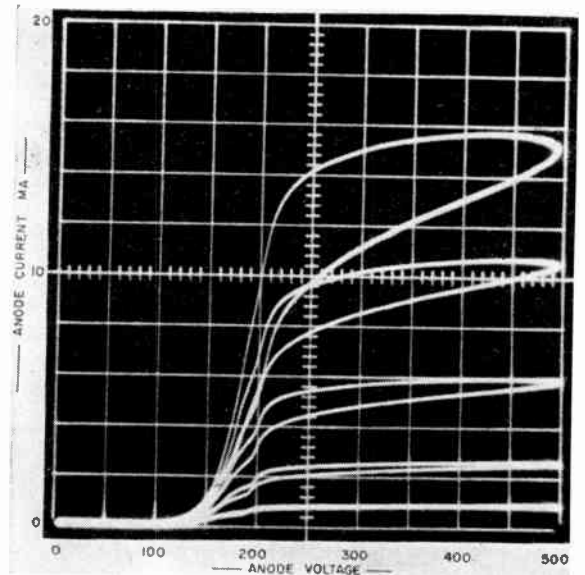


Fig. 13—Family of curves of plate current vs plate voltage for the pentode. The different curves were taken at 160, 170, 180, 190, and 200 volts on the control grids. The sustaining grid was operating at an average value of 420 volts.

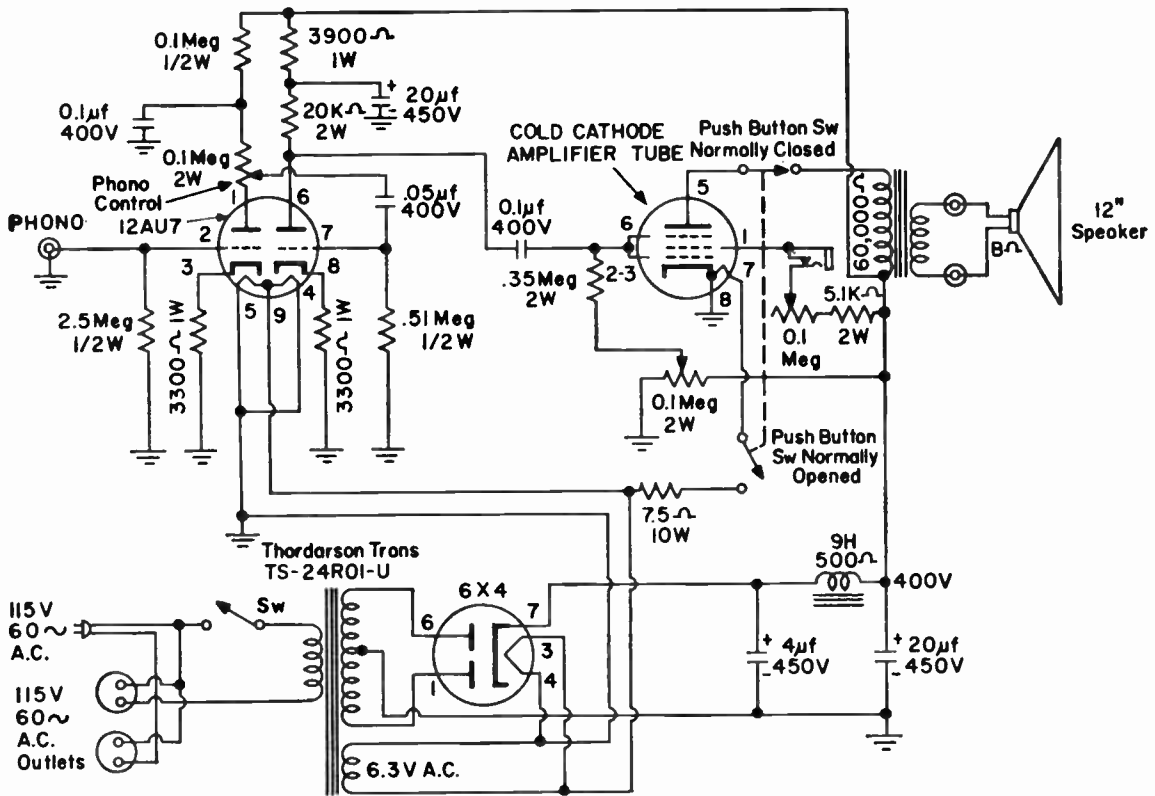


Fig. 14—Circuit of audio amplifier employing the cold cathode pentode in the output stage, which was used for demonstration.

taken on an automatic curve tracer with a repetition rate of 60 cycles. The loops that appear at the higher values of plate current appear to be due to a lag in surface charge, *i.e.*, surface potential, as the applied potential is varied.

The following are the operating characteristics.

Plate supply voltage	500 volts
Plate current	10 ma
Sustaining grid (G_2) voltage supply	350 volts
Sustaining grid (G_2) resistor	10,000 ohms
Sustaining grid (G_2) current	3 ma
Control grid ($G_1 + G_3$) voltage	175 volts
Transconductance	600 micromhos
Amplification factor	33½
Plate resistance	55,500 ohms

Fig. 14 shows the circuit that was used with the pentode in the output stage of a small phonograph for

demonstration purposes.¹² The output was 900 milliwatts of audio power with less than 5 per cent distortion. The signal to noise ratio in the output circuit was 52 db.

ACKNOWLEDGMENT

The authors wish to acknowledge the many helpful discussions with L. L. Kaplan and Dr. D. Dobischek of the Signal Corps, during the preparation of this paper.

A number of members of the technical staff of the Tung-Sol Research Division have contributed significantly. In particular the names of W. J. Shattes, R. L. Simpson, and W. C. Johnson should be mentioned.

¹² Demonstrated at the Meeting of Electron Devices Section of the IRE, Washington, D. C., October 31, 1958.

The Quadrupole Amplifier, a Low-Noise Parametric Device*

R. ADLER†, FELLOW, IRE, G. HRBEK‡, ASSOCIATE MEMBER, IRE AND
G. WADE‡, SENIOR MEMBER, IRE

Summary—Unusually low noise, combined with high stable gain over fairly wide bands, has been obtained with electron beam amplifiers of a new kind. This paper explains how this performance is achieved by the action of a transverse quadrupole field upon a fast cyclotron wave.

The first two sections give a qualitative description of the device and of the amplifying mechanism. A physical picture of the fast cyclotron wave is used to explain the interchange of signal and noise in the input coupler and the mechanism of parametric amplification in the quadrupole region.

The third section presents a detailed analysis of the amplification process. It shows that the fast cyclotron wave is amplified in accordance with a cosh function of distance traveled through the quadrupole, and that a new cyclotron wave at idler frequency (difference between pump and signal frequencies) is generated which grows as a sinh function of distance.

The fourth section describes experimental tubes built to date. These operate on frequency bands between 400 and 800 mc. Typical bandwidth is 40 to 50 mc independent of gain, which may be adjusted to 20 or 30 db. Residual noise temperature of the electron beam in good specimens within this experimental lot is 70°K; input coupler loss raises this figure to about 100°K. This is equivalent to a noise figure of 1.4 db if the device is used, for instance, in radio astronomy. As with other parametric devices, a correction must be added in many other applications; its amount depends on the specific arrangement. This is explained in some detail in the fourth section.

The last section attempts to state precisely the concepts on which the quadrupole amplifier is based and which distinguish it from conventional devices. These concepts may generate a variety of new tube structures in addition to the one described.

INTRODUCTION

THE quadrupole amplifier is a tube in which quadrupole fields act parametrically upon the fast cyclotron wave of an electron beam to produce the amplification.¹ In more conventional microwave tubes such as the traveling-wave tube and the klystron, it is through interaction with a slow wave of the beam that amplification results.^{2,3} The slow wave used can be either a space-charge wave or a cyclotron wave (although the use of space-charge waves is more common in this respect). It has been established theoretically that after the beam emerges from the gun the noise present in slow waves of either type cannot be com-

pletely removed or cancelled.^{4,5} On the other hand, complete noise removal or cancellation is possible, in principle, for a fast wave of either type. Consequently workers have recognized for some time that amplification by means of a fast wave could well be an attractive method of obtaining low-noise amplification.⁶⁻⁹ In the quadrupole tube, amplification by this means is accomplished.

Several of these tubes, all designed to operate in the 400 to 800 mc region, have been built and tested. They exhibit a number of unusual properties. Noise temperature in the liquid nitrogen range has been measured. The tubes are completely unilateral and unconditionally stable. The present tubes have bandwidths of about 10 per cent. Inherently such tubes are capable of much greater bandwidth since, as is shown in a later section, the amplifying process does not limit the bandwidth at all. The bandwidth for a given tube is determined substantially by the bandwidth of the input and output couplers. These and other experimental results are described in more detail in a section to follow.

The quadrupole amplifier is shown diagrammatically in Fig. 1. The electron gun produces a beam which flows successively through an input coupler, an amplifying region, and an output coupler. The entire beam is immersed in a uniform magnetic field (not shown in the diagram) and flows parallel to the flux lines. Most

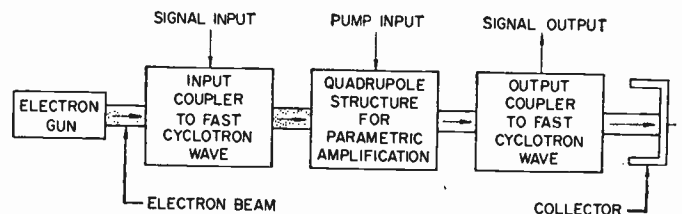


Fig. 1—Diagram of quadrupole amplifier.

* Original manuscript received by the IRE, May 4, 1959.

† Research Dept., Zenith Radio Corp., Chicago, Ill.

‡ Electronics Res. Lab., Stanford University, Stanford, Calif.

¹ R. Adler, G. Hrbek and G. Wade, "A low-noise electron-beam parametric amplifier," *Proc. IRE*, vol. 46, pp. 1756-1757; October, 1958.

² J. R. Pierce, "The wave picture of microwave tubes," *Bell Sys. Tech. J.*, vol. 33, pp. 1343-1372; November, 1954.

³ R. W. Gould, "A coupled mode description of the backward-wave oscillator and the Kompfner dip condition," *IRE TRANS. ON ELECTRON DEVICES*, vol. ED-2, pp. 37-42; October, 1955.

⁴ H. A. Haus and F. N. H. Robinson, "The minimum noise figure of microwave beam amplifiers," *Proc. IRE*, vol. 43, pp. 981-991; August, 1955.

⁵ H. A. Haus and D. L. Bobroff, "Small signal power theorem for electron beams," *J. Appl. Phys.*, vol. 28, pp. 694-704; June, 1957.

⁶ R. Adler, "A new principle of signal amplification," presented at Conf. on Electron Tube Research, Berkeley, Calif.; June, 1957.

⁷ W. H. Louisell and C. F. Quate, "Parametric amplification of space-charge waves," *Proc. IRE*, vol. 46, pp. 707-716; April, 1958.

⁸ R. Adler, "Parametric amplification of the fast electron wave," *Proc. IRE*, vol. 46, pp. 1300-1301; June, 1958.

⁹ G. Wade and R. Adler, "A new method for pumping a fast space-charge wave," *Proc. IRE*, vol. 47, pp. 79-80; January, 1959.

of the tubes thus far built operate with the magnetic field intensity such that the corresponding cyclotron frequency is approximately equal to the frequency of the signal to be amplified. For these tubes, the input and output couplers are of the Cuccia type.^{8,10} This type of coupler interacts with the fast cyclotron wave only. The input coupler serves two functions. It demodulates the beam as far as the entering fast-wave component of beam noise is concerned, and at the same time it modulates the beam with a new fast wave corresponding to the input signal. Thus it extracts noise and inserts signal simultaneously. The beam then passes through the quadrupole structure which provides a means for amplifying the signal modulation. In the present tubes the quadrupole is fed by a pumping signal at precisely twice the cyclotron frequency. Parametric action of the quadrupole field upon the modulated beam results in amplification. Finally, the amplified fast-wave modulation is extracted from the beam by the output coupler and appears as the signal output for the device.

Since the action of the quadrupole field is parametric in nature, these amplifiers exhibit a number of the characteristics usually associated with parametric amplifiers. For example, a modulation at the idler frequency (the difference between the pump frequency and the input signal frequency) is excited on the beam by the quadrupole fields and will appear at the output if the output coupler is sensitive to the idler frequency.

Although certain similarities do exist between the various types of parametric amplifiers, there are also some wide differences. For example, the quadrupole amplifier is not inherently narrow band, bilateral nor unstable, as is common in many cavity type, solid-state versions. The quadrupole has opposite characteristics in these respects. In many ways it resembles the tube of Louisell, Quate and Ashkin^{7,11} which utilizes parametric amplification of space-charge waves. However, there are some significant differences having to do with the nature of the quadrupole pumping and with the inherent behavior of cyclotron waves relative to space-charge waves.¹²

In the sections to follow, this paper presents a more detailed physical description of the amplifier and how it works, an analysis of the amplifying mechanism associated with the quadrupole fields, a discussion of the experimental results, and some conclusions regarding the significance of this work. Although the noise behavior is discussed in a general way and the results of noise figure measurements are given, an analysis of

the noise characteristics of cyclotron waves is not presented, since this appears in the literature elsewhere.^{5,13}

PHYSICAL DESCRIPTION OF THE DEVICE AND THE MECHANISMS FOR COUPLING AND AMPLIFYING

Since this device amplifies the fast cyclotron wave, it is necessary to know something about the nature of the fast cyclotron wave in order to understand how the device works. Analyses of the various cyclotron waves are available in the literature.¹³⁻¹⁶ It will suffice here to summarize briefly what the analyses say with particular emphasis on the fast wave.

Consider an electron beam drifting in a region of uniform magnetic field. The unmodulated beam flow is parallel to the flux lines of the field. If the beam is modulated by a signal that produces velocity components in the transverse direction, in general, the modulation components are propagated along the beam corresponding to two fundamental modes, a fast-wave mode and a slow-wave mode.¹⁷ The phase velocities of propagation for these modes are, respectively,

$$v_f = \frac{u_0}{1 - \frac{\omega_c}{\omega}}$$

and

$$v_s = \frac{u_0}{1 + \frac{\omega_c}{\omega}}$$

where

- u_0 = the electron velocity in the axial direction (the direction of unmodulated beam flow),
- $\omega_c = \eta B$, the radian cyclotron frequency,
- ω = the radian frequency of the signal modulation,
- η = the electronic charge to mass ratio,
- B = the strength of the axial magnetic field.

As the signal frequency approaches the cyclotron frequency from above, the separation of the velocities increases. For the case where the signal frequency equals the cyclotron frequency, the phase velocity for the fast

¹⁰ C. L. Cuccia, "The electron coupler," *RCA Rev.*, vol. 10, pp. 270-303; June, 1949.

¹¹ A. Ashkin, "Parametric amplification of space charge waves," *J. Appl. Phys.*, vol. 29, pp. 1646-1651; December, 1958.

¹² For example, the pumping fields producing the amplification are supplied by the quadrupole structure rather than through a separate modulation of the beam. This eliminates the problem of beam saturation and the detrimental by-products associated with beam saturation. Also, with cyclotron waves the fast and slow waves can be more easily separated in velocity than with space-charge waves.

¹³ G. Wade, K. Amo, and D. A. Watkins, "Noise in transverse-field traveling-wave tubes," *J. Appl. Phys.*, vol. 25, pp. 1514-1520; December, 1954.

¹⁴ J. R. Pierce, "Traveling-Wave Tubes," D. Van Nostrand Co., Inc., New York, N. Y., ch. 13; 1950.

¹⁵ R. Adler, "An equivalence principle in high frequency tubes," 1953 IRE NATIONAL CONVENTION RECORD, pt. 6, pp. 54-61.

¹⁶ R. Adler, O. M. Kromhout, and P. A. Clavier, "Transverse-field traveling-wave tubes with periodic electrostatic focusing," *Proc. IRE*, vol. 44, pp. 82-89; January, 1956. See particularly "Transverse electron waves," pp. 84-85.

¹⁷ Transverse waves can also propagate at an intermediate velocity equal to the electron stream velocity u_0 . These waves involve transverse displacements only, with zero transverse velocity components (see reference 13). These waves are not germane to the present discussion since they are not generated by the input coupler and are not amplified by the quadrupole structure.

wave is infinite. The phase velocity for the slow wave is one-half the axial electron velocity. The two velocities are then very different, and it is easy to couple to the fast wave only. The quadrupole amplifiers thus far built have operated over a range of signal frequencies close to the cyclotron frequency.

For a moment, consider the electron pattern corresponding to fast wave modulation only. Fig. 2 illustrates the pattern as it would appear at a particular instant of time for the condition that $\omega > \omega_c$. The imaginary center conductor is included as a convenience for indicating the sense of the helical pattern. As time passes, the pattern maintains its form but moves forward in the plus z direction at the fast-wave velocity. Each electron individually moves forward at u_0 , which is less than the fast-wave velocity. It is possible for the pattern to move faster than the electrons because each electron has angular velocity in the plus θ direction (*i.e.*, coming out of the paper above the center conductor and going into the paper below the center conductor) as well as linear velocity in the plus z direction. The angular velocity of each electron in the plus θ direction is precisely ω_c , the radian cyclotron frequency. The point of intersection of the beam with any transverse plane at constant z describes a circle and moves with an angular velocity of precisely ω , the radian frequency of the modulation.

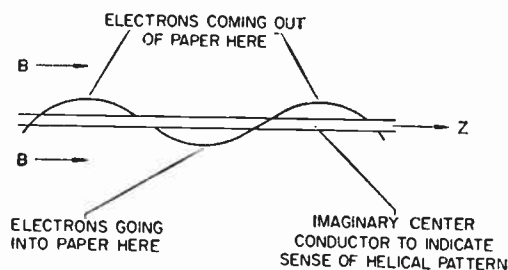


Fig. 2—Electron pattern corresponding to fast-wave modulation on a drifting beam for an instant of time. The beam is assumed to be immersed in a uniform magnetic field B . Also it is assumed that $\omega > \omega_c$.

As stated, Fig. 2 gives the pattern under the condition $\omega > \omega_c$. As ω is reduced, both the fast-wave velocity and the wavelength increase. The helical beam pattern becomes less tightly wound. It is important to note that in spite of these changes in the beam pattern, the individual electrons continue to move in the axial direction with velocity u_0 and in the θ direction with angular velocity ω_c . In the limit, as ω approaches ω_c , the beam pattern becomes a straight horizontal line which revolves about the axis (or the imaginary center conductor of Fig. 2) with angular velocity $\omega = \omega_c$. The phase velocity and the wavelength are both infinite for this condition.

For $\omega < \omega_c$, the phase velocity becomes negative. This merely means that the beam pattern shown in Fig. 2 begins to wind up the other way, becoming a right-handed instead of a left-handed screw. The indi-

vidual electrons still revolve with angular velocity ω_c while moving forward with velocity u_0 .

For operation where the cyclotron and the modulation frequencies are about equal, the phase velocities are so high that we can neglect the time of propagation and use lumped electrodes, as in the present quadrupole tubes. For example, each coupler consists of a pair of flat, parallel plates between which the beam flows. Let us examine briefly the nature of the couplers by following a beam as it passes from an electron gun successively through an input coupler of this type, a drift region, and an output coupler of this type. Fig. 3 illustrates the operation when the cyclotron and modulation frequencies are precisely equal. In the input coupler, each electron follows a spiral path of increasing radius. Then it continues on a helical path of constant radius in the drift region preceding the output coupler. Cuccia has shown that if the output coupler is loaded properly, the circling electrons can be made to give up all their transverse motion as they pass through it.¹⁰ There is no energy interchange between transverse and longitudinal electron motion. There is also no gain. To the signal source, the electron stream in the input section looks like a purely resistive load. All the energy delivered by the source is turned into transverse electron motion and it all reappears in the output coupler.

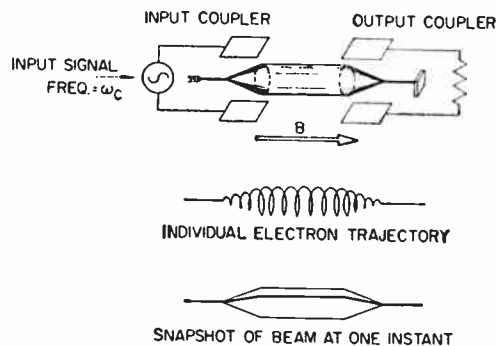


Fig. 3—Diagram showing an electron beam passing through an input coupler and an output coupler which are separated by a drift region. The individual electrons follow spiral and helical paths, while the beam pattern for any instant of time consists of straight line segments.

The mechanism of energy interchange between beam and coupler is similar to energy interchange in two coupled transmission lines. For properly designed coupling between two transmission lines, all of the energy originally fed into one of the two lines is transferred to the second one over a distance of a quarter of a coupling wavelength. If at this point we separate the two lines, the first line remains with none of its original energy and the second line carries away all of it. The same process, of course, works just as well in the opposite direction. In fact, if we have two sources of energy initially feeding the two lines (one source feeding each line) at the end of the coupling region the energy is completely interchanged. Assume that we label the energy fed to the first line "signal" and the energy fed

to the second line "noise." Then "signal" and "noise" are interchanged on the lines by the coupling.

The electron beam and the Cuccia coupler can be thought of as two coupled transmission lines each supporting waves of infinite phase velocity. A signal fed to the coupler is transferred to the fast wave of the beam while fast-wave noise entering with the beam is transferred to the coupler. Ideally the device shown in Fig. 3 transmits all of the signal and adds no noise to it.

We may regard each coupler as a three-port circulator. The first port consists of the beam as it enters; the second port, the leads to the two parallel plates; and the third port, the beam as it leaves. The fast-wave noise which enters the first port (i.e., with the beam) goes out the second port to the signal source which also acts as a noise sink. The signal energy from the source enters the second port and is routed to the third port (the departing beam). If the noise sink is not properly matched, a fraction of the beam noise is reflected and re-applied to the beam.

The Cuccia coupler, because of its requirement of infinite phase velocity, represents a special case among fast-wave couplers. Such couplers may also be designed for finite phase velocity; helices are a familiar example. Signal input and beam noise output terminals may be physically separated on such a coupler, making it effectively a four-port circulator.

As shown in Fig. 3, when $\omega = \omega_c$, the beam pattern in the drift region forms a straight, horizontal line segment which revolves about the axis with an angular frequency ω_c . Each electron in the drift region follows a helical path of constant radius. The fact that the radius is constant signifies that no amplification takes place. Any mechanism which increases the radius of the electron path will produce amplification. For the amplification to be linear, the rate of growth of the radius must be proportional to the radius.

The problem of producing amplification is one of finding a mechanism for increasing the radii of the individual electrons. Consider a single electron which in the absence of such a mechanism describes a circular path as far as its transverse motion is concerned. It seems intuitively obvious that the radius of the circular path could be increased by arranging for the electron to experience constantly a tangential force in the direction of its transverse motion. Such a force would serve to accelerate the electron, increasing its transverse velocity and consequently increasing the radius of curvature of its path. In this regard, the electron motion would be somewhat similar to the motion of the bob of a circular pendulum (one which traces a circular orbit in a horizontal plane) when the bob is acted upon continuously by a tangential force which increases its velocity.

For the operation to be proper, the magnitude of such a tangential force on the electron would have to be a function of the position of the electron. An unmodulated electron, corresponding to no signal present, would travel without any transverse motion down the axis of

the tube, in the absence of our hypothetical force system. This electron should be left undisturbed by our hypothetical force system. In order for the amplification of electron radii to be linear, an electron which carries a weak signal and consequently describes a path of small radius, should encounter only a weak tangential force. By the same token, an electron which is strongly modulated should encounter a strong tangential force. As the radius of curvature of the electron path increases, the magnitude of the force encountered should likewise increase.

Fig. 4 shows an electrode structure which is ideally suited to supply the forces necessary to amplify the radii of all electrons which enter with the proper phase. The figure represents the cross section at the entrance to a quadrupole structure. The structure is assumed to extend out of the paper in the positive z direction. The polarities indicated in the figure correspond to an instant when the top and bottom electrodes are at their maximum positive potential and, consequently, when the left and right electrodes are at their maximum negative potential. The arrows show the forces which would be exerted upon electrons in the corresponding positions.

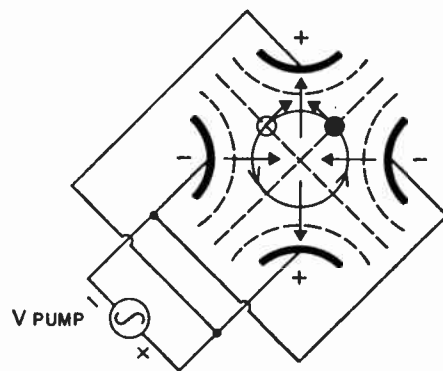


Fig. 4—Cross section at the entrance to the quadrupole structure, illustrating the forces exerted upon electrons (arrows) and the equipotential surfaces (dashed lines).

The beam flow is out of the paper and the sense of the helical electron motion is counter-clockwise as seen by an observer looking up stream at the cross section. The dashed lines indicate the equipotential surfaces of the quadrupole region. We see that the electron at the top right, which is shown solid, encounters a force which accelerates it along its counter-clockwise path. The other electron, shown as an empty circle, is subjected to a force which decelerates its orbital motion. Any electron which occupies a position along the equipotential line extending from upper right to lower left has the proper phase for maximum acceleration and therefore maximum amplification. Those occupying positions along the equipotential line extending from upper left to lower right will experience maximum deceleration.

Two entirely different approaches may be used to analyze the amplification process. The mathematical

treatment given in the following section resolves the orbital electron motion into two orthogonal periodic motions; it shows how each of these is made to grow by the application of a time-varying restoring force. This is the parametric viewpoint. It is helpful because it elucidates the analogies between the quadrupole amplifier and other parametric devices; it is also general enough to be applicable to other electron beam devices which use periodic electron motion about one coordinate only.⁹

But in the present device, the magnetic field forces the two orthogonal periodic motions to be always in phase quadrature and of equal amplitude. This restriction permits us to use a simpler method of analysis, less general but better suited to convey an intuitive understanding of the specific device.

We may resolve the alternating quadrupole field pattern into two counter-rotating component patterns, in the manner commonly used with electrical machines. Because our stator has four poles, the component patterns complete one revolution for every two cycles of the pump frequency. If we choose the pump frequency to be just twice the cyclotron frequency, one of the patterns will revolve synchronously with the orbiting electrons. The other pattern we may ignore, as far as our present description is concerned, because its influence is small.

For the moment, let us consider an electron which enters the quadrupole region with a phase corresponding to maximum acceleration. Half of the accelerating field may be ascribed to the quadrupole field pattern just referred to which rotates synchronously. Our electron, which entered with optimum phase, remains in that phase throughout its passage through the quadrupole. Note that there is no field at all at the center and that the field intensity increases linearly with distance from the center. Thus, the forces exerted upon our orbiting electron are proportional to the radius of the circle in which it moves. As a result, the radius increases exponentially and the amplification is linear.

Now let us consider an electron which enters with a phase corresponding to maximum deceleration. For this electron, the force field produces an exponential decrease in the radius which is equivalent to a linear attenuation. The rate of decrease in the radius for this electron and the rate of increase in the radius for the previous electron are the same. Fig. 5 shows the curved surfaces generated by the motion of two electrons with best and worst phase. Both are assumed to enter from the left along the same cylindrical surface. One radius becomes very large and the other negligibly small.

Thus far we have been discussing the motion of individual electrons. Fig. 5 can also be used to illustrate beam patterns. For example, assume that the pump frequency is precisely twice the cyclotron frequency and that the input frequency is accurately synchronized with one-half the pump frequency. A specific phase condition, for instance that of maximum gain, will then be maintained. Under these conditions the outer surface of Fig.

5 is a figure of revolution of the beam pattern. If the phase condition is changed to that of maximum attenuation, then the inner surface of Fig. 5 becomes the figure of revolution of the beam pattern. If the signal frequency is then altered slightly, conditions of maximum gain and maximum loss occur alternately. At any plane in the quadrupole the radius of the electron pattern as a function of time is periodic, swinging alternately from that corresponding to maximum gain to that corresponding to maximum attenuation. If the difference between one-half the pump frequency and the signal frequency is great enough, the electron pattern at any instant of time will touch several times both the maximum gain surface and the maximum attenuation surface. This condition is illustrated by the plot in Fig. 6. On the average, the resulting output signal is larger than the input signal because the exponential growth always outweighs the exponential drop. The output signal contains a beat with round tops and sharply pointed dips. It consists of two sine wave components, one at the signal frequency, and the other at the idler frequency, the difference between pump and signal frequencies.

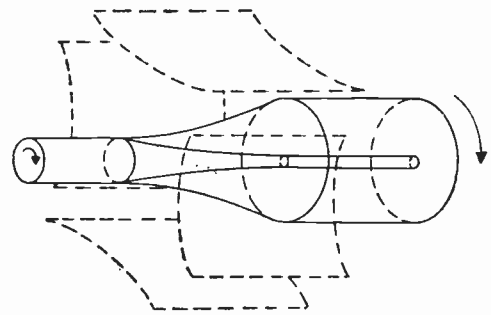


Fig. 5—Surfaces generated by the motion of electrons with best and worst phase for amplification. The dashed lines depict the outlines of the quadrupole structure.

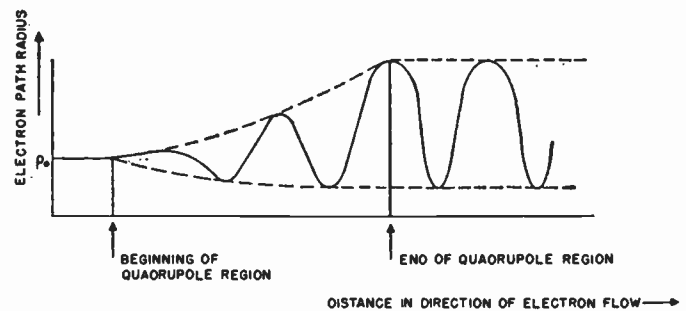


Fig. 6—Electron path radius as a function of distance for a particular instant of time.

It is now possible to see why the amplifying process does not limit the bandwidth. The waveform shown in Fig. 6 was obtained by altering the signal frequency. The pump frequency and the magnetic field were not changed. Gain resulted from averaging over many electrons entering with every possible phase. This mechanism remains the same regardless of signal frequency.

Thus the amplifying process does not have any frequency selectivity. By using wide-band couplers, we may produce fast waves at any signal frequency. The individual electrons which make up these waves must still orbit at the cyclotron frequency, and we can amplify their motion by pumping at twice that frequency. The bandwidth of the tube, therefore, is determined only by the couplers.

In comparing the action of the quadrupole with older amplifying mechanisms, one is struck by the absence of a familiar concept. There is no two-way interaction between a stream and a field, as in a traveling wave tube, or between two streams, as in a double-stream amplifier; instead, there is only the one-way action of an externally imposed field upon individual electrons.

ANALYSIS OF AMPLIFYING MECHANISM

This section presents a derivation of an equation describing the beam pattern in the quadrupole region. By comparing the amplitude and the character of the transverse excursions at the end of the quadrupole region to the amplitude and character at the beginning, we obtain a measure of the gain of the amplifying signal and of the growth of the idling signal which is excited. The derivation proceeds by examining the nature of the quadrupole field and its effect upon the electrons of the beam.

Consider a quadrupole structure which is formed by placing four similar electrodes symmetrically about an axis. The electrodes are shaped so that the transverse cross sections of the structure are identical through all points of the axis. The structure is driven by tying together the electrodes having opposite positions, and connecting the pump generator between the resulting pairs as illustrated in Fig. 4. The electrodes conceivably can have any of a wide variety of shapes. However, regardless of the shape, the equipotentials near the axis tend to have the form of equilateral hyperbolas. Equipotentials with precisely this form, not only near the axis but throughout the entire region, result if the electrodes themselves are shaped like equilateral hyperbolas. Since this shape gives the simplest field configuration for analysis and since all other shapes give field configurations which approximate this one near the axis (in the small signal region), we will assume that the electrodes are so shaped.

The potential anywhere in the quadrupole region is given by the following expression:

$$V = k(y^2 - x^2), \quad (1)$$

where x and y are the transverse coordinates specifying the position of the electrons. Fig. 7 illustrates the orientation of the coordinate system and the position of the electrodes. Electrodes 1 and 3 of Fig. 7 are connected together, as are electrodes 2 and 4. These connections were previously indicated in Fig. 4. The full pump voltage appears across the two pairs of electrodes.

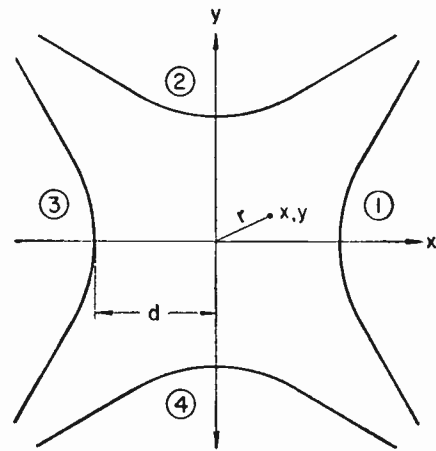


Fig. 7—Orientation of xy coordinates in the quadrupole region. Electron flow and magnetic flux lines are assumed to be in the z direction (out of the paper).

The quantity k is given by

$$k = \frac{V_{\text{pump}}}{2d^2}, \quad (2)$$

where V_{pump} is the instantaneous pump voltage and d is a distance defined in Fig. 7. As previously stated, the pump frequency is chosen to be just double the cyclotron frequency. Hence we have

$$k = \frac{V_m \sin 2\omega_c t}{2d^2} = k_m \sin 2\omega_c t \quad (3)$$

where k_m is a constant representing the maximum value of k . The x and y components of the electric field resulting from the pump voltage can be calculated from (1) as follows:

$$\begin{aligned} E_x &= -\frac{\partial V}{\partial x} = 2kx \\ E_y &= -\frac{\partial V}{\partial y} = -2ky. \end{aligned} \quad (4)$$

Note that these field components are proportional to distance from the origin. The forces they produce upon electrons are therefore like elastic restoring forces. They vary in time at a rate corresponding to the pump frequency $2\omega_c$. This is characteristic of parametric processes.

We can determine the gain of the amplifier by observing the growth in the transverse displacement of the electrons as they traverse the quadrupole region. The procedure will be to consider the forces acting on a single electron. From this consideration we derive a general equation giving the transverse coordinates of the electron as a function of the time it remains in the quadrupole region. As we shall see, the relative phase of the pump voltage greatly influences the change in the transverse displacement of the electron. By applying the general equation thus derived to the whole train of electrons which make up the beam pattern, we obtain the

expression for beam position as a function of time at the plane marking the exit from the quadrupole region.

The force equation for a single electron is

$$\bar{F} = m \frac{d\bar{v}}{dt} = -e(\bar{E} + \bar{v} \times \bar{B}). \tag{5}$$

By expanding into x and y components of force, and using (4), we obtain

$$\begin{aligned} \ddot{x} &= -\eta 2kx - \omega_c \dot{y} \\ \ddot{y} &= \eta 2ky + \omega_c \dot{x}, \end{aligned} \tag{6}$$

where ω_c , the cyclotron frequency, is given by $(e/m)B$.

The electron beam which approaches the quadrupole region has already passed through the input coupler where it has been fast-wave modulated in the fashion previously described. The intersection of the beam pattern and the entrance plane to the quadrupole region moves in accordance with the following equations:

$$\begin{aligned} y &= r_0 \sin \omega t \\ x &= r_0 \cos \omega t, \end{aligned} \tag{7}$$

where ω = the modulating frequency (the input signal frequency). Eqs. (7) are consistent with the previous description of fast-wave modulation. The point of intersection of the beam and the entrance plane describes a circle and moves in the counter-clockwise direction at an angular velocity ω .

Let us consider a particular electron which enters at a time $t=t_1$. At that moment the electron has a transverse position given by

$$\begin{aligned} y &= r_0 \sin \omega t_1 \\ x &= r_0 \cos \omega t_1. \end{aligned} \tag{8}$$

In solving for the effect of the quadrupole fields on the transverse motion of the electron, it is helpful first to note the transverse motion of the electron under the condition that the quadrupole fields are zero. This transverse motion is readily obtained from (6) by letting k be zero and by using (8) to give the boundary conditions. For time $t > t_1$, the electron has been in the quadrupole region an amount of time $\tau = t - t_1$. The transverse motion of the electron is

$$\begin{aligned} y &= r_0 \sin (\omega_c \tau + \omega t_1) \\ x &= r_0 \cos (\omega_c \tau + \omega t_1). \end{aligned} \tag{9}$$

Eqs. (9) are consistent with intuitive concepts. After entering the quadrupole region with a transverse position given by (8), the electron describes a circle moving with angular velocity ω_c in the counter-clockwise direction.

For reasons which become apparent shortly let us expand (9), through the use of trigonometric identities, to give the following:

$$\begin{aligned} y &= r_0' \sin (\omega_c \tau + \omega_c t_1) + r_0'' \cos (\omega_c \tau + \omega_c t_1) \\ x &= r_0' \cos (\omega_c \tau + \omega_c t_1) - r_0'' \sin (\omega_c \tau + \omega_c t_1) \end{aligned} \tag{10}$$

where

$$\begin{aligned} r_0' &\equiv r_0 \cos (\omega t_1 - \omega_c t_1) \\ r_0'' &\equiv r_0 \sin (\omega t_1 - \omega_c t_1). \end{aligned}$$

Since $t = \tau + t_1$, (3) can be rewritten as follows:

$$k = k_m \sin [2(\omega_c \tau + \omega_c t_1)]. \tag{11}$$

We recognize that (10) is the solution for (6) in the limit as k_m approaches zero. For $k_m > 0$, the solutions must be modifications of (10), which approach (10) as k_m approaches zero. We are now in a position to determine the modifications.

An easy method for finding the modifications (in fact, the method originally used by the authors) involves making use of the descriptive information previously given concerning the operation of the tube. We simply choose convenient entrance conditions to consider for the electrons and guess at the corresponding solutions. The accuracy of each guess is quickly determined by substituting the assumed solution in (6) and checking for equality. In this fashion we very rapidly arrive at the general solution which holds for all electrons regardless of entrance condition. As is shown below, only two choices of the entrance conditions are needed in finding the general solution.

For the first choice let us assume that t_1 is such that

$$\omega t_1 - \omega_c t_1 = \pi 2n \quad n = 0, 1, 2, \dots$$

Then

$$r_0' = r_0$$

and

$$r_0'' = 0.$$

If we compare (10) with (11) we see that for the above condition the electron has a phase which corresponds to that of the electron shown solid in Fig. 4, and therefore the electron experiences maximum amplification, as previously discussed. We might reasonably expect its radius to increase approximately as $e^{\alpha' \tau}$ where α' is some positive number. Hence, we guess that the solution is

$$\begin{aligned} y &= r_0 e^{\alpha' \tau} \sin (\omega_c \tau + \omega_c t_1) \\ x &= r_0 e^{\alpha' \tau} \cos (\omega_c \tau + \omega_c t_1). \end{aligned}$$

When we substitute this assumed solution in (6) we find that equalities result for

$$\alpha' = \frac{k_m}{B}$$

under the condition that

$$\alpha' \ll \omega_c.$$

This is the condition of usual interest.

For the second choice of entrance conditions let us assume that t_1 is such that

$$\omega t_1 - \omega_c t_1 = \pi(2n + 1) \quad n = 0, 1, 2, \dots$$

Then

$$r_0' = 0$$

and

$$r_0'' = r_0.$$

This time the electron has a phase corresponding to that of the electron shown as the empty circle in Fig. 4. Hence, the electron experiences maximum attenuation. We might expect the radius to decrease approximately as $e^{-\alpha''\tau}$ where α'' is a positive number. Consequently, our assumed solution is

$$\begin{aligned} y &= r_0 e^{-\alpha''\tau} \cos(\omega_c\tau + \omega_c t_1) \\ x &= -r_0 e^{-\alpha''\tau} \sin(\omega_c\tau + \omega_c t_1). \end{aligned}$$

By substituting these equations in (6) we find that equalities result for

$$\alpha'' = \frac{k_m}{B},$$

when

$$\alpha'' \ll \omega_c.$$

For the general case, we must assume that neither r_0' nor r_0'' is zero. The expected solution would be a superposition of the respective solutions for the preceding two cases, the portion of the equation associated with r_0' increasing as $e^{(k_m/B)\tau}$ and the portion associated with r_0'' decreasing as $e^{-(k_m/B)\tau}$. Hence, the assumed solution is

$$\begin{aligned} y &= r_0' e^{(k_m/B)\tau} \sin(\omega_c\tau + \omega_c t_1) \\ &\quad + r_0'' e^{-(k_m/B)\tau} \cos(\omega_c\tau + \omega_c t_1) \\ x &= r_0' e^{(k_m/B)\tau} \cos(\omega_c\tau + \omega_c t_1) \\ &\quad - r_0'' e^{-(k_m/B)\tau} \sin(\omega_c\tau + \omega_c t_1). \end{aligned} \quad (12)$$

That (12) is correct is easily demonstrated by substituting (12) in (6) and checking the equality. Equality results under the condition that

$$\frac{k_m}{B} \ll \omega_e.$$

As previously stated, this is the case of usual interest.

Consider further the solution for y . If the plates of the output coupler are parallel to the x axis, then it is the motion in the y direction which is important in inducing the signal from the beam to the coupler. By using the definitions of r_0' and r_0'' and by manipulating the terms of (12), we obtain

$$\begin{aligned} y &= r_0 \left\{ \sin[\omega_c\tau + \omega t_1] \cosh \frac{k_m}{B} \tau \right. \\ &\quad \left. + \sin[\omega_c\tau + (2\omega_c - \omega)t_1] \sinh \frac{k_m}{B} \tau \right\}. \end{aligned} \quad (13)$$

The electron remains within the quadrupole region for a time τ given by

$$\tau = \frac{L}{u_0},$$

where

L = the length of the quadrupole region.

Hence we have

$$\omega_c\tau = \frac{\omega_c}{u_0} L \equiv \beta_m L$$

and

$$\frac{k_m}{B} \tau = \frac{k_m}{Bu_0} L \equiv \alpha L,$$

where

β_m = the cyclotron wave number

α = the growth factor.

Using these definitions in (13) we have

$$\begin{aligned} y &= r_0 \left\{ \cosh \alpha L \sin[\omega t_1 + \beta_m L] \right. \\ &\quad \left. + \sinh \alpha L \sin[(2\omega_c - \omega)t_1 + \beta_m L] \right\}. \end{aligned} \quad (14)$$

Eq. (14) was derived specifically to apply to a single electron which enters the quadrupole region at $t = t_1$. We recognize that the equation applies to any electron of the whole train of electrons which make up the beam pattern. Each electron, of course, has a different t_1 . Thus, by permitting t_1 to range through all values of time, (14) generates the y component of the beam position at the exit plane as a function of time.

A comparison of (14) with (8) shows that the signal is amplified by the factor $\cosh \alpha L$. In addition, an idler signal is generated at a frequency equal to the difference between the pump and the input signal frequencies. The idler signal has a magnitude proportional to $\sinh \alpha L$.

EXPERIMENTAL RESULTS

The equations derived in the preceding section permit us to calculate the gain of a quadrupole amplifier. By inserting numerical values which correspond to a practical structure, one finds that substantial gain may be obtained with surprising ease.

According to (14), the gain is $\cosh \alpha L$, where $\alpha L = (k_m/Bu_0)L$. Eq. (3) defines k_m as $k_m = V_m/2d^2$, where V_m is the peak pump voltage applied across adjacent quadrupole elements as shown in Fig. 4, and d is the half spacing illustrated in Fig. 7. Thus,

$$\alpha L = \frac{V_m L}{2d^2 Bu_0}. \quad (15)$$

Let us now insert the numbers which were selected for the first experimental model. The signal-and-cyclotron frequency was chosen to be 560 mc, corresponding to a magnetic field of 200 gauss (2×10^{-2} Webers per square meter). To keep the over-all dimensions of the tube small, a slow electron beam was used. It was known from previous experiments that a beam carrying about 50 micro-

amperes at less than 10 volts could be held to a diameter of about one-half millimeter in a 200 gauss field without difficulty. A velocity of $u_0 = 1.5 \cdot 10^6$ m/sec or 1/200 of light velocity was chosen corresponding to 6.25 volts accelerating potential.¹⁸

The transverse dimensions of the quadrupole structure were chosen large enough to allow ample clearance for the beam, since electron interception is highly undesirable in a low-noise tube. A spacing of 0.030 inch or 0.75 millimeter between opposite elements would have been sufficient from this standpoint. It was believed, however, that it would be advantageous to obtain a better approximation of a purely hyperbolic potential distribution in the beam region by keeping the quadrupole electrodes farther apart, and a spacing of 0.080 inch or 2 millimeters between opposite elements, corresponding to $d = 107_0$ meter, was chosen.

The axial length of the quadrupole structure was 0.4 inch or 1 cm; thus $L = 10^{-2}$ meter. For a 6-volt beam, this corresponds to a transit time of $6.7 \cdot 10^{-9}$ seconds, or nearly four cycles at the cyclotron frequency of 560 mc.

Substituting now the numerical values into (15), we find

$$\alpha L = \frac{V_m \cdot 10^{-2}}{2 \cdot 10^{-6} \cdot 2 \cdot 10^{-2} \cdot 1.5 \cdot 10^6} = \frac{V_m}{6}$$

Thus, $\alpha L = 1$ for a pump voltage of as little as 6 volts peak-to-peak; with $V_m = 18$ volts, we obtain $\alpha L = 3$ and $\cosh \alpha L = 10$, corresponding to a gain of 20 db.

Very little pump power is required to maintain the quadrupole field. To obtain a rough estimate, let us assume the capacity between each pair of adjacent quadrupole elements to be $0.5 \mu\mu$ farads; then at the pump frequency of 1120 mc, the circulating reactive power at $V_m = 18$ volts is about 2.3 volt-amperes, and if the capacity of the elements is tuned out by inductances having a Q of 100, the required driving power is 23 mw. Clearly, these figures do not represent an optimum design; they approximate the behavior of the early experimental models.

Fig. 8 schematically shows the arrangement of the input coupler, quadrupole and output coupler in the experimental tubes. The two Cuccia couplers are tuned to the center of the signal frequency band by built-in coils; balanced transmission lines with a characteristic impedance of about 300 ohms are connected to taps on the coils. These taps are positioned for good impedance match to the electron beam; signal source and output load are matched to the 300-ohm lines by adjustable impedance transformers. The total power loss in each coupler, including transmission lines and external transformer, ranges from 0.2 db at 400 mc to about 0.5 db at 800 mc. Improvement through better design appears quite possible, particularly at the higher frequency.

¹⁸ The Brillouin flow current for a 6.25 volt beam of $\frac{1}{2}$ millimeter diameter at 200 gauss is 90 microamperes.

The quadrupole structure is tuned to the pump frequency by means of four built-in coils interconnecting the four structural elements. To insure operation only in the desired π -mode (180° phase shift between adjacent elements), low-inductance straps are connected across opposite elements. Pump power is introduced into the quadrupole through a balanced two-wire line which ends in a single-turn loop closely coupled to one of the four coils.

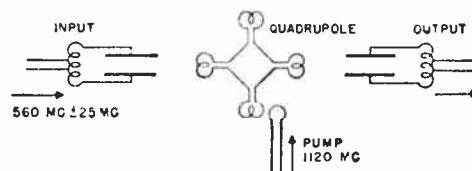


Fig. 8—Schematic diagram of first experimental quadrupole amplifier.

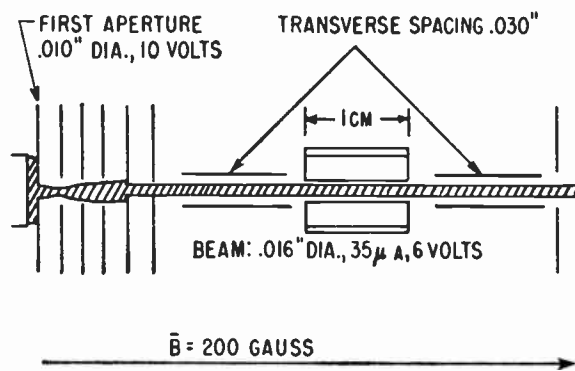


Fig. 9—Constructional features of experimental quadrupole amplifier.

Fig. 9 illustrates the construction of an experimental tube. The electron gun is designed to approximate Brillouin flow. The narrow aperture in the first electrode selects a very small cylindrical portion from the wide parallel stream emitted by the cathode. Next, this portion is made to converge violently, with the result that it diverges rapidly after passing a minimum radius in the vicinity of the second, highly positive electrode. The divergent beam is then gradually slowed down and bent parallel to the axis by the combined effect of the third and fourth apertures. Finally, marginal portions of the beam are sliced off by the last two apertures.

The entire gun is immersed in the same homogeneous magnetic field which serves to maintain the desired cyclotron frequency in the radio-frequency portion of the tube. Theoretically, Brillouin flow could be obtained if all electrons started from a single point on the cathode. The small aperture in the first electrode approximates such a point source.

A typical 560-mc tube (see Fig. 10) uses a beam current of about 35 microamperes. Because the magnetic field is proportional to the center frequency, correspondingly higher or lower beam currents are used at 800 and 400 mc.

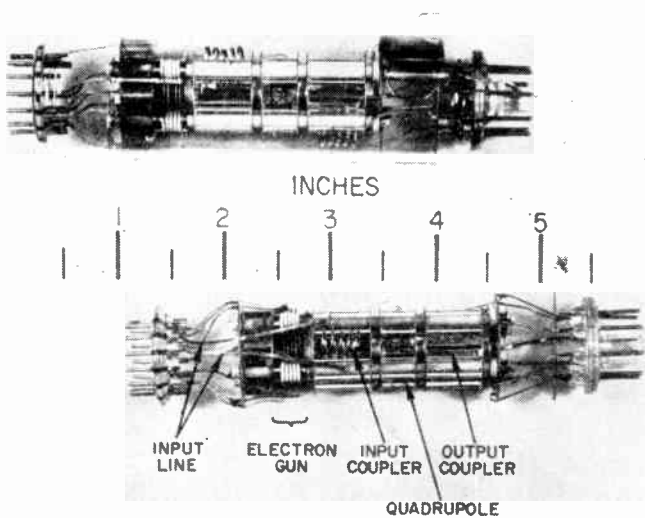


Fig. 10—Experimental quadrupole amplifiers, the lower one without glass envelope.

When a tube is operated without pump power, it acts as a unidirectional transmission device or isolator; input and output couplers behave like loaded tuned circuits and may, by adding external reactances, be broad-banded to provide essentially resistive terminations over a band equal to about 8 per cent of the center frequency (see Fig. 11). Unidirectional signal transmission over this band is essentially flat. In addition to the coupler losses mentioned previously, some loss occurs in the signal transmission along the beam; this is not yet understood. Total insertion loss for tubes built to date varies from 0.8 db to 2 db.

When pump power is applied, gain is obtained in proportion. The increase in output signal level is the same regardless of signal frequency. This is clearly illustrated in Fig. 12. The lowest curve represents signal transmission with the pump turned off; there is an insertion loss of about 1.5 db which gradually increases toward the edges of the band. Application of pump power simply lifts the entire curve by 17 and 31 db, respectively; the amplification process is not frequency dependent and thus adds no selectivity.

The impedances of input and output coupler are in no way affected by the application of pump power. This is of great practical value; to take full advantage of the possibility of absorbing the fast-wave noise in the input coupler, the signal source must be matched to the input impedance of the coupler. This match, once accomplished, remains correct, regardless of the gain for which the pump power is adjusted.

With perfect input match, one might assume that all the fast-wave noise could be extracted from the beam. The noise figure of the tube, measured with a wide-band noise generator, should then be equal to the input coupler loss of 0.2 to 0.5 db. Measured noise figures are not that good; 1.5 to 1.6 db is measured regularly on good tubes, and 1.4 db is measured occasionally. Allow-

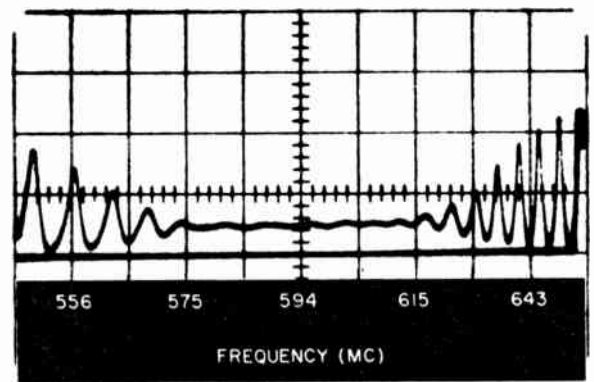


Fig. 11—Standing-wave ratio vs frequency at the input of a 600-mc quadrupole amplifier. Ordinate represents the square of the sum of incident and reflected voltage waves, measured at the sending end of a long 50-ohm line which is terminated at its receiving end by the input coupler.

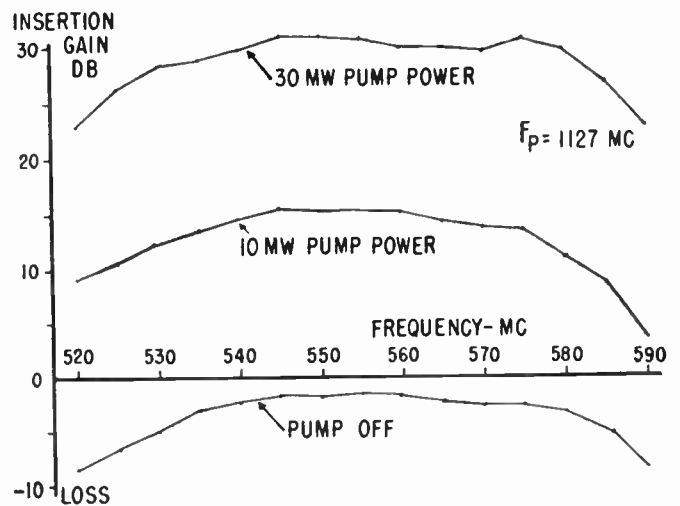


Fig. 12—Insertion gain of a 560-mc amplifier as a function of frequency, with pump power as a parameter.

ing for 0.4-db coupler loss, this leaves 1 db, or a noise temperature of about 70°K, unaccounted for. Similar to the signal loss along the beam mentioned previously, this is not yet understood.

Fig. 13 illustrates the behavior of the noise figure for an experimental tube with couplers tuned to 420 mc, broad-banded by appropriate coupling to tuned baluns outside the tube. The pump frequency was held at 840 mc and a receiver following the tube was tuned over the frequency range from 390 mc to 450 mc. Noise figures were determined by observing the power output from the receiver, with the input balun alternately connected to a 50-ohm resistance at room temperature and to a similar resistance immersed in liquid nitrogen.

In interpreting these noise figures, it is important to remember that we are dealing with a parametric amplifier which generates in its output two frequencies—signal and idler—for any given input signal frequency. Conversely, if the tube is followed by a receiver tuned to a given output signal frequency, there are two in-

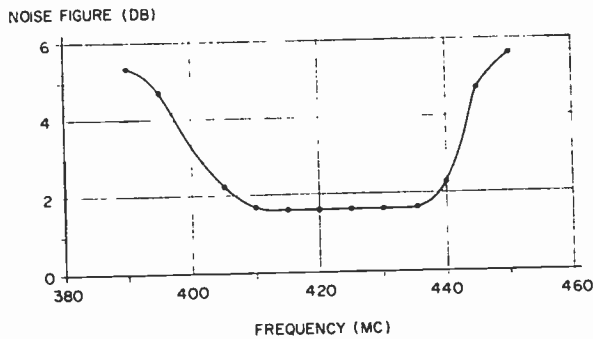


Fig. 13—Noise figure vs frequency for a 420-mc quadrupole amplifier.

put frequency channels—the signal channel and the idler channel—through which input noise may enter the receiver. Essentially, the parametric amplifier doubles the noise bandwidth of the receiver. This is observed as expected; in agreement with (14), receiver sensitivity on the two channels is essentially equal for tube gains higher than about 10 db. It is important to select the pump frequency so that the idler channel as well as the signal channel fall well within the pass band of the input coupler, allowing the beam noise on both channels to be absorbed by the signal source.

The noise figures quoted above were measured with noise generators broad enough to cover both signal and idler channels. They are valid without correction for applications which put both channels to use; radio astronomy is the best-known example. For use with single-channel signals, a correction must be made because of the noise generated in the idler channel. Where the idler and signal channels are substantially alike, as with the present quadrupole tubes, 3 db may be added to the broadband noise figure to obtain a single-channel noise figure. For example, 1.4 db would be increased to 4.4 db.

However, the performance of the amplifier under actual operating conditions can be much better than is suggested by such a noise figure. Most of the idler noise originates outside the tube; its magnitude, therefore, depends primarily on the temperature of the idler termination. Only when this termination is at room temperature will the performance be accurately indicated by the above single-channel noise figure. For the interesting case of an antenna having an equivalent source temperature of 100°K, the single-channel performance of the same amplifier (broad band $NF=1.4$ db) is equivalent to that of a conventional receiver whose noise figure is 3.24 db. With an antenna of only 50°K, the idler noise is reduced further and the single-channel performance becomes equal to that of a conventional receiver having a noise figure of only 2.86 db.

CONCLUSION

Low-noise electron beam parametric amplifiers employ a combination of two separate concepts. The first of these involves the use of the fast wave to carry signals along the beam. This makes possible the interchange of signal and noise in the input coupler, but it also prevents amplification by conventional methods which draw upon the dc energy of the beam. The second concept calls for the use of a nonhomogeneous alternating field to enhance the signal-induced motion of the electrons while they travel from input to output coupler.

In the quadrupole amplifier, we have selected the transverse cyclotron wave in preference to other types of electron waves. By choosing a cyclotron frequency close to the signal frequency, we obtain a fast cyclotron wave of nearly infinite phase velocity. This permits the use of lumped input and output couplers which are simple to build and easy to match. The quadrupole arrangement is specially suited for pumping the transverse cyclotron wave; again, because of the high phase velocity, a lumped quadrupole structure suffices.

Interaction between beam and metallic circuit, in the sense which this term has acquired in the traveling wave tube art, takes place only in the couplers. The growth process in the quadrupole is of a different nature: Here we have unilateral action of the pumping field on the moving electrons. The gain is calculated by tracing the path of individual electrons as they travel through the quadrupole, then averaging the over-all possible conditions of relative phase. Currents induced in the quadrupole by the moving electrons are of no significance.

The computation shows that high gain is easily obtained. Experimental tubes bear this out; they also demonstrate remarkably low noise, together with broad bandwidth and unconditional stability regardless of gain. They exhibit the idler frequency phenomenon characteristic of parametric devices.

The near-infinite phase velocity employed in these tubes represents a special case within a more general class of devices. Other tubes may be designed in which signal frequency and cyclotron frequency are quite different from each other, so that the phase velocity of the fast cyclotron wave is finite. Input and output couplers must then be adapted to this finite velocity. In most respects, such tubes will be quite similar to those described above.

It also appears possible to modify the geometry of the quadrupole in several different ways so as to permit the use of pump frequencies either lower or higher than twice the cyclotron frequency. A discussion of these variations would transcend the scope of this paper.

Generation of Harmonics and Subharmonics at Microwave Frequencies with P - N Junction Diodes*

D. LEENOV† AND A. UHLIR, JR.‡, ASSOCIATE MEMBER, IRE

Summary—The performances of a nonlinear resistance and a nonlinear capacitance in a broadband harmonic generator circuit are analyzed. The nonlinear capacitance is shown to have a considerably higher efficiency. Some results of harmonic and subharmonic generation experiments with a graded-junction silicon nonlinear capacitance diode are given.

INTRODUCTION

A SMALL, efficient harmonic generator has numerous applications at the present time. In connection with a transistor oscillator, it can be a source of microwave power; used with available generators it might generate significant power in the millimeter wave region. As another application, a harmonic generator can be used to multiply the output of a crystal stabilized oscillator to obtain a standard frequency in the microwave region. Similarly, a compact subharmonic generator operating at microwave frequencies would be desirable. It could be used to subdivide an atomic or molecular microwave resonant frequency to obtain a standard low frequency.

Semiconductor devices can perform both of these tasks and possess a number of advantages. They have small-size, low-power requirements, and ruggedness. Point-contact crystal rectifiers and welded-contact diodes have for some time been known to be effective harmonic generators. Studies of the efficiencies of these devices were reported upon in 1945–46 [1]. It was found that the welded contact diodes were superior to the rectifiers, up into the millimeter wave region, for generating the second or third harmonic. However, more recent work has shown that silicon point contact diodes are considerably better generators of high harmonics at millimeter and submillimeter frequencies [2], [3], [4].

Recently a diffused p - n junction silicon diode has been developed which acts as a voltage variable capacitance [5]. It has been named the “nonlinear capacitance diode.” Tests have shown that this device is an unusually efficient harmonic generator.

In this paper, the use of semiconductor diodes for frequency multiplication and division is discussed. The existing theory of harmonic generation, as related to these devices, is reviewed briefly, and the calculation of the harmonic generation efficiency for a broadband circuit is presented. Following this is a collection of ex-

perimental results obtained with the nonlinear capacitance diode.

REVIEW OF THEORY

In theoretical discussions of harmonic generation, two classes of nonlinear elements have been analyzed, nonlinear resistances and nonlinear reactances. The former group is exemplified by the point-contact rectifier, the latter by the recently developed nonlinear capacitance diode. The original welded-contact diodes developed and tested by H. North [1] were charge storage devices and hence behaved somewhat like nonlinear capacitors.

The theory of the nonlinear resistor as a frequency converter has been developed by C. H. Page [6] who gives an expression for the maximum harmonic generation efficiencies obtainable. His results are summarized in (1).

$$P_1 = P_0 + \sum_{n>1} P_n \geq \sum_{n>1} n^2 P_n \geq k^2 P_k \quad \text{for any } k. \quad (1)$$

Here P_n represents the power developed at the n th harmonic, and P_1 represents the amount of fundamental power converted to other frequencies. From this we obtain the relations (2), for any particular value of n .

$$P_n \leq \frac{1}{n^2} P_1 \quad (2a)$$

$$P_0 \geq (n^2 - 1)P_n. \quad (2b)$$

Eq. (2a) states that even if all the fundamental power is converted, the efficiency for generating n th the harmonic cannot exceed $1/n^2$ when all other harmonics are absent. Eq. (2b) states that when the equality holds, the remaining fundamental power is converted to dc. If there is no dc loss, there is no harmonic generation.

On the other hand, greater efficiency might be expected from a nonlinear device which does not rectify, and hence does not convert any input power to dc. In their theory of frequency conversion by nonlinear reactances, Manley and Rowe [7] show that a lossless nonlinear capacitance as a harmonic generator can convert up to 100 per cent of the available generator power into any single harmonic, with proper tuning.

Another result obtained by Page is that a nonlinear resistor cannot generate subharmonics [6]. On the other hand, the theory of Manley and Rowe predicts that a nonlinear capacitance will generate subharmonics. These authors give relations which specify the power

* Original manuscript received by the IRE, March 19, 1959. This manuscript is based in part on investigations supported by the U. S. Army Signal Corps on Contract DA-36-039-sc-73224.

† Bell Telephone Laboratories, Inc., Murray Hill, N. J.

‡ Microwave Associates, Burlington, Mass.; formerly with Bell Telephone Laboratories, Inc., Murray Hill, N. J.

converted by a nonlinear reactance into sideband frequencies, when the device is driven by a beat oscillator (frequency b) and a signal generator (frequency s). Let us consider the case that the upper sideband and all harmonic images are reactively terminated, so that power is transferred only at the beat oscillator frequency b , the signal frequency s , and the lower sideband frequency $b-s$. Then the Manley-Rowe equations reduce to (3a) and (3b).

$$\frac{P_{b-s}}{b-s} + \frac{P_b}{b} = 0 \tag{3a}$$

$$-\frac{P_{b-s}}{(b-s)} + \frac{P_s}{s} = 0. \tag{3b}$$

By combining (3a) and (3b) we obtain (4):

$$-P_b = P_s + P_{b-s}. \tag{4}$$

This indicates that pump power is converted into power at two lower frequencies, s and $b-s$. Thus, if the device is terminated by resonant circuits tuned to these frequencies, a signal s , for example, can be amplified; this process is the basis of the varactor amplifier. With less circuit damping, spontaneous oscillations may be set up. In particular, if $s=b/2$, then $s=b-s$, and one resonant termination tuned to one-half the pump frequency should be readily excited. The one-third harmonic could be obtained with a termination (or terminations) resonating at frequencies $\frac{1}{3}b$ and $\frac{2}{3}b$. An infinite number of such examples can be chosen, of course, involving pairs of frequencies whose sum equals b . However, one would expect locking in to occur most readily for the lowest orders of subharmonics (one-half or one-third) since these frequencies when generated undergo harmonic generation, and the second or third harmonics would excite other resonant terminations of the circuit.

BROADBAND ANALYSIS

In the previous section we discussed the theoretical upper limits of harmonic generation efficiency obtainable with nonlinear resistors and nonlinear capacitors. The superiority of the nonlinear capacitor was indicated. However, a better intuitive understanding of these nonlinear elements may be achieved through a study of broadband harmonic generation. This type of operation is analyzed in the present section.

A broadband harmonic generation circuit (resistive terminations at all frequencies) can be approximated experimentally and is not difficult to analyze. The efficiencies of a nonlinear resistor (N-R) and a nonlinear capacitor (N-C) are calculated below for this type of operation.

A further simplification is contained in the analysis. By way of explanation, we shall briefly discuss the way in which harmonic power depends upon fundamental power. In the range of very small applied voltages, the harmonic output increases faster than the first power of the fundamental input. With increasing input, the out-

put climbs more slowly and eventually becomes proportional to the input. It is this limiting output efficiency, expressed as a conversion loss, that is calculated.

In the large voltage limit assumed for this calculation, the diodes are approximately ideal. The N-R diode is nearly a perfect rectifier, with an I-V characteristic given by Fig. 1. The N-C diode may be approximated by a device with infinite capacitance under forward bias, with complete recovery of charge when the voltage drops to zero, and with zero capacitance under reverse bias. The corresponding Q-V characteristic is also represented by Fig. 1. The equivalent circuit for broadband harmonic generation with an N-R diode or an N-C diode is shown in Fig. 2. The resulting current vs time relations, for the diodes under reverse bias, are illustrated in Fig. 3(a) and (b).

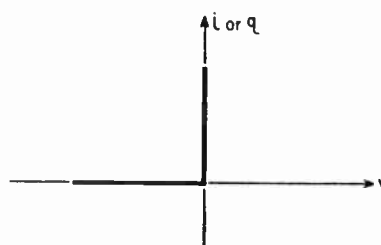


Fig. 1—Characteristic of ideal diodes.

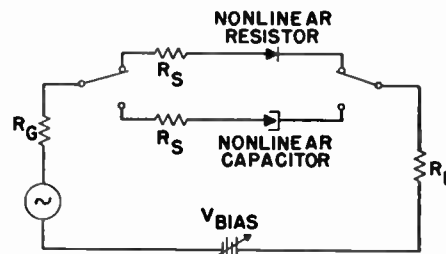
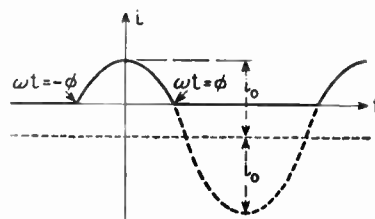
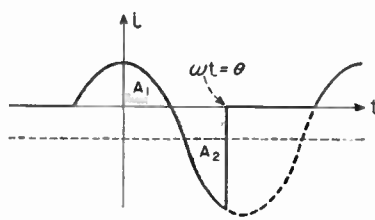


Fig. 2—Equivalent circuit of broadband harmonic generator.



(a)



(b)

Fig. 3—Current vs time curves for ideal diodes; (a) nonlinear resistor, (b) nonlinear capacitor.

Fig. 3(a) is the well-known rectifier characteristic. The dotted curve represents the current which would flow if the diode were absent; the displacement of the horizontal dotted line from the time axis is the effect of the reverse bias.

Fig. 3(b) represents the behavior of an ideal nonlinear capacitor. When the net applied voltage is in the forward direction, the device has a very large capacitance; hence negligible impedance, and the magnitude of the current is determined by the remaining circuit impedances. When the applied voltage is reversed, all of the charge which was stored during the forward part of the cycle is recovered; graphically this means that the area $A_2 = A_1$. At $\omega t = \theta$, the current drops discontinuously to zero. This discontinuity causes the curve in Fig. 3(b) to be richer in harmonics than that in Fig. 3(a).

The harmonic generation efficiencies are obtained from the Fourier amplitudes of the current vs time curves. The power absorbed by the load at a particular harmonic is readily calculated from the corresponding Fourier amplitude of current. The efficiencies are expressed as conversion losses, defined by (5).

$$L_n = 10 \log \frac{\text{available power from generator}}{\text{power output in } n\text{th harmonic}} \text{ (decibels).} \quad (5)$$

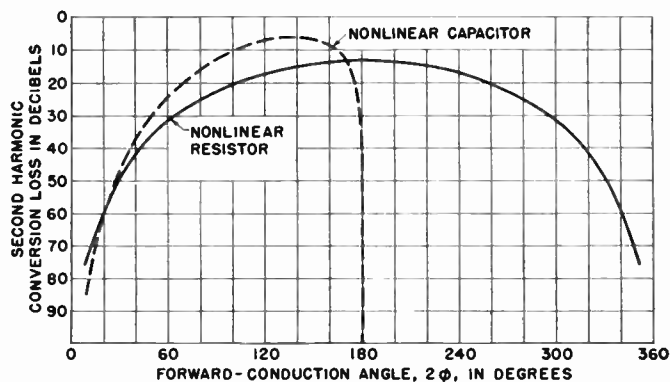
The conversion losses have been obtained as functions of bias voltage for a number of harmonics. Details of the calculation are given in the Appendix. In Fig. 4 several curves are presented of L_n vs the forward conduction angle, 2ϕ . This quantity is related to the bias voltage V_b by the equation $V_b = -V_0 \cos \phi$, where V_0 is the peak generator voltage.

In Fig. 4 we see that each curve for the nonlinear resistor has several peaks. Note that on these graphs the coordinate L_n increases in the downward direction. Thus the peaks represent maximum values of output, corresponding to minimum values of L_n .

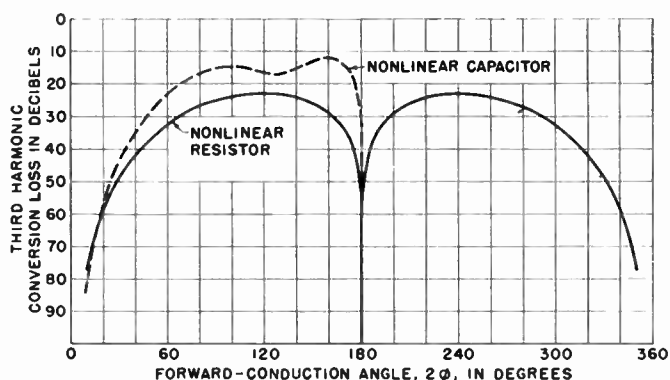
We see that in every case the number of relative minima of L_n is equal to $n - 1$. In the Appendix this relation is proved analytically for all n . There it is shown that minimum values of L_n occur for $\phi = s\pi/n$, where s is any integer such that $1 \leq s \leq n - 1$. We note that the first of these minima occurs when the forward conduction angle $2\phi = 2\pi/n$. This means a relative maximum in output occurs when the duration of the forward current equals the period of the harmonic, an effect which would be expected intuitively.

In the case of the nonlinear capacitor, each curve also possesses $n - 1$ humps (not necessarily maxima), but no general proof for such a relation has been developed because the expressions for L_n have not been obtained in closed form.

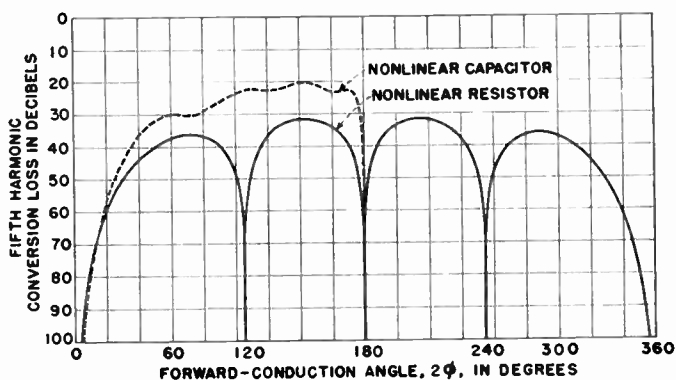
When diodes are operated so as to approximate the ideal behavior assumed above, the relation between the number of humps and the harmonic should provide a convenient means for identifying a particular harmon-



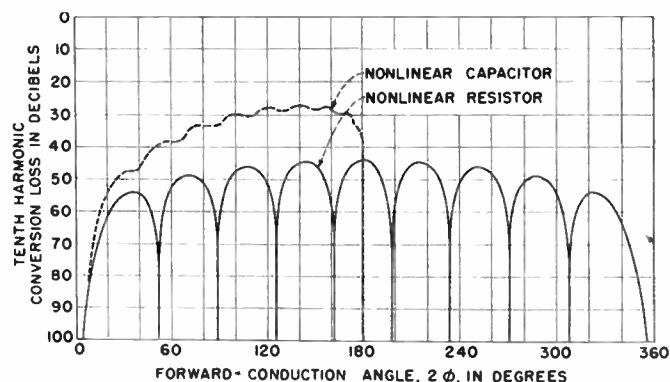
(a)



(b)



(c)



(d)

Fig. 4—Harmonic conversion loss vs forward-conduction angle for broadband operation.

ic, obtained from a broadband circuit and filtered from the rest of the output. The identification of the harmonic can then be obtained from an oscilloscope presentation of rectified power output vs bias voltage, when the latter is swept over an adequate range at a low frequency.

The minimum conversion loss for each harmonic is also of considerable interest. Values are given in Table I for a number of harmonics. (As noted previously, these results apply only in the limit of high drive.) To compare the N-C diode with the N-R diode, the difference between the corresponding conversion losses, expressed in db, is given for each harmonic in the column labeled "Advantage of N-C over N-R." The advantage in efficiency obtainable with an N-C diode is seen to increase for the higher harmonics.

The calculation of efficiencies discussed above applies only to ideal nonlinear elements. The parasitics of real diodes will cause their efficiencies to be diminished. A preliminary analysis for broadband operation has shown that the parasitics of the N-C diode should cause the efficiency to drop off rapidly as the output approaches a certain "cut-off" frequency f_c , where

$$f_c = \frac{1}{2\pi R_s C_{min}}$$

(Here R_s is the diode series resistance, assumed constant, and C_{min} is the smallest capacitance attainable, limited by the value of the breakdown voltage.) The cutoff effect is expected to become significant for output frequencies $f \cong 1/10 f_c$, and to become large for $f \cong f_c$.

DESCRIPTION OF EXPERIMENTS

The silicon nonlinear capacitance diodes have been used to generate harmonics in broadband and tuned circuits, and also to generate the one-half harmonic. Representative results are given in Table II.

The broadband circuit used is shown in Fig. 5. The attenuators provide resistive terminations in conformity with the equivalent circuit in Fig. 2. The efficiencies at the second and third harmonics have been measured. On referring to the theoretical values for broadband (Table I), we see that the experimental values (Table II) were better than predicted for the ideal nonlinear resistor, but not nearly as high as predicted for the ideal nonlinear capacitor. This may have been due to the fact that wave shapes were not as sharp as in the ideal case. Deviations from the predicted values may also have been caused by circuit inductance and unaccounted losses. No power measurements were attempted in the experiments of multiplying 35 mnc, but the harmonic was identified from the shape of an oscilloscope trace of output power vs bias (see section on Broadband Analysis). It is also noteworthy that the trace obtained for the third harmonic was distinctly unsymmetrical. Thus its shape resembled the curve calculated for the nonlinear capacitor [Fig. 4(b)].

TABLE I
LIMITING CONVERSION LOSSES FOR IDEAL DIODES

$$\left[\text{Minimum } L_n - 10 \log \frac{R_a + R_s}{R_a} \right]$$

Harmonic	N-R Diode (db)	N-C Diode (db)	Advantage of N-C over N-R Diode (db)
2	13.5	9.2	4.3
3	23.2	15.1	8.1
4	27.5	18.5	9.0
5	32.0	20.4	11.6
6	34.7	22.6	12.1
7	37.7	24.2	13.5
8	39.9	25.7	14.2
9	41.9	26.4	15.5
10	43.8	27.3	16.5
100	83.9	47.9	36.0

TABLE II

Fundamental Frequency (mc)	Harmonic or Subharmonic Frequency (mc)	Conversion Loss (db)	Kind of Terminations
320	960	4.0	Tuned [8]
324	19,000	35	Tuned [9]
900	10,200	22.5	Tuned [9]
35,000	70,000	—	Broadband
35,000	105,000	—	Broadband
400	800	11	Broadband
300	900	19.7	Broadband
700	350	6	Tuned [10]

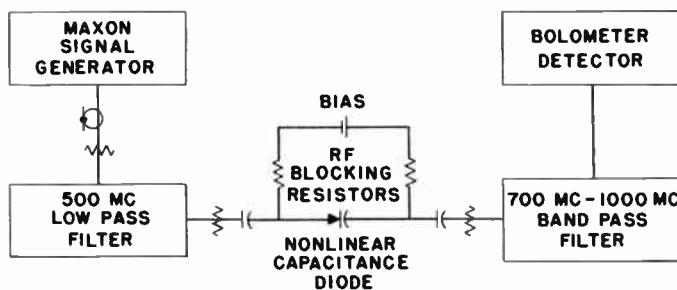


Fig. 5—Broadband harmonic generator.

The experiments performed under tuned conditions used either circuits similar to that in Fig. 5 with tuning elements replacing the pads, or resonant cavities tuned to the desired harmonic frequency. Unusually high harmonic yields were obtained in some of these experiments, exceeding the outputs to be expected from an ideal nonlinear capacitor in broadband operation, or from a tuned nonlinear resistor.

The generation of one-half harmonic by the junction diode is further evidence that the device is functioning essentially as a nonlinear capacitor, since this effect is not to be expected with a nonlinear resistor.

CONCLUSION

Theory indicates that a pure nonlinear capacitance should be superior to a nonlinear resistance for harmonic generation, when the characteristics of the two devices have the same degree of nonlinearity. It appears that

the welded contact diodes of North [1] were superior for generating low harmonics because of their nonlinear capacitance action. The recently developed diffused silicon diodes have been found to be quite efficient harmonic generators for obtaining frequencies up into the microwave region. This performance is due to their high "Q," or otherwise stated, their high "cut-off" frequency. Aside from their higher efficiency, the nonlinear capacitance diodes have a further advantage over point-contact rectifiers, in their greater power-handling capability and ruggedness.

At millimeter wave frequencies, the nonlinear capacitance diode harmonic generator, despite reduced efficiency, should still be superior to other sources of power. This is because the diode can be driven by a *K*-band klystron supplying considerable power at the fundamental frequency. The efficiencies obtained will be considerably smaller than predicted by the ideal theory, for two reasons: first, due to the cutoff effect described above; second, because the capacitance of the diode may be frequency dependent.

APPENDIX

CALCULATION OF CONVERSION LOSS

The conversion loss has been defined by

$$L_n = 10 \log \frac{\text{available power from generator}}{\text{power output in } n\text{th harmonic}} \text{ (in db).} \quad (5)$$

The available input power is defined as

$$P_{in} = \frac{V^2}{8R_G} \quad (6)$$

where *V* is the peak generator voltage. The output power is given by (7).

$$P_{out} = \frac{1}{2} \frac{V^2}{(R_G + R_L + R_S)^2} (g_n^2 + h_n^2) R_L. \quad (7)$$

Here *g_n* and *h_n* are, respectively, the coefficients of $\cos n\omega t$ and $\sin n\omega t$ in the Fourier expansion of the current waves in Fig. 3, assuming the dotted curves to be sine waves of unit amplitude. The actual amplitudes of the dotted curves are $V/(R_G + R_L + R_S)$.

On substituting (6) and (7) into (5), we obtain

$$L_n = 10 \log \frac{(R_G + R_L + R_S)^2}{4R_G R_L (g_n^2 + h_n^2)} \text{ (in db).} \quad (8)$$

We shall assume a matched load, $R_L = R_G + R_S$. For this case

$$L_n = 10 \log \frac{R_G + R_S}{R_G} - 10 \log (g_n^2 + h_n^2) \text{ (in db).} \quad (9)$$

To calculate *L_n* for the nonlinear resistor we refer to the current waveform in Fig. 3(a). We note that the current, being an even function of time, is representable by a cosine series. Then only *g_n* appears in (7), (8), and (9). For the case that the dotted sine wave has unit

amplitude, the current is given by (10) for the interval $-\pi < \omega t < \pi$.

$$\begin{aligned} i &= \cos \omega t - \cos \phi & -\phi < \omega t < \phi \\ i &= 0 & |\omega t| > \phi. \end{aligned} \quad (10)$$

The *n*th harmonic of this wave, *g_n*, is given by (11).

$$g_n = \frac{1}{\pi} \left[\frac{\sin (n-1)\phi}{n(n-1)} - \frac{\sin (n+1)\phi}{n(n+1)} \right]. \quad (11)$$

The curves of *L_n* vs 2ϕ , plotted in Fig. 4, were calculated by substituting (11) into (9).

Using (11) it is possible to calculate the values of ϕ given relative maximum values of $|g_n|$, and hence maximum harmonic power output. These determine the relative minima of *L_n*, which are the peaks of the curves in Fig. 4. By differentiation, we find the condition for maximum $|g_n|$ to be given by (12):

$$\sin n\phi \sin \phi = 0$$

or

$$\phi = \frac{s\pi}{n} \quad (12)$$

where *s* is any integer such that $1 \leq s \leq n-1$. Hence the function *L_n*(ϕ) should have *n*-1 minima in the range $0 < \phi < \pi$. As plotted in Fig. 4 these minimum values of *L_n* appear as peaks, to show that they correspond to maximum values of output.

The maximum values of $|g_n|$, obtained from (12), are given by (13). The one over-all

$$|(g_n)|_{max} = \frac{2}{\pi} \frac{\sin (s\pi/n)}{n^2 - 1} \quad (13)$$

maximum will occur when *s/n* approaches $\frac{1}{2}$: hence at $s = n/2$, *n* even; $s = (n-1)/2$ and $s = (n+1)/2$, *n* odd. From these, the minimum values of *L_n* are obtained, given by (14).

$$\begin{aligned} (L_n)_{min} &= 10 \log \frac{R_G + R_S}{R_G} \\ &\quad - 20 \log \frac{2}{\pi} \frac{\sin [(n-1)\pi/2n]}{n^2 - 1} \text{ (db) } [n \text{ odd}] \\ (L_n)_{min} &= 10 \log \frac{R_G + R_S}{R_G} \\ &\quad - 20 \log \frac{2}{\pi(n^2 - 1)} \text{ (db) } [n \text{ even}]. \end{aligned} \quad (14)$$

Values of $(L_n)_{min}$ for several values of *n*, calculated from (14), are given in Table I.

The nonlinear capacitor current waveform is represented by Fig. 3(b). The equation for this current (again assuming unit amplitude for the dotted curve) is given by (15), for the interval $0 < \omega t < 2\pi$.

$$\begin{aligned} i &= \cos \omega t - \cos \phi & 0 < \omega t < \theta \\ i &= 0 & \theta < \omega t < 2\pi - \phi \\ i &= \cos \omega t - \cos \phi & 2\pi - \phi < \omega t < 2\pi. \end{aligned} \quad (15)$$

The angle θ is determined in accordance with the assumption that the charge stored by the nonlinear capacitance during the interval of forward current, $-\phi < \omega t < \phi$, is completely recovered during the interval of reverse current, $\phi < \omega t < \theta$. This condition is expressed in (16) where

$$\int_{\omega t = -\phi}^{\omega t = \phi} i dt = - \int_{\omega t = \phi}^{\omega t = \theta} i dt \quad (16)$$

which is equivalent to (17).

$$\int_{-\phi}^{\theta} (\cos x - \cos \phi) dx = 0 \quad (17)$$

or

$$\sin \theta + \sin \phi - (\theta + \phi) \cos \phi = 0.$$

Solution of this transcendental equation gives values of θ corresponding to specified values of ϕ .

Having obtained numerical values of θ , the Fourier coefficients of the expansion of (15) may be calculated. Expressions for these are given in (18).

$$g_n = \frac{1}{\pi} \left[\frac{\sin(n+1)x}{2(n+1)} + \frac{\sin(n-1)x}{2(n-1)} - \frac{\cos \phi}{n} \sin nx \right]_{-\phi}^{\theta}$$

$$h_n = \frac{1}{\pi} \left[-\frac{\cos(n+1)x}{2(n+1)} - \frac{\cos(n-1)x}{2(n-1)} + \frac{\cos \phi}{n} \cos nx \right]_{-\phi}^{\theta} \quad (18)$$

Values of L_n as a function of ϕ are obtained by substituting the results of (18) into (9). Since θ is the solution of a transcendental equation, L_n is not expressed

in closed form, and no analytic expressions for $(L_n)_{\min}$ are available. Therefore the minimum conversion losses given in Table I were obtained directly from the numerical results.

The numerical solutions for the nonlinear capacitor are readily obtained with an electronic computer. All the calculations described above were performed on the IBM 650 Magnetic Drum Calculator.

ACKNOWLEDGMENT

We wish to thank the several authors for permission to quote their measurements prior to publication.

REFERENCES

- [1] H. C. Torrey and C. A. Whitmer, "Crystal Rectifiers," ch. 13, pp. 398-416, McGraw-Hill Book Co., Inc., New York, N. Y.; 1948.
- [2] W. C. King and W. Gordy, "One to two millimeter wave spectroscopy. I," *Phys. Rev.*, vol. 90, pp. 319-320; April, 1953.
- [3] C. A. Burrus and W. Gordy, "Submillimeter wave spectroscopy," *Phys. Rev.*, vol. 93, pp. 897-898; February, 1954.
- [4] M. Cowan and W. Gordy, "Further extension of microwave spectroscopy in the submillimeter wave region," *Phys. Rev.*, vol. 104, pp. 551-552; October, 1956.
- [5] A. Uhler, Jr., "The potential of semiconductors in high frequency communications," *PROC. IRE*, vol. 46, pp. 1099-1115; June, 1958.
- [6] C. H. Page, "Frequency conversion with positive nonlinear resistors," *J. Res. NBS*, vol. 56, pp. 179-182; April, 1956.
- [7] J. M. Manley and H. E. Rowe, "Some general properties of nonlinear elements—I," *PROC. IRE*, vol. 44, pp. 904-913; July, 1956.
- [8] L. R. Malling, private communication.
- [9] W. G. Matthei, private communication.
- [10] R. S. Englebrect, private communication.
- [11] S. Kita, "A harmonic generator by use of the nonlinear capacitance of germanium diode," *PROC. IRE*, vol. 46, p. 1307; June, 1958.
- [12] K. K. N. Chang, "Harmonic generation with nonlinear reactances," *RCA Rev.*, vol. 19, pp. 455-464; September, 1958.

Comparison and Evaluation of Cesium Atomic Beam Frequency Standards*

J. HOLLOWAY†, W. MAINBERGER†, MEMBER, IRE, F. H. REDER‡, MEMBER, IRE, G. M. R. WINKLER‡, L. ESSEN§, AND J. V. L. PARRY§

Summary—Cesium atomic beam frequency standards of different design have been compared, and the principal sources of errors in these devices have been studied. The unresolved discrepancy found between the standards was about 2 parts in 10^{10} . The characteristics of the standard, sources of errors, and the details of the comparison tests are discussed in this paper.

INTRODUCTION

FOR many years the most accurate of all physical measurements has been that of frequency, and its practical applications have kept pace with the technique. Atomic standards have provided a major advance in the reproducibility and stability of frequency references, so that it has become important to examine their performance critically.

Investigation [1] of an atomic beam standard at the National Physical Laboratory (NPL), Teddington, England, led to the conclusion that it could be used to calibrate¹ quartz oscillators in terms of the natural resonance frequency of cesium (at zero magnetic field) to 1 part in 10^{10} . Similar work at the National Company, Malden, Mass., established that their atomic beam standards, which are called Atomichrons[®], agreed with one another to 3 in 10^{10} .

The two atomic beam standards were compared by means of transatlantic radio transmissions. The frequencies of the phase-stable transmissions from MSF (60 kc) and GBR (16 kc), Rugby, England, were measured at Teddington in terms of the NPL standard, and at Harvard by J. A. Pierce in terms of a local quartz oscillator, which in turn was compared by means of another stable transmission with an Atomichron in Camden, N. Y. [2]. The comparisons indicated that there was probably an average systematic difference (NPL-Atomichron) = 4 parts in 10^{10} . Other comparisons of time signals related to the two standards, made by Dr. William Markowitz of the Naval Observatory, indicated a larger discrepancy. It clearly became important,

therefore, to make a more direct comparison. This was emphasized by both the International Committee of Weights and Measures and the International Scientific Radio Union. The comparison, made since at Teddington, is described here. The results are given briefly in *Nature* [3].

PRINCIPLE OF OPERATION

Before the tests are described in detail, a brief review of the principle of operation of the atomic frequency standards is presented. As the name implies, the frequency produced or measured by an atomic standard is uniquely related to a time-invariant resonance of an atom—in this case to the magnetic field-insensitive resonance in cesium 133. The atomic beam tube is the device used to compare the frequency of an external RF generator with that of the cesium. Fig. 1 illustrates the atomic beam tube schematically. The tube functions in the following manner. A beam of neutral cesium atoms effuses from the source, with thermal velocities of about 200 meters/sec. An atom in the beam will proceed in a straight line until it is acted on by the inhomogeneous magnetic field of a deflecting magnet, or until it strikes and is absorbed by an obstacle or the walls of the beam tube. The pressure in the tube must be low enough so that scattering of the beam is negligible. The source, deflecting magnets, and detector are arranged so that only a certain class of the atoms emitted from the source may reach the detector. The atoms which reach the collector undergo a transition in the region between the deflecting magnets. The transition, which amounts physically to a rearrangement of the internal structure of the atom, will be induced only when the atom is irradiated with an RF signal having a frequency nearly equal to that of the atomic resonance. At other frequencies the RF signal has no effect.

If an atom undergoes a transition, it will be deflected in the second magnet so that it will follow the path to the collector, where it is converted to an ion and ultimately to an electric current. If the atom does not undergo a transition, it will follow the path which misses the collector. Hence, the presence of beam current at the detector indicates that transitions are induced, which in turn means that the frequency of the RF signal applied to the beam is very close to the atomic resonance frequency.

If the frequency of the RF generator is swept slowly through the resonance frequency, and the detector beam

* Original manuscript received by the IRE, March 5, 1959; revised manuscript received June 16, 1959.

† National Company, Inc., Malden, Mass.

‡ Frequency Control Div., U. S. Army Signal Res. and Dev. Laboratories, Ft. Monmouth, N. J.

§ National Physical Lab., Teddington, Middlesex, England.

¹ The accuracy of the calibration procedure mentioned above merely expresses how well the ratio (the number of oscillations of a quartz oscillator in a given interval of time/number of oscillations made by a cesium atom over the same interval of time) is known. The accuracy to which the cesium resonance frequency is known in terms of the traditional astronomical standard of time does not enter here.

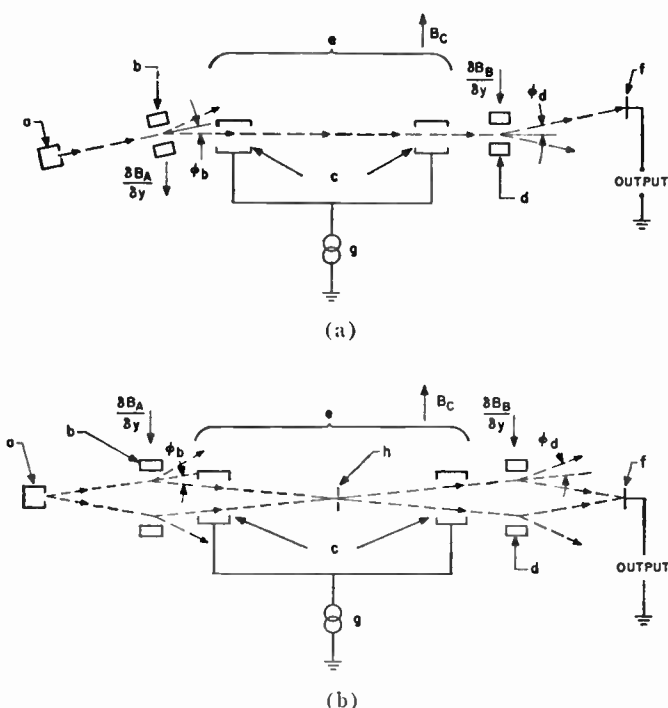


Fig. 1—Path of atoms through magnetic fields. (a) Atomichron. (b) NPL. The deflection angle is ϕ_d which in practice is very small, a typical value being 10^{-2} radian. a=source. b="A" magnet, strong inhomogeneous magnetic field; c=RF cavities; d="B" magnet, strong inhomogeneous field; e=weak dc field; f=ionizer collector; g=RF generator 9192 mc; h=slit.

current is plotted as a function of the generator frequency, the result will be as shown in Fig. 2(a), if a single RF cavity is used to irradiate the beam (the Rabi method), or as in Fig. 2(b), if two separated cavities are used (the Ramsey method). The center frequencies of both patterns will be equal to the atomic resonance frequency provided no distortions are present. The full width of the resonance between the points of half the maximum amplitude is 120 cps for the Atomichron and 330 cps for the NPL tube, and the nominal center frequency is 9192.631830 mc, the unit of time being the second of UT2 in June, 1955 [4]. The line width in cps is given approximately by $1/T$, where T is the time in seconds that an atom of average velocity spends in the space between the two cavities.

A complete exposition of the theory of the atomic beam tube, the cesium resonance, and the interaction between the RF fields and the atoms can be found in ref. [5].

PRINCIPAL DIFFERENCES IN CONSTRUCTION OF THE TWO STANDARDS

Beam Path

In the Atomichrons the detector is placed so that it is reached only by atoms which have been deflected in one direction [Fig. 1(a)], whereas in the NPL tube atoms in both parts of the beam are detected. This necessitates the use of a central slit [Fig. 1(b)].

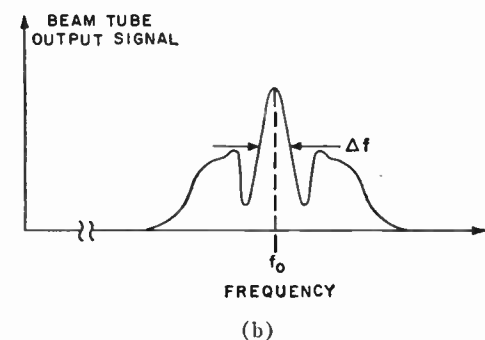
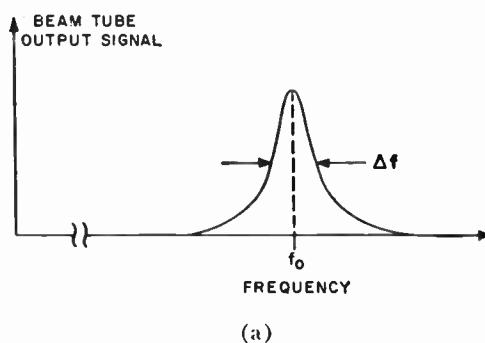


Fig. 2—Resonance curves; (a) Rabi method, (b) Ramsey method.

Beam Tube RF Structure

Both the NPL tube and the Atomichrons use the Ramsey method of separated cavities to stimulate the transitions, but the waveguide structures are of different design (Fig. 3). The ideal waveguide structure for use with the Ramsey method should have uniform oscillating fields of equal amplitude, which are in phase in the two regions where the beam is exposed to the RF. The structures of Fig. 3(a) and 3(c) can most closely approximate this ideal. The structure in Fig. 3(b), in addition to exposing the beam to the cavity fields, exposes it to that in the feed guides, where the maximum oscillating field amplitude is about one-fourth that in the cavities. An analysis of this structure has shown it to be satisfactory, provided the electrical lengths of the feed guides, the cavity tunings, and field distributions are correct.

Generation of the RF Signal

The NPL system generates the cesium resonance frequency by multiplying the frequency of a crystal oscillator which operates at a subharmonic of the cesium frequency in the neighborhood of 5 mc. In the Atomichron, the cesium frequency is generated from a crystal oscillator which runs at exactly 5 mc,² so that a considerable amount of synthesizing is required. As a result, the spectrum applied to the beam tube in the Atomichron is not as free of undesirable sidebands as the NPL system.

² As a matter of practical convenience, the cesium frequency at zero magnetic field has been defined to be 9192.631840 mc in the Atomichrons. The difference between this value and the value in use at NPL (ref. [4]) has been allowed for in the data processing.

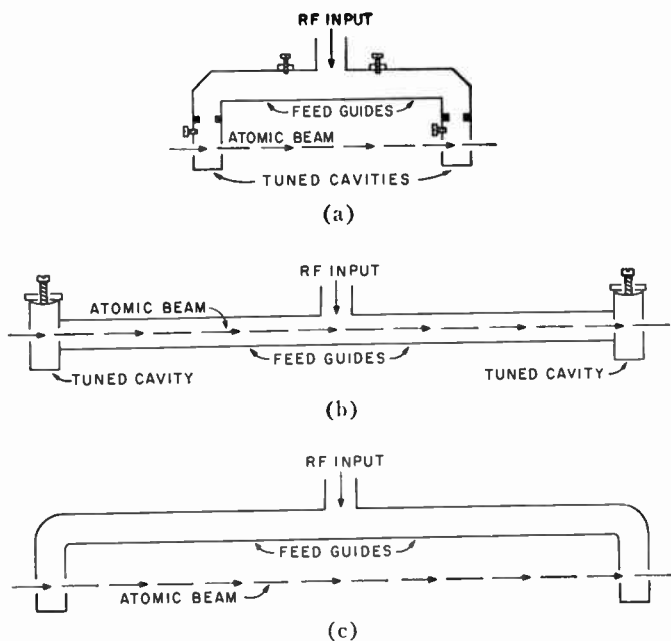


Fig. 3—(a) NPL RF section, (b) standard Atomichron RF section, (c) experimental Atomichron RF section.

Servo Control

There is no provision in the NPL system for locking the crystal oscillator to a subharmonic of the cesium frequency. The oscillator is tuned manually to study the resonance. Hence, the cesium tube is used as a resonator to calibrate a crystal standard. The Atomichron crystal oscillator is locked, through a servo system, to a frequency uniquely related to the cesium frequency. The system block diagrams are shown in Fig. 4.

FREQUENCY DISTORTIONS

The term "distortion" is used to describe anything which can cause the frequency of an atomic standard to be different from the atomic resonance frequency. The most important distortions are listed in the following paragraphs.

Magnetic Field

The frequency of the field-insensitive cesium transition is given by [5]

$$f = f_0 + 427 B^2 \tag{1}$$

where

- f_0 = frequency at zero field ($0.919263183 \times 10^{10}$ cps),
- B = magnetic field in gauss,
- f = cesium resonance frequency in cps at a field of B gauss.

For various reasons, it is not possible to operate at zero field. NPL operates at 0.043 gauss and the Atomichrons at 0.060 gauss. The standards are, therefore, offset from the zero field frequency by 0.77 and 1.54 cps respectively. Hence, the magnetic field in the transition region must be carefully measured and controlled if

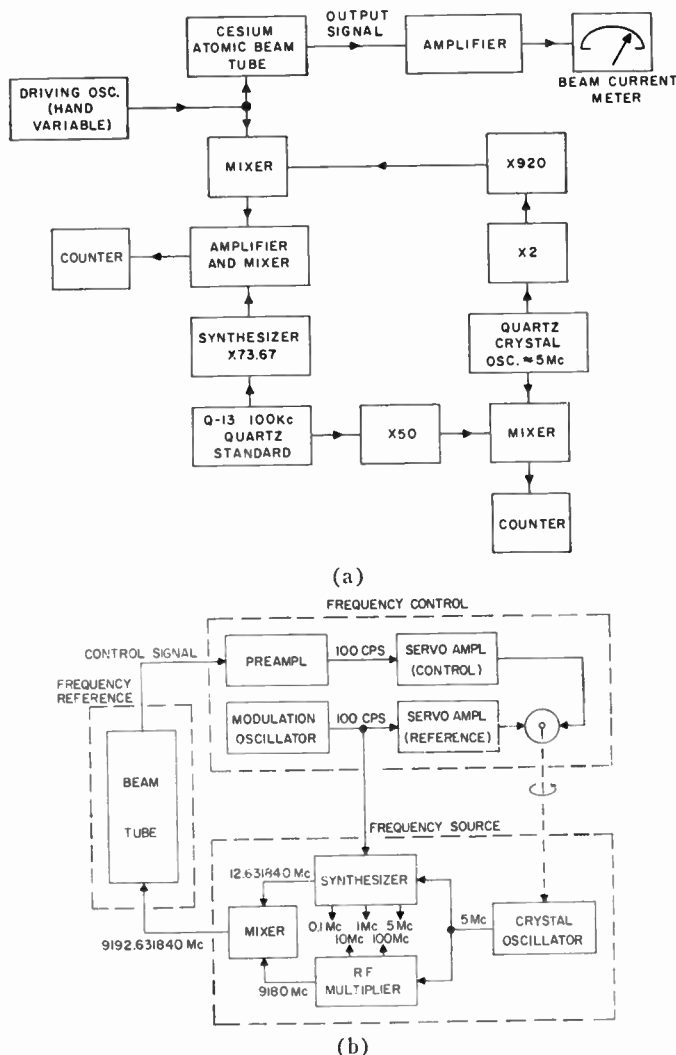


Fig. 4—(a) Block diagram of NPL system, (b) Atomichron block diagram.

accuracies exceeding 1 part in 10^9 are required. The field is measured by observation of a field-sensitive resonance in cesium, so that an accurate, internally consistent field determination is achieved.

Relative Cavity Phase

In the separated-oscillating field technique employed, any lack of synchronism between the two oscillating fields will cause a distortion in the observed resonance. The shift in the frequency of the peak of the resonance is given by

$$\delta f_\phi = \frac{\delta\phi}{180} W \tag{2}$$

where

- δf_ϕ = shift of peak frequency in cps,
- $\delta\phi$ = phase shift between oscillating fields in degrees,
- W = width of the resonance at half maximum amplitude in cps.

The presence of a phase shift can be detected by observation of the symmetry of the resonance curve; perfect symmetry is obtained only when the phase shift is

zero. The amount of asymmetry caused by a given phase shift depends on the velocity distribution of the beam which reaches the detector; this distribution is in general substantially different from the beam-velocity distribution directly in front of the source. A calculation of asymmetry as a function of phase shift was made through the use of a velocity distribution calculated for the Atomichron at the detector. The equation relating asymmetry to phase shift is [6]

$$\delta\phi = 3.2S \tag{3}$$

(Require $SS < 2\%$ for applicability of Eq. 3)

where

$\delta\phi$ = phase shift in degrees,

S = percentage asymmetry, as defined from Fig. 5.

Through the combined use of (2) and (3), the frequency error arising from cavity phase shifts can be estimated from the characteristics of the observed resonance. Unfortunately, cavity phase shifts are not the only source of asymmetry in the curve. Thus, in order to measure the cavity phase-shift effect through the symmetry measurement, one must have the guarantee that there are no other sources of distortion in the system. This is not entirely possible with the standard Atomichron RF structure [see Fig. 3(b)], because some of the RF fields between the cavities can conceivably contribute to an asymmetry. In this paper the slight asymmetry found to be present is treated as if it had arisen solely from cavity phase shift, and an appropriate correction is applied.

Another approximation made in the application of this correction is that the beam-velocity distribution is assumed to be the calculated one. There is also a mathematical effect where a modulated signal is used to study the resonance curve. In this case the resonance frequency is determined by the criterion that the amplitude of the fundamental component of the output signal equals zero. When the curve is asymmetrical, this does not result in the same determination of the resonance frequency as given by the peak of the dc curve obtained with a nonmodulated RF signal. A calculation indicates that the shift of the zero crossing (modulated case) is roughly two-thirds the shift of the peak of the dc curve. The estimated accuracy of the correction is included in later tables containing the experimental results.

RF Sidebands

Any sidebands not symmetrical about the cesium frequency will cause a frequency shift.

This problem has not been completely analyzed. Therefore, experimental measurements have been made on both the NPL tube and the Atomichron. The NPL results are reported in ref. [1].

In these experiments a single sideband of controlled amplitude and frequency was added to the RF signal

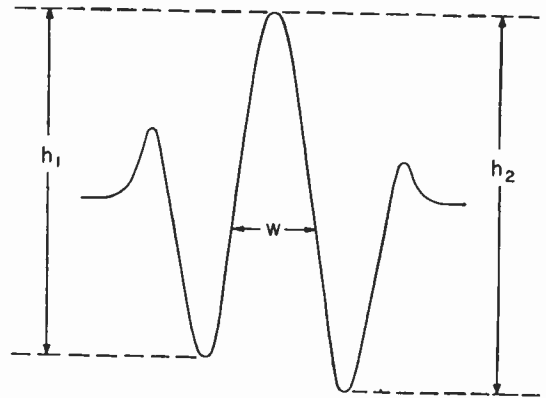


Fig. 5—Asymmetric resonance due to cavity phase error.

$$S = \frac{h_2 - h_1}{\frac{1}{2}(h_2 + h_1)} \times 100$$

$$\delta\phi = 3.2S \text{ (Degrees)}$$

$$\delta f_\phi = \frac{\delta\phi}{180} W$$

driving the beam tube. The results on an Atomichron for a sideband with a frequency (f_s) 200 kc away from the cesium frequency (f_0) obey an equation of the form:

$$f_r - f_0 = \frac{\alpha(P_s/P_0)}{f_0 - f_s} \tag{4}$$

where

f_r is the observed resonance frequency, and α is a constant equal to 1.5×10^4 (cps)²,

P_s/P_0 = ratio of sideband power to optimum power at f_0 .

When the sideband is in the frequency range of the neighboring transitions, the frequency shifts do not obey such a simple equation and must be plotted experimentally.

Distortions Arising from Frequency Modulation of the RF

This class of distortions is associated only with the Atomichron, since the NPL system does not use frequency modulation. There are two results of interest. The first is that the use of FM does not in itself introduce any symmetry distortion. However, if there is second-harmonic distortion on the FM, there may be an attendant frequency shift. The shift, which has been calculated for a single velocity beam, is given by

$$f_r - f_0 \approx \left[0.45 \sin \phi \cos \left(\frac{\omega_m T}{2} \right) \right] HW \tag{5a}$$

when the RF signal is in the form

$$E_{RF} = \cos \{ \omega t - K [\cos \omega_m t + H \cos (2\omega_m t + \phi)] \}. \tag{5b}$$

It is assumed that K is adjusted to its normal operating value. In the above equations the notation is:

- 100 H = percentage 2nd harmonic distortion on the modulation,
- ω_m = modulation frequency,
- T = time atom spends between RF cavities,
- W = full width of resonance at half max. amplitude (cps),
- ϕ = angle between first and second harmonic modulation.

From (5a) it is evident that, in any case:

$$|f_r - f_0| < 0.45HW. \tag{5c}$$

When a second harmonic distortion of controlled amplitude and phase was injected into an Atomichron, the maximum frequency shift observed was about half that given by the right-hand side of (5c). The dependence of the shift on $\sin \phi$ was verified.

There are probably other sources of distortion, but it is believed that those listed above are the major ones.

DETAILS OF TEST CARRIED OUT AT NPL

Standard Comparison Procedure

The tests carried out at NPL may be divided into two classes—those which compared the Atomichrons under standard operating conditions with the NPL system and those which sought to measure the sources of difference in the systems. The experimental arrangement for the first class of tests is shown in Fig. 6. It can be shown that

$$\frac{f_{c0} - f_{n0}}{f_{n0}} = \frac{f_m - 1160 - \delta_c + \delta_n + 0.18}{f_{n0}} \tag{6}$$

where

- f_{n0} = cesium zero field frequency as measured by the NPL system,
- f_{c0} = cesium zero field frequency as measured by an Atomichron,
- δ_n = offset from zero field frequency due to the magnetic field in the NPL system,

- δ_c = offset from zero field frequency due to the magnetic field in the Atomichrons,
- f_m = measured audio frequency,
- Δ = the deviation of the Q^{13} oscillator from nominal [taken as 2.5 parts in 10^8 in (6)].

The data obtained from the standard comparison tests are given in Table I. In this table the Atomichrons are identified by their serial numbers; the 857X1 experimental tube was used with the electronic system of the No. 111 Atomichron. For all the data of March 12 and thereafter, the Atomichrons underwent a basic alignment before comparison. This consisted of having the critical electronic controls misadjusted, then having different operators realign the system according to a standard procedure. This practice was intended to show up any frequency dependence due to system adjustment.

Distortion Measurements

The asymmetry of the resonance was measured on all the beam tubes, with the use of RF without modulation. The RF signal from the NPL electronics was studied and found to yield a very pure note at X band, and since any sideband effects should be negligible with only 5-mc sidebands, the NPL electronics was selected to drive all the beam tubes for the asymmetry measurements. It was assumed that any observed asymmetry was due to a beam-tube effect.

If a beam tube were to exhibit an asymmetrical resonance, it would be expected that the asymmetry would be a function of RF power and that the center of the resonance would shift with the RF power. This phenomenon is referred to as the power shift. With the use of nonmodulated RF, both the asymmetry and the resonance frequency were measured as a function of power. The results of these measurements are applied in Table II as corrections to the data from Table I. The power shift associated with asymmetric resonance curves is caused by the variation of the velocity distribution function with power.

Proceeding on the assumption that the NPL electronics were not causing any distortions, those performing the tests sought a measure of the distortions associated with the Atomichron RF signal and servo control. First, the normal closed-loop operating frequencies of the Atomichrons were compared with open loop frequencies, with NPL electronics driving the Atomichron beam tubes. The tubes ran consistently lower with the NPL electronics. This is referred to as the "electronic effect," and the measurement results are listed and applied as corrections in Table II. To complete the experiment, the NPL beam tube was driven, open loop and without modulation, with the electronics of the No. 117 Atomichron system. In this case, the NPL tube ran 0.8 part in 10^{10} higher than it did with its own electronics. This series of measurements was not sufficient to determine how much of the "electronic effect"

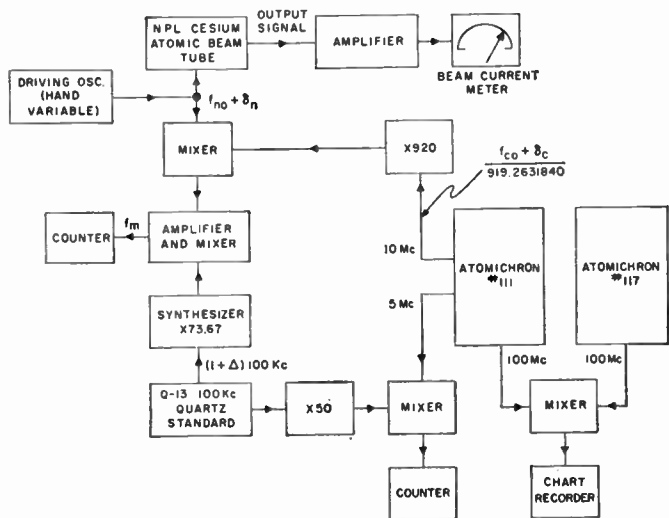


Fig. 6—Block diagram for frequency comparison tests.

in the Atomichrons was contributed by the various elements in the electronics; only the total effect was determined. Any attempt to isolate the effects is complicated by the fact that the resonance curve widths of the NPL system and Atomichron systems are different.

Discussion of Results

After the corrections inferred from the distortion measurements have been applied to the data of Table I, one would expect the corrected results to show the Atomichrons and NPL system to agree. The discrepancy in the corrected results is not well understood at present. It may be due partially to the approximate nature of the asymmetry correction.

While the comparisons were being carried out at NPL, the transatlantic frequency measurement programs, carried on by Prof. J. A. Pierce at Harvard and Dr. W. Markowitz at the U. S. Naval Observatory in collaboration with NRL, were active. The Atomichron at Harvard had been carefully measured against those which were shipped to NPL, just before they left. The

data accumulated should supply definitive information on the accuracy of transatlantic frequency measurements.

SUBSEQUENT MEASUREMENTS

J. V. L. Parry, one of the authors of this paper, has continued to make weekly basic alignments, measurements and comparison. The results are compiled in Table III. The limits given to the average values are slightly higher than those of Table I because of a small systematic change in the relative values of the Atomichrons and the NPL standard. Since the changes are little more than the standard deviation of a single observation, it is not possible to say definitely when they occurred, but the value of 111-NPL appears to have decreased gradually, whereas that of 117-NPL appears

TABLE I
FREQUENCY REPRODUCIBILITY AFTER REALIGNMENT
UNIT 1×10^{-10}

Date 1958	Frequency Difference			
	111-NPL	117-NPL	857X1-NPL	Q13-NPL
March 6	3.6	3.5		230.0
7	3.8	3.6		231.8
10		3.3		233.5
11		4.0		233.6
12		3.2	4.7	234.5
14		2.5	4.2	235.3
17	4.1	3.5		238.2
18 (A.M.)	3.7	3.7		239.4
18 (P.M.)	3.6	2.7		238.1
19 (A.M.)	4.3	3.3		240.2
19 (P.M.)	4.0	3.2		240.0
20 (A.M.)	3.9	3.1		240.7
20 (P.M.)	4.5			241.4
24 (A.M.)	3.5	3.4		244.7
24 (P.M.)	3.6	2.8		244.8
24 (P.M.)	3.8	3.3		245.5
26	3.4			244.1
28	3.2			245.8
April 1 (A.M.)	3.5	3.0		249.2
1 (P.M.)	3.7	2.9		247.6
2	3.5	3.2		250.7
Mean	3.7 ± 0.3	3.2 ± 0.4	4.5 ± 0.3	

TABLE II
BEAM TUBES TESTED AS RESONATORS
UNIT 1×10^{-11}

Effect	Frequency Error			
	111	117	857X1	NPL
Servo and electronics	$+8 \pm 4$	$+6 \pm 4$	$+20 \pm 4$	0
Asymmetry	-2 ± 9	-11 ± 9	0 ± 7	-10 ± 10

The measured errors due to the servo, electronics and asymmetry can legitimately be applied as corrections to the mean frequencies of Table I, and the corrected results of the comparison are as follows:

111-NPL	$2.1 \pm 1.4 \times 10^{-10}$
117-NPL	$2.7 \pm 1.4 \times 10^{-10}$
857X1-NPL	$1.5 \pm 1.4 \times 10^{-10}$

TABLE III
UNIT 1×10^{-10}

		Atomichron No. 111-NPL Standard	Atomichron No. 117-NPL Standard
April	8	3.6	3.0
	9	2.8	—
	14	1.8	2.4
	15	1.9	2.3
	28	1.7	2.1
May	5	4.1	3.4
	12	3.7	3.0
	19	3.0	3.1
	27	3.4	3.4
	29	3.9	3.7
June	2	3.5	3.0
	9	3.3	—
	16	3.2	—
	23	3.9	3.9
	27	3.5	3.5
July	1	3.3	3.4
	4	3.4	3.0
	7	3.4	3.0
	14	2.6	2.6
	15	3.5	3.5
	21	3.0	2.7
	25	3.0	2.9
August	11	2.2	2.5
	18	3.2	—
	26	3.7	—
	27 (A.M.)	3.5	2.8
	27 (P.M.)	3.0	—
	28 (A.M.)	2.0	2.5
	28 (P.M.)	2.0	2.5
September	1	2.5	3.0
	2 (A.M.)	2.0	3.1
	2 (P.M.)	2.5	3.5
	3 (A.M.)	2.6	3.7
	3 (P.M.)	1.7	2.7
	5 (A.M.)	2.5	4.2
	5 (P.M.)	2.7	—
	15	2.7	—
	22	2.0	—
	24	1.5	1.9
	29	1.7	—
October	30	0.2	—
November	3	-0.8	0.2
Mean of all results from March to November		3.1 ± 0.8	3.1 ± 0.5

to have changed rather suddenly in September, 1958. It might be mentioned that by November 18, 1958, the operational time of 111 was 1036 hours and that of 117 was 662 hours.

In August, 1958, changes were made to the NPL standard with the object of eliminating the asymmetry recorded in Table II. A new cavity system, shown in Fig. 7, was designed, with provision for the sensitive adjustment of the relative phases in the two cavities. The phase bridge arm was an odd number of half-wavelengths long and was adjusted to resonance at the cesium frequency. It was coupled to both cavities through very small holes, and the signal was observed at a detector in the middle. When the phases at *A* and *B* are equal there is a minimum signal, and the setting to the minimum was found to be extremely sharp.

The new system gave a symmetrical resonance, as nearly as could be judged experimentally, and for a time both the new and old systems were used to find a statistical value for the frequency difference. The value found

was -1.7×10^{-10} . Since August 26, 1958, only the new system has been used, but the values in Table III have been adjusted to correspond to the initial condition of the NPL standard.

Through the use of the mean values for the whole period of the comparisons, together with the new measured value of the asymmetry error of the NPL standard in place of that given in Table II, the following final results were achieved:

111-NPL	$0.8 \pm 1.5 \times 10^{-10}$
117-NPL	$1.9 \pm 1.5 \times 10^{-10}$

ACKNOWLEDGMENT

The work was carried out at the Natl. Phys. Lab. and the results are published by permission of the Director. The Atomichrons and support for the Natl. Co. effort in this program were made available by the U. S. Army Signal Res. and Dev. Lab. under contract number DA-36-039 SC-74863. The cooperation of all the agencies involved is gratefully acknowledged.

BIBLIOGRAPHY

- [1] L. Essen and J. V. L. Parry, "The caesium resonator as a standard of frequency and time," *Phil. Trans. Royal Soc. London, A*, vol. 250, pp. 45-69; August 8, 1957.
- [2] L. Essen, J. V. L. Parry, and J. A. Pierce, "Comparison of caesium resonators by transatlantic radio transmission," *Nature*, vol. 180, pp. 526-528; September 14, 1957.
- [3] L. Essen, J. V. L. Parry, J. H. Holloway, W. A. Mainberger, F. H. Reder and G. M. R. Winkler, "Comparison of caesium frequency standards of different construction," *Nature*, vol. 182, pp. 41-42; July 5, 1958.
- [4] L. Essen and J. V. L. Parry, "An atomic standard of frequency and time intervals" *Nature*, vol. 176, pp. 280-282; August, 1955.
- [5] N. F. Ramsey, "Molecular Beams," Oxford University Press, New York, N. Y., pp. 115-144; 1956.
- [6] C. W. Franklin, private communication.

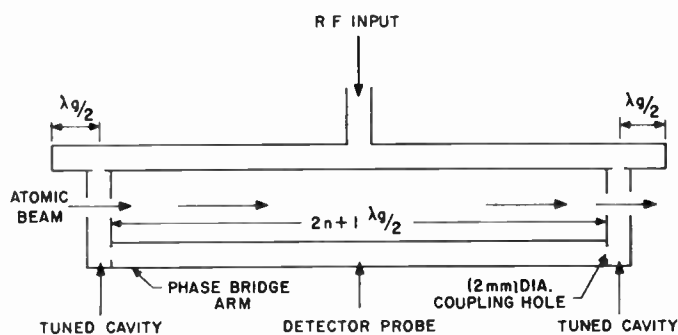


Fig. 7—New NPL RF section.

Pattern Detection and Recognition*

S. H. UNGER†, MEMBER, IRE

Summary—Two types of pattern-processing problems are discussed in this paper. The first, termed “pattern detection,” consists of examining an arbitrary set of figures and selecting those having some specified form. The second problem, “pattern recognition,” consists of identifying a given figure which is known to belong to one of a finite set of classes. This is the problem encountered when reading alphanumeric characters.

Both recognition and detection have been successfully carried out on an IBM 704 computer which was programmed to simulate a spatial computer¹ (a stored-program machine comprised of a master control unit directing a network of logical modules). One of the programs tested consisted of a recognition process for reading hand-lettered sans-serif alphanumeric characters. This process permits large variations in the size, shape, and proportions of the input figures and can tolerate random noise when it is well scattered in small specks.

Programs for detecting L-shaped (or A-shaped) figures in the presence of other randomly drawn patterns have also been successfully tested.

I. INTRODUCTION

A PRINCIPAL goal of the research upon which this report is based is to determine how machines can be made to duplicate some of the remarkable feats that humans perform daily when dealing with visual images. For example:

- 1) Presented with a new coloring book, a five-year-old child quickly points out all outlines of dogs.
- 2) A post-office clerk deciphers the name of a city in a carelessly written address.
- 3) A hold-up victim selects a photograph of his assailant from among the collection in police files.
- 4) A frequent visitor to an art museum identifies the creator of a newly acquired painting merely from its general appearance and style, and the knowledge that it was done by one of the better known nineteenth-century artists.

Examples 1 and 3 illustrate what we shall term *pattern detection*. This is the process of examining a set of figures and selecting those that fall into some particular class of patterns, defined as the *target set*. Examples 2 and 4 involve a different kind of operation, which we shall define as *pattern recognition*. Here a single input pattern known to belong to one of several known classes is to be identified. In other words, the problem is to specify which of a finite number of labels should be attached to the input. Thus, in example 2, the postal clerk knew that the scrawled word that he was trying

to decipher was the name of one of the cities in the state of New Jersey, and his object was to decide *which* one. Compare this with the detection problem of example 1. Here, the child was required to search through an assortment of patterns selected from an unlimited ensemble and to indicate which, if any, were pictures of dogs. Note that detection subsumes recognition in that any recognition problem can be treated as a finite number of detection problems. The converse is not true.

Both detection and recognition will be discussed here in some detail with alphanumeric characters being used as the patterns of interest. Systems have been devised and successfully tested for accomplishing the following:

- 1) Recognizing any given hand-printed alphanumeric character.
- 2) Examining an input field consisting of a set of randomly drawn patterns and detecting all L-shaped figures that are present. (A-shaped figures have also been detected.)

The above-mentioned systems consist of programs written for the spatial computer.¹ A brief description of this machine (abbreviated SPAC) follows, and a somewhat more detailed description including the order structure, is included in an appendix.

SPAC consists of a rectangular network of logical modules directed by a master control unit. Each module has direct contact with its four immediate neighbors (Fig. 1) and receives orders from the master control, which issues identical commands to all modules in the network.

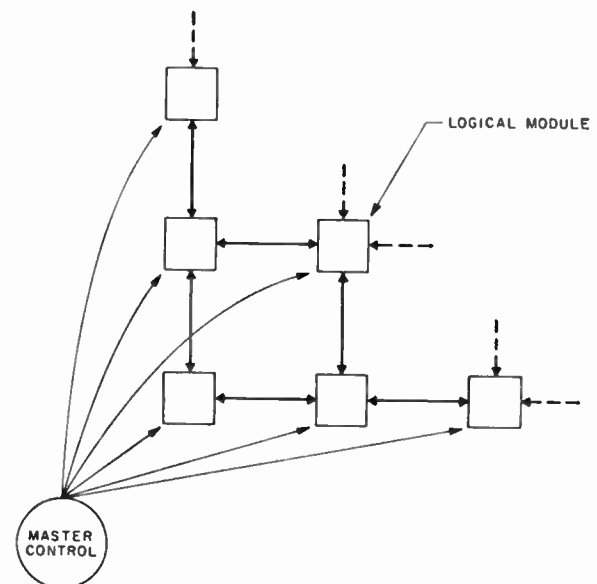


Fig. 1—Structure of spatial computer.

* Original manuscript received by the IRE, April 30, 1959; revised manuscript received, May 9, 1959.

† Bell Telephone Laboratories, Inc., Whippany, N. J.

¹ S. H. Unger, “A computer oriented toward spatial problems,” *Proc. IRE*, vol. 46, pp. 1744–1750; October, 1958.

A module consists of some logical circuitry, a one-bit principal register (PR), and a set of one-bit memory registers (MR's) individually addressable as MR1, MR2, etc. (In the original description of SPAC,¹ the PR's are called accumulators.) A pattern can be stored in the PR's or in any of the MR arrays.

The master control includes a random-access memory for storing instructions, an instruction counter, and decoding circuitry. It operates like the control unit of a conventional digital computer, reading instructions out of memory in sequence, decoding them and sending appropriate control signals out on a set of buses feeding the modules.

The SPAC programs that will be discussed here were tested by means of a simulation program on an IBM 704 Computer. The simulated SPAC has a 36×36 array of modules, and there are nine MR's per module.

Important work in the pattern processing area has been done by Selfridge^{2,3} and Dinneen⁴ who performed a number of interesting experiments on a digital computer which indicated that much could be accomplished through the use of a small number of very elementary operations, such as local averaging, spatial differentiation, and blob counting. Their primary goal was to investigate the learning process and they were not concerned with finding efficient recognition or detection procedures.

Kirsch⁵ and some of his colleagues at the Bureau of Standards have made use of the SEAC computer to study various pattern processing operations. Their objective was to develop a library of computer subroutines that might be useful in pattern processing. In addition to operations similar to those used by Selfridge and Dinneen, the Bureau of Standards group has demonstrated some interesting properties of an operation in which patterns are alternately complemented and spatially differentiated. No effort was made to develop specific recognition or detection systems.

A report by Greanias *et al.*⁶ describes a system for recognizing members of a sixteen character alphabet (numerals and some miscellaneous printer symbols). The system has been tested via a computer program and has successfully identified samples of printed characters in the presence of background noise. As described in the paper, this method does not permit variations in the size and proportions of the input characters.

² O. G. Selfridge, "Pattern recognition and learning," Symp. on Information Theory, London, Eng.; 1955.

³ O. G. Selfridge, "Pattern recognition and modern computers," 1955 Proc. WJCC, pp. 91-93.

⁴ G. T. Dinneen, "Programming pattern recognition," 1955 Proc. WJCC, pp. 94-100.

⁵ R. A. Kirsch, L. C. Ray, L. Cahn and G. H. Urban, "Experiments in processing pictorial information with a digital computer," 1957 Proc. EJCC, pp. 221-230.

⁶ E. C. Greanias, *et al.*, "Design of logic for recognition of printed characters by simulation," IBM J., vol. 1, pp. 8-18; January, 1957.

T. L. Dimond⁷ has developed a process for reading hand-printed numerals, provided that they are drawn in accordance with certain constraints that restrict size, proportion, and location.

The Solartron electronic reading automaton,⁸ produced commercially in England, can read 120 printed numerals per second. Only small variations in size and style are permissible.

The amount of work being done on pattern processing problems is increasing too rapidly to permit a complete review of the field, but the preceding summary represents a reasonable cross section.

II. THE EFFECTS OF QUANTIZING PATTERNS ON A GRID

We shall not consider multi-color patterns or those represented in half-tones. The original inputs will be assumed to be representable in black and white.

As a first step in processing patterns, it is desirable to reduce the input field to a discrete form. This can be done by superimposing a grid or matrix of squares over the figure (assumed to be black on white) and placing a one in each square if the black area within that square exceeds a certain threshold. Zeros are filled in elsewhere (although zero-cells will usually be left blank in the diagrams). All of our input fields will be of this form.

Such a quantizing process (which can be physically realized by devices such as flying spot scanners) results in a loss of information concerning the original pattern, but this loss can always be reduced by decreasing the mesh of the grid (that is, by increasing the number of squares per unit area). If the grid is too coarse, certain details of the pattern will be lost. This effect can sometimes be made to serve a useful function in filtering out insignificant irregularities that might cause confusion. For example, if a character printed by a typewriter is magnified by a factor of several thousand diameters and projected on a screen it is generally somewhat difficult to identify because of the apparently random distribution of tiny blobs of ink on the paper. Thus, for a given input field, there is a limit on the amount of useful grid resolution.

Regardless of how fine a grid is used, there are still important transformations which occur when a continuous line is mapped onto a discrete grid. Assume that the threshold is set so that a one is placed in every cell touched by any portion of a black area. A straight vertical line will be mapped as a set of one-cells (squares with ones in them) one above the other, as shown in Fig. 2(a). Except for the change in thickness, if the one cells are blacked in the resulting picture will be the same as the original line.

⁷ T. L. Dimond, "Devices for reading handwritten characters," 1957 Proc. EJCC, pp. 232-237.

⁸ "Typed figures translated into computer code," *Engineering*, vol. 183, pp. 348-349; March 15, 1957.

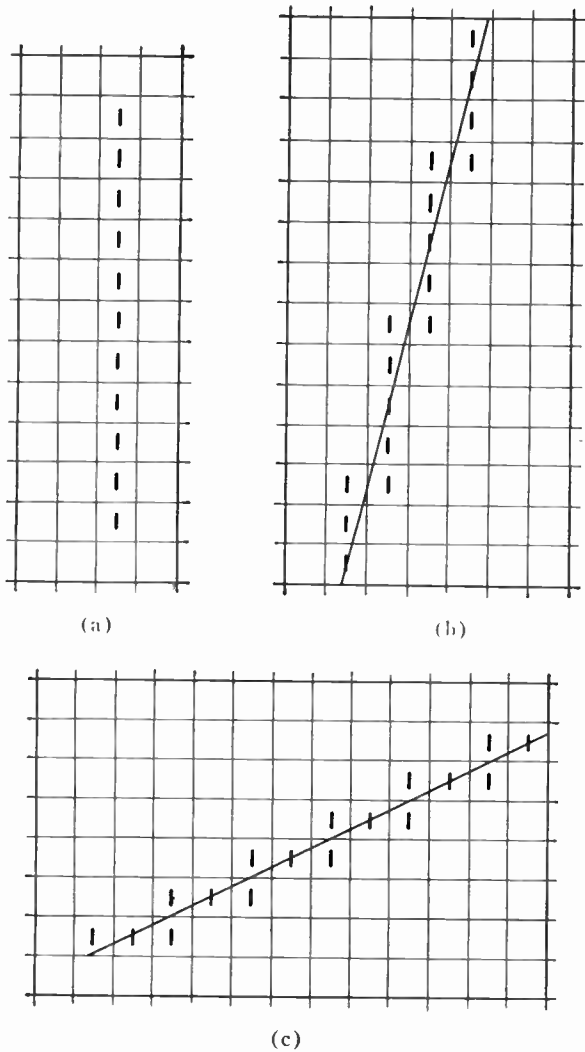


Fig. 2—Mappings of straight lines on a grid.

Consider now the mapping of a straight line whose slope exceeds unity, but is not infinite [Fig. 2(b)]. Such a map must have slope discontinuities, since the edges of the array of squares in the map must be either vertical or horizontal at all points. Thus, a map of a line with a slope anywhere between $+1$ and ∞ consists of a chain of vertical strips, with the top cell of each strip to the left of the bottom cell of the strip above. The numbers of cells in the strips corresponding to a particular straight line differ from one another by at most one (except for the uppermost and lowermost strips which may have fewer cells), and are approximately equal to the slope. Lines with absolute slopes less than one (lines closer to being horizontal) are similarly mapped into chains of overlapping horizontal strips, as shown in Fig. 2(c). In such cases, the number of one-cells per strip approximates the inverse slope of the line.

If a line is not quite straight, its map will still be qualitatively as above. The difference will show up in the form of variations in the lengths of some of the strips.

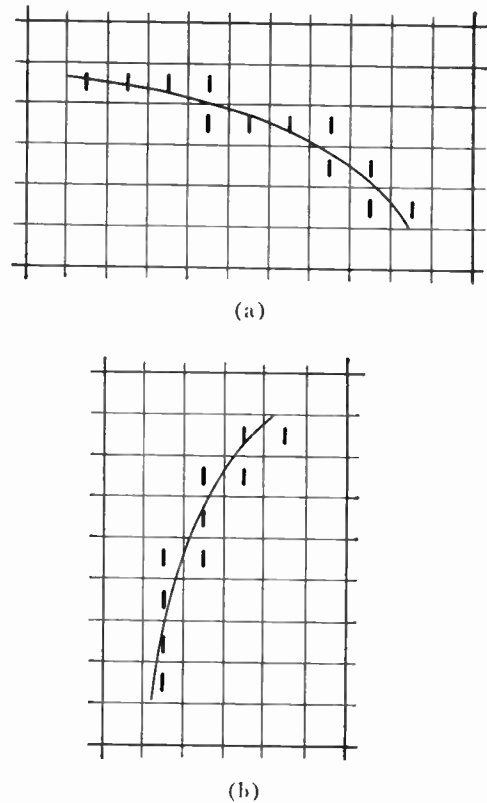


Fig. 3—Mappings of curved lines on a grid.

The mapping of a curved line onto a discrete matrix can be thought of as the union of a set of maps derived from a series of nearly straight line segments approximating the curve. A more precise approach is suggested by an examination of Fig. 3(a), a mapping of a section of a curve that is convex upward. Note that the lengths of the horizontal strips that constitute the mapping decrease monotonically from the top down. In other words, the map consists of a staircase in which every step is as long as, or longer than, the step below.

Fig. 3(b) is a map of a curve convex to the left, with slope between $+\infty$ and $+1$. Here the lengths of the vertical strips decrease monotonically to the right. This monotonicity property can be used to characterize the curvatures of given lines.

III. SMOOTHING

It is important that any system for pattern detection or recognition be relatively insensitive to minor irregularities in the input fields. Interchanging zeros for ones in a few isolated cells should not cause significant changes in the output of a pattern processing system. As was pointed out previously, some smoothing is achieved merely by quantizing the input. This however is not adequate, and in some cases the quantization itself introduces irregularities.

There are at least two basic approaches to this problem. One is to carry out a preliminary smoothing opera-

tion on the input fields prior to the main task. Another approach is to incorporate the smoothing into the basic recognition or detection operations by making them insensitive to variations confined to any small area. Both of these techniques are used in the programs that will be described here.

The explicit smoothing process,

- 1) Fills in isolated holes in otherwise black areas,
- 2) Fills in small notches in straight edge segments,
- 3) Eliminates isolated ones,
- 4) Eliminates small bumps along straight edge segments,
- 5) Replaces missing corner points (under certain conditions).

Fig. 4 shows a cell x , and the eight cells around it. Treat each cell as a binary variable. That is, $b = 1$ if cell b contains a one and $b = 0$ if cell b contains a zero.

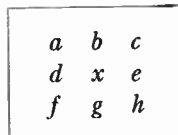


Fig. 4—Points involved in smoothing operations.

The first step in the smoothing operation places a one in x if the Boolean function $f_1 = x + bg(d + e) + de(b + g)$ is unity. (That is, x is changed from zero to one if three of the four variables $b, d, e,$ and f are ones.) If this process is carried out simultaneously for every cell in the matrix, then steps 1 and 2 will be accomplished. (In the preceding sentence, "simultaneously" means that the next state of each cell is determined before any of the other cells have been changed.)

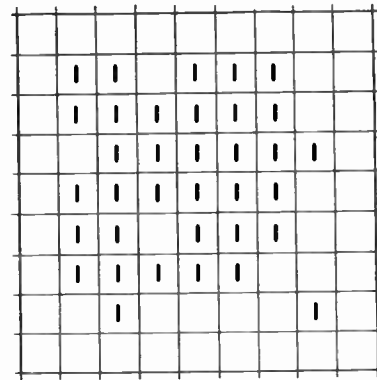
Steps 3 and 4 can be accomplished by replacing the contents of each cell x with $f_2 = x[(a + b + d)(e + g + h) + (b + c + e)(d + f + g)]$. A series of four more operations of a similar nature serve to carry out step 5. The smoothing will transform Fig. 5(a) into Fig. 5(b).

About one hundred SPAC orders (each executed once) are required to accomplish the preceding operations.

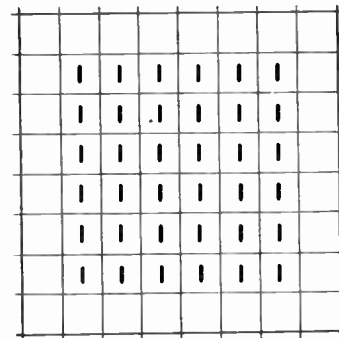
A simple 25-step subroutine which closes breaks in lines, if the gaps are no wider than one unit, can be inserted ahead of the above described smoothing routine.

These programs will clean up only small noise "specks" affecting isolated cells or in some cases pairs of cells. However, smoothing operations for eliminating larger irregularities might be devised by considering larger regions around each cell and exploiting continuity properties.

Note that the smoothing operations discussed thus far are size dependent in an absolute sense. That is, the irregularities are smoothed out on the basis of absolute size, not on the basis of size relative to that of the overall figure.



(a)



(b)

Fig. 5—Effects of smoothing.

This situation is satisfactory only if the figures being processed do not vary in size by more than a factor of two or three in magnitude. If wider variations are to be permitted in the sizes of the input figures, then it would be necessary to insert parameters in the smoothing programs which would be functions of some dimension of the input figure, such as the over-all height. A preliminary part of the program would then measure this dimension and insert appropriate parameters in the smoothing program. These parameters would control the sizes of the irregularities to be smoothed out. All of this is doubtless possible, but it would add considerable complexity to the program. Possibly, the way to avoid the necessity for such an approach would be to use some sort of analog controlled lens system that would keep the sizes of input figures within a range of two or three to one.

IV. EDGE SEQUENCES

In order to be able to detect patterns in the sense defined in the introduction, it is necessary to be able to state precisely, for any target set, just what characteristics distinguish this set from all others. For most interesting target sets these characteristics must be independent of size, location, and, to a considerable extent, of the proportions of component parts.

An important property which goes far toward satisfying these requirements will now be introduced.

Consider the letter "L" in Fig. 6(a) (regarding it as a figure covering a non-zero area, not as a pair of intersecting line segments). Beginning at the starred corner and proceeding in a counter-clockwise direction along the edges (boundaries) of the figure, the following succession of edges is found: top, left, bottom, right, top, right. This sequence, abbreviated at TLBRTR (T for top, L for left, etc.), is cyclic, and if another starting point is used, then an equivalent form such as BRTRTL will be found. Such a sequence, which will be referred to as an *edge sequence*, is not affected by changes in size, proportion, or location.

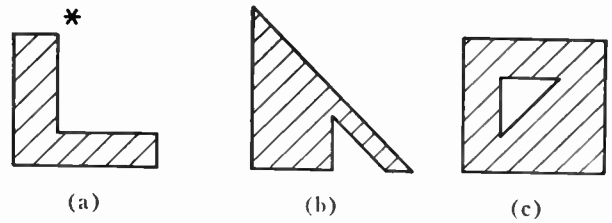


Fig. 6—Illustrating the use of edge sequences.

The edge sequence of Fig. 6(b) is LBR (BL) B (TR), where (BL) and (TR) represent diagonal edges facing "bottom-leftward" and "top-rightward" respectively. Similar notation can be devised for curved edges.

In the case of a figure with a hole, such as is shown in Fig. 6(c), two edge sequences are required for a description; one for the outside, and one for the inside. For this case they are LBRT and R (TL) B, respectively.

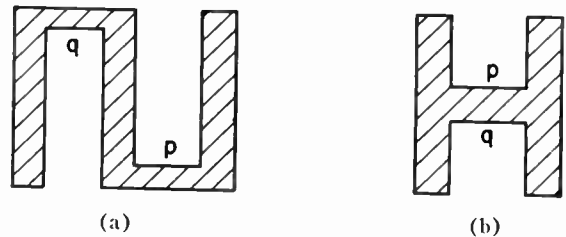


Fig. 7—Limitations of edge sequence description.

Edge sequences constitute a powerful tool for pattern detection. As will be shown in a later section, the ideas concerning edges that were introduced earlier can be utilized by a machine to find the figures in a given input field that have edge sequences corresponding to the target set.

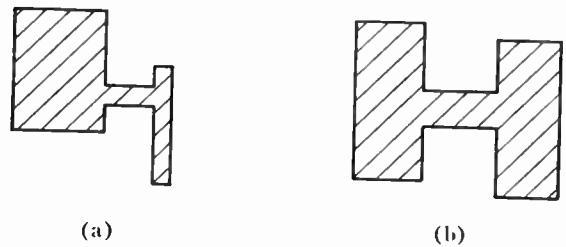


Fig. 8—Variations in proportion.

Edge sequences alone are not in general sufficient to completely characterize many interesting target sets. A particular edge sequence may, for example, be a necessary condition for membership in some target set, but there may be other requirements as well. Consider for example Fig. 7(a). This figure has the same edge sequence as a certain alphabetic character drawn in block capital form without serifs. But few readers would classify this figure as an H, although both (a) and (b) of Fig. 7 share the same edge sequence. An additional constraint that must be satisfied before a figure can be classified with 7(b) as an "H" is that the edge labelled p in Fig. 7(b) be directly above the edge labelled q. This condition is not satisfied by the corresponding edges in Fig. 7(a). Such "relative-edge-position" tests are frequently necessary after the edge sequence requirement has been met.

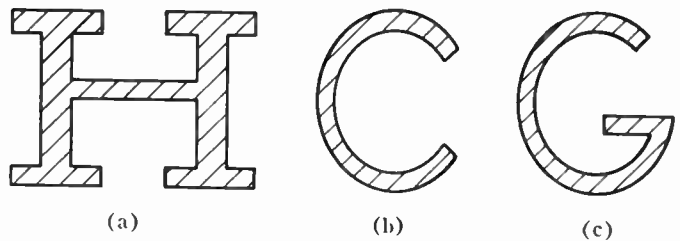


Fig. 9—Serifs.

Questions of proportion may also arise. For example, it would be reasonable to exclude Fig. 8(a) from the H-set, while admitting Fig. 8(b). Both have the appropriate edge sequences and their edges are in the proper relation to one another. It is difficult to specify precisely which figures intermediate between the pair in Fig. 8 should be considered as acceptable H's. However, an arbitrary set of standards may be chosen for each target set, such as the requirement (as applied to the present example): "the width of the wider leg must not exceed twice the width of the narrower leg." The research reported on here has not yielded any more specific results concerning this aspect of the problem.

Still another question is posed by Fig. 9(a). Is this a respectable member of the H-set previously discussed? At first, the results of a lifetime of conditioning would lead one to immediately answer "yes." But, on second thought, it becomes obvious that the form of Fig. 9(a) is certainly significantly different from that of a block capital H without serifs, which is the target set under discussion [see Fig. 7(b)]. Only long established custom decrees that this is also an "H," and it would be perfectly possible to devise an alphabet in which the two forms represented different letters. The difference between Fig. 9(b) and Fig. 9(c) is of the same nature, and is smaller in magnitude than the difference between the two H's, and yet one is called a "C," and the other a "G."

Thus, it may be convenient to think of certain target sets as being *compound*; that is to say, of being composed of the union of two or more simpler sets. Just as it would not be wise to expect a single description to suffice for both a small "h" and a capital "H," it is similarly unreasonable to expect the same description to cover different styles of capital "H's."

detection program does, the results of one of the experimental 704 runs will be presented now.

The input to the system is a set of figures drawn free-hand on a sheet of coordinate paper (Fig. 10). Since a suitable automatic scanning device was not yet available, its action was simulated by a key-punch operator, who was instructed to punch a set of IBM cards to represent the pattern; one column corresponding to each cell of the coordinate paper. A one was punched where the corresponding cell was black and a blank where the corresponding cell was blank. The resulting deck of cards served as the input to the machine. (As can be seen in Fig. 10, a 36x36 array was used.) A print-out of this quantized input is shown in Fig. 11, with x's replacing ones in order to make the form of the figures more conspicuous.

The first step by SPAC was to smooth the input field using a routine carrying out the steps described in the section on smoothing. Details of the smoothing routine will not be presented here.

SPAC then executed the L-detection program, which will be discussed next, and then printed out the result shown in Fig. 12, in which only L-shaped figures (after smoothing) remain.

The program first selects those figures whose edge sequences include LBRTRT, where the first R-edge and the second T-edge can be arbitrarily small, while the other four edges must each be at least four units long. (This permits the detection of "thin" as well as "thick" L's.) From this set, the program eliminates all figures with any edges not in the LBRTRT sequence, leaving figures such as those shown in Fig. 6(b) and Fig. 13(a).

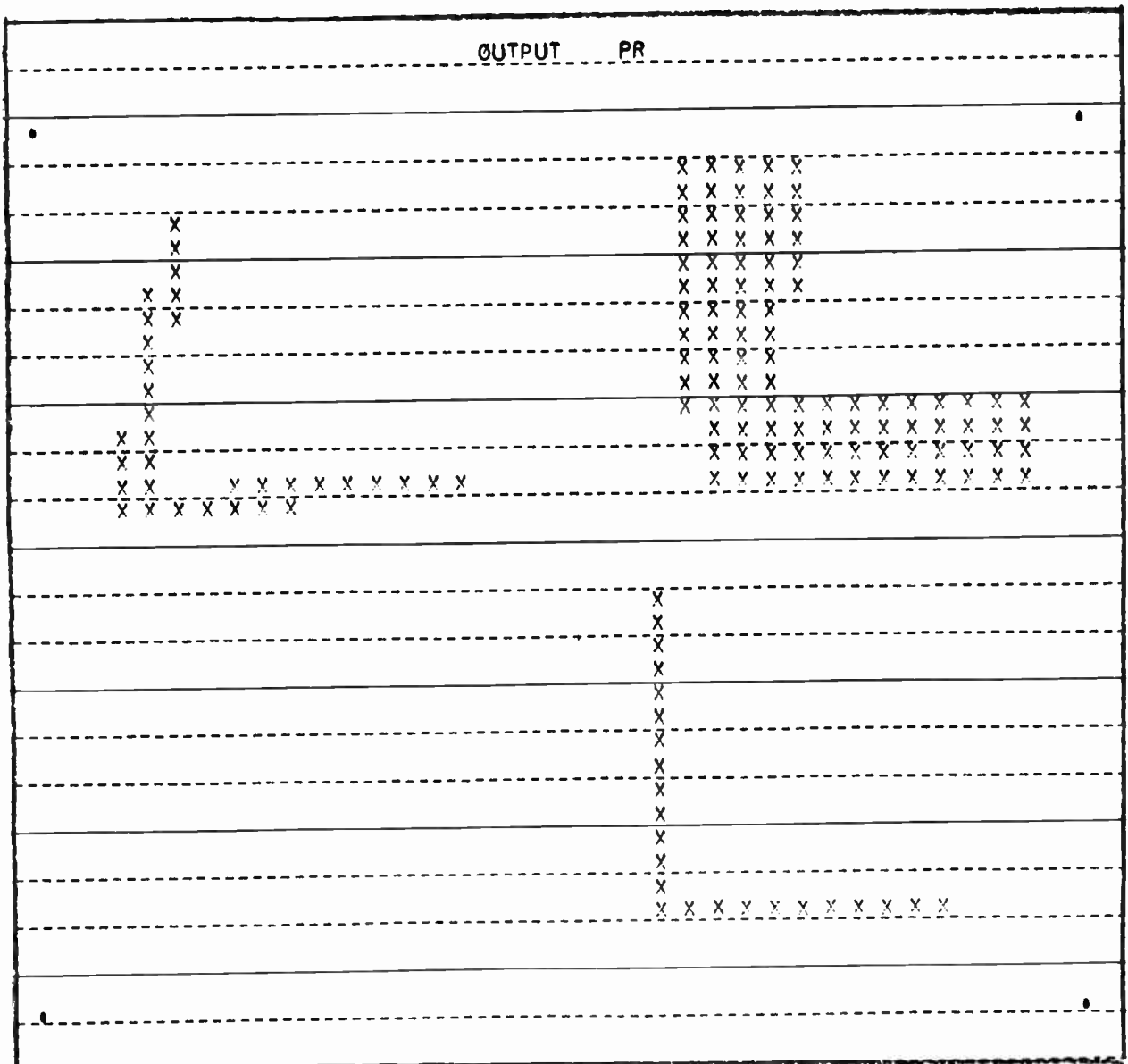


Fig. 12—SPAC output.

The following explanatory notes correspond to the parenthetically numbered points in the program shown in Table I, and the references to lettered edges in these notes pertain to Fig. 13(a).

- (1) Left edge points (one-points with zeros to the left) which are in vertical strips of length at least equal to 4 (a-edges).
- (2) Adds b-edges (vertical strips of left edge points diagonally below a-edges) to the a-edges found in (1).
- (3) Corner points such as the one common to b and c.
- (4) MR5 now includes edges a, b, c, and d.
- (5) Adds edge e to MR5.
- (6) Adds edge f to the edges already in MR5. Note that whereas the left edge of the L, consisting of m, a, and b-edges, must include an a-edge which is at least 4 units long, the portion of the L corresponding to f can be as small as one unit.
- (7) Adds g-edge to MR5.
- (8) Adds edge h to MR5.
- (9) Edge i is added to MR5. The inside corner was "turned" 10 instructions prior to this order by the SHF L and SHF U instructions.
- (10)-(13) Edges j, k, and l, are added to MR5.
- (14) The PR now contains edge m (which is now also in MR3).
- (15) MR2 now contains all edges which are in LBRTR sequences (or subsequences) and *only* such edges.
- (16) MR3 now contains the edges found in (15) and the regions enclosed by these edges. In the case of Fig. 13(a), MR3 contains the entire figure. Since only the darkened edges of Fig. 13(b) comprise LBRTR sequences, MR3 will contain only that part of this figure which is in MR2 (the darkened edges—which enclose no area). MR3 will contain Fig. 13(c) with the hole filled in. Thus, only in the case of true L's such as Fig. 13(a) will MR3 include the whole figure without additions. The remainder of the program consists of eliminating figures which are only partially contained in MR3 [Fig. 13(b)] and figures such as Fig. 13(c) which do not completely cover their counterparts in MR3.
- (17) Figures such as 13(c) which have holes.
- (18) PR now contains figures such as 12(b) with outer edge sequences including edges other than those in MR2.
- (19) Figures found in (17) and (18) are eliminated, leaving only the desired L-shaped figures.

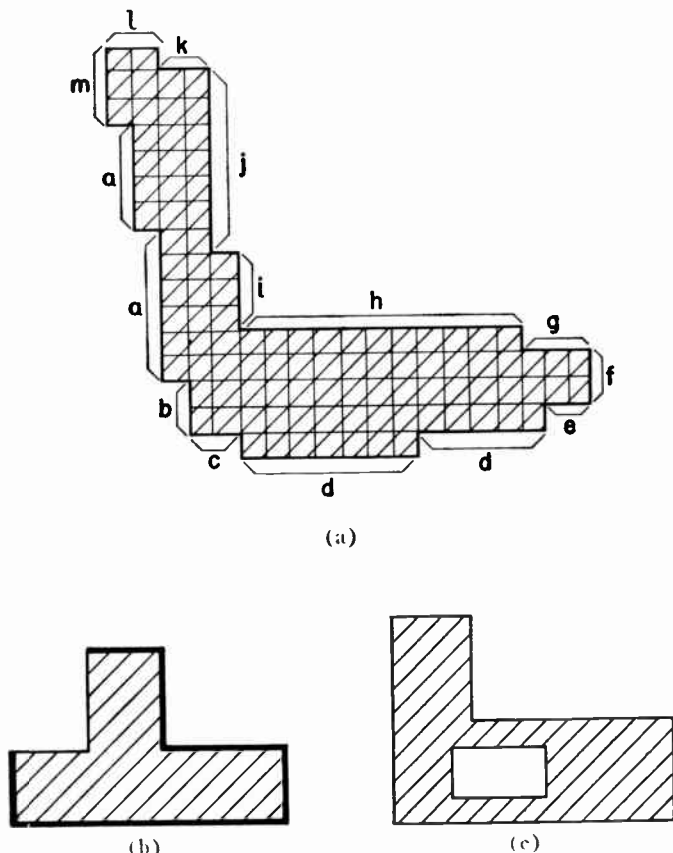


Fig. 13—Illustrating L-detection program.

TABLE I
L-DETECTION PROGRAM

SMOOTH	WRT 3	STR 3
WRT 1	SHF U	WRT 1
SHF R	ADD L, R	SHF D
INV	MPY 4	INV
MPY 1	EXP V, P, N	MPY 1
STR 2	ADD 3	STR 2
LNK	ADM 5 (6)	LNK
MPY U	SHF U	WRT 1
MPY U	ADD L, R	SHF L
MPY U	ADM 3	SHF D
ADD D	WRT 2	INV
ADD D	LNK	MPY 2, 3
ADD D	MPY 3	EXP H
STR 5 (1)	EXP V	STR 3
SHF D	ADM 5	WRT 2
ADD L, R	STR 3	MPY R
MPY 2	WRT 1	MPY R
EXP V	SHF D	MPY R
STR 3	INV	ADD L
ADM 5 (2)	MPY 1	ADD L
WRT 1	STR 2	ADD L
SHF U	LNK	LNK
INV	WRT 1	STR 4
MPY 1	SHF L	WRT 3
STR 2	SHF D	SHF L
LNK	INV	ADD U, D
MPM 3	MPY 2, 3	MPY 4
WRT 1	EXP H	EXP H, P, N
SHF R	ADM 5 (7)	ADD 3
SHF U	SHF L	ADM 5 (12)
INV	ADD U, D	SHF L
MPY 3 (3)	STR 3	ADD U, D
EXP H	WRT 2	ADM 3
ADM 5	MPY L	WRT 2
SHF R	MPY L	LNK
ADD U, D	MPY L	MPY 3
STR 3	ADD R	EXP H
WRT 2	ADD R	ADM 5 (13)
MPY R	ADD R	STR 3
MPY R	LNK	WRT 1
MPY R	MPY 3	SHF R
ADD L	EXP H, P, N	INV
ADD L	ADM 5 (8)	MPY 1
ADD L	SHF L	LNK
LNK	ADD U, D	STR 2
MPY 3	STR 3	WRT 1
EXP HPN	WRT 2	SHF R
ADM 5 (4)	LNK	SHF D
SHF R	MPY 3	INV
ADD U, D	EXP H	MPY 2, 3
STR 3	ADM 5	EXP V
WRT 2	SHF L	STR 3 (14)
LNK	SHF U	ADD 5
MPY 3	STR 3	LNK
EXP H	WRT 1	WRT 3
STR 3	SHF L	EXP H, V, P, N
ADM 5 (5)	INV	STR 2 (15)
WRT 1	MPY 1	INV
SHF L	STR 2	LNK
INV	LNK	MPY 2
MPY 1	MPY 3	ADR
STR 2	EXP V	EXP H, V
LNK	ADM 5 (9)	INV
WRT 1	SHF U	STR 3 (16)
SHF L	ADD L, R	LNK
SHF U	STR 3	WRT 1
INV	WRT 4	INV
MPY 2, 3	LNK	MPY 3
EXP V	MPY 3	EXP H, V, P, N
STR 3	EXP V, P, N	STR 4 (17)
WRT 2	ADM 5 (10)	WRT 1
MPY D	SHF U	LNK
MPY D	ADD L, R	WRT 3
MPY D	STR 3	INV
ADD U	WRT 2	MPY 1 (18)
ADD U	LNK	ADD 4
ADD U	MPY 3	EXP H, V, P, N
LNK	EXP V	INV
STR 4	ADM 5 (11)	MPY 1 (19)

Note that there are no loops in the program, so that each of the 237 SPAC instructions is executed exactly once.

Programs for detecting figures with holes are somewhat more complex. Both inner and outer edge sequences are traced, and, in place of the contents of MR3 described in (16) it is necessary to find the area enclosed between the outer and inner borders. This area is then used in the same manner as the MR3 contents were used in the L-program. However, it is then necessary to eliminate figures with the wrong number of holes, or with improperly located holes. This can be done in a variety of ways. One method is to eliminate points between one outer edge of the figure and the hole(s) and then check the edge sequence of the resulting figure, which no longer has any holes.

Figs. 14, 15 and 16 show the results of a test of an A-

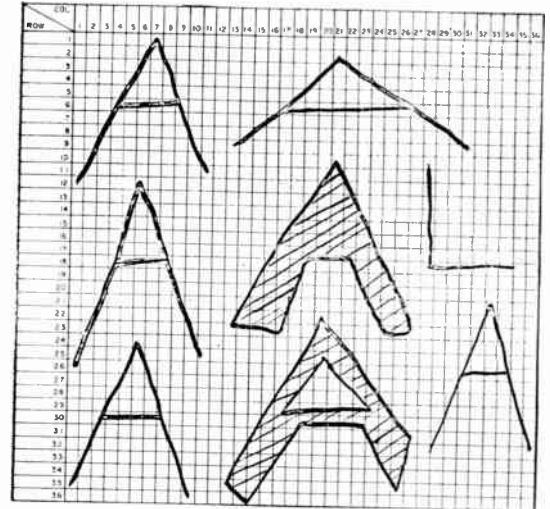


Fig. 14—Original drawing.

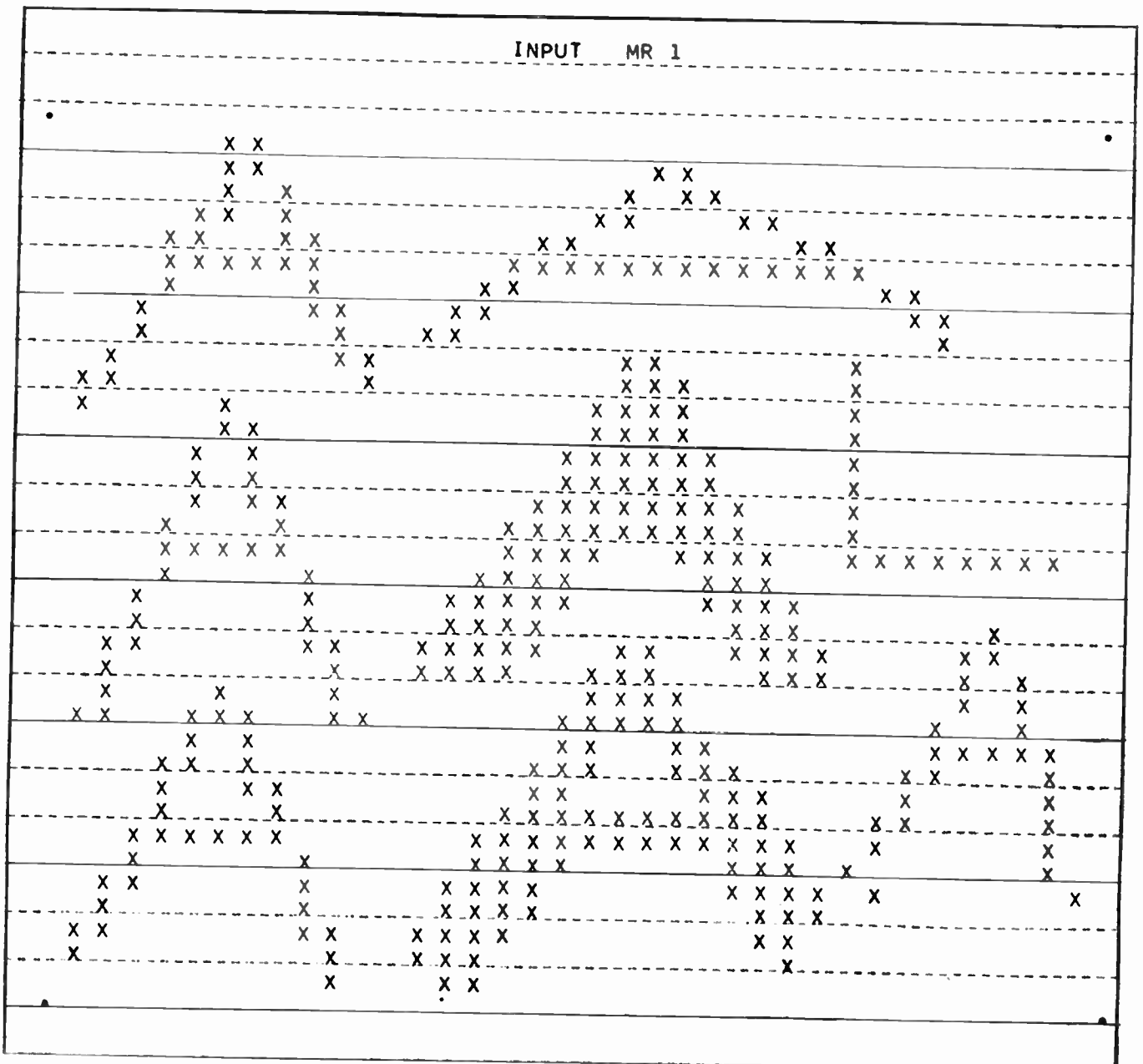


Fig. 15—Input to SPAC L-detection program.

detection program consisting of about 500 orders (including smoothing).

VI. PATTERN RECOGNITION

The pattern recognition problem defined earlier in this paper consists of identifying an input figure, given that it belongs to some member of a finite set of categories. For example, the set of categories (henceforth to be referred to as the *alphabet*) might consist of the digits from zero through nine inclusive.

For any alphabet there must exist at least one finite set of characteristics that can be used to distinguish amongst the members. That is, there must exist a set of yes or no questions, such that if these questions are answered with respect to any given figure, then there will be only one member of the alphabet to which this

figure can belong. The questions might, for example, concern the presence or absence of such features as holes, straight left edges, or concavities open to the right.

It is not necessary to ask all of the questions in every case. A sequential process can be carried out in which the answer to the first question determines a subset of the alphabet to which the input figure may belong. Depending upon the subset, a second question is asked, the answer to which further narrows the field of possible categories. This process is repeated until a single candidate remains. If the questions can be so chosen that each one halves the number of remaining candidates, then the number of questions necessary to identify any given figure is about $\log_2 n$, where n is the number of members of the alphabet. This is the minimum average

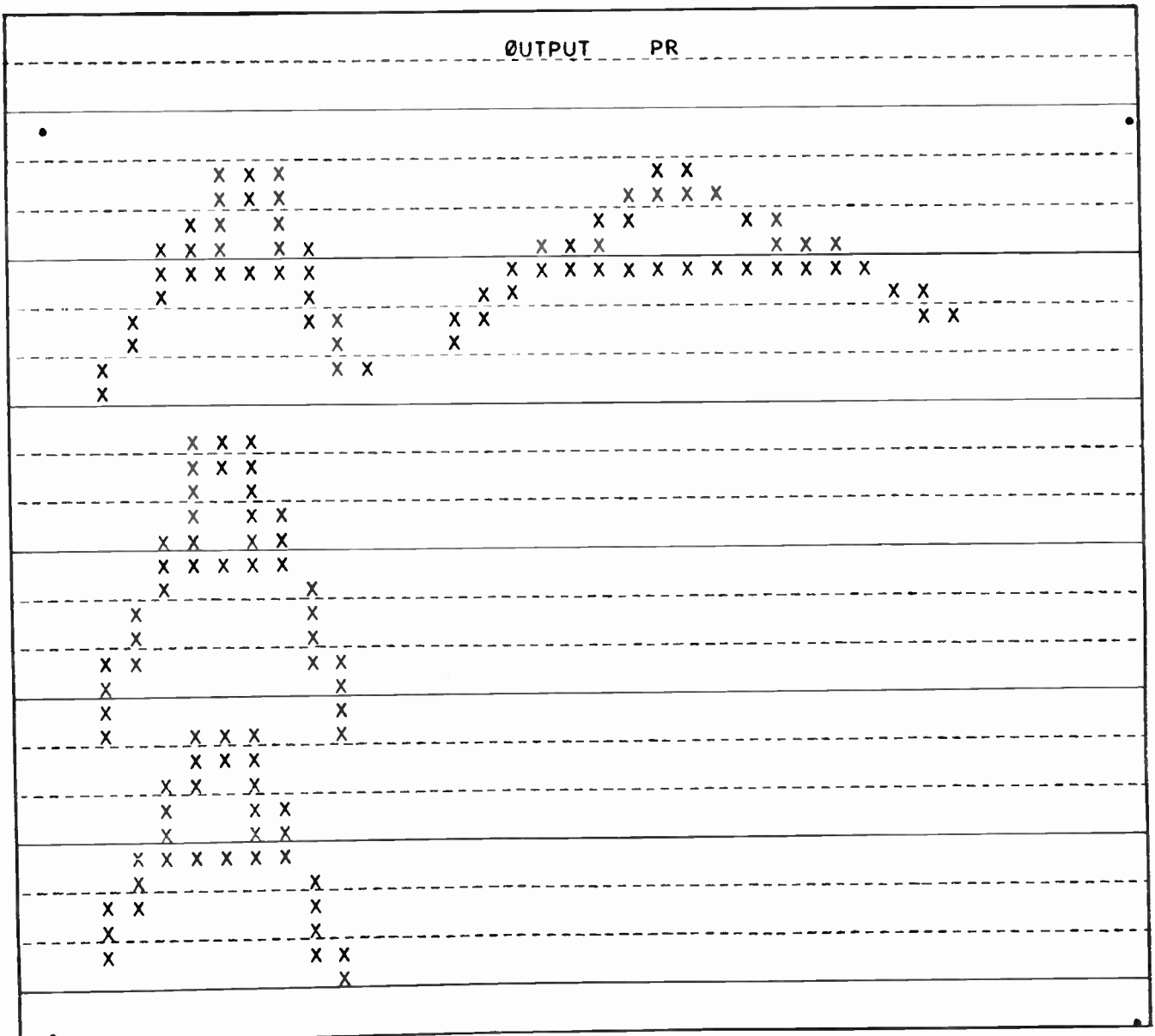


Fig. 16—SPAC output.

number of questions, assuming that the input figure is equally likely to belong to any of the n categories.

A good set of questions should have the following characteristics (insofar as they are mutually compatible):

- 1) They should be sufficient to distinguish any pair of allowable input patterns that belong to different members of the alphabet.
- 2) The necessary number of tests that must be performed for each identification should be minimal.
- 3) The number of orders necessary to perform each test should be minimal.
- 4) The total number of tests should be minimal.

An ideal property is thus easy to test for, possessed by half of the members of the alphabet (each test must produce a *different* dichotomy), and invariant with respect to all distortions that leave a pattern in the same category within the alphabet. Needless to say, it is not generally possible to attain such an ideal.

A pattern recognition scheme for alphanumeric characters will now be described. It is intended to recognize hand drawn sans-serif capital letters and numerals with very broad limits on the permissible over-all sizes and thicknesses of the input figures. A preliminary smoothing routine as described in Section III serves to cancel out the effects of noise, provided that the noise is not concentrated in any one locale.

The 34 properties described in Table II are used to distinguish among the 34 members of the alphabet (ones do not differ from I's, and zeroes do not differ from O's). Fig. 17 is a flow chart indicating how the tests are used. Starting with property 2 at the top, movement is downward. At each branch point the left branch is taken if the answer to the question referred to by the number is no. The right branch is taken for a yes answer. The following two definitions pertain to Table II:

- 1) A figure is *vertically concave* if there exist points not on the figure whose vertical projections *both* upward and downward touch the figure. Such points constitute *vertical cavities*. Similar definitions apply to horizontally concave figures, and to $+45^\circ$ and -45° concave figures. Parts (a), (b), (c), and (d) of Fig. 18 illustrate vertical, horizontal, -45° and $+45^\circ$ concave figures respectively, the dotted regions indicating the respective cavities. (This definition will be further qualified later on in the text.)
- 2) A cavity is *open to the right* if a directed path can be found starting at a point in the cavity, passing through points not on the figure, with no component in a leftward direction, and terminating at a point on the margin of the matrix. Cavities open to the left, or in other specified directions, are similarly defined.

TABLE II

FEATURES USED IN CHARACTER RECOGNITION PROGRAM

- 1) Horizontal cavity open above, (begj).
- 2) Vertical cavity open to the right, (aghk).
- 3) Vertical cavity open to the left, (efghl).
- 4) Horizontal cavity open below, (fhk).
- 5) Horizontal cavity, (befghijkl).
- 6) A hole, (eil).
- 7) Two vertical cavities lying on a common vertical line with the region between them consisting of points on the figure. For at least part of each cavity, no points on the figure are directly to the left of the cavity. (This latter requirement is a somewhat stricter version of "open to the left"), (e).
- 8) $+45^\circ$ concave, (defghijkl).
- 9) A region such that a vertical line segment can be drawn starting on the figure, passing down through a vertical cavity, passing through points on the figure again, then (still moving down) entering another vertical cavity, and finally terminating on the figure, (efghl).
- 10) Not used.
- 11) Same as 9), but with a horizontal instead of vertical orientation, (ijk).
- 12) Vertical cavity, (aefghikl).
- 13) -45° cavity, (cefghijkl).
- 14) -45° cavity open in a "left-bottomward" direction, (efghkl).
- 15) Horizontal cavity not part of a hole, (befghjk).
- 16) $+45^\circ$ cavity not part of a hole, (defghjkl).
- 17) Holes whose inverse (complement) is horizontally concave, (i).
- 18) -45° cavity not part of a hole, (cefghjkl).
- 19) A vertical left edge with right-angled corners above and below, (acdefjkl).
- 20) Two holes, (i).
- 21) A horizontal top edge with inside corners on both ends, (ej).
- 22) Same as 7) except that the cavities are horizontal and they face upward, (j).
- 23) Same as 7) except that the cavities are horizontal and they face downward, (k).
- 24) A vertical cavity, the lower end of which is above a bottom edge connected to an upper-left inside corner, (the intersections of a bottom edge and a right edge), (ek).
- 25) A cavity which is both vertical and horizontal, (efghil).
- 26) Hole whose inverse is vertically concave, (e).
- 27) Same as 9) except that the lower vertical cavity is inside a hole, (e).
- 28) Leftmost point of a vertical cavity open to right higher than the rightmost point of a vertical cavity open to the left, (g).
- 29) Right vertical edge, (bcdefijk).
- 30) Not used.
- 31) Height of the left leg of a U-shaped figure less than half the height of the right leg. (Used only to distinguish a "J" from a "U".)
- 32) Vertical cavity open to the left. This differs from 3 in that it includes cases where the boundaries of the cavity have nearly vertical slopes. (A fuller explanation of this distinction will be presented in the text.)
- 33) A right vertical edge with no horizontal cavity on the same level with it. (A Y has this property—but not a V.)
- 34) Leftmost point of a vertical cavity open to the right lies in the upper two thirds of the figure.
- 35) Vertical cavity open to right. (See 32.)
- 36) Horizontal cavity above a vertical cavity separated by part of the figure (efh).

Some of the descriptions in the table are of a qualitative nature, since more detailed statements would be beyond the scope of this paper. Following the description of each feature in the table is a parenthetic note referring to just those parts of Fig. 18 which have that feature. It is hoped that these illustrations will serve to clarify some of the more complex descriptions.

Before discussing some of the interesting features of this problem and our solution let us see how the system would operate in a particular case. Suppose, for example, that the figure to be identified happens to be an

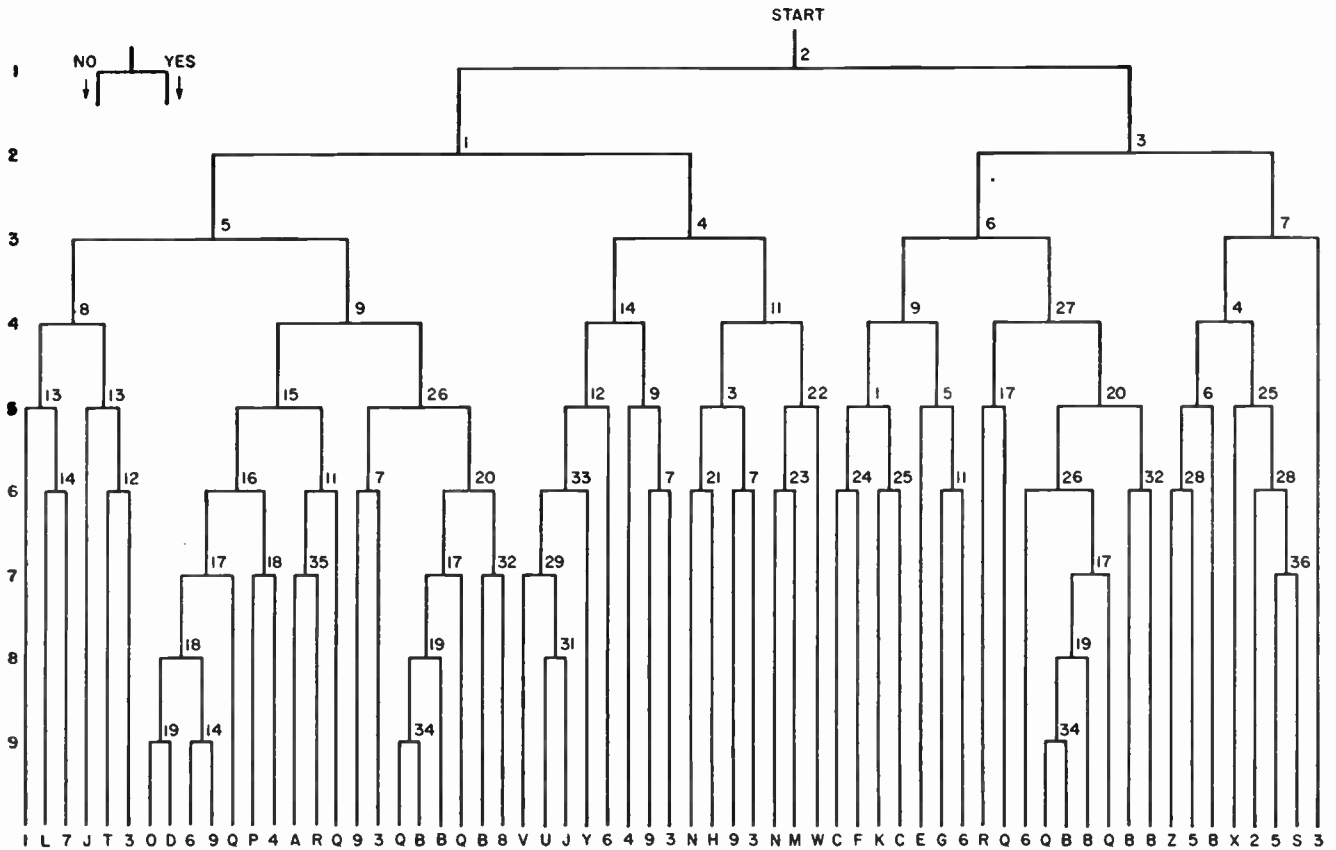


Fig. 17—Flow chart for recognition program.

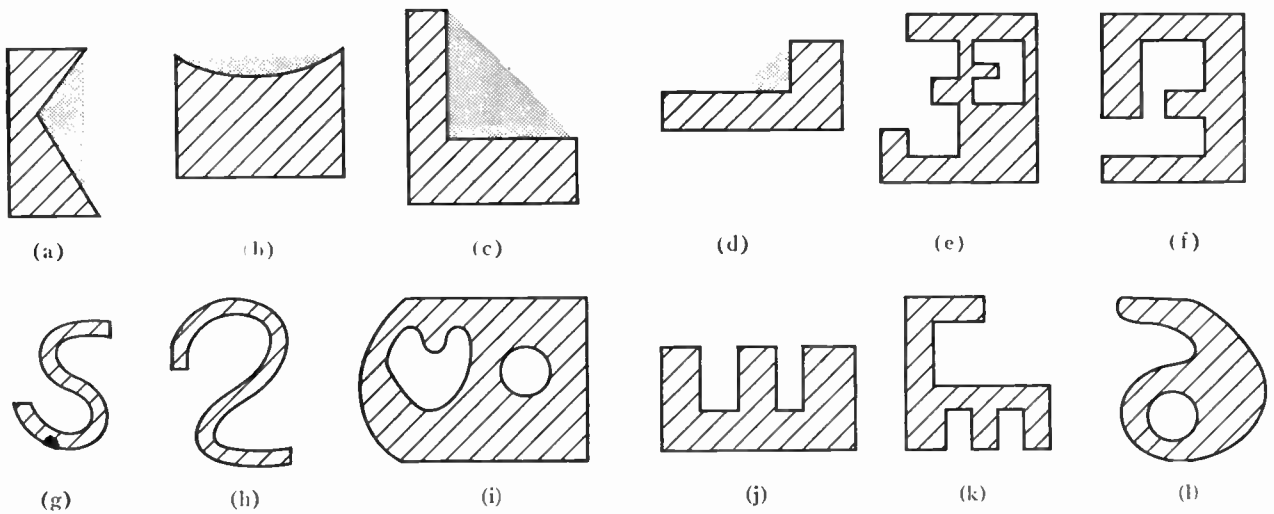


Fig. 18—Illustrations for recognition program features.

“E.” Referring to Fig. 18 we see that the first question (2) tests whether there is a concavity open to the right. Since the answer is yes, the right branch is taken, and the next question is 3, “Is there a concavity open to the left?” The answer being no, the left branch is taken and the next question is 6. Questions 9 and 5 follow in succession and a negative answer to the latter leads to the conclusion that the input is an “E.”

In order to allow for variations in the forms of cer-

tain characters, these characters (such as “3” and “Q”) appear at several different terminal points of the flow chart. A “9” for instance may be successfully recognized as drawn in either (a) or (b) of Fig. 19. Thus there are 63 termination points for the 34 characters.

Tests for each characteristic listed in Table II can be carried out by means of subroutines for SPAC. An average of about forty-five orders are required for each test. Thus, roughly three to five hundred orders are re-

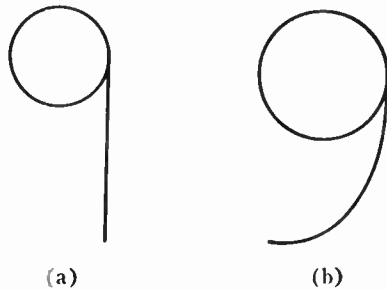


Fig. 19—Illustrating allowable style variations.

quired for each input figure (including one hundred orders to carry out the smoothing process described in Section III). There are about 1600 orders in the entire program, which has been successfully tested by means of the simulated SPAC. A lack of space precludes the presentation of the entire program in this paper, but a representative subroutine will be included.

The subroutine for each test consists of a series of operations carried out on the given figure so that at the end of the routine the field is cleared unless the figure has the property being tested for. Table III consists of a portion of a calling sequence that realizes the first few levels of the flow chart of Fig. 17. The order SBR XXX calls in the subroutine XXX. (For example, to test for property 2 we use the order SBR RO2.) After this subroutine has been executed the next order in the sequence is carried out. The order JMP PRY causes the computer to print a statement to the effect that the input character is a Y.

TABLE III

SBR RO2	TRZ 3
TRZ 1	JMP PR3
SBR RO3	TRA 60 (where a stop order is located)
TRZ 2	1 SBR RO1
SBR RO7	TRZ 4 etc.

An example of a SPAC program for carrying out a typical test is shown in Table IV.

TABLE IV
SPAC SUBROUTINE FOR TEST 9 (TABLE II)

WRT 1	MPY 9	ADD U
ADD L, R	EXP V (3)	STR 7
INV	ADD U	WRT 9
STR 9 (1)	SHF D	LNK
LNK	MPY 1 (4)	MPY 7
WRT 1	STR 7	EXP V
INV	WRT 1	ADD U
STR 8	LNK	SHF D
WRT 1	WRT 7	MPY 1 (6)
SHF D	EXP V	STP
MPY 8 (2)	SHF D	
ADD U	MPY 8 (5)	

The following explanatory notes refer to the numbered instructions in the program.

- (1) Zeros, with zeros to the left and right of them.
- (2) Points just below bottom edges.
- (3) Zeros with upward projections touching ones.

- (4) Zeros just below parts of the figure which are below vertical cavities.
- (5) Zeros just below parts of the figure which are below vertical cavities.
- (6) Ones below two vertical cavities, as required in Table II.

Note that the use of the points obtained in (1) as the possible vertical cavity points prevents a slightly crooked vertical line from being considered as vertically concave.

It will not be possible to discuss in detail all of the problems that lead to the use of the various tests employed in the system described here, but a few samples may serve to give the general flavor.

Consider first the test for a vertical cavity open to the right (test 2). A strict interpretation of this test would mean that a positive result would be obtained in cases typified by a "T" whose vertical member is slanted as shown in Fig. 20. In order to prevent this,

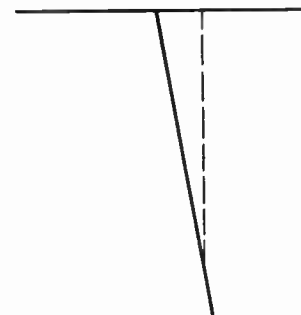


Fig. 20—Illustrating test 2.

the program for test 2 is written so that necessary conditions for a point to be considered as being in a vertical cavity are:

- 1) It must not be horizontally adjacent to a one-cell;
- 2) All zero-points in the cavity that are in the same column as the given point must meet condition 1, except possibly those at the top and bottom of the cavity.

These requirements insure that parts of the upper and lower borders of a vertical cavity must both be nearly horizontal. Hence Fig. 18(a) does *not* possess feature 2 as indicated in Table II. In certain cases it may be desirable to detect the presence of vertical cavities whose boundaries do not meet condition 2. Such a cavity is shown in Fig. 21. Test 35 accomplishes this function, in that it does not require the upper and lower cavity boundaries to be nearly horizontal. This characteristic is useful in distinguishing R's from A's.

In order to distinguish Y's from V's, it was found necessary to look for a right vertical edge below the V-shaped notch at the top of the figure. This is property 33 in Table II. A right vertical edge in this case is defined as an edge containing either one vertical strip of



Fig. 21—Illustrating need for test 35.

length at least equal to six or two vertical strips each of length at least equal to three.

The recognition program is preceded by the smoothing routine described earlier in this paper, which eliminates small irregularities. In addition, the various sub-routines for detecting features are generally insensitive to fine details, so that the over-all system will operate fairly well in the presence of scattered noise. Fig. 22 is a photograph of a 704 print-out which consists of an input figure and the output statement produced by the recognition program. Such tests have been carried out on about 90 figures. The clumsiness of the procedure for generating input data has precluded more exhaustive experimentation, but the success of the program has been clearly established.

VII. CONCLUSION

Methods applicable to two classes of problems, pattern recognition and pattern detection, have been developed. Solutions to several specific problems in these areas have been described, namely the recognition of alphanumeric characters, and the detection of L-shaped patterns. The methods and solutions presented here have all been successfully tested by means of a 704 simulation program, and some of the results of these tests have been included.

The matrix size of 36×36 used in these experiments was chosen for its convenience in simulating on the 704, and because it is a reasonably satisfactory size for the complexity of the patterns used in the tests. For applications in which fine details of more complex figures must be studied, a larger matrix will be necessary. A smaller matrix might suffice for simpler applications, although for small matrices the permissible variation in the size of the input image is quite limited, and an important advantage of the techniques described here is lost. On the other hand, as was mentioned in Section II, a matrix that is not too fine will smooth out some of the random irregularities in the input. Of course the principal reason for limiting the matrix size is economic.

Since SPAC does not yet exist as hardware, it is not possible to give actual execution times for the programs included here. However, in view of the simplicity of the

logic required for each SPAC order,¹ and the speed of components now in the development stage, it is not unreasonable to assume that, within five years, a speed of one microsecond per order will be attainable. Under this assumption, the character recognition program given here could operate at a rate of about 2500 characters per second (ignoring input time). The time required by the 704 simulation program to execute each SPAC order varies widely as a function of both the data and the instruction. A rough estimate of the time for a "typical" program is 10 msec per order.

In addition to being a fascinating field of study, automatic pattern processing has numerous conceivable applications. Primary interest today is in devices for character recognition, and it is easy to list applications such as transmitting hand written programs and input data to computers without the need for key punch operators, automatic sorting of mail, machine reading of telephone toll tickets written by operators, and machine reading of texts to be automatically translated into other languages.

Pattern detection methods might be useful in biological studies where searches must be made for particular cell structures, bacteria, or viruses among large numbers of microphotographs.⁹ Organic chemistry is another field in which important data exist in pictorial form, namely molecular diagrams. Searches for particular kinds of molecular structures among large numbers of records (perhaps in a patent office) may well be facilitated by machines.¹⁰ No doubt other applications will be found as the techniques improve.

VIII. APPENDIX

THE ORDER STRUCTURE OF THE SPATIAL COMPUTER (SPAC)

The order structure of SPAC is summarized in Table V, and a brief amplification of some of the descriptions follows. A more complete treatment will be found in a paper mentioned earlier.¹ (Note that some of the abbreviations in this paper will differ slightly from those used in the original description of SPAC.¹)

Suppose, for example, that the order ADD 1, 4 is given. Then, within every module, simultaneously, the contents of MR1 and MR4 will be added to the PR contents (Boolean additions). Note that each module operates on the data in its own memory cells, independently of what is going on in the other modules. The order ADD L, 2 results in the contents of the PR of each module being incremented (again Boolean addition) by the contents of MR2 and the *original* contents of the PR of the neighboring module to the left. Note that ADD L, 2 is not equivalent to ADD 2 followed by ADD L. Other references to neighboring modules used

⁹ H. P. Mansberg, "Automatic particle and bacterial colony counter," *Science*, pp. 823-827; October 25, 1957.

¹⁰ L. C. Ray, R. A. Kirsch, "Finding chemical records by digital computers," *Science*, pp. 814-819; October 25, 1957.

TABLE V
SPAC ORDER STRUCTURE

Order	Symbol	Interpretation
Write	WRT	Write the contents of the indicated MR into the PR without altering the MR contents.
Store	STR	Store the contents of the PR in each of the specified memory cells without altering the PR contents.
Invert	INV	Change the contents of every PR.
Add in memory	ADM	Add logically to the contents of each specified MR, the contents of the PR, without changing the latter.
Multiply in memory	MPM	Multiply logically the contents of each specified MR by the contents of the PR, leaving the PR contents undisturbed.
Add	ADD	Add logically to the contents of each PR, the contents of the specified MR's and neighboring PR's.
Multiply	MPY	Multiply logically the contents of the PR, the specified MR's and neighboring PR's, placing the result in the PR.
Add Reference	ADR	Add a one to the PR of the module in the lower left corner of the matrix.
Shift	SHF	Write the contents of each PR in the contents of the PR of the module in the specified direction (L, R, U, or D).
Transfer	TRA	Execute the instruction at the indicated address and then continue from there in sequence.
Transfer if zero	TRZ	If every PR contains a zero, then TRA to the indicated address. Otherwise continue with next order.
Link	LNK	Activate link elements between those adjacent pairs of modules in which both PR's contain ones. De-activate all other link elements.
Expand	EXP	Add ones to all PR's connected to PR's with ones through a chain of activated link elements of the orientation(s) specified in this order (H, V, P, N—or any combinations).
Stop	STP	End of program or subroutine.

with the ADD, MPY and SHF orders are R, U, and D referring to right, above (up) and below (down) respectively. Incidentally, it is assumed that a border of modules whose PR contents are permanently zero surrounds the entire matrix.

The link and expand orders require some further clarification. Although they are not shown in Fig. 1, there are one-bit memory elements between every adjacent pair of modules, including diagonal neighbors (so that each module shares eight such elements with its neighbors). These link cells become activated (or de-activated) only when a link order is given, in accordance with the description of that order in Table V. Note that there are four kinds of link cells, depending upon the orientation of the line connecting the two modules that they connect. These are horizontal (H), vertical (V), diagonal with positive slope (P), and diagonal with negative slope (N). An expand order can refer to any combination of these four orientations. When an expand order is given, the activated link cells of the specified orientation(s) establish two-way channels between the modules they connect. A propagation of ones takes place starting from those PR's which contained ones when the EXP order was given, and spreading to all other PR's connected to them via the network of channels.

Although not specifically discussed here, there are means for loading patterns into the module array prior to the executions of a program, and also means for unloading the output. There are also instructions making possible a printed output (required for the recognition program). At this time SPAC exists only in simulated form.

ACKNOWLEDGMENT

The author would like to thank Miss D. M. Habbart of the Bell Telephone Laboratories who wrote the SPAC simulation program which made possible the testing of the ideas described in this paper.

A Unified Analysis of Range Performance of CW, Pulse, and Pulse Doppler Radar*

J. J. BUSSGANG†, SENIOR MEMBER, IRE, P. NESBEDA†, AND H. SAFRAN†

Summary—This paper presents a unified method for computing detection range of pulse, multi-channel pulse Doppler, and CW radars.

The method assumes that detection occurs when a set threshold is exceeded and is based on 1) a modification of the conventional radar equation which relates range with the signal-to-noise ratio; 2) a simplified analysis of a single channel consisting of range gate, bandpass filter, square-law detector, and post-detection integrator which leads to an approximate calculation of the probability of detection; 3) a consideration of multi-channel effects.

Although pulse radar has been extensively analyzed, the literature on the performance of CW and pulse Doppler radars is meager. This paper attempts to fill this gap.

The method should prove useful for evaluating changes in a radar or comparing two radars. In order to estimate the radar range of a single radar, experiments to "calibrate" the model are required. A radar whose range is experimentally known can serve as a standard of comparison for predicting the behavior of radars under development.

Examples illustrate the method and suitable graphs are given.

INTRODUCTION

IT is by now well established that the problem of predicting the detection range of radars is of a statistical nature. The radar literature contains extensive descriptions and performance analyses of pulse radar systems.¹⁻¹² In comparison, with few exceptions such as

* Original manuscript received by the IRE, October 10, 1958; revised manuscript received, May 20, 1959.

† Missile Electronics and Controls Dept., RCA, Burlington, Mass.

¹ J. I. Marcum, "A Statistical Theory of Target Detection by Pulsed Radar," The RAND Corp., Res. Memo, RM-754; December 1, 1947.

² J. I. Marcum, "A Statistical Theory of Target Detection by Pulsed Radar; Mathematical Appendix," The RAND Corp., Res. Memo RM-753; July 1, 1958.

³ A. V. Haefl, "Minimum detectable radar signal and its dependence upon parameters of radar systems," PROC. IRE, vol. 34, pp. 857-862; November, 1946.

⁴ K. A. Norton and A. C. Omberg, "The maximum range of a radar set," PROC. IRE, vol. 35, pp. 2-24; January, 1947.

⁵ W. H. Hall, "Prediction of pulse radar performance," PROC. IRE, vol. 44, pp. 224-231; February, 1956.

⁶ J. L. Lawson and G. E. Uhlenbeck, "Threshold Signals," MIT Rad. Lab. Ser., McGraw-Hill Book Co., Inc., New York, N. Y., vol. 24; 1947.

⁷ D. O. North, "An Analysis of the Factors which Determine Signal-to-Noise Discrimination in Pulsed-Carrier Systems," RCA Labs., Princeton, N. J., Tech. Rept. No. PTR-6C; 1943.

⁸ H. Hance, "The Optimization and Analysis of Systems for the Detection of Pulsed Signals in Random Noise," Ph.D. dissertation, Mass. Inst. Tech., Cambridge, Mass.; January, 1951.

⁹ M. Schwartz, "A Statistical Approach to the Automatic Search Problem," Ph.D. dissertation, Harvard University, Cambridge, Mass.; June, 1951.

¹⁰ S. M. Kaplan and R. W. McFall, "The statistical properties of noise applied to radar-range performance," PROC. IRE, vol. 39, pp. 56-60; January, 1951.

¹¹ E. L. Kaplan, "Signal-detection studies with application," *Bell Sys. Tech. J.*, vol. 34, p. 403; March, 1955.

¹² P. Swerling, "Probability of Detection for Fluctuating Targets," The RAND Corp., Res. Memo RM-1217; March 17, 1954.

Barlow,¹³ little has been published regarding the performance analysis of CW and pulse Doppler radars. This paper is an attempt to fill the gap by presenting a unified method for computing the range performance of CW, pulse, and pulse Doppler radars. A common ground is thereby established on which different types of radars and similar radars with different design characteristics can be compared.

In evaluating range performance, it was found useful to follow concepts and methods established for pulse radar. This has the advantage that engineers familiar with the pulse radar method will need a minimum of reorientation. Results are reduced to a simple graphical presentation and to equations employing well-tabulated functions in order to facilitate application even further. No attempt is made either to employ the work on optimum detection techniques¹⁴⁻¹⁸ or to consider fluctuating signals. The latter can be readily treated following the work of Swerling.¹² The detection device assumed is of the type quite likely to be encountered in practice.

The analysis is carried through for a pulse Doppler radar, since the CW and standard pulse radars can be regarded as special cases of the pulse Doppler radar.

The paper begins with a brief description of a pulse Doppler radar. Then some results known to the radar engineer are reiterated. The relationship between radar parameters, target cross section, and a *normalizing radar range* R_0 is re-established with modifications necessary to adapt R_0 to a pulse Doppler radar. These modifications consist of appropriate adjustments in the signal power entering the (square-law) detector and integrator; these adjustments are a consequence of 1) a range gate which eclipses part of the returned pulse, and 2) a filter which passes only the central spectral line. Once the adjustment in signal power is calculated

¹³ E. J. Barlow, "Doppler radar," PROC. IRE, vol. 37, pp. 340-355; April, 1949.

¹⁴ P. M. Woodward, "Probability and Information Theory," McGraw-Hill Book Co., Inc., New York, N. Y., pp. 31-35; 1953.

¹⁵ J. J. Bussgang and D. Middleton, "Optimum sequential detection of signal in noise," IRE TRANS. ON INFORMATION THEORY, vol. IT-1, pp. 5-18; December, 1955.

¹⁶ W. W. Peterson, T. G. Birdsall, and W. C. Fox, "The theory of signal detectability," IRE TRANS. ON INFORMATION THEORY, no. PGIT-4, pp. 171-212; September, 1954.

¹⁷ D. Middleton and D. Van Meter, "Detection and extraction of signals in noise from the point of view of statistical decision theory," *J. Soc. Ind. and Appl. Math.*, vol. 3, pt. 1, pp. 192-253; December, 1955; vol. 4, pt. 2, pp. 86-119; June, 1956.

¹⁸ R. F. Drenick, S. Gartenhaus, and P. Nesbeda, "Detection of coherent and noncoherent pulsed signals," PROC. IRE, vol. 43, p. 370; March, 1955.

for each type of radar, the treatment of the problem is identical for the several types of radar. The statistical problem of analyzing a single channel consisting of a square-law detector, a post-detection integrator, and a threshold is handled by approximating the detector output with a staircase wave made up of independent segments. The technique used here reduces the analysis of the continuous process to the treatment of a sum of discrete variables. The distribution of the sum which represents the output of the post-detection integrator is assumed to have the form of a Gamma distribution having a mean and a variance which can be calculated from the mean and the variance of the input distribution function. This assumption is suggested by the fact that 1) the output of the integrator is a non-negative quantity, 2) for the case of noise alone the assumed distribution is exact when the predetection filter is ideal and a close approximation when the predetection filter is narrow-band RLC,^{19,20} and 3) a check of the present method against values computed using Incomplete Gamma Functions^{1,2} shows excellent agreement. This approach of assuming an appropriate distribution of integrator voltage at the outset permits the analysis not only of a simple integrator which sums up the last N pulses but also of a weighted integrator such as an RC low-pass filter without recourse to the characteristic function employed by Emerson²¹ and Kac and Siegert.²² In particular, the present method simplifies actual computations.²³

Probabilities of detection and false alarm are obtained by integrating the distribution discussed above. The integrals yield incomplete Gamma functions which are tabulated only for limited values of parameters. This difficulty is, however, overcome by applying the approximation of Wilson and Hilferty to the Incomplete Gamma Function²⁴ which involves only the well-tabulated Error Function.²⁵ A check against values tabulated by Pachares²⁶ of high percentage points of the Gamma distribution reveals agreement within the accuracy of the graphs.

¹⁹ S. O. Rice, "Mathematical Analysis of Random Noise," Bell Telephone Systems, Monograph B-1589; 1944-1945.

²⁰ D. Slepian, "Fluctuations of random noise power," *Bell Sys. Tech. J.*, vol. 37, pp. 163-184; January, 1958.

²¹ R. C. Emerson, "First probability densities for receivers with square-law detectors," *J. Appl. Phys.*, vol. 24, pp. 1168-1176; September, 1953.

²² M. Kac and A. J. F. Siegert, "On the theory of noise in radio receivers with square-law detectors," *J. Appl. Phys.*, vol. 18, pp. 383-397; April, 1947.

²³ Since the first two moments are sufficient to represent the assumed distribution, the method used is straightforward for a large class of filters. Emerson, *op. cit.*, on the other hand, first derives the characteristic function of the integrator output, then computes the cumulants or semi-invariants from it and uses these cumulants to get an asymptotic expression for the output distribution. The characteristic function method is involved because the characteristic values of a difficult integral equation have to be found.

²⁴ M. G. Kendall, "Advanced Theory of Statistics," Hafner Publ. Co., New York, N. Y., vol. 1; 1952.

²⁵ This approximation has been suggested by R. Terzian, RCA, West Coast Electronic Products Div., Los Angeles, California.

²⁶ J. Pachares, "A table of bias levels useful in radar detection problems," *IRE TRANS. ON INFORMATION THEORY*, vol. IT-4, pp. 38-45; March, 1958.

Finally, results are extended to the multiple-channel case. Special graphs of probability of detection vs normalized range are given for an unweighted integrator as an aid to practical computation and their use is illustrated by an example. The graphs are of different form from those of Marcum^{1,2} since they eliminate threshold as an explicit parameter and use only radar design quantities, such as false alarm rate, number of filter channels, filter bandwidth, and time on target as entries. These graphs can be used for both the CW and pulse radar analysis.

While different workers in the field have been using various methods for radar range evaluation, the outline of an over-all procedure, the construction of helpful graphs, and the emphasis on simplicity of presentation are in themselves an important contribution towards unifying the methods of realistically evaluating the performance of different radars. An abbreviated and partial version of this work was presented by the authors at the National Conference on Aeronautical Electronics held in Dayton, Ohio, on May 12-14, 1958.

BRIEF DESCRIPTION OF A SIMPLE PULSE DOPPLER RADAR

A block diagram of a simple Doppler radar adequate for the purpose of this analysis is given in Fig. 1(a). The energy transmitted by the radar consists of a coherent train of pulses at carrier frequency f_0 . The envelope of these pulses is shown in Fig. 2(a). Pulse duration τ and pulse repetition $\cdot T$ are assumed constant. Echoes from a target compose the train of a duration corresponding to target illumination time T_i , as shown in Fig. 2(b). The carrier frequency of the returning radiation is shifted from the transmitted frequency f_0 by an amount f_D called the "Doppler frequency" which is twice the ratio of the relative velocity (of the transmitter and the reflector) to the wavelength of transmitted radiation. The returned pulses, after amplification, are passed through a range gate.

The detection device is illustrated in Fig. 3. It consists of a certain number of narrow band-pass filters covering the Doppler region of interest. A narrow-band filter extracts only one spectral line from the pulse spectrum, thus converting the pulse train to a continuous wave. Each (predetection) band-pass filter is followed by an envelope detector and by a post-detection integrator (PDI). Normally, a square-law envelope detector followed by a linear integrator is the most convenient case to handle. The output of the integrator is applied to a threshold device. An alarm results if the integrated voltage exceeds the threshold. More than one range gate could be used, each followed by a detection device. If the range gate is omitted, and CW transmission used, Fig. 1(a) represents a model of a CW radar.

A common modification of the system in Fig. 1(a) is shown in Fig. 1(b). After (or before) range gating, the returned signal is applied to a coherent detector. This detector is, in essence, a mixer which uses for its refer-

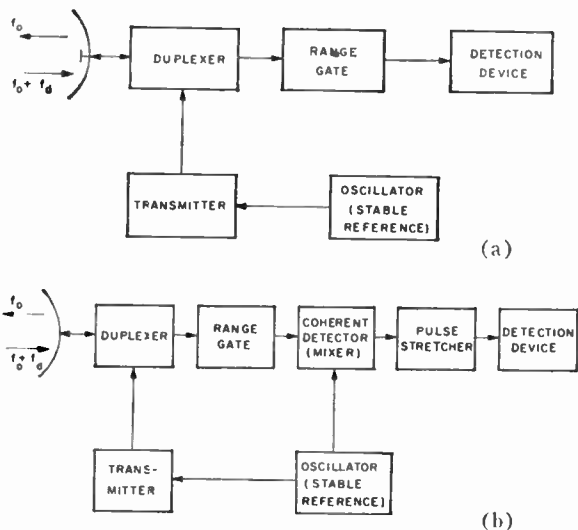


Fig. 1—(a) Block diagram of a simple pulse Doppler radar. (b) Block diagram of a modification of a pulse Doppler radar.

ence a signal from the oscillator employed to generate pulses. The output of the coherent detector is a series of pulses amplitude-modulated by the Doppler frequency. In order to produce an amplifying effect, these pulses are stretched by a "boxcar" circuit. The stretched pulse train is applied to the detection device of Fig. 3, properly positioned in frequency.

In practice, heterodyning operations may increase the complexity of the system but this in no way detracts from the generality of the model.

SIGNAL-TO-NOISE RATIO AND THE NORMALIZING RANGE R_0

The fundamental quantity in radar detection theory is the ratio of signal energy available for detection in a particular detection scheme to the competing noise energy.¹⁴ When signal and noise are present over the same period of time, which is the case here, their energy ratio is equivalent to the *average power ratio*. Since, in practice, the physical quantity measured is power, an analysis in terms of average power rather than energy has been preferred. The average is taken over the period of activity of the signal source.

As the first step in the analysis, the signal-to-noise average power ratio at the output of a single narrow band-pass filter and entering the (square-law) detector and integrator is calculated.

Because of receiver gating and filtering, not all the transmitter power is ultimately used for detection. Let \bar{P}_E be that portion of average transmitted power which is actually used in the detection process and termed by us the *effective signal power*. The concept of effective signal power, \bar{P}_E , is introduced in order to apply effects of receiver processing directly to transmitted quantities.

Similarly, we define the effective noise power, N_E , as that amount of noise generated at the receiver input which competes with signal at the input of the detector. Then the average signal-to-noise power ratio, X , at the input to the detector is given by

$$X = \frac{\bar{P}_E G^2 \lambda^2 \sigma_T L}{(4\pi)^3 N_E R^4} \tag{1}$$

where

\bar{P}_E = effective signal power (that portion of the transmitted average power which is used in detection).

G = one-way antenna gain.

λ = wavelength of transmission.

σ_T = target radar cross section.

L = product of system losses in two directions, such as losses due to plumbing, radome, propagation, and beam shape.

N_E = effective noise power (that portion of receiver input noise which interferes with detection).

In (1) \bar{P}_E and N_E take into account modifications in both signal and noise powers due to gating and filtering. For example, for the system of Fig. 1(a), the range gate

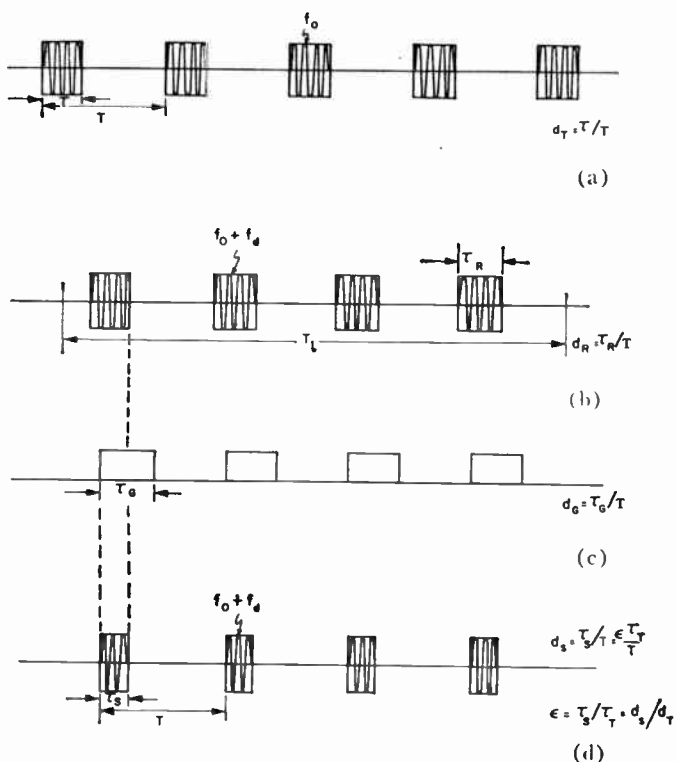


Fig. 2—(a) Transmitted pulses. (b) Returned pulses. (c) Receiver gate. (d) Signal pulses available for detection after gating.

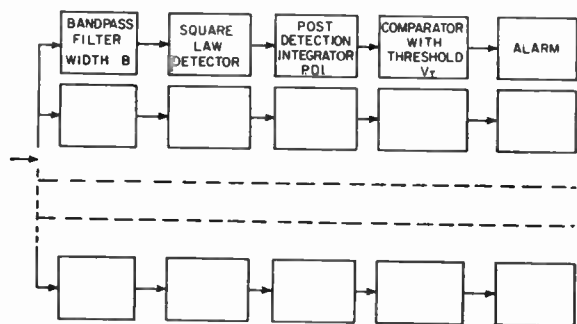


Fig. 3—Block diagram of the detection device.

admits, in general, only a fraction ϵ of each transmitted pulse, where ϵ is the ratio of pulse width after gating to the transmitted pulse width; ϵ can be termed the *eclipsing factor* (see Fig. 2). If the transmitter duty ratio is d_T and the duty ratio of signal pulses after gating is d_s , $\epsilon = d_s/d_T$. Following the range gate a filter extracts only that fraction of signal energy which is contained in the principal spectral line. A simple Fourier analysis shows that this fraction is only d_s of the total. Since the average power transmitted is the product of peak transmitted power \hat{P}_T and the duty ratio d_T , one concludes that for the example of Fig. 1, the *effective signal power* is

$$\bar{P}_E = (\hat{P}_T d_T) \cdot \epsilon \cdot d_s = \hat{P}_T d_s^2 = \hat{P}_T \epsilon^2 d_T^2 \quad (\epsilon \leq 1). \quad (2)$$

By the same token, a Fourier analysis of gated noise shows that noise power per cps after gating is reduced approximately by the receiver duty ratio, d_G , from the standard $kT(NF)$.

Hence, for the example of Fig. 1, the effective noise power at the output of narrow-band filter is

$$N_E = kT(NF)Bd_G \quad (3)$$

where

kT = product of Boltzmann's constant and the absolute temperature.

(NF) = over-all average receiver noise figure.

B = noise bandwidth of the band pass filter (Fig. 3).²⁷

d_G = gating duty factor [Fig. 2(c)].

Substituting into (1), one finds that, for a single channel of the system of Fig. 1, the signal-to-noise ratio at the detector input is

$$X = \frac{\hat{P}_T d_T^2 \epsilon^2 G^2 \lambda^2 \sigma_T L}{(4\pi)^2 kT(NF)Bd_G R^4}. \quad (4)$$

In practice d_G and d_T may be equal.

For the model of pulse Doppler radar involving pulse stretching prior to filtering [see Fig. 1(b)], both the effective signal power and the effective noise power are modified by the envelope of the spectrum of stretched pulses.²⁸ It follows that the signal-to-noise ratio given by (4) is still a good approximation if each filter extracts only a narrow band of Doppler frequency and rejects repetition rate sidebands.

Define a *normalizing range* R_0 as the range for which $X = 1$. Letting $\hat{P}_T d_T = \bar{P}_T$ (transmitted average power), we have from (4)

$$R_0 = \left[\frac{\bar{P}_T d_T \epsilon^2 G^2 \lambda^2 \sigma_T L}{(4\pi)^2 kT(NF)Bd_G} \right]^{1/4}. \quad (5)$$

All the radar parameters are locked in R_0 . R_0 is just a normalizing quantity for a single channel and should not be treated as the actual detection range. The operation of the detector itself and of multiple channels is not yet taken into account in R_0 .

It can be shown with simple arguments that (5) can be applied to various types of radar.

Case 1—Pulse Doppler Radar

This case is discussed above in transition from (1) to (4). Eq. (5) applies to both the model of Fig. 1 and the modified model of Fig. 1(a).

Case 2—CW Radar

In a CW radar, the transmitter and receiver are on continuously; thus, in (5), d_T , d_G , and ϵ are equal to unity.

Case 3—Pulse Radar

The noise bandwidth is now the IF bandwidth B_{IF} which is wide enough to pass all the significant components of the pulse spectrum and not just the principal spectral line; hence, the factor $d_T \epsilon = d_s$ in (5) has to be omitted. If effects of eclipsing can be neglected and hence ϵ set equal to unity and if $d_T/d_G = 1$, (5) becomes

$$R_0 = \left[\frac{\hat{P}_T G^2 \lambda^2 \sigma_T L}{(4\pi)^2 kT(NF)B_{IF}} \right]^{1/4}. \quad (6)$$

In (6) B_{IF} is assumed to match the pulse width. This is the standard radar range equation (see Ridenour²⁹).

Case 4—Delay-Line MTI Radar

A delay-line MTI operating at a repetition rate f_R acts as a linear filter modifying the spectrum of the signal with Doppler frequency f_D and the spectrum of noise by the same factor $\sin(\pi f_D/f_R)$. Therefore, if the output of the delay line canceller is passed through a narrow-band filter, (4) still represents approximately the average signal-to-noise power ratio at the output of the narrow-band filter. Hence the normalizing range R_0 is still given by (5). This is identical with the argument above on the effect of pulse stretching. In the presence of clutter signal-to-clutter ratio is more significant than signal-to-noise ratio.

²⁷ The "noise bandwidth" of a narrow-band filter is defined by $B = \int_0^\infty |y(f)|^2 df / |y(f_c)|^2$ where $y(f)$ is the transfer characteristic of the filter and f_c its center frequency. Other definitions of bandwidth in current use can be related to the "noise bandwidth" using the $y(f)$ of each given filter. For an ideal filter $|y(f)| = |y(f_c)|$ for $f_a < f < f_b$ and 0 elsewhere. Hence for an ideal filter $B = f_b - f_a$.

²⁸ Lawson and Uhlenbeck, *op. cit.*, see sections 3.4 and 10.4.

²⁹ L. N. Ridenour, "Radar System Engineering," M.I.T. Rad. Lab. Ser., McGraw-Hill Book Co., Inc., New York, N. Y., vol. 1, chaps. 5, 16, 1947.

In summary, although in the standard radar range (6) only the peak signal power appears, the broader concept of *energy ratio* expressed by (1) is more fundamental and includes the radar cases listed above as special examples.

In the discussion that follows, it is possible to relate immediately the signal-to-noise average power ratio (or energy ratio) X to the normalized, dimensionless range quantity R/R_0 , since from (4) and (5)

$$R/R_0 = X^{-1/4} \tag{7}$$

The analysis of a single-channel square-law detector and integrator which follows is carried out in terms of the quantity X . A system of M adjacent ideal filters, each of width B , has a noise power MN_B . Hence the over-all signal-to-noise ratio X_0 at the input of the filter bank is

$$X_0 = X/M, \tag{7a}$$

and

$$R = R_0/(MX_0)^{1/4} \tag{7b}$$

REPRESENTATION OF DETECTOR OUTPUT

Since detection is said to occur when a threshold is exceeded, the problem becomes ultimately one of determining the probability of such an event. This involves tracing the probability distribution of amplitudes through various operations. First we consider the voltage $g(t)$ at the output of the narrow-band filter and input to the square-law detector. This voltage consists of a sine wave plus noise. Let $f(t)$ be the envelope of $g(t)$.

The associated signal-to-noise ratio X was discussed above. The voltage, $v(t)$, at the output of a square-law detector is, by definition, $v(t) = \frac{1}{2}f^2(t)$, where the arbitrary factor $\frac{1}{2}$ is of no consequence and is selected to simplify (8) and (9) which follow. Let v be the normalized variable representing the output of this square-law detector in units of mean square noise. The probability density function of the envelope is for noise alone,¹⁹

$$P_N(v)dv = \begin{cases} e^{-v}dv & v > 0 \\ 0 & v < 0 \end{cases} \tag{8}$$

and for signal-plus-noise

$$p_{S+N}(v)dv = \begin{cases} e^{-v-X} I_0(2\sqrt{vX})dv & v > 0 \\ 0 & v < 0 \end{cases} \tag{9}$$

We now introduce a simplified mathematical model of the voltage at the output of a square law envelope detector. The continuous voltage is approximated by a function which is constant for intervals of duration $1/B$ and statistically independent in different intervals. The times at which the function changes its value are assumed unknown. An example of such a function is shown in Fig. 4. The height of v_i of each segment follows the same probability density function as

(8) and (9). For the ideal predetection filter, Maximon and Ruina²⁰ have justified this model by showing excellent agreement between the results of integrating the continuous noise process due to Rice¹⁹ and the results of integrating the model waveform, both for noise alone and signal-plus-noise.

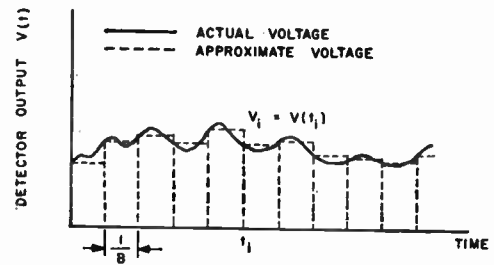


Fig. 4—Approximation of the detector output.

For predetection filters with RLC and Gaussian transfer characteristics, the agreement is still excellent for a large signal-to-noise ratio and moderately good for small signal-to-noise ratio provided enough segments are considered.³⁰

With the representation of the detector output assumed above, the normalized input voltage of the PDI is given by

$$v(t) = \sum_{n=-\infty}^{N-1} v_n a\left(t - \frac{n}{B}\right) \tag{10}$$

where N/B is the expected duration of the signal, where

$$a(t) = \begin{cases} 1 & 0 < t < 1/B \\ 0 & \text{elsewhere,} \end{cases}$$

and where the v_n are independent and follow the density laws of (8) and (9). The initial point has been arbitrarily selected and is of no importance.

If a detector which is not quadratic were to be considered, the model (10) of output voltage could still be used, but a different density function would have to replace (9). For the pulse radar, N is the actual number of pulses.

REPRESENTATION OF PDI FILTER OUTPUT

The problem of determining exactly the probability density function of the voltage at the output of a post-detection integrator has been treated by Kac and Siegert.²² Their method is not suitable for engineering computations. A simpler approximate approach is adopted here. We assume immediately a reasonable representation of the density function of voltage, V , at the output of PDI. The form which suggests itself whenever the

³⁰ L. C. Maximon and J. P. Ruina, "Some statistical properties of signal plus narrow band noise integrated over a finite time interval," *J. Appl. Phys.*, vol. 27, pp. 1442-1448; December, 1956.

required probability density $P(V)$ is zero for all negative values of V is given by

$$P(V)dV = \frac{\lambda_1}{\lambda_2} \frac{1}{\Gamma\left(\frac{\lambda_1^2}{\lambda_2}\right)} \left(\frac{\lambda_1}{\lambda_2} V\right)^{\lambda_1^2/\lambda_2-1} e^{-(\lambda_1/\lambda_2)V} dV \quad (11)$$

where λ_1 and λ_2 are, respectively, the mean and the variance of V .³¹ The probability density defined by (11) is exactly the distribution of V if noise alone is present and the integrator is an unweighted adder. If signal is also present, the quality of the approximation depends on the signal strength. Combined with the voltage model of (10), this method permits an approximate treatment of integrators with complicated weighting functions and even infinite samples with the use of just the average and the variance of detector output voltage.³² The procedure connecting V and v is outlined below.

Let $h(t)$ be the impulse response of the PDI filter. Then the output of the filter is given by

$$V(t) = \int_0^t h(\tau) \sum_n v_n a\left(t - \tau - \frac{n}{B}\right) d\tau \quad (12)$$

or

$$V(t) = \sum_{n=-\infty}^{n=N-1} v_n A_n(t) \quad (13)$$

in which

$$A_n(t) = \int_0^{1/B} h\left(t - \tau - \frac{n}{B}\right) d\tau. \quad (14)$$

Eq. (13) indicates that the output of the PDI filter can be regarded as a weighted sum of independent samples of the detector output v . This means that if the mean \bar{v} and variance σ_v^2 of the voltage at the detector output are known, then the mean λ_1 and the variance λ_2 of V at the output of PDI are

$$\bar{V} = \lambda_1 = \bar{v}_0 \sum_{n=-\infty}^{-1} A_n + \bar{v}_s \sum_{n=0}^{N-1} A_n \quad (15)$$

$$\sigma_V^2 = \lambda_2 = \sigma_{v_0}^2 \sum_{n=-\infty}^{-1} A_n^2 + \sigma_{v_s}^2 \sum_{n=0}^{N-1} A_n^2 \quad (16)$$

where subscripts 0 and s denote noise alone ($X=0$) and signal-plus-noise ($X \neq 0$). For each specific integrator only the evaluation of (15) and (16) and substitution of λ_1 and λ_2 thus obtained in (11) is required. Two examples of integrators follow.

³¹ Eq. (11) represents a density function known in statistics as Pearson Type III. (See Kendall, *op. cit.*) It can also be regarded as the first term of the expansion in a series of generalized Laguerre functions

$$P(V) = \sum_{n=0}^{\infty} c_n e^{-V} V^n L_n^d(V).$$

³² P. Nesbeda, "The Metrephon as a Practical Signal Integrator," RCA internal memo., May, 1954.

EXAMPLES OF SPECIFIC PDI INTEGRATORS

Example 1—Unweighted Integrator Matched to Signal Duration

The simplest case is that of integration with uniform weight over a finite time T_i corresponding to signal duration (target illumination time). With the application of the model input, the integrator becomes an unweighted adder of $N=BT_i$ independent samples containing signal-plus-noise. From (9), which describes statistics of the PDI input, we have

$$\bar{v} = 1 + X \quad \text{and} \quad \sigma_v^2 = 1 + 2X. \quad (17)$$

Hence (15) and (16) for this integrator are

$$\bar{V} = \lambda_1 = BT_i(1 + X) \quad (18)$$

and

$$\sigma_V^2 = \lambda_2 = BT_i(1 + 2X). \quad (19)$$

On substitution into (11) the probability density of PDI output follows.

Example 2—RC Filter

The weighting function of an RC filter is

$$h(t) = \begin{cases} \frac{1}{T} e^{-t/T} & \text{for } t > 0 \\ 0 & \text{for } t < 0 \end{cases} \quad (20)$$

where $T=RC$ is the time constant of the network. This filter performs both integration and averaging. We assume that noise alone is integrated from $t=-\infty$ to the time $t=0$ at which signal appears, and signal-plus-noise is integrated from $t=0$ to $t=T_i$, where T_i is the duration of the signal.

Applying again (15) and (16), we find that the PDI output at time $t=T_i$ is characterized by

$$\lambda_1 = \bar{V} = 1 + X(1 - e^{-T_i/T}) \quad (21)$$

and

$$\lambda_2 = \sigma_V^2 = \frac{(1 - e^{-1/BT})}{(1 + e^{-1/BT})} [1 + 2X(1 - e^{-2T_i/T})]. \quad (22)$$

While the technique for treating an RC post-detection integration filter is only approximate, results are in a form eminently suitable for numerical evaluations.

DEFINITION OF SIGNAL DETECTION, FALSE ALARM AND BIAS LEVEL

We give first a definition of detection. A signal is said to be detected whenever the channel output exceeds a certain predetermined value V_T , hereafter called the *bias level* or *threshold*.

The probability of detection, P_D , of signal-plus-noise in a single channel is then by definition

$$P_D = \int_{V_T}^{\infty} P_S(V) dV \quad (23)$$

where $P_S(V)dV$ denotes the probability density function of the voltage at the output of PDI when signal is present [cf. $P(V)dV$ in (11) with a suitable λ_1 and λ_2].

In the absence of any signal this bias level will, on occasion, be exceeded by noise alone, thus causing a false alarm. The higher the bias level is set, the less frequently this happens.

Let P_{FA}' denote the probability of false alarm in a single channel; then by definition

$$P_{FA}' = \int_{V_T}^{\infty} P_0(V)dV \quad (24)$$

where $P_0(V)dV$ denotes the probability density of the output of the PDI for noise alone, $X=0$; [cf. $P(V)dV$ in (11)].

In a multi-channel system, e.g., the one described in Fig. 3, the false alarm is said to have occurred if the bias level is exceeded by noise alone in at least one of the channels. If the receiver consists of M parallel channels, the probability of false alarm of the system is then

$$P_{FA} = 1 - (1 - P_{FA}')^M \quad (25)$$

with the assumption that the output of a channel be independent of that of other channels, i.e., that any channel is equally likely to produce a false alarm.³³ For a small probability of false alarms (25) becomes

$$P_{FA} \doteq MP_{FA}' \text{ for } P_{FA}' \ll 1. \quad (26)$$

In practice, the average time T_{FA} between alarms, rather than P_{FA} , is specified. Let T_{FA} denote the system false alarm time and T_{FA}' denote the single channel false alarm time. Then we have for a system consisting of M independent channels

$$T_{FA} = T_{FA}'/M. \quad (27)$$

To relate the system false alarm time with the bias level one needs to express the single channel probability of false alarm, P_{FA}' , as a function of the false alarm time. This can be expressed by³⁴

$$T_{FA}' = T_i/P_{FA}' \quad (28)$$

where T_i is the integration time which ordinarily corresponds to the signal duration. Hence

$$P_{FA}' = T_i/(MT_{FA}). \quad (29)$$

The bias level can be therefore determined by eliminating P_{FA}' between (24) and (29).

EVALUATION OF P_D AND V_T

The evaluation of the probability of detection follows by substituting (11) for $P_S(V)$ in (23).

If one defines, after Pearson,³⁵ the integral

³³ These channels can be frequency channels associated with different range gates. The sum total of identical individual channels is M .

³⁴ Hance, *op. cit.*, p. 23.

³⁵ K. Pearson, "Tables of the Incomplete Gamma-Function," Cambridge University Press, Cambridge, Eng., published by *Biometrika*; 1946.

$$I(u, p) = \int_0^{u\sqrt{p+1}} \frac{e^{-x}x^p dx}{p!} \quad (30)$$

as the Incomplete Gamma Function, the probability of detection is given by

$$P_D = 1 - I\left[\frac{V_T}{\sqrt{\lambda_2}}, \frac{\lambda_1^2}{\lambda_2} - 1\right]. \quad (31)$$

The function I is tabulated only for a limited range of its argument

$$\lambda_1^2/\lambda_2 - 1 < 50.^{35}$$

Using the method developed by Wilson and Hilferty and described in Kendall,³⁶ we can approximate the Incomplete Gamma Function with the aid of Error Integrals. Wilson and Hilferty noted that if the distribution of V is of the form given by (11), for large values of λ_1^2/λ_2 the distribution of the variable $(V/\lambda_1)^{1/3}$ approaches a normal distribution with the mean $m = 1 - \lambda_2/(9\lambda_1^2)$ and a standard deviation, $\sigma = (\lambda_2/9\lambda_1^2)^{1/2}$. Hence, we obtain

$$P_D \approx \frac{1}{\sqrt{2\pi}} \int_s^{\infty} \exp(-\frac{1}{2}u^2) du \quad (32)$$

in which

$$s = \left[\left(\frac{V_T}{\lambda_1} \right)^{1/3} - \left(1 - \frac{\lambda_2}{9\lambda_1^2} \right) \right] + \left(\frac{\lambda_2}{9\lambda_1^2} \right)^{1/2} \quad (33)$$

and λ_1 and λ_2 are the mean and variance of PDI output in the presence of signal, e.g., (18) and (19) or (21) and (22). This approximation is considerably better than the usual one that V itself tends to a normal distribution.

Since P_{FA}' is given by the same expression as P_D , cf. (23) and (24), except that λ_1 and λ_2 are evaluated for $X=0$ (no signal), it follows that (32) and (33) can be used to derive the threshold V_T for a given false alarm probability P_{FA}' or false alarm time, T_{FA}' .

The threshold value can therefore be eliminated from the expressions for P_D (32) and (33) once P_{FA}' or T_{FA}' is specified. This has been done for certain illustrative values. By applying successively (6), (32) and (33), graphs of the probability of detection P_D vs the normalized range R/R_0 have been constructed.

THE USE OF GRAPHS

A set of graphs is included in this paper to assist the designer in the task of determining the detection range in specific instances. These graphs have been constructed in order that computations specified by (32) and (33) be averted. The usefulness of these graphs rests on their compactness and on the fact that only known radar design parameters are needed to read them.

Figs. 5-9 give the probability of detection for an un-

³⁶ Kendall, *op. cit.*, pp. 294-297.

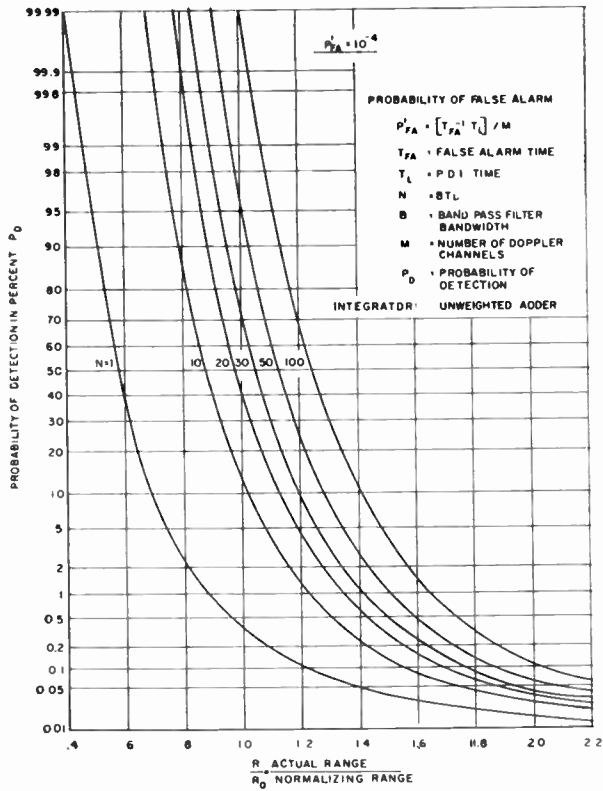


Fig. 5—Probability of detecting target at range R in terms of R/R_0 .

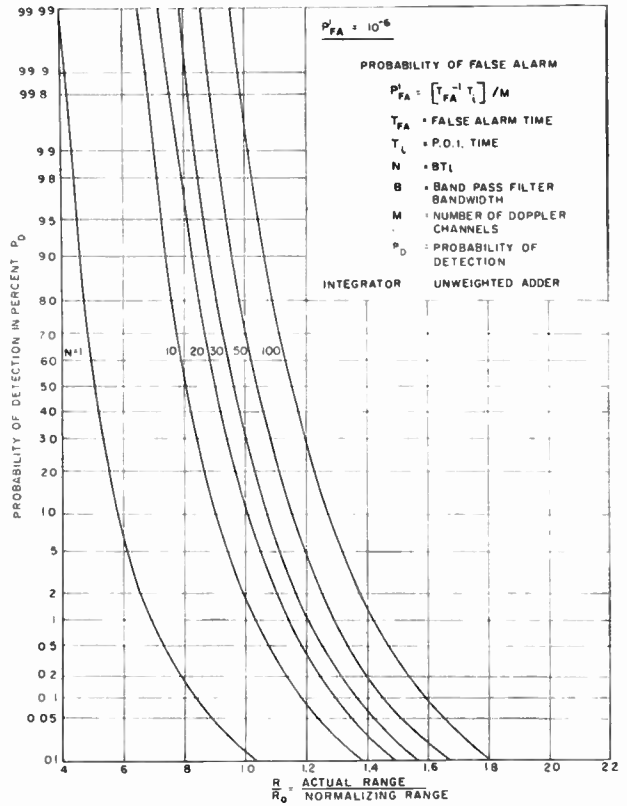


Fig. 7—Probability of detecting target at range R in terms of R/R_0 .

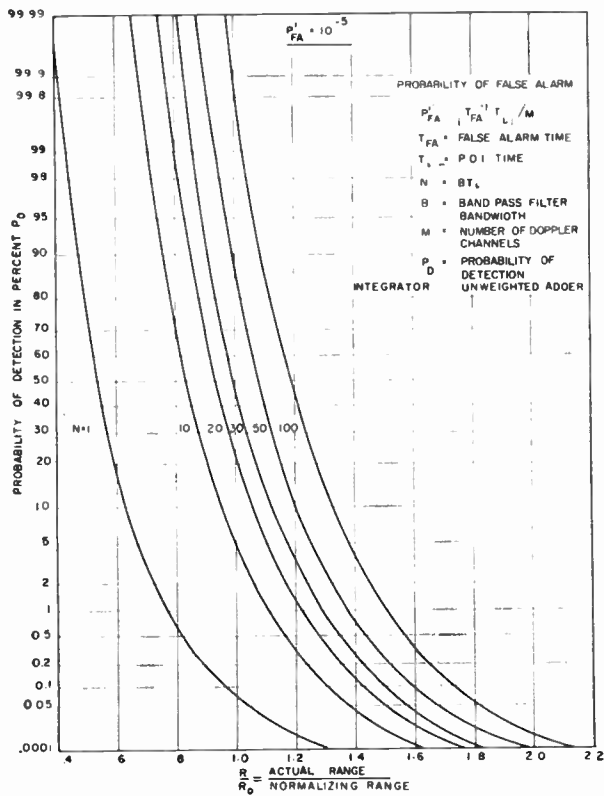


Fig. 6—Probability of detecting target at range R in terms of R/R_0 .

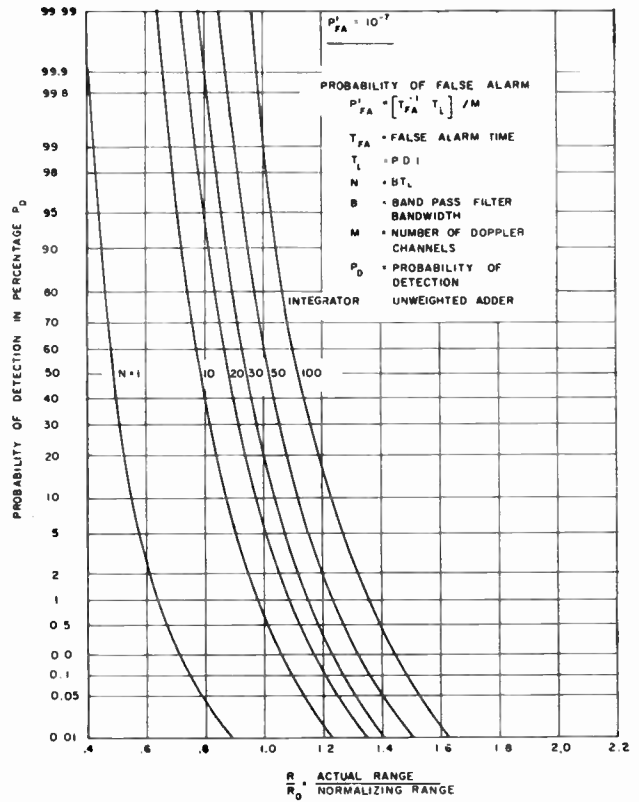


Fig. 8—Probability of detecting target at range R in terms of R/R_0 .

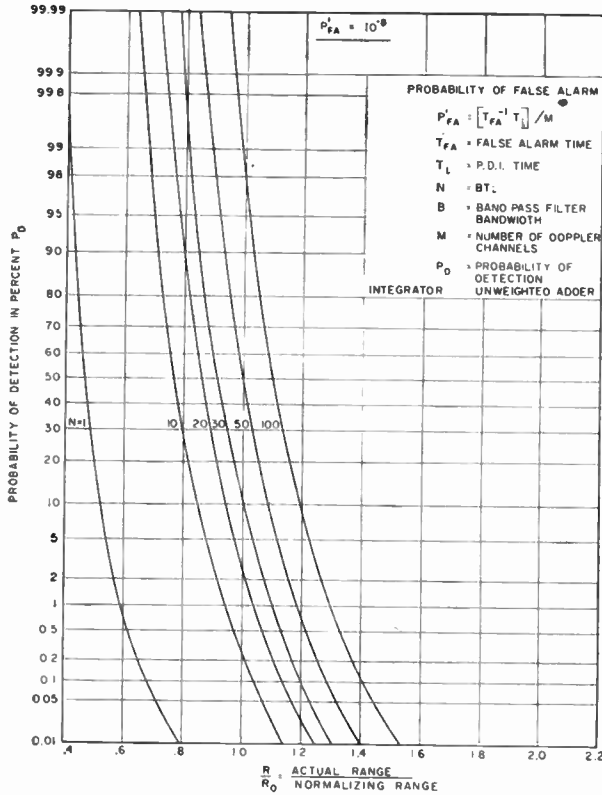


Fig. 9—Probability of detecting target at range R in terms of R/R_0 .

weighted integrator as a function of R/R_0 for the probability of false alarm in a single channel, P_{FA}' of 10^{-4} , 10^{-5} , 10^{-6} , 10^{-7} , 10^{-8} and $N=1$, $N=10$, $N=20$, $N=50$. These curves have been computed using the normal probability function tables³⁷ and (7), (32) and (33) for $X=0$. Examples illustrate the use of the graphs.

Example 1—Single-Channel Detection Range

Let the range for 90 per cent probability of detection be derived when radar design parameters are as follows:

- False alarm time $T_{FA} = 500$ seconds.
- Number of channels $M = 100$.
- Time on target $T_i = 0.05$ second.
- Bandwidth of the filter $B = 200$ cps.

Then from (29), $P_{FA}' = 10^{-6}$. This case is given in Fig. 7. From the relation $N = BT_i$, $N = 10$. On the curve $N = 10$, one reads $R/R_0 = 0.74$ corresponding to the 90 per cent probability of detection. Hence the range R for the 90 per cent probability of detection is $0.74 R_0$ where R_0 is the normalizing range given by (5).

Example 2—Effect of the Number of Channels

Suppose the problem is to compare the detection range of radars which differ from each other only in the num-

ber of Doppler filter channels M . Assume for all three radars:

- Probability of detection $P_D = 0.90$.
- False alarm time $T_{FA} = 1000$ seconds.
- Time on target $T_i = 0.1$ second.

Let each radar have a filter bank covering the same total Doppler bandwidth $B_0 = 10,000$ cps, where $B_0 = MB$.

Let $M = 10, 100, 1000$. The range $(R)_m$ corresponding to M channels is compared to the range, $(R)_{100}$, of the radar with 100 channels.

$$\frac{(R)_M}{(R)_{100}} = \frac{(R/R_0)_M}{(R/R_0)_{100}} \frac{(R_0)_M}{(R_0)_{100}}$$

Calculations are summarized in Table I.

TABLE I

M	10	100	1000
P_{FA}'	10^{-6}	10^{-6}	10^{-7}
Fig. No.	6	7	8
B	1000	100	10
N	100	10	1
$(R/R_0)_M$	1.1	0.74	0.45
$(R/R_0)_M / (R/R_0)_{100}$	1.5	1.0	0.61
$(R_0)_M / (R_0)_{100}$	0.56	1.0	1.8
$(R)_M / (R)_{100}$	0.84	1.0	1.1

In this particular example, then, a hundredfold increase in the number of channels improves the detection range by a factor of 1.27 ($= 1.1/0.84$).

Example 3—Comparison of Pulse and Pulse Doppler Radars

Another useful example is that of comparing detection ranges of a conventional pulse radar $(R)_p$ and a pulse Doppler radar $(R)_d$, assuming equal values of average transmitted power \bar{P}_T .

- Assume the following conditions for both radars:
- Probability of detection $P_d = 0.9$.
- Time on target $T_i = 0.02$ second.
- False alarm time $T_{FA} = 200$ seconds.
- IF bandwidth of pulse radar $B_{IF} = 5 \times 10^6$ cps.
- Pulse repetition frequency $PRF = 500$ pps.
- Doppler channel bandwidth $B = 500$ cps.
- Number of Doppler channels $M = 10$.
- (Hence total Doppler bandwidth $MB = 5000$ cps).

From (5) and (7), the ratio of normalizing ranges for the two radars is

$$(R_0)_p / (R_0)_d = [(B/B_{IF})(\hat{P}_T)_p / \bar{P}_T]^{1/4}$$

If the pulse radar duty ratio is 0.001, we get

$$(R_0)_p / (R_0)_d = 0.55. \tag{34}$$

³⁷ "Tables of Normal Probability Functions," Natl. Bur. of Standards, Washington, D. C., Appl. Math. Ser. 23; 1953.

Now, for the pulse radar

$$P_{FA}' = (T_i/T_{FA}) = 10^{-4}$$

$$N = T_i \times PRF = 10.$$

Hence from Fig. 5, we read

$$(R/R_0)_p = 0.79. \quad (35)$$

For the pulse Doppler radar

$$P_{FA}' = T_i/(MT_{FA}) = 10^{-5}$$

$$N = BT_i = 10.$$

Hence from Fig. 6, we read

$$(R/R_0)_d = 0.76. \quad (36)$$

Combining (34), (35), and (36):

$$(R)_d/(R)_p = \frac{(R/R_0)_d}{(R/R_0)_p [(R_0)_p/(R_0)_d]} = 1.8.$$

Thus, in this particular example, the pulse Doppler radar has 80 per cent more detection range.

CONCLUSIONS

This paper shows how one should modify the standard radar range equation to accommodate CW and pulse Doppler radars. A method of computing the probability of detection has been developed. This method is simple and its application requires only the use of tables of normal probability functions. The approximation introduced affords sufficiently good values for the probability of detection even for a small number of integrated samples and for small values of signal-to-noise ratio, which are the most interesting and practical cases. Graphs suitable for handling a large number of typical numerical examples have been given to simplify computational problems.

ACKNOWLEDGMENT

Thanks are due to Dr. G. M. Nonnemaker for encouragement and guidance, to Miss Janet Heineman for the computational work, and to Profs. W. M. Siebert and J. P. Ruina for helpful comments on an earlier version of this paper.

Absorptive Filters for Microwave Harmonic Power*

VIKTOR MET†

Summary—Utilizing the cutoff properties of certain lossy periodic waveguide structures, low reflection absorptive filters for harmonic power at microwave frequencies have been obtained.

Various approaches to specific absorptive filters are discussed, and the experimental results presented demonstrate the validity of the concepts developed. Insertion loss of up to 50 db for second harmonic power (TE₁₀ or TE₂₀ mode) and less than 0.1 db for the fundamental at S-band could be accomplished using a waveguide filter of eight inches length. The VSWR is of the order of 1.5 or better throughout the entire useful frequency range. The wide band performance of the filters is characterized by the fact that satisfactory operation results if the frequency of the fundamental falls within the range of dominant TE₁₀ mode propagation in rectangular guide, excluding the extreme edges of the band.

INTRODUCTION

THE progressive utilization of the microwave spectrum for general communication purposes brings the problem of interference more and more into the focus of attention. Thus the design of microwave filters, both on the transmitter as well as on the receiver side, has evolved as a well-controlled art¹ to

fill the needs created by the increase in the number of operating systems.

The fact that all power generators used in one system also produce an appreciable amount of harmonic power results in direct interference with other systems which operate at harmonic frequencies. Thus, as a specific example, the third harmonic of an S-band transmitter might interfere with an X-band system unless the harmonics are suppressed at the source. Consequently, filters which are capable of withstanding the high power levels found in modern microwave transmitters are required to reject or absorb harmonic power.

Since the resonant elements commonly used in conventional filters lead to excessively large field strengths, evacuation of such structures becomes necessary for high power applications. On the other hand, the conventional design procedures may be modified to avoid breakdown by spreading the resonance fields as much as possible. Such approaches toward reflective high power filters have been reported by Cohn and Vogelman. Cohn² employs inductive irises in rectangular guide and imposes conditions that lead to equal maximum electric field strength in the cavities thus formed.

* Original manuscript received by the IRE, March 4, 1959; revised manuscript received, June 8, 1959.

† General Electric Microwave Lab., Palo Alto, Calif.

¹ S. B. Cohn, *et al.*, "Final Report, Research on Design Criteria for Microwave Filters," Stanford Res. Inst., Palo Alto, Calif., Contract period covered March, 1955 to April, 1957, DA 36-039-SC-64625; June, 1957.

² S. B. Cohn, "Direct-Coupled-Resonator Filters," Proc. IRE, vol. 45, pp. 187-196; February, 1957.

This optimizes the power-handling capacity, and it is claimed that the breakdown properties of the unperturbed guide may be approached. Vogelman³ deliberately introduces higher order mode propagation in his structure by increasing the b -dimension of standard rectangular waveguide. The higher order mode resonances obtained in various tapered sections produce a good filter characteristic, and the high power capabilities are reported to be excellent.

The concept of introducing perturbations in the original waveguide to obtain selectivity always suffers from the propagation of higher order modes at harmonic frequencies, which lead in turn to spurious passbands. Thus, for suppression of harmonic power, special changes in guide geometry such as ridge guide or toll-ticket guide become necessary. The number of propagating modes is minimized accordingly, and extended frequency range filters may be designed.¹ These suffer from the effects of high power breakdown, mentioned before, due to reduced dimensions.

Thus we have pointed out two disadvantages of high power reflective filters: either spurious passbands at harmonic frequencies within the range of the second and especially the third harmonic, or breakdown problems. Since most high power generators are fairly sensitive to reflections, there appears another principal difficulty for reflective filters, the elimination of which would require ferrite isolators. These in turn are not very desirable if we consider insertion loss, higher order mode propagation problems, and complexity. Consequently, for certain applications absorptive filters may be highly desirable.

The concept of the absorptive harmonic power filter has been given some thought by Edson and Cohn. Edson⁴ suggests an arrangement of resonant slots on a waveguide of largely arbitrary cross section which is surrounded by lossy material, which in turn is shielded to form a closed system. This structure is quite similar to a muffler, and was named accordingly. The disadvantage of Edson's scheme is excessive attenuation of the fundamental by leakage through the slots. Cohn⁵ recognizes the importance of the wall thickness to introduce cutoff properties in his structure, which otherwise is very similar to Edson's. This scheme would suffer from undesired resonances at harmonic frequencies, due both to large dimensions of the apertures in the direction of propagation, as well as to mutual coupling through the lossy region.

Although the concepts to be described in the following have been arrived at by taking an entirely different approach, that of lossy periodic structures, there is a certain amount of resemblance to the previous schemes in

the appearance of the physical structures developed. Thus, they should be considered as only an extension of the basic principle described by Edson or Cohn.

The author is also aware of development efforts for absorptive ferrite filters, which have not yet been reported in detail in the literature. Therefore, it seems premature to make a comparison between such structures, and the filters to be described in the following. For this one would have to take into consideration such factors as power handling capacity, broadband performance, insertion-loss, and VSWR in the passband as well as in the stopband for the entity of propagating modes; also weight, size and, finally, cost. It is believed at this time that absorptive filters of the type to be described here offer several important advantages over corresponding ferrite structures.

LOSSY ARRAY TYPE ABSORPTIVE FILTERS

Frequency selective energy absorption in the microwave region may conveniently be accomplished by the arrangements illustrated in Fig. 1. Both Figs. 1(a) and 1(b) show a main guide propagating fundamental and harmonic power and an auxiliary guide or absorber.

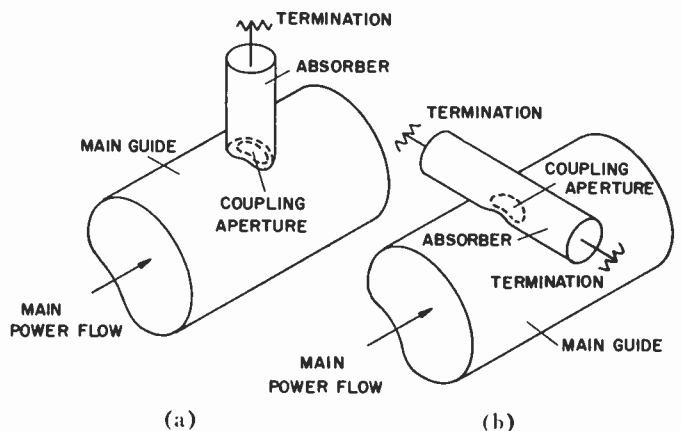


Fig. 1—Principle of harmonic absorbers.

Coupling from the main guide to the absorber is obtained through a suitably chosen aperture or apertures, designed to match the fields of the waves propagating from the main guide into the absorber. Energy entering the absorber is dissipated in a low-reflective wide band load or loads. The frequency selectivity of power dissipation in the device results from the cutoff properties of the absorber below a certain frequency, denoting the upper end of the passband of the absorptive filter.⁶ Below the cutoff frequency of the absorber, the coupling apertures merely represent a reactive loading of the main guide, while at frequencies above cutoff, energy will enter the absorber to be dissipated in its load.

Two basically different principal arrangements of the absorber with respect to the main guide are illustrated

³ J. H. Vogelman, "High-power microwave filters," IRE TRANS. ON MICROWAVE THEORY AND TECHNIQUES, vol. MTT-6, pp. 429-439; October, 1958.

⁴ W. A. Edson, private communication.

⁵ S. B. Cohn, "Microwave filter design for interference suppression," Proc. Symp. on Electromagnetic Interference, U. S. Army Signal Corps, pp. 230-251; June, 1958.

⁶ Very recently a patent came to the author's knowledge, where these concepts are expressed quite similarly. Compare: W. L. Pritchard, et al., "Selective Absorbers," U. S. Patent No. 2,869,085; January 13, 1959.

in Figs. 1(a) and 1(b). The choice of configuration will ultimately depend on the mode composition in the main guide, as well as on manufacturing techniques.

The main guide may be any type of microwave transmission line such as waveguide or coaxial line. Waveguide has to be used for the absorbers to obtain the cutoff characteristic essential for the functioning of the device. The coupling apertures have to be chosen in accordance with the fields in the main and auxiliary guide, and optimum power transfer into the absorber in the desired stopband of the filter should be aimed for. With regard to the size of the coupling apertures, it should be kept in mind that, for a flat absorption characteristic, some dimensions have to be small compared with the wavelength of the highest frequency, in order to avoid resonances. This will limit the amount of power which can be diverted into the auxiliary guide by one aperture. On the other hand, resonance apertures or the tuning of the apertures inside of the absorber may be useful to obtain maximum power transfer into the absorber and to control the frequency dependence of absorption.

Practically, a single absorber will not be sufficient to effect any substantial amount of energy dissipation in the desired stopband, and in a physical case there will always be an array of absorbers.

It is readily seen that a periodic structure consisting of a section of main guide loaded by a large number of equally spaced and oriented apertures, each coupling to its broadband-terminated absorber cell, is most advantageous in view of both the passband as well as the stopband transmission. Then we face a situation very similar to that in slow-wave circuits, which have been extensively described,⁷ and which are well understood. Considering reactive as well as resistive loading of the main guide by the apertures, for the two characteristic ranges of operation, we obtain a structure with a minimum amount of electrical dissimilarity from the main guide if the circuit period is small compared with one wavelength for all frequencies to be considered.⁸ Accordingly, we may expect the possibility of an extremely broadbanded transition from the main guide to the filter section.

Indeed, it turns out that even abrupt changes between periodic structure and main guide lead to VSWR values not larger than from 1.20 to 1.50 (depending on the type of structure) at frequencies below the circuit-spacing resonance, and excluding the immediate vicinity of the absorber cutoff frequency.

Depending on the choice of size and orientation of the apertures, the absorber array will cause a certain amount of attenuation per unit length in the stopband of the filter, for each propagating higher order mode. For some modes the structure will be more effective than for others, according to the specific field and aper-

ture configurations, but all modes will be attenuated to some significant extent if absorbers are properly placed at the critical locations on the main guide.

A multitude of array compositions based on a periodic repetition of the arrangements of Figs. 1(a) and 1(b) may be prescribed. Several typical examples will be discussed in the experimental part of this paper.

DISTRIBUTED LOSS ABSORPTIVE FILTER

In the previous section, types of filters were introduced which utilize the cutoff properties of the absorber in its usual direction of propagation. Additionally, Fig. 1 merely showed one absorber and its typical arrangement, but not the entire array. In Fig. 2, on the other hand, an absorptive filter is shown which consist of only two coupled waveguides. As in Figs. 1(a) and 1(b), there is a main guide which provides power flow, as indicated, at both the fundamental and harmonic frequencies, and with several modes of propagation. On the other hand, the absorber is beyond cutoff for the fundamental, but propagates harmonic frequencies. The two guides are coupled by a series of apertures periodically arranged with a spacing, d . The shape of these apertures is largely arbitrary, but one dimension will always be small as compared with the dimensions of the absorber cross section.

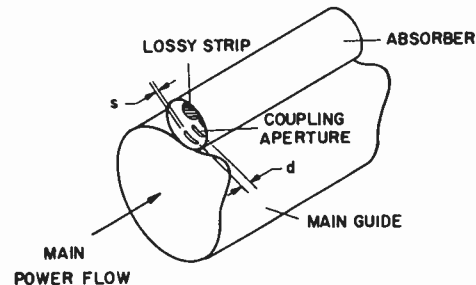


Fig. 2—Distributed loss absorptive filter.

Additionally, a strip of lossy material extends all the way along the absorber such that it is at the maximum distance from the coupling apertures. Thus the absorber provides a certain attenuation per unit length for waves propagating in its interior. (Using carbonized ceramic strips in rectangular X-band waveguide, attenuations of 4 db/cm are readily accomplished.)

Again, the spacing and size of the coupling apertures are chosen to accomplish optimum wide band power transfer from the main guide into the absorber at higher harmonic frequencies. In the passband of the filter, the periodic array of reactively loaded apertures will represent an excellent wide band structure for the fundamental. For higher harmonic frequencies which enter the absorber, the frequency sensitivity of coupling energy from the main guide will, to a large extent, depend on the loss per unit length accomplished. For appreciable attenuation between adjacent apertures, directive effects due to the accumulative interaction of the individual apertures should be negligible. To obtain good

⁷ L. Brillouin, "Wave Propagation in Periodic Structures," Dover Publications, New York, N. Y.; 1953.

⁸ Needless to say, this also implies good high-power performance and reduced breakdown problems, since the individual apertures represent only small perturbations of the main guide.

field matching through the apertures, the dimensions of absorber and main guide should be properly chosen with special attention to the specific modal distribution.

Since the critical width, s , of the apertures is chosen to be small with respect to the dimensions of the absorber cross section, as well as the aperture spacing, d , the nonpropagating fields of the fundamental penetrate into the absorber only a few distances, s , to any practical extent. As mentioned before, the lossy material is spaced at the maximum distance from the coupling apertures, and thus has negligible influence on the fundamental. Experiments show the validity of the principle described, which is also very attractive in view of manufacturing considerations.

LABORATORY TESTS ON SPECIFIC FILTER STRUCTURES

Grill-Type Cross Section Periodic Structures

Based on the principle outlined in Fig. 1(a), an array of rectangular guides has been constructed and is illustrated in Fig. 3. The face of the absorber-array in the photograph replaces a section of broad wall of standard rectangular *S*-band waveguide. The resistive card terminations in each absorber cell, visible in Fig. 3, are practically without reflection for a large range of frequencies. For reasons of convenience in mechanical construction, the dividing vane at half the distance of the *S*-band a -dimension extends only partially into the lossy region. The position of the absorber on the main guide is shown in Fig. 4 (further explanation to be given later). The individual absorber cells represent rectangular waveguides of the dimensions $a = 1.375$ inches and $b = 0.250$ inch. Accordingly, a TE_{10} cutoff frequency of 4.29 kmc results, denoting the lower limit of absorption of energy in the device. The b -dimension of the cells is chosen small as compared with a wavelength of the highest frequency of interest, *i.e.*, that of the third harmonic of *S*-band which lies in the *X*-band range. Early experiments showed that otherwise resonances appear, which are to be expected according to the theory of slow-wave circuits. (This corresponds to the well-known situation where the circuit spacing becomes of the order of half a wavelength of the propagating slow-wave.)

Transmission tests in standard *S*-band guide with the structure of Fig. 3 replacing a section of broad wall showed excellent VSWR performance in the passband (2.2 kmc to 4.0 kmc) and insertion loss of the order of 12 db to 15 db in the stopband (at frequencies from 5.5 kmc to 7 kmc). Insertion loss in the passband was as low as 0.03 db. For these tests only one side of the waveguide was replaced by an absorber; insertion loss of better than 20 db may be expected for a filter section of eight inches length with two absorbers (as shown in Fig. 3) on opposite broad walls.⁹ High power tests have shown that the breakdown properties of the structure are excellent.

⁹ V. G. Price, R. Stone, and V. Met, "Leaky wall filters for harmonic suppression," to be presented at the 1959 WESCON CONVENTION, San Francisco, Calif.; August 18-21.

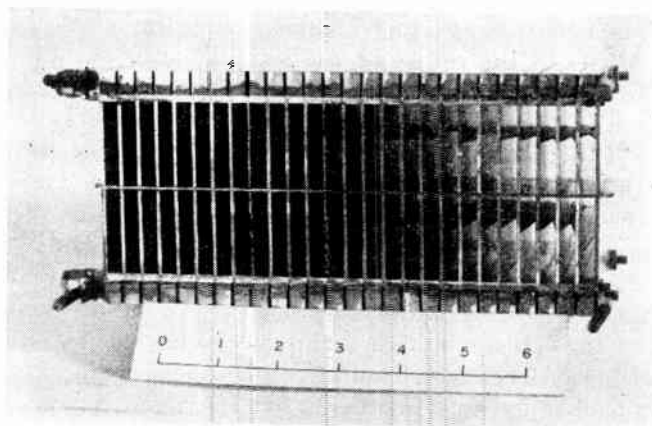


Fig. 3—Grill-type absorber array.

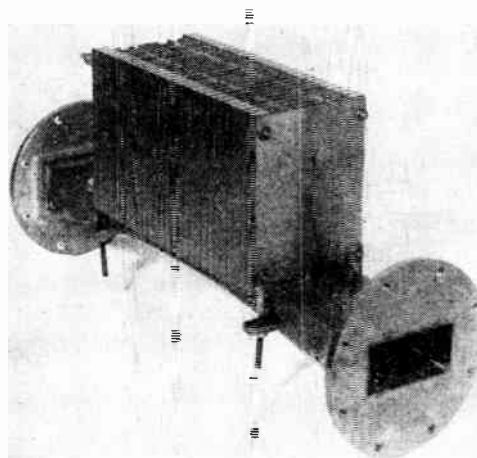


Fig. 4—Assembled absorptive harmonic filter.

To investigate the limits of the insertion loss obtainable for harmonic power for a prescribed length of waveguide, the b -dimension, and thus the impedance of the main guide, was reduced to render better coupling due to improved field matching into the absorber cells. This resulted in the double logarithmic cosine taper of the main guide employed in the filter shown in Fig. 4. A taper of this sort has several advantages. a) It increases the coupling to the absorber cells according to improved field matching as outlined above. Thus, for a given length of main guide, a greater amount of insertion loss for harmonic power may be accomplished. b) The dissipative structure intercepts harmonic energy more gradually, *i.e.*, there is a less abrupt change of the main guide as far as harmonic power flow is concerned. c) For harmonic power, each absorber cell is connected essentially in series with the main guide. Thus, the main guide impedance should gradually decrease in the direction of propagation to assure continuous impedance as seen by the waves to be absorbed, which situation may be approximated by a tapered section suitably chosen.

Disadvantages of the reduction of height are the increased breakdown problems and the larger VSWR for the fundamental in the passband of the filter. The main advantage is the more compact structure thus obtained.

The results of the transmission and reflection measurements in the region of the second harmonic of S -band are summarized in Fig. 5. It is apparent that, except for the range close to the cutoff of the absorber cells, the properties of the filter are quite satisfactory. Insertion loss in the passband stays below 0.1 db for frequencies up to about 3.5 kmc, and is determined on the short-circuited filter by a VSWR measurement. The increase of the insertion loss in the range from 3.5 kmc to 4 kmc is most probably due to excessive surface loss along the periodic structure, and may be reduced by improving surfaces and rounding corners. Also, a widening of the dividing vane, in order to have a narrow conducting path along the center of the absorber, should improve the situation as well as the high-power handling capabilities.

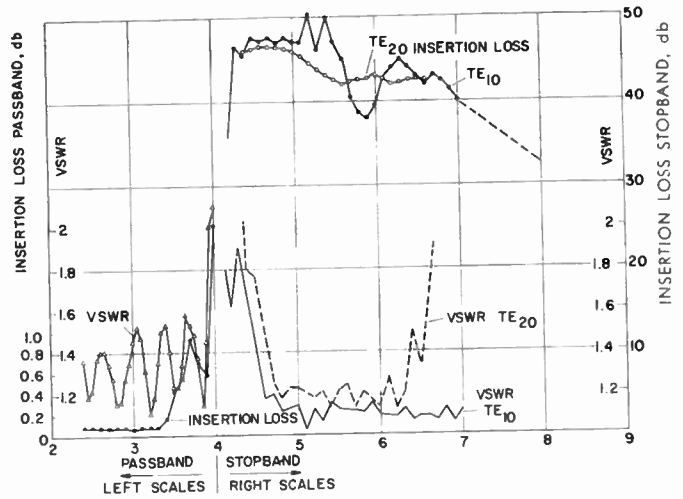


Fig. 5—Transmission characteristic of the filter shown in Fig. 4.

The VSWR in the passband shows a periodic variation, and thus it should be possible to further reduce reflection by a series of tuning elements appropriately located along the periodic structure. In the stopband, the VSWR is low throughout. It should be kept in mind that for the TE_{20} mode, the VSWR is measured in the E -plane arm of the folded hybrid serving as a mode launcher in conjunction with a taper. Thus the VSWR increases rapidly outside of its passband (*i.e.*, the frequency range from 4.8 kmc to 6.3 kmc). A linear taper served as a mode launcher for the TE_{10} mode; both mode launchers are shown in Fig. 6.

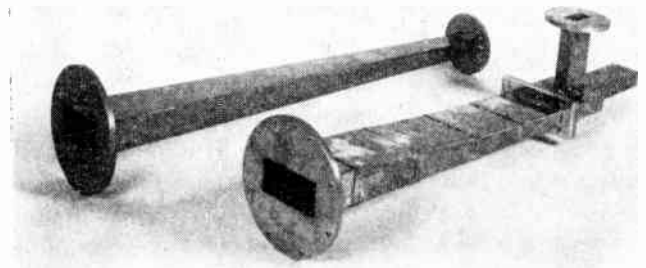


Fig. 6—Mode launchers for the TE_{10} and TE_{20} modes.

The insertion loss at harmonic frequencies is also plotted in Fig. 5. While the insertion loss for the TE_{20} mode remains fairly constant, at least for the frequency range of the measurements, that for the TE_{10} mode decreases gradually above the TE_{30} cutoff of the main guide. This may be explained with the following simple logic. As mentioned before, the absorber replaces a section of main guide broad wall, and the fields have to propagate along a structure, as sketched in Fig. 7. If a TE_{n0} mode propagates in the main guide, it is conceivable that the nature of the fields in the section with the periodic structure does not change drastically, although it can no longer be called a waveguide mode. Thus, modes of odd symmetry like the TE_{20} should couple better to the absorber cells than modes of even symmetry since the dividing vane presents less of a perturbation. For modes of odd symmetry, we may introduce a center dividing vane in the main guide without disturbing the fields, and this should also be reasonably true in the periodic structure. Then, our problem may be resolved into that of propagation in two separate waveguides and periodic structures, which phenomenon has been extensively studied. Since the absorber cells are all assumed to be terminated in their characteristic impedance, a much simpler situation results than in the case of the usual slow-wave circuit with reactive terminations. By the simplified analogy to the case of a plane wave over an array of semi-infinite parallel plates, it may then be stated that, theoretically, there is no propagation along the periodic structure. Practically,

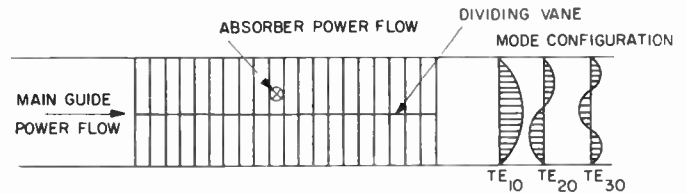


Fig. 7—Cross-sectional view of the absorber.

this is almost true, as illustrated by the insertion loss exceeding 40 db for an absorber extending eight inches along the main guide. For modes of even symmetry, the presence of the center vane will be of appreciable influence, and it is conceivable that at high frequencies the periodic structure will support a mode of propagation with large field concentration along the center vane and a corresponding reduction of coupling to the individual absorber cells. This seems to be the cause of the reduction in insertion loss for the TE_{10} mode at higher frequencies above 7 kmc.

Transmission at higher frequencies was checked by the crude but satisfactory method of launching and receiving with ordinary X -band waveguide detector mounts. Insertion loss of about 30 db to 35 db could be observed at frequencies above 7 kmc, for symmetrical as well as asymmetrical excitation and pickup. For frequencies above the TE_{30} mode cutoff in the main guide, a varying amount of the TE_{10} to TE_{30} mode conversion from input to output could be observed. This is probably due to the fact that there is strong coupling, by way

of the apertures of the individual absorber cells, between TE_{10} and TE_{30} type fields in the periodic structure. A periodic structure with three rows of absorber cells may exhibit different behavior and, due to the absence of a center vane effect, might also render better insertion loss at higher frequencies.

No experimental data are available at present to illustrate the absorber properties of the grill-type cross section structures for other modes than that of the TE_{n0} type. All measurements have to be somewhat specialized or even crude at this stage of investigation, since reasonably accurate measurements of transmission and reflection for frequencies including the third harmonic are complex and costly. A multiple probe measurement and analysis would have to be performed^{10,11} which, in order to include reflection and mode conversion, would involve a complex programming scheme for a digital computer.

Special structures like the double logarithmic cosine taper used for the filter of Fig. 4 will, by themselves, suppress a number of modes due to the change in guide geometry. Fig. 8 shows the respective cutoff frequencies for a typical example. Little is known about the percentage of conversion and reflection of higher order modes incident to such a change of geometry.

The grill-type structure combined with the double cosine taper also presents a fairly simple case, with three different modes at the most, for the frequency range of interest. Thus the cutoff region in Fig. 5 can be examined quite carefully. Only two mode launchers are needed for frequencies up to about 7 kmc, and measurements with a cross-guide sliding probe in the main guide show good agreement with the theoretical field distributions at higher harmonic frequencies, for both the TE_{10} and the TE_{20} mode.

Distributed Loss Absorptive Filter

For this type of filter the case of rectangular waveguide, both for the main guide as well as the absorber, is of particular interest.

Preliminary tests were conducted by placing lossy strips into standard slotted waveguide sections and directly measuring the attenuation per unit length by means of the probe. Carbonized ceramic strips were found to be a material excellently suited for the purpose, especially in view of eventual operation in a hard vacuum. In X-band waveguide, for a strip with a 0.5 inch \times 0.125 inch cross section, the attenuation per centimeter obtained is tabulated below.

<i>f</i>	8	8.5	9	9.5	10	kmc
Attenuation	2	3	4	4.5	5.5	db/cm

¹⁰ M. P. Forrer and K. Tomiyasu, "Determination of higher order propagating modes in waveguide systems," *J. Appl. Phys.*, vol. 29, pp. 1040-1045; July, 1958.

¹¹ V. G. Price, "Measurement of harmonic power generated by microwave transmitters," *IRE TRANS. ON MICROWAVE THEORY AND TECHNIQUES*, vol. MTT-7, pp. 116-120; January, 1959.

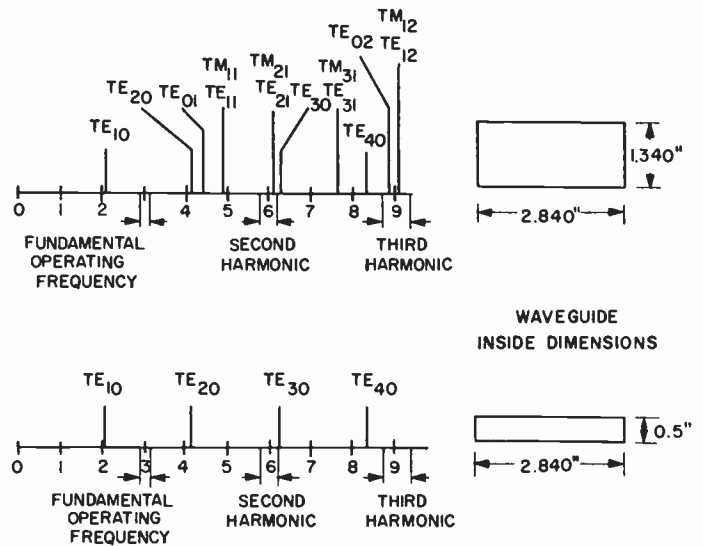


Fig. 8—Higher order mode cutoff frequencies for different cross sections of rectangular waveguide.

From these values one can roughly estimate the amount of aperture interaction to be expected for each specific spacing, *d* (Fig. 2).

Using the double cosine taper available from previous experiments, the filter illustrated in Figs. 9 and 10 was constructed. Note the absorber design and the lossy strips in position in Fig. 9, with a single absorptive strip placed outside for comparison. The assembled filter is shown in Fig. 10.

Fig. 11 demonstrates the performance of the filter. The over-all transmission characteristic for the fundamental as well as the third harmonic¹² is characterized by very low VSWR. The insertion loss for the fundamental is seen to be better than 0.1 db for a large range. For this, again a VSWR measurement of the short-circuited filter was employed.

The influence of the presence of the lossy strips on the fundamental was also investigated. Measurements of the short-circuited filter, with and without lossy strips, were practically identical and showed minor difference only above 3.5 kmc. Thus the validity of the basic concept was established by an exact method: the fundamental does not penetrate to the lossy strips to any practical extent for the proper dimensions of the apertures and the absorber cross section.

The desired insertion loss occurs at frequencies of the third harmonic according to the particular absorber configuration of the filter, shown in Figs. 9 and 10. Although the structure is by far not as effective as the one described previously, it has definite merit from the manufacturing point of view. At harmonic frequencies, the apparent decrease of the insertion loss with frequency, as observed in Fig. 11, is not yet completely understood. Most probably this occurs due to the fact that the impedance as well as the guide wavelength of the

¹² In Fig. 11, the VSWR grid lines for the stop band should be labeled analogously to those for the pass band.

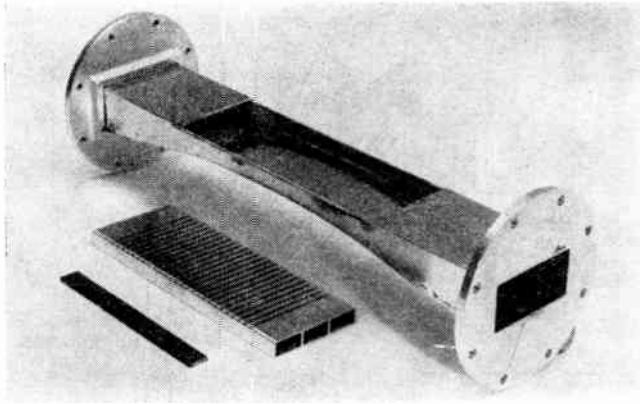


Fig. 9—Disassembled double cosine tapered distributed loss harmonic filter for the third harmonic.

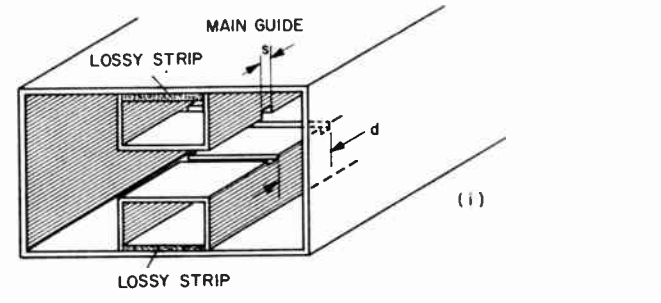
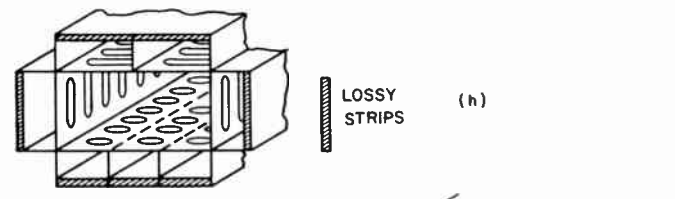
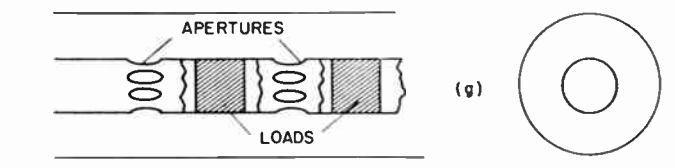
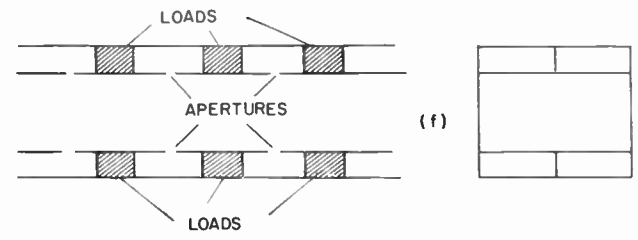
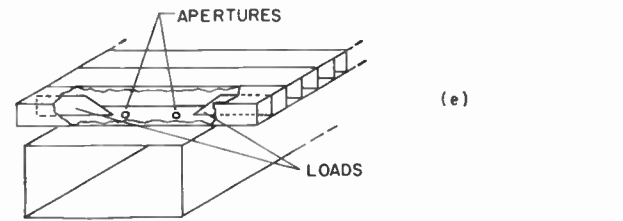
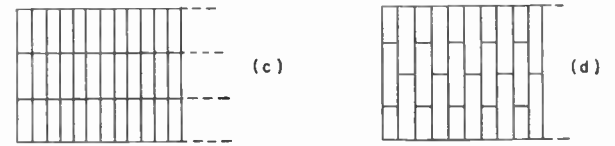
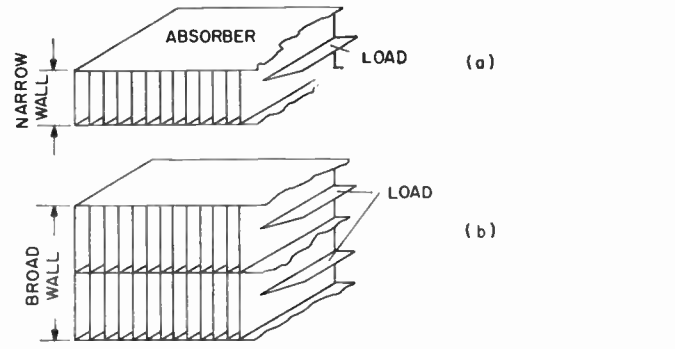


Fig. 12—Absorber configurations.

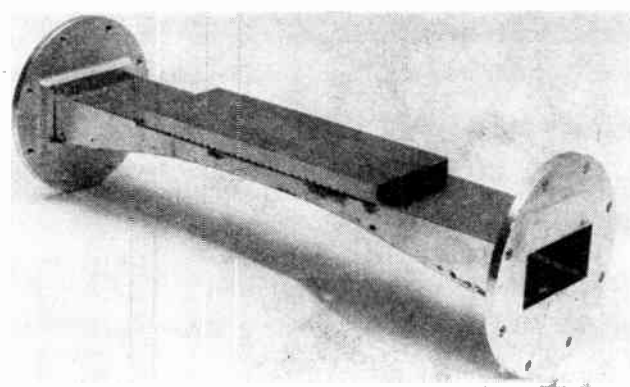


Fig. 10—Assembled filter.

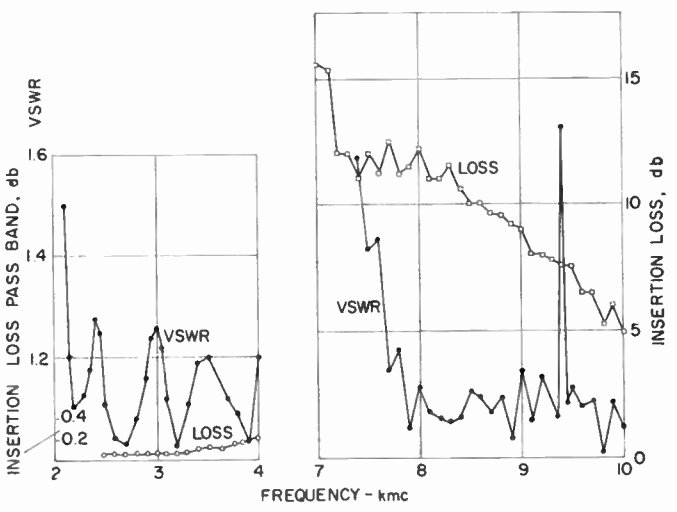


Fig. 11—Transmission characteristic of the absorptive filter shown in Figs. 9 and 10, TE₁₀ mode.

secondary guide increase considerably when approaching cutoff conditions.

Geometric Configurations for Absorptive Filters

Various arrangements for absorptive filters which are based on the principles outlined in the previous sections are sketched in Fig. 12. They are briefly discussed in consecutive order in the following paragraph.

Figs. 12(a)–12(d) illustrate the grill-type cross section absorber type filter with locations on broad or narrow walls of the main guide. Figs. 12(c) and 12(d) merely show the cross sections, and one can think of a large variety of combinations of these and other basic types of structures on all four sides of rectangular guide. Corresponding structures may be designed for a main guide which is not rectangular. Fig. 12(e) illustrates an absorber arrangement based on cross-guide coupling, resulting from Fig. 1(b).

The principle of periodic loading, which is also based on the arrangement of Fig. 1(b), is illustrated by Figs. 12(f) and 12(g). The former shows a combination of rectangular guides, the other shows a coaxial system with a circular guide which serves as a center conductor and an absorber. The loads are sufficiently remote from the apertures to utilize the absorber cutoff properties at the fundamental. Finally, the isometric views of Figs. 12(h) and 12(i) demonstrate a possible configuration of lossy strip absorbers with slot type apertures on the main guide. Again, one can think of a variety of combinations of absorbers.

CONCLUSION

The theoretical investigations have led to three basically different types of structures for absorptive filters. All three utilize the cutoff properties of waveguide to achieve power transfer into an absorber at high frequencies, with negligible loss for the lower frequencies to be

propagated in the main guide. Experimental investigations on several typical structures have been conducted which show the validity of the suggested schemes. Satisfactory match and very low insertion loss in the pass band, and low-reflection absorption of energy in the stop band were demonstrated. Such filters thus lend themselves readily to be incorporated in high-power systems, for purposes of harmonic suppression and interference reduction.

Since many practical higher order mode problems result from resonance effects, loading of the particular section of "main guide" (in a very general sense) with a very simple absorptive filter of low insertion loss, *i.e.*, a "harmonic pad," will eliminate such problems completely. Especially when located close to or within the generator, such a pad will sufficiently load all resonances at harmonic frequencies. For example, these may otherwise trigger off a high power breakdown in a system operated close to its power-carrying capabilities for the fundamental.

Thus, it appears that absorptive filters of the type described should find various applications in present and future high power system and tube design at microwave frequencies. Although the experiments reported here are of a somewhat specialized nature, taking into account only the TE_{10} , TE_{20} , and TE_{30} modes in rectangular waveguide, it is believed that the principles developed are most readily applicable to more general modal configurations.

Simple Methods for Computing Tropospheric and Ionospheric Refractive Effects on Radio Waves*

S. WEISBROD†, MEMBER, IRE, AND L. J. ANDERSON†

Summary—The paper describes a simple and accurate method for computing ionospheric and tropospheric bending. The only assumptions made are that the refractive gradient is radial and that the refractive index profile can be approximated by a finite number of linear segments whose thickness is small compared with the earth's radius. These assumptions are readily justifiable in all practical cases. Since there are no limitations on the angle of elevation and the shape of the refractive index profile, the method has a wide application and it is extended to cover other refractive effects such as retardation, Doppler error and Faraday Rotation.

INTRODUCTION

THE bending of radio waves passing through the troposphere and ionosphere has aroused considerable interest in recent years. Such bending bears directly on the accuracy of tracking radio stars, satellites, missiles and other high-altitude objects. This problem has been attacked by a number of investigators and several different methods have been developed.¹⁻⁶ Most of these, however, are either of limited accuracy or too laborious for routine application where both speed and accuracy are required.

A method is presented in this paper which is particularly simple and which can be applied to both tropospheric and ionospheric bending. There are no limitations on the shape of the profile or angle of elevation. The only assumptions are that the refractive index gradient is only in the vertical plane, that the index of refraction profile can be approximated by a number of linear segments, and that the thickness of these steps is small compared to earth's radius. Since these assumptions are readily justifiable in all practical cases, the method has a wide application.

In addition to refractive bending, the closely related problem of signal retardation is also considered and a simple approximate method, analogous to the one used for computing the bending, is developed.

* Original manuscript received by the IRE, November 17, 1958; revised manuscript received, June 12, 1959. Sponsored by Rome Air Dev. Center, Air Res. and Dev. Command, Griffiss Air Force Base, Rome, N. Y., in connection with Contract AF 30(602)-1624.

† Smyth Research Associates, San Diego, Calif.

¹ M. Shulkin, "Average radio ray refraction in the lower atmosphere," *PROC. IRE*, vol. 40, pp. 554-561; May, 1952.

² V. A. Counter, "Propagation through the troposphere and ionosphere," presented at the IRE and URSI Joint Meeting, Washington, D. C.; May, 1956.

³ B. M. Fannin and K. H. Jehu, "A study of radar elevation-angle errors due to atmospheric refraction," *IRE TRANS. ON ANTENNAS AND PROPAGATION*, vol. AP-5, pp. 71-77; January, 1957.

⁴ L. J. Anderson, "Tropospheric bending of radio waves," *Trans. AGU*, vol. 39, pp. 208-212; April, 1958.

⁵ B. R. Bean and G. D. Thayer, "A Model Radio Refractivity Atmosphere," *Natl. Bur. Stand. Rept. 5576*, pp. 18-22; June, 1958.

⁶ G. H. Millman, "Atmospheric effects on VHF and UHF propagation," *PROC. IRE*, vol. 46, pp. 1492-1501; August, 1958.

DEVELOPMENT OF THE METHOD

Referring to Fig. 1, consider a ray entering at angle β an infinitesimal layer of thickness $d\rho$. Since the curvature of the ray is equal to the component of the refractive gradient normal to the ray, divided by the index of refraction, it follows that:

$$\frac{1}{K} = \frac{1}{n} \frac{dn}{d\rho} \cos \beta \tag{1}$$

where K is the radius of curvature.

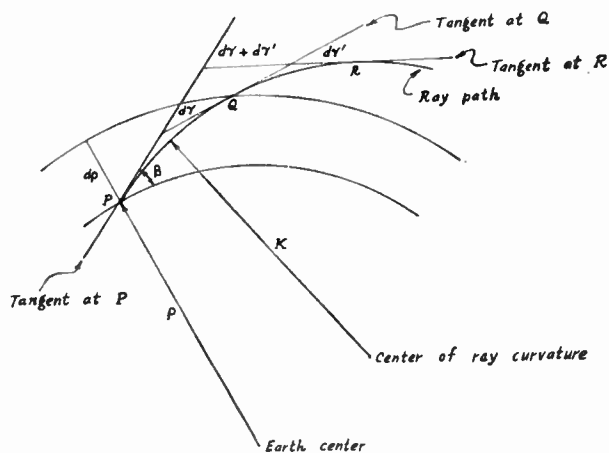


Fig. 1—Geometry of bending through an infinitesimal layer.

The length of the ray path in the layer is

$$K d\gamma = \csc \beta d\rho \tag{2}$$

which, combined with (1), gives

$$d\gamma = \frac{1}{n} \frac{dn}{d\rho} \cot \beta d\rho. \tag{3}$$

Since $d\gamma$'s of all elementary layers are directly additive, as shown in Fig. 1, by considering $d\gamma'$ due to bending between points Q and R , it follows that the contribution to the total bending γ , due to a layer bounded by the heights ρ_j and ρ_k is

$$\gamma_{jk} = \int_{\rho_j}^{\rho_k} \frac{1}{n} \frac{dn}{d\rho} \cot \beta d\rho. \tag{4}$$

If the ray departs from the earth's surface with the elevation angle of α_0 , Snell's Law for spherical stratification states:

$$n_0 a \cos \alpha_0 = n \rho \cos \beta = \text{constant} \tag{5}$$

where

- n_0 = surface index of refraction,
- a = Earth's radius,
- $\rho = a + h$,
- h = height above earth,
- n = index of refraction at the specified height.

From (5) we get

$$\cos \beta = (n_0 a / n \rho) \cos \alpha_0 = (n_j \rho_j / n \rho) \cos \beta_j \quad (6)$$

$$\begin{aligned} \sin \beta &= (n_0 a / n \rho) [(n \rho / n_0 a)^2 - \cos^2 \alpha_0]^{1/2} \\ &= (n_j \rho_j / n \rho) [(n \rho / n_j \rho_j)^2 - \cos^2 \beta_j]^{1/2} \end{aligned} \quad (7)$$

$$\begin{aligned} \cot \beta &= [(n \rho / n_0 a)^2 - \cos^2 \alpha_0]^{-1/2} \cos \alpha_0 \\ &= [(n \rho / n_j \rho_j)^2 - \cos^2 \beta_j]^{-1/2} \cos \beta_j \end{aligned} \quad (8)$$

where n , ρ and β are the values of these parameters at some height h .

Eq. (8) can be substituted in (4) to give the general equation for refractive bending.

$$\begin{aligned} \gamma_{jk} &= \int_{\rho_j}^{\rho_k} \frac{1}{n} \frac{dn}{d\rho} \frac{\cos \alpha_0}{[(n \rho / n_0 a)^2 - \cos^2 \beta_j]^{1/2}} d\rho \\ &= \int_{\rho_j}^{\rho_k} \frac{1}{n} \frac{dn}{d\rho} \frac{\cos \beta_j}{[(n \rho / n_j \rho_j)^2 - \cos^2 \beta_j]^{1/2}} d\rho. \end{aligned} \quad (9)$$

We now assume that a) $dn/d\rho = -k = \text{constant}$, b) $\rho_k - \rho_j \ll \rho_j$, and c) index of refraction n is very nearly equal to unity. On the basis of these assumptions we can write:

$$k = \frac{(N_j - N_k) \times 10^{-6}}{\rho_k - \rho_j} = \frac{(N_j - N) \times 10^{-6}}{\rho - \rho_j} \quad (10)$$

where $N = (n - 1) \times 10^6$

$$\begin{aligned} (n \rho / n_j \rho_j)^2 &= \{ [1 - (N_j - N) \times 10^{-6}] [1 + (\rho - \rho_j) / \rho_j] \}^2 \\ &\cong 1 + 2(\rho - \rho_j)(1 - k \rho_j) / \rho_j \end{aligned} \quad (11)$$

and, substituting in (9) we get

$$\begin{aligned} \gamma_{jk} &= k \cos \beta_j \int_{\rho_j}^{\rho_k} [\sin^2 \beta_j + 2(\rho - \rho_j)(1 - k \rho_j) / \rho_j]^{-1/2} d\rho \\ &= \frac{k \rho_j \cos \beta_j}{1 - k \rho_j} \{ [\sin^2 \beta_j + 2(\rho_k - \rho_j)(1 - k \rho_j) / \rho_j]^{1/2} \\ &\quad - \sin \beta_j \}. \end{aligned} \quad (12)$$

From (6), (7), and (11)

$$\begin{aligned} \sin \beta_k &= (n_j \rho_j / n_k \rho_k) [(n_k \rho_k / n_j \rho_j)^2 - \cos^2 \beta_j]^{1/2} \\ &= (\cos \beta_k / \cos \beta_j) [\sin^2 \beta_j + 2(\rho_k - \rho_j)(1 - k \rho_j) / \rho_j]^{1/2}. \end{aligned} \quad (13)$$

Combining with (12)

$$\gamma_{jk} = \frac{k \rho_j \cos^2 \beta_j}{1 - k \rho_j} (\tan \beta_k - \tan \beta_j). \quad (14)$$

From (6), (10), and (11)

$$\begin{aligned} \frac{k \rho_j}{1 - k \rho_j} &= \frac{2(N_j - N_k) \times 10^{-6} \sec^2 \beta_j}{\sec^2 \beta_k - \sec^2 \beta_j} \\ &= \frac{2(N_j - N_k) \times 10^{-6} \sec^2 \beta_j}{\tan^2 \beta_k - \tan^2 \beta_j} \end{aligned} \quad (15)$$

which, substituted in (14), gives the desired expression for γ_{jk}

$$\begin{aligned} \gamma_{jk} &= \frac{(N_j - N_k) \times 10^{-6}}{\frac{1}{2}(\tan \beta_j + \tan \beta_k)} \\ &= \frac{N_j - N_k}{500(\tan \beta_j + \tan \beta_k)} \text{ milliradians} \end{aligned} \quad (16)$$

where N is expressed in N units, $(n - 1) \times 10^6$.

Total bending through the atmosphere is simply the sum of individual contributions.

$$\gamma(mr) = \sum_{k=0}^{n-1} \frac{(N_k - N_{k+1})}{500(\tan \beta_k + \tan \beta_{k+1})}. \quad (17)$$

REFRACTIVE BENDING REFERRED TO EARTH CENTER

It is frequently convenient to measure the refractive error in terms of the angle subtended from the earth's center. This quantity, denoted by ϵ , can be readily obtained from Fig. 2.

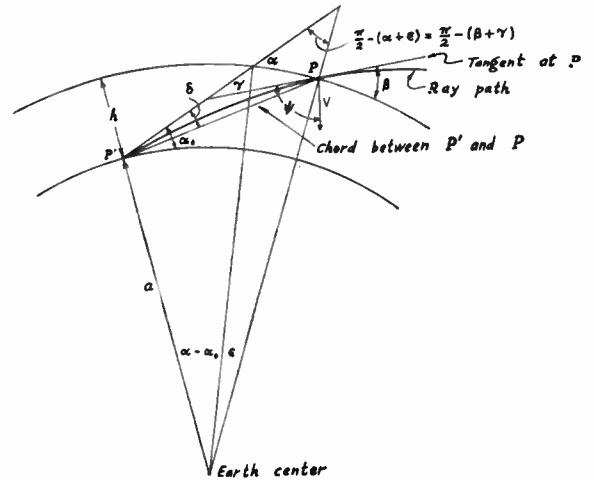


Fig. 2—Geometry of bending through a refractive layer.

$$\epsilon = \gamma - (\alpha - \beta). \quad (18)$$

The quantity $\alpha - \beta$ may be conveniently found in the following manner. From Snell's law we have

$$n_0 \cos \alpha = n \cos \beta$$

or

$$\begin{aligned} \cos \beta &= \cos [\alpha - (\alpha - \beta)] \\ &= [1 + (N_0 - N) \times 10^{-6}] \cos \alpha \end{aligned} \quad (19a)$$

$$\begin{aligned} \cos \alpha &= \cos [\beta + (\alpha - \beta)] \\ &= [1 - (N_0 - N) \times 10^{-6}] \cos \beta. \end{aligned} \quad (19b)$$

Expansion of (19) and the application of small angle approximations results in

$$\alpha - \beta = \{1 - [1 - 2(N_0 - N) \times 10^{-6} \cot^2 \alpha]^{1/2}\} \tan \alpha \quad (20a)$$

$$= \{[1 + 2(N_0 - N) \times 10^{-6} \cot^2 \beta]^{1/2} - 1\} \tan \beta. \quad (20b)$$

At heights above the troposphere for rays departing tangentially, or for angles of elevation greater than 100 milliradians at any height, α and β are very nearly equal and (20) reduces to:

$$\begin{aligned} \alpha - \beta &\cong (N_0 - N) \times 10^{-6} \cot \alpha \\ &\cong (N_0 - N) \times 10^{-6} \cot \beta. \end{aligned} \quad (21)$$

ELEVATION ANGLE ERROR

In most practical applications the quantity of greatest interest is the elevation angle error. This quantity denoted by δ can be obtained from Fig. 2 by the use of the law of sines.

$$\begin{aligned} a \cos \alpha_0 &= \rho \cos \alpha \\ a \cos (\alpha_0 - \delta) &= \rho \cos [(\alpha + \epsilon) - \delta]. \end{aligned} \quad (22)$$

From (22) we get

$$\tan \delta = \frac{\sin \epsilon \tan \alpha + (1 - \cos \epsilon)}{\sin \epsilon + \cos \epsilon \tan \alpha - \tan \alpha_0}$$

or

$$\delta = \frac{\epsilon \tan \alpha + \epsilon^2/2}{\epsilon + \tan \alpha - \tan \alpha_0}. \quad (23)$$

From (5), (18), and (22) an alternate form of (23) may be obtained

$$\delta = \frac{\gamma \tan \beta - (N_0 - N) \times 10^{-6} + \gamma^2/2}{\gamma + \tan \beta - \tan \alpha_0}. \quad (24)$$

Omitting $\epsilon^2/2$ in the numerator of (23) results in an error of about five per cent in the troposphere for a tangentially departing ray. At higher angles of elevation or greater heights, this error becomes negligible.

It should be noted that whereas γ and ϵ , due to the passage of the ray through various layers, are directly additive, δ 's are not. Thus, to evaluate δ at ionospheric heights or above, it is first necessary to combine the tropospheric and the ionospheric ϵ 's or γ 's and then use (23) or (24). However, it turns out that in nearly all practical cases above the troposphere $\epsilon^2/2 \ll \epsilon$ and $\epsilon \ll \tan \alpha - \tan \alpha_0$; consequently the omission of $\epsilon^2/2$ in the numerator and ϵ in the denominator usually results in less than five per cent error at *F* region heights.

Eq. (23) may thus be approximated by

$$\delta = \frac{\epsilon \tan \alpha}{\tan \alpha - \tan \alpha_0}. \quad (25)$$

It is, therefore, usually justifiable to add directly the tropospheric and ionospheric δ 's to obtain the total elevation angle error.

At astronomical distances all three quantities (γ , ϵ and δ) become numerically equal.

DOPPLER ERROR

Due to the refractive bending, there will generally be an error in the measurement of the radial component of the target velocity. The equation describing this can be readily derived with the aid of Fig. 2. Let V be the component of the target velocity in a plane determined by the transmitter beam and the earth's center. If ψ is the angle between V and the apparent direction, then the following statements can be made:

a) measured radial velocity is

$$V_m = V \cos \psi, \quad (26)$$

b) true radial velocity

$$V_r = V \cos [\psi - (\gamma - \delta)], \text{ and} \quad (27a)$$

c) apparent radial velocity

$$V_a = V \cos (\psi - \delta). \quad (27b)$$

Since γ and δ are at most on the order of a few milliradians, expansion of (27) using the usual small angle approximations results in

$$V_a - V_m = \Delta V_a = V \gamma \sin \psi \quad (28a)$$

$$V_r - V_m = \Delta V_r = V(\gamma - \delta) \sin \psi. \quad (28b)$$

The quantity which is usually of interest is ΔV_r , although for some applications ΔV_a may be the more convenient to use since beyond the refractive regions it is independent of height and range.

RETARDATION OF THE SIGNAL PASSING THROUGH A REGION OF A CONSTANT REFRACTIVE GRADIENT

Signal retardation $d\tau$ caused by a layer of thickness $d\rho$ (Fig. 1) is given by

$$\begin{aligned} d\tau &= (1/v - 1/c) \csc \beta d\rho \\ &= (c/v - 1) \csc \beta d\rho / c = N \times 10^{-6} c^{-1} \csc \beta d\rho \end{aligned} \quad (29)$$

where c and v are signal velocities in free space and the medium, respectively.

The range error is given by

$$\Delta r_{jk} = \int_{\rho_j}^{\rho_k} c d\tau = \int_{\rho_j}^{\rho_k} \frac{N \times 10^{-6} d\rho}{\sin \beta}. \quad (30)$$

In evaluating γ we found (16)

$$\gamma_{jk} = \int_{\rho_j}^{\rho_k} \frac{(dn/d\rho) d\rho}{\tan \beta} = \int_{\rho_j}^{\rho_k} \frac{dn}{\tan \beta} = \frac{(N_j - N_k) \times 10^{-6}}{\frac{1}{2}(\tan \beta_j + \tan \beta_k)}.$$

In other words, the value of the integral for the case of a constant radial gradient was found to be very nearly equal to the one that would have been obtained had we taken the average value of the denominator of the integrand and treated it as a constant. We are therefore tempted to treat the integral of (30) in a similar manner. Furthermore, we can argue that at low angles sine and

tangent are nearly the same and at high angles the rate of change of $\sin \beta$ is so slow that such procedure is certainly justifiable.

Thus we evaluate (30) by setting

$$\Delta r_{jk} = \int_{\rho_j}^{\rho_k} \frac{N \times 10^{-6} d\rho}{\sin \beta} = \frac{2 \times 10^{-6}}{\sin \beta_j + \sin \beta_k} \int_{\rho_j}^{\rho_k} N d\rho,$$

but from (10)

$$\begin{aligned} \int_{\rho_j}^{\rho_k} N d\rho &= \int_{\rho_j}^{\rho_k} [N_j - k(\rho - \rho_j)] d\rho \\ &= N_j(\rho_k - \rho_j) - \frac{1}{2}(N_j - N_k)(\rho_k - \rho_j) \\ &= \frac{1}{2}(N_j + N_k)(\rho_k - \rho_j). \end{aligned}$$

Substituting in (30) we get

$$\Delta r_{jk} = \frac{(N_k + N_j)(\rho_k - \rho_j) \times 10^{-6}}{\sin \beta_k + \sin \beta_j}. \quad (31)$$

To compute retardation for a double passage through the layer, (31) must be doubled.

The integral of (30) can be evaluated exactly. The resulting expression, however, is quite involved. Comparison of the exact solution with (31) indicates an error of a few hundredths of one per cent for the case of the tropospheric propagation. In the ionosphere, the errors are somewhat larger, although still sufficiently small to justify the use of (31). This is discussed in more detail in the section on Application to the Ionosphere.

APPLICATION TO THE TROPOSPHERE

In computing the refractive effects of the troposphere, one normally uses radiosonde data in which the temperature, pressure, and dewpoint are given at "significant" levels above the earth's surface. These levels have been selected so that linear interpolation between adjacent levels is a good approximation to the measured temperature and dewpoint profiles. The refractivity N at each significant level is computed from the expression

$$N = (n - 1) \times 10^6 = (77.6/T)(P + 4810e/T)$$

where

- n = refractive index,
- T = absolute temperature in degrees Kelvin,
- P = total atmospheric pressure in millibars,
- e = water vapor pressure in millibars.

The index of refraction is virtually independent of frequency up to 30,000 megacycles.

To compute the refractive bending we tabulate $N_0 - N$ at significant levels and use (17).

$$\gamma = \sum_{k=0}^{n-1} \frac{N_k - N_{k+1}}{500(\tan \beta_k + \tan \beta_{k+1})} \text{ milliradians.}$$

The above expression is quite exact for the bending in a layer of constant gradient as long as the layer thickness is small compared with the earth's radius. For a layer thickness of 50,000 feet, which is much greater

than ever found in the troposphere, the error is less than 0.06 per cent.

To determine the various β 's in terms of the angle of elevation α_0 and height h , we use Snell's Law, (5),

$$\cos \beta_h = \frac{\cos \alpha_0}{(1 + h/a)[1 - (N_0 - N) \times 10^{-6}]}$$

We note that β , the ray inclination angle, is a function only of height h and the difference in the refractive index between the surface and h . It is independent of the shape of the refractive profile. This fact allows us to determine β_h at each significant level independently of other levels. Thus, it is not necessary to start at the surface and work up layer by layer as is necessary in many other computation methods.

Fig. 3 is a graphical representation of Snell's Law

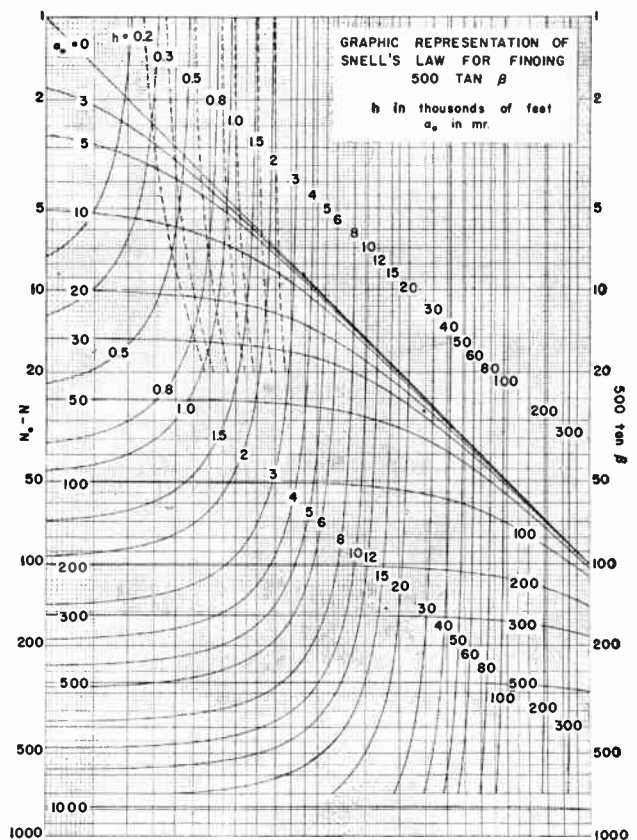


Fig. 3

from which $500 \tan \beta$ may be read off directly. The procedure in using the plot is as follows. Enter on the left margin at the appropriate $N_0 - N_h$. Proceed horizontally to the proper height, interpolating between curves if necessary. Use the solid height curves when $N_0 - N_h$ is positive and the dashed curves when $N_0 - N_h$ is negative. Then proceed vertically to the assumed α_0 and read off $500 \tan \beta$ along the right margin.

Suppose, for example, that $h = 4500$ feet and $N_0 - N_h$ is 58 units and $\alpha_0 = 0^\circ$. Enter the left margin at 58, move to the right to $h = 4500$ (midway between 4000 and 5000 feet height curves), then move up vertically to $\alpha_0 = 0$ line and

read $500 \tan \beta = 8.7$ on the right margin. If α_0 were 50 milliradians instead of 0, $500 \tan \beta = 26.5$.

A convenient procedure for computing-ray bending for a given refractive index profile is as follows.

- 1) Tabulate N , $N - N_0$ and h at each significant level.
- 2) Find $500 \tan \beta_k$ at each level using chart of Fig. 3.
- 3) For each adjacent pair of levels use (16) to determine $\Delta\gamma$'s.
- 4) Add $\Delta\gamma$'s from the surface up to the height at which total tropospheric bending is desired.
- 5) To obtain refractive error referred to the observer use (24),

$$\delta = \frac{\gamma \tan \beta - (N_0 - N) \times 10^{-6} + \gamma^2/2}{\gamma + \tan \beta - \tan \alpha_0}$$

At greater heights or higher angles of elevation, the alternate form of (24); i.e., (23) will be found more convenient.

$$\delta = \frac{\epsilon \tan \alpha + \epsilon^2/2}{\epsilon + \tan \alpha - \tan \alpha_0}$$

where ϵ may be obtained from (18) and (21).

$\cot \beta$ may be obtained from Fig. 3. For ionospheric heights and above, $\cot \alpha$ may be obtained from Fig. 5. If ϵ has been calculated, δ may be approximately evaluated from Fig. 6, which is a graphic representation of (25).

Atmospheric retardation in any one layer may be computed from (31).

$$\Delta r_{jk} = \frac{(N_k + N_j)(h_k - h_j)}{1000(\sin \beta_k + \sin \beta_j)}$$

where Δr_{jk} is the range error for one-way passage through the layer. $1000 \sin \beta$ can be obtained from Fig. 4 in a manner analogous to that of obtaining $500 \tan \beta$ from Fig. 3. Height is expressed in thousands of feet and Δr_{jk} is expressed in feet. Values of Δr for a passage through the troposphere at zero elevation angle are on the order of 350 feet.

The Doppler error for targets in or above the troposphere but below the ionosphere can be readily computed from (28).

For a standard atmosphere at the height of 100,000 feet and $\alpha_0 = 0$ assuming $\Psi = 90^\circ$, the Doppler error is on the order of one-half per cent.

APPLICATION TO THE IONOSPHERE

In considering the effect of the ionosphere on the passage of electromagnetic waves, we will limit ourselves to frequencies above 100 mc, since this represents the situation of most interest and also will enable us to be simplified the various equations.

The force exerted by a plane electromagnetic wave on an electron of mass m and charge e , in the presence of a steady magnetic field B , is

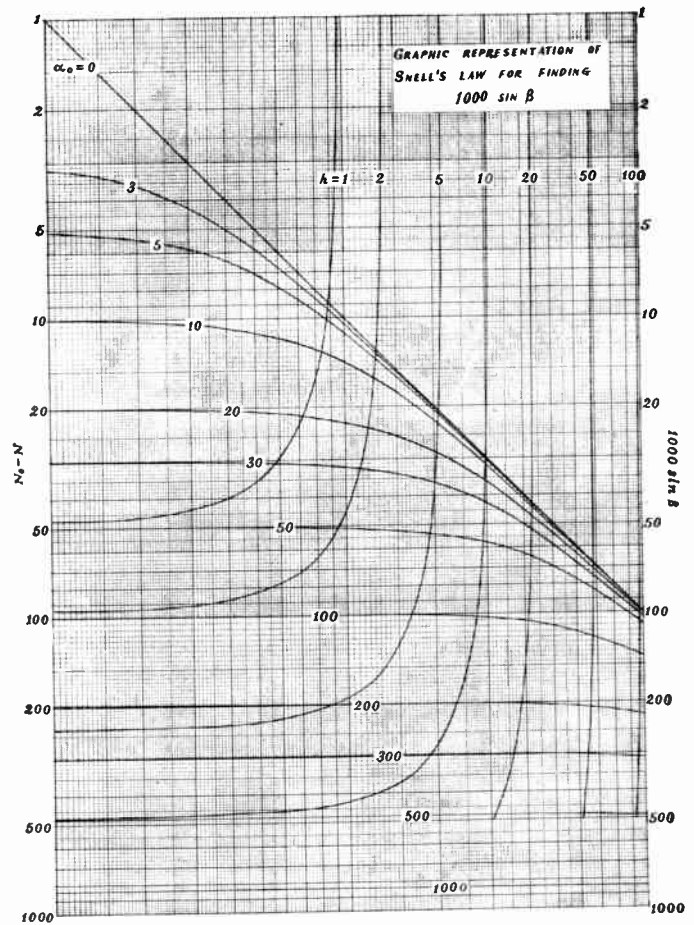


Fig. 4—Graphic representation of Snell's law for finding $1000 \sin \beta$.

$$\begin{aligned} \mathbf{F} &= e[\mathbf{E} + (\mathbf{V} \times \mathbf{B})] = m d\mathbf{V}/dt + m\mathbf{v}\mathbf{V} \\ &= j\omega m\mathbf{V}(1 - j\nu/\omega) = j\omega m\mathbf{V}(1 - j\nu/\omega), \end{aligned} \quad (33)$$

where

\mathbf{E} = the incident electric vector,

ν = angular collision frequency of electrons with air molecules,

ω = angular frequency of the incident signal,

\mathbf{V} = velocity of the electron.

The phase term multiplying each term of (33) is

$$\exp [j\omega(t - \mathbf{n} \cdot \mathbf{R}/v)]$$

where

\mathbf{n} = unit vector along direction of travel,

\mathbf{R} = vector from the origin of the coordinate system to the point of interest,

v = phase velocity of the wave.

The formal solution of (33), in conjunction with Maxwell's field equations leads to the well known Appleton-Hartree equations which give the refractive index of the ionized medium. At very high radio frequencies the absorption is negligible since the ratio of collision fre-

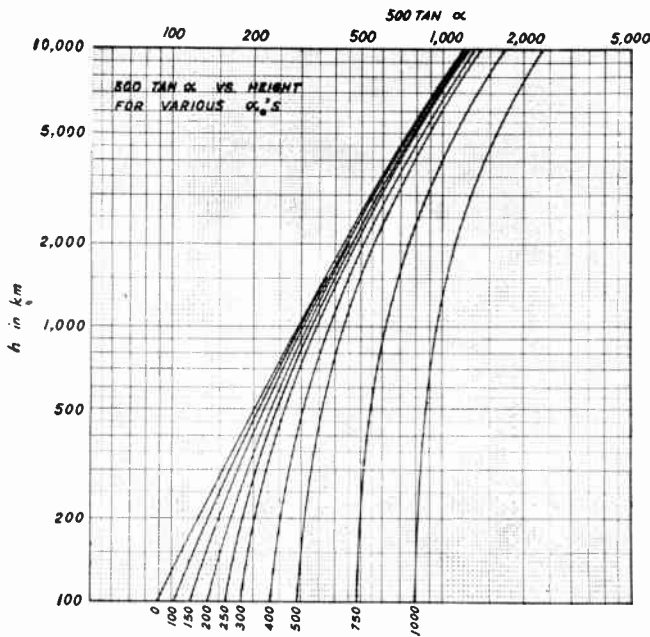


Fig. 5—500 tan α vs height for various angles of elevation in milliradians.

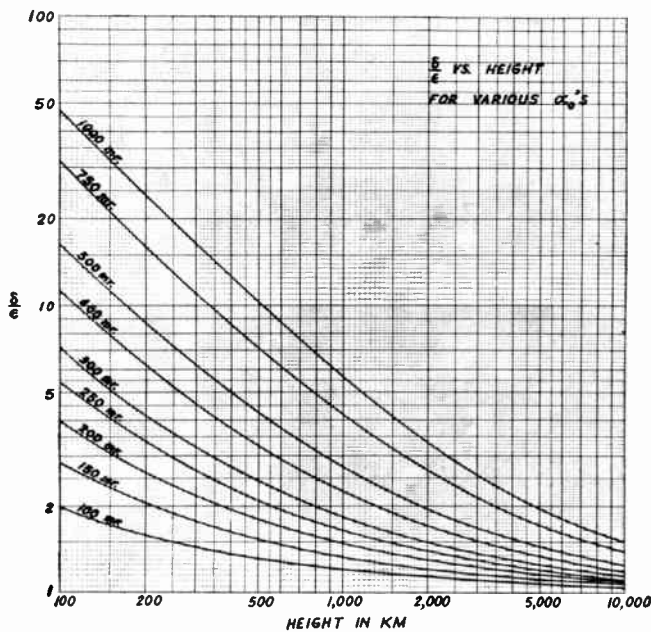


Fig. 6— δ/ϵ vs height for various angles of elevation in milliradians.

quency to operating frequency in the ionized region is extremely small. In addition, a number of simplifying assumptions are possible, and the resulting expression for the index of refraction is⁷

$$n^2 = (c/v)^2 = 1 - p^2 \pm p^2 g \cos \theta \quad (34)$$

⁷ S. Weisbrod and J. L. Heritage, "Ionospheric Refraction and the Faraday Effect at Frequencies above 100 mc," ASTIA Document No. AD-138621, pp. 8-16; March, 1956.

where

- p = ratio of plasma to operating frequency,
- $p = [(N_e e^2) / (m \epsilon_0 \omega^2)]^{1/2}$; $p^2 \ll 1$,
- N_e = electron density per cubic meter,
- ϵ_0 = permittivity of free space = 8.854×10^{-12} farads/meter,
- v = phase velocity of the wave,
- c = velocity of light in vacuum,
- g = ratio of gyro to operating frequency = $(eB/m\omega) \ll 1$,
- θ = angle between the magnetic field and the direction of propagation. For values of θ very nearly 90° , (34) becomes inaccurate, but this is not a serious limitation since in most cases it does not apply.

It follows from (34) that, upon entering an ionized layer, the wave splits up into two components, each traveling with a different phase velocity. It can also be readily demonstrated that, if the coordinate system is chosen so that the magnetic field is along the z axis, and the direction of propagation is in the $x-z$ plane, the two components of the electric vector are:⁷

$$\begin{aligned} E_{1,2} &= |E_y| (\pm j \cos \theta i + j + j \sin \theta k) \\ &= |E_y| (j \pm jt) \end{aligned} \quad (35)$$

where i, j, k are unit vectors along x, y, z axis, and

$$t = n \times j = -\cos \theta i + \sin \theta k.$$

It is seen from (35) that the two vectors represent two circularly polarized waves, each with an opposite sense of rotation. Since each travels with a slightly different velocity, the resultant of the two waves forms a plane wave whose plane of polarization rotates as it traverses through the ionized region. We shall now derive the equation of the combined wave

$$E \text{ total} = E_1 \exp [j\omega(t - r/v_1)] + E_2 \exp [j\omega(t - r/v_2)] \quad (36)$$

where

$$r = x \sin \theta + z \cos \theta,$$

but from (34)

$$\begin{aligned} \frac{1}{v_{1,2}} &= \frac{\sqrt{1 - p^2}}{c} \left(1 \pm \frac{p^2 g}{1 - p^2} \cos \theta \right)^{1/2} \\ &\cong \frac{\sqrt{1 - p^2}}{c} (1 \pm \frac{1}{2} p^2 g \cos \theta) \\ &= \frac{1}{v_0} \pm \frac{p^2 g \cos \theta}{2v_0} \cong \frac{1}{v_0} \pm \frac{p^2 g \cos \theta}{2c} \end{aligned} \quad (37)$$

where $v_0 = c/(1 - p^2)^{1/2}$ = phase velocity in the absence of a magnetic field. Combining (35), (36), and (37) we obtain

$$E_{\text{total}} = 2 |E_y| (\cos \beta r_j + \sin \beta r_t) \exp j\omega(t - r/v_0) \quad (38)$$

where

$$\beta = \frac{\dot{p}^2 g}{2c} \omega \cos \theta.$$

Eq. (38) represents a plane wave whose plane of polarization rotates β radians per unit distance and whose phase velocity is v_0 . In other words, while the earth's magnetic field has only a negligible effect on the phase velocity of the wave of very-high-frequency radio waves, it produces the so-called Faraday rotation and thus plays an important role in ionospheric propagation.

IONOSPHERIC REFRACTION

In the preceding discussion it was shown that the index of refraction in the ionosphere, as far as the refractive bending is concerned, is given by

$$n = [1 - (N_e e^2)/(m \epsilon_0 \omega^2)]^{1/2} = (1 - b^2)^{1/2} \\ = 1 - \frac{1}{2} b^2 = 1 + N^i \times 10^{-6} \quad (39)$$

where N^i , the ionospheric N , is defined in complete analogy to the tropospheric N .

Numerically N^i is given by

$$N^i = -4.03(N_e/f^2) \times 10^{-6}, \quad (40)$$

where f = signal frequency in megacycles, and N_e = electrons per cubic meter.

The two important differences between the ionospheric and the tropospheric N units are:

- 1) N^i is a negative quantity,
- 2) N^i is inversely proportional to the square of radio frequency.

At 100 mc the maximum value of N^i rarely exceeds -4000 units.

Ionospheric bending may be computed directly from (17). However, since the minimum angle of entrance into the ionospheric region is on the order of 160 milliradians, α and β are very nearly equal and only a small error will result if (16) is written as

$$\gamma_{jk} = \frac{|N_k^i| - |N_j^i|}{500(\tan \alpha_k + \tan \alpha_j)} \text{ milliradians.} \quad (41)$$

In Fig. 5, $500 \tan \alpha$, corrected for nominal atmospheric refraction, is plotted vs height for various angles of elevation α_0 . The correction for tropospheric refraction is less than two milliradians at very oblique incidence, and is based on the assumption that the surface value of index of refraction is 320 N units.

If $|N^i|$ is greater than a few thousand units, or if a high accuracy is required, α in (41) should be replaced with β . The relationship between the quantities is given by (21) and (40). If values of α are obtained from Fig. 5, which incorporates the tropospheric correction, (21) reduces to

$$\alpha - \beta = |N^i| \times 10^{-6} \cot \alpha. \quad (42)$$

Total bending γ is simply the sum of tropospheric and ionospheric contributions

$$\gamma_{\text{total}} = \gamma^t + \gamma^i \quad (43)$$

where superscript t and i refer to troposphere and ionosphere, respectively.

The ionospheric contribution to the refractive bending referred to the earth's center at a given height is, from (18) and (21),

$$\epsilon^i = \gamma^i - |N^i| \times 10^{-6} \cot \alpha. \quad (44)$$

Total ϵ is

$$\epsilon_{\text{total}} = (\gamma^t - N_0 \times 10^{-6} \cot \alpha) \\ + (\gamma^i - |N^i| \times 10^{-6} \cot \alpha) = \epsilon^t + \epsilon^i. \quad (45)$$

The elevation-angle error is obtained most conveniently from (23), or approximately from (25) and Fig. 5.

When γ and δ have been determined, the Doppler error due to refraction can be readily obtained from (28). At 100 mc, the maximum magnitude of Doppler error will be on the order of one per cent, and will approach zero at very great distances since γ and δ approach each other. The error will rapidly decrease for larger angles of elevation or higher frequencies.

In discussing the retardation effect of the ionosphere, one must remember that the ionosphere is a dispersive medium, and a distinction must be made between the group and phase velocities. For computing the refractive effects we used the phase velocity which exceeds velocity of light in free space, but, in considering the retardation, we must use the group velocity which represents the velocity with which energy propagates through the medium. The relation between the two is

$$c/v_p = v_g/c \quad (46)$$

and

$$c/v_g - 1 = v_p/c - 1 = (1 - n^2)/n^2 = -N^i \times 10^{-6} \\ = |N^i| \times 10^{-6}. \quad (47)$$

Comparison with (29) shows that the computing of ionospheric retardation (31) is perfectly valid, provided that the absolute value of N^i is used. As in the case of refractive computations, we can replace β with α without causing a serious error.

Thus, if h is in kilometers

$$\Delta r_{jk} = \frac{(|N_k^i| + |N_j^i|)(h_k - h_j)}{1000(\sin \alpha_k + \sin \alpha_j)} \text{ meters.} \quad (48)$$

In Fig. 7, $1000 \sin \alpha$ corrected for tropospheric refraction is plotted vs h for various α_0 's. As before, the assumed value of N_0 was taken at 320 units. Since this correction is very small, the exact value of N_0 is unimportant.

The value of Δr_{jk} as given by (48) [or (31)] was compared with the exact solution of (30). It was found that for $\alpha_j = 150$ milliradians and layer thickness of 20, 50 and 100 kilometers, the values were 1.4, 3.9 and 7.2

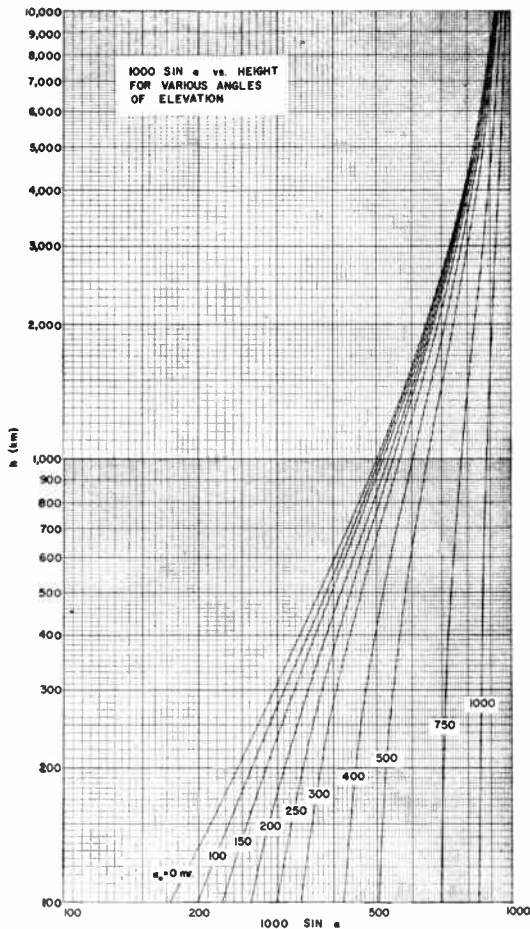


Fig. 7—1000 sin α vs height for various angles of elevation in milliradians.

per cent too high. With the angle of entrance of 200 milliradians, these errors dropped to 1.15, 2.7 and 4.7 per cent. From the above comparisons it is obvious that (48) is adequate for all practical applications.

One effect which is unique to ionospheric propagation is the Faraday rotation. From (38) this rotation amounts to $(p^2 g \omega / 2c) \cos \theta$ radians per unit distance for a single passage through the layer. Since distances under consideration are small compared to earth's radius, the strength of the magnetic field, and hence g , the ratio of the gyro to operating frequency, is very nearly constant.

Also, the rate of change of electron density per unit distance of the ray path is small compared with the wavelength of the signals. Thus we can state that the number of rotations of the plane of polarization for a double passage through the layer bounded by heights ρ_k and ρ_j is

$$\Omega = \int_{\rho_j}^{\rho_k} (\rho^2 g \omega / 2nc) \cos \theta dr = \lambda_g^{-1} \int_{\rho_j}^{\rho_k} \rho^2 \cos \theta dr \quad (49)$$

where

$$\lambda_g = c / f_g = \text{gyro wavelength inside the layer} = 109 / B \text{ meters}$$

B = intensity of the terrestrial field in gauss.

At ionospheric heights typical values of λ_g are on the order of 250 meters.

From (2) and (39) we have

$$dr = K d\gamma = \csc \beta d\rho$$

$$p^2 = 2 |N^i| \times 10^{-6}$$

Also, in any one lamination which does not exceed fifty or a hundred kilometers in thickness (which certainly represents the practical case), λ_g and $\cos \theta$ are nearly constant and (49) may be written as

$$\Omega_{jk} = 2\lambda_g^{-1} \cos \theta \int_{\rho_j}^{\rho_k} |N^i| \times 10^{-6} \csc \beta d\rho \quad (50)$$

which, compared with (30), yields

$$\Omega_{jk} = 2\lambda_g^{-1} \cos \theta \Delta r_{jk} \quad (51)$$

where $\cos \theta_{jk}$ = value of $\cos \theta$ in the middle of the layer.

From (51) it appears that ionospheric retardation is very closely related to the Faraday rotation. In most practical applications λ_g and $\cos \theta$ are not rapidly varying functions of the ray path. If we use a constant value for $\cos \theta$ equal to that encountered at the midpoint of the path, or, in the case of very long paths, in the region of maximum electron density, no serious error will result; and, according to (51) Faraday rotation will be directly proportional to the total ionospheric retardation. The constant of proportionality $2\lambda_g^{-1} \cos \theta$ is, of course, a function of geometric and geomagnetic factors of the transmission path.

Discussion of Relativity and Space Travel

There appear below four letters commenting on a recent PROCEEDINGS paper. The author's reply to all four correspondents follows the fourth letter.—The Editor.

Comment on Relativity and Space Travel*

Pierce's recent article on relativity¹ gave a very good summary of current opinions, and is to be commended for being free of the sensationalism with which semipopular articles (and, alas, even textbook discussions) only too often abound. It is a pity that the comments under "Scanning the Issue" chose to go a little further, in speaking of "leaving his familiar Newtonian world. . . ." Just how "unfamiliar" will the "new, relativistic, world" be?

At present, it is barely possible to attain escape velocity, about 11 km/sec. Suppose that, in the not-too-distant future, it becomes possible to attain velocities ten times that figure. The earth's velocity in its orbital motion, about 30 km/sec., might be added to that, giving about 150 km/sec. For the sake of round figures, double that, to suppose that velocities around 300 km/sec might be foreseeable. This figure is just 10^{-3} times the speed of light. In the relativistic equations, the factors supposed to be involved with the peculiar effects are usually of the form $(1 - V^2/C^2)^{1/2}$. Thus, since $V/C = 10^{-3}$, it appears that the space traveler might find his "new world" "unfamiliar" to the extent of about one part per million. So it would take a rather precise experiment to see that the "new world" was "unfamiliar" at all.

This communication, however, is not intended just to raise a quibble. There are two matters of some importance which deserve comment.

In the first place, the article brings up again the proposal of launching a very accurate oscillator in a satellite so that its behavior may test the theory of relativity. The writer maintains that the experiment would test nothing except the behavior of an oscillator of such-and-such a design traveling in a satellite under such-and-such conditions. How many alleged "crucial experiments" have been performed in the past, and can any of them "prove" any theory, in the sense of showing that the theory in question is not only *sufficient* but also *necessary*, to explain the results? It is generally (although, perhaps, not very openly) admitted now that the "crucial experiments" which were once supposed to prove the theory of relativity did not accomplish that aim.² On the basis of Ritz's electrodynamics,³ e.g., the outcome

of the Michelson-Morley⁴ and Trouton-Noble⁵ experiments was a foregone conclusion. The advance in the perihelion of Mercury could be explained in various ways,² and the other experiments, such as the "bending of light rays" near the sun do not agree at all well with the theoretical value.^{2,6} Perhaps, then, some rather critical consideration is indicated before deciding on a great expense of money and effort to launch the oscillator in the satellite.

The second point which deserves to be made is this. Some rather pointed arguments against certain of the conclusions of relativity, and even more against some of the arguments offered in support of those conclusions, have been advanced, and it seems only right that the readers should at least have heard of them. Brown^{2,7,8} has given some very interesting discussions of these matters, Moon and Spencer⁹ have carried out some interesting analyses bearing on the subject, and, last but by no means least, O'Rahilly's book¹⁰ offers a stimulating and critical investigation of some of these points.

H. L. ARMSTRONG
Queen's University
Kingston, Ontario, Canada

The Clock Paradox¹¹

In a recent paper¹ Pierce discussed the clock paradox in the special theory of relativity. According to this paradox, one of two identical twins goes off in a starship at 99.5 per cent of the speed of light. As observed from earth, his clock runs only 1/10 of normal speed. Ten years after takeoff he lands back on earth. The "traveling" twin has aged during this time by only 1 year while his "stationary" brother is 10 years older than when the ship started.

The clock paradox controversy is almost as old as the special theory of relativity itself. On one side there are the authors who state that the clock paradox is a *physical*

reality.¹²⁻¹⁷ On the other side there are the authors who cannot accept it as a physical reality and try to explain the paradox by different theories.¹⁸⁻²⁴ One author, who will remain nameless, even suggested that we could never reach any great velocities at all, so the clock paradox does not really exist. To his credit I should say that his paper was published before the satellites started to rotate around the earth.

In his original paper^{25,26} Einstein based his special theory of relativity on two postulates:

1) If a system of coordinates K is chosen so that, in relation to it, physical laws hold good in their simplest form, the *same* laws also hold good in relation to any other system of coordinates K' moving in a *uniform* translation relative to K .

2) The light is always propagated in empty space with a definite velocity c , which is independent of the state of motion of the emitting body.

We have to realize in the clock paradox that the "traveling" twin, in order to reach velocities close to the velocity of light, should *accelerate* and *decelerate* his space vehicle before he will come back to the exact same position as his brother. As we see above, *no* discussion of the effects of acceleration is possible at all in the special theory of relativity.

In his paper on the general theory of relativity^{26,27} Einstein has discussed gravitation fields and acceleration. However, this part of his theory is far from being perfect and has been checked with any real accuracy in only *two* observations. Extensive discussions on the general theory of relativity and *other* possible theories of gravitation may be found in several places.²⁸

The author of this letter and quite a few others find it impossible to believe (unless a definite experiment proves otherwise!) in the physical reality of the clock paradox and in two twins where one is younger than

¹² H. Dingle, *Proc. Phys. Soc. (London) A*, vol. 69, p. 925; 1956.

¹³ E. M. McMillan, "The clock paradox and space travel," *Science*, vol. 126, pp. 381-384; August 30, 1957. See references cited therein.

¹⁴ H. Dingle, *Science*, vol. 127, p. 158, 1958.

¹⁵ E. M. McMillan, *Science*, vol. 127, p. 160; 1958.

¹⁶ R. M. Frye and V. M. Brigham, *Amer. J. Phys.*, vol. 25, p. 553; 1957.

¹⁷ R. H. Romer, *Amer. J. Phys.*, vol. 27, p. 131; 1959.

¹⁸ C. Moller, "The Theory of Relativity," Oxford University Press, London, Eng., p. 258; 1952.

¹⁹ E. G. Cullwick, "Electromagnetism and Relativity," Longmans, London, Eng., p. 70; 1957.

²⁰ R. C. Tolman, "Relativity, Thermodynamics, and Cosmology," Oxford University Press, London, Eng., p. 166; 1934.

²¹ J. W. Campbell, *Phil. Mag.*, vol. 15, p. 48; 1933.

²² W. Campbell, *Phil. Mag.*, vol. 16, p. 529; 1933.

²³ F. L. Hill, *Phys. Rev.*, vol. 72, p. 236; 1947.

²⁴ C. B. Leffert and T. M. Donahue, *Amer. J. Phys.*, vol. 26, p. 8; 1958.

²⁵ A. Einstein, "Zur Elektrodynamik bewegter Körper (On the electrodynamics of moving bodies)," *Ann. der Phys.*, vol. 17; 1905.

²⁶ H. A. Lorentz, A. Einstein, H. Minkowski, and H. Weyl, "The Principle of Relativity," Methuen, London, Eng.; 1923.

²⁷ A. Einstein, "Die Grundlage der allgemeinen Relativitätstheorie (The foundation of the general theory of relativity)," *Ann. der Phys.*, vol. 49, 1916.

²⁸ *Revs. Modern Phys.*, vol. 29, pp. 325-546, July 3, 1957 includes quite a few references.

* Received by the IRE, June 29, 1959.

¹ J. R. Pierce, "Relativity and space travel," *Proc. IRE*, vol. 47, pp. 1053-1061; June, 1959.

² G. B. Brown, "Have we abandoned the physical theory of nature?" *Science Progress*, vol. 44, pp. 619-634; October, 1956.

³ Ritz's original work is not very accessible nowadays. A discussion may be found in chapter 11 of O'Rahilly's book (see footnote 10).

⁴ G. Joos, "Theoretical Physics," Blackie and Son Ltd., London, Eng., 1st ed., p. 226; 1934.

⁵ *Ibid.*, p. 447.

⁶ E. Finlay-Freundlich, "Du déplacement general vers la rouge des raies du spectre solaire," *Ann. Phys.*, ser. 13, vol. 2, pp. 765-777; November-December, 1957.

⁷ G. B. Brown, "A theory of action—at-a-distance," *Proc. Phys. Soc. B*, vol. 68, pp. 672-678; September, 1955.

⁸ G. B. Brown, "The unification of macroscopic physics," *Science Progress*, vol. 46, pp. 15-29; January, 1959.

⁹ P. Moon and D. E. Spencer, "Interpretation of the ampere experiment," *J. Franklin Inst.*, vol. 257, pp. 203-220; March, 1954; "The coulomb force and the ampere force," pp. 305-315; April, 1954; and "A new electrodynamics," pp. 369-382; May, 1954.

¹⁰ A. O'Rahilly, "Electromagnetics," Longmans, Green, and Co., London, Eng.; 1938.

¹¹ Received by the IRE, June 29, 1959.

the other. The explanation of the clock paradox probably lies somewhere in the acceleration and the deceleration of one system compared to the other. Therefore the author suggests the following *postulate*:

Two identical material bodies at the same position at the same time t_0 and at rest with respect to the same coordinate system will remain identical at any future time t_1 under the above conditions, regardless of their relative movements between the times t_0 and t_1 . This basic postulate could be made into an additional check²⁸ on any general theory of relativity.

H. UNZ
Elec. Engrg. Dept.
University of Kansas
Lawrence, Kans.

Relativity and Space Travel²⁹

Pierce¹ has given his solution of the famous "clock paradox," and finds that the crew on a starship age less rapidly than those left behind on earth. He does mention the fact that there are those who do not agree with this. This note is written to present the opposing point of view.

Let us start with the postulates of the special theory.

Postulate I—The laws of electrodynamics (including, of course, the propagation of light with the velocity c in free space), as well as the laws of mechanics, are the same in all inertial frames.

Postulate II—It is impossible to devise an experiment defining a state of absolute motion, or to determine for any physical phenomena a preferred inertial frame having special properties.

In a general sense, Postulate II is all that is required to show that Pierce's solution is incorrect. Since, in common with most modern writers on this subject, he has ruled out any effect of acceleration on clocks, his problem becomes that of two inertial frames with uniform relative velocity. Then the measurement of the elapsed time between the two events, the departure of the starship from earth and its return thereto, must be the same on the earth's clock as well as the starship's, since they have measured the same events, at the same place, and in a state of relative rest. Otherwise Postulate II is violated. A solution giving different elapsed times is impossible, or, to quote Pierce, "we simply can't have such a thing and relativity too; one or the other will have to go."

This argument is conclusive, but probably not very satisfying. The trouble is that one of the logical consequences of Postulates I and II can be stated loosely as, "moving clocks go more slowly than stationary ones." As a result, one intuitively, but wrongly, thinks that the moving clock must show a

shorter elapsed time after its return. This is what leads to the famous paradox, since the relativist can draw no distinction between earth and starship, and has both clocks running slow, depending on the viewing point. He infers that the elapsed times are impossible—both observers cannot be right, and hence the paradox.

Actually, in making this inference, both observers would be equally wrong. If they reasoned accurately from Postulates I and II, each would be prepared to find the other's clock agreeing with his, after coming to rest for a comparison. Hence, the paradox does not exist—it is merely wrong reasoning that makes it appear to be present.

Let us examine this further. Postulates I and II have certain logical consequences, the mathematical expression of which is the Lorentz transformation. If A and B are two inertial frames moving with uniform relative velocity, three effects occur which are of particular interest. If A looks at B 's measuring rods, he finds them shorter than his own, in the direction of motion. If B has a system of clocks spaced along his direction of motion, and nicely synchronized according to B , A finds that they are not synchronized. Finally, A observes that B 's measurement of the time interval between two events occurring at the same place in A 's frame does not agree with A 's measurement, and, in fact, indicates a shorter time than A measures. From this, A infers that B 's clocks must be running at a slower rate than his own.

An essential part of special relativity is that the effects mentioned in the preceding paragraph are completely reciprocal and symmetrical. That is, if B is substituted for A , and A for B , in the paragraph, it will still be true. Both observers are right in their observations.

Having concluded that the clocks on both the earth and starship will show exactly the same elapsed time for the round trip, what will this time be? If the observer on the earth knows the velocity of the spaceship relative to him, and the distance covered in the round trip, he can calculate the total elapsed time, and this is exactly what his clock will show him. The same is true for the observer in the starship, and his clock will show the same time.

If the two observers measure the rate of each other's clocks, each will find the other's going slower than his own, and both will be right. If they infer from this, however, that the other man's clock will show an elapsed time less than his own, they will be wrong.

Further elaboration of this theme is found in Dingle.³⁰ A detailed solution of the earth and starship problem is given by Cullwick.³¹

Referring specifically to Pierce's argument, this is a mathematically dressed up version of one already put forward by Darwin.³² This was criticized by Dingle,³³ who pointed out the error, namely, that in a problem based on the postulates of the

special theory, you cannot introduce a preferred frame of reference. In essence, this is what both Darwin and Pierce do when they say that things look different to the starship's observer because he is the one who pushes the button that fires the rockets.

In some ways the clock paradox is a trivial problem. McMillan,³⁴ who makes the same error of the preferred frame in his treatment, has calculated the energy required to drive a practical starship to the velocities required to gain some appreciable age advantage. This turns out to be some orders of magnitude greater than any energy source in the foreseeable future.

The main reason for still belaboring the clock paradox is that it is a fallacy based on erroneous reasoning, and can do great harm in confusing future students of relativity. Further, when asymmetrical aging is seriously presented to Congressional committees as another reason for exploration of space, it is time to call a halt, before our scientific advisers are embarrassed.

C. WESLEY CARNAHAN
Menlo Park, Calif.

The Clock Paradox³⁴

I was sorry to see a further confusion of the clock paradox published in the PROCEEDINGS.¹ It is hoped that the following explanation will settle this controversy once and for all.

First let me point out the fallacy in Pierce's "resolution" of the paradox. His argument is correct up to the sentence:² "But, when we reach * we change our motion . . ." which leads to the erroneous (49). The statement here should be: "But, when we reach * the earth appears to turn around at a distance LS ." The derivation then proceeds precisely as for (45), except that the apparent distance is now LS instead of L ; then (49) becomes:

$$N_e = 2L/c \gamma^{-1} [1 - (v/c)^2] = SN_e.$$

Thus when the earth-bound twin "comes back" he will have aged *less* than the ship-bound twin by the shrinking factor $S = [1 - (v/c)^2]^{1/2}$. To use the figures in the article, the earth twin seems to have aged 1/10 year while the starship twin has aged 1 year;³ from the earth twin's point of view the traveler has still aged 1 year, but he himself has aged 10 years. This is the paradox!

The only way to clear up the paradox is to take account of the acceleration required to reach the velocity v and the deceleration needed to stop before turning around. The earth is approximately an inertial system,

²⁹ H. Dingle, "What does relativity mean?," *Bull. Inst. Phys.*, vol. 7, pp. 314-323; December, 1956.

³⁰ Cullwick, *op. cit.*, footnote 19, pp. 70-76.

³¹ C. G. Darwin, "The clock paradox in relativity," *Nature*, vol. 180, pp. 976-977; November 9, 1957.

³² H. Dingle, "The clock paradox in relativity," *Nature*, vol. 180, pp. 1275-1276; December 7, 1957.

³³ Received by the IRE, June 15, 1959.

³⁴ Pierce, *op. cit.*, p. 1058, column 2, line 4.

³⁵ The statement "Should we say . . . ?" in Pierce's article, *ibid.*, p. 1057, column 1, line 6 from bottom, does not give a valid comparison; the apparent distance has shrunk to 1/10 so the times should be smaller in the same ratio.

²⁸ Received by the IRE, July 6, 1959.

while the spaceship must be treated as an accelerated or noninertial system; this destroys the symmetry which gives rise to the paradox. Suppose, for simplicity, that the spaceship goes half the distance out at an acceleration g , goes the remaining half while decelerating at the same rate, and returns in the same manner. These accelerations are taken to be the *subjective* accelerations of the traveler, that is, with respect to an inertial frame in which the ship is instantaneously at rest. From the point of view of an observer on earth the ship's acceleration is:

$$du/dt = [1 - (u/c)^2]^{3/2}g,$$

where u is the velocity of the ship in the earth's reference frame and t is earth time.³⁷ Hence:

$$t_e = 4 \int_0^v dt = 4 \int_0^v g^{-1} [1 - (u/c)^2]^{-3/2} du \\ = 4vg^{-1} [1 - (v/c)^2]^{-1/2},$$

where v is the final velocity attained.³⁸ On the other hand, increments of time on the ship are related to increments of time on earth by:

$$dt' = [1 - (u/c)^2]^{1/2} dt,$$

so that:

$$t_s = 4 \int_0^v dt' = 4 \int_0^v g^{-1} [1 - (u/c)^2]^{-1/2} du \\ = 2cg^{-1} \ln \frac{1 + (v/c)}{1 - (v/c)},$$

which is always less than the time t_e because of the shrinking factor. For the distance (one-way) one has the relation:

$$L = 2 \int_0^v u dt = 2 \int_0^v g^{-1} [1 - (u/c)^2]^{-3/2} u du \\ = 2c^2 g^{-1} \{ [1 - (v/c)^2]^{-1/2} - 1 \}.$$

For example, if $v=0.995c$ and $g=9.88$ m/sec² (normal gravity), $t_e=64$ years, $t_s=19.23$ years, and $L=29.9$ light-years.

CHRISTOPHER P. GADSDEN
Dept. of Elec. Engrg.
Tulane University
New Orleans, La.

³⁷ A derivation of this relation may be found in the book by I. Landau and E. Lifshitz, "The Classical Theory of Fields," Addison-Wesley Press, Inc., Cambridge, Mass., p. 23; 1951.

³⁸ The factor 4 arises from the four legs of the trip each of which takes the same time.

The Clock Paradox³⁹

There is some overlap in the comments of various correspondents on my paper,¹ and perhaps it will be adequate if I reply in a rather general way.

Special relativity asserts that the same physical laws apply in all unaccelerated coordinate systems regardless of the relative velocities of the different systems. Nowhere in my paper would the addition of a constant velocity to a coordinate system have changed any of the conclusions. In any particular unaccelerated coordinate system, one can make valid calculations of acceleration, as Gadsden does.

Special relativity does *not* say that events in a coordinate system tied to an accelerated object must or can be computed in exactly the same way as events in an unaccelerated coordinate system. However, a false assumption to this effect repeatedly creeps into discussions of the "clock paradox."

The fact is that on reaching the star, when the ship (or the rest of the universe) turns around, the frequency received by the ship from the earth changes, and it does not change again during the "return trip." This fact we can express from more than one point of view, but it is always different from the case of the radiation reaching the earth from the ship, which does *not*, in anyone's book, change frequency when the ship is in the vicinity of * ("turning around").

If we wish to allow the space pilot to insist that ship coordinates are as good and as universal as any others, then something beyond special relativity is needed. We must note that if the spaceship observer insists that he remain stationary at all times, then he must assume a gravitational field which acts *not only* on the earth, but on the *intervening radiation as well*. This I point out in my paper¹ in the second column of page 1059, just prior to Section VI. This field would presumably change the frequency of the radiation reaching him immediately following "turnaround."

We must also note that while there are many experimental verifications of special relativity, alleged verifications of general relativity are widely regarded as inconclusive.

The laws of motion of special relativity are attested by the fact that such devices as the billion-volt Stanford electron accelerator work as planned, and by many atomic phenomena. The time dilatation is attested by the lengthened life of fast mesons and by Ives' experiments which showed a fre-

quency reduction in the radiation from rapidly moving molecules.⁴⁰ The tests of general relativity (the red shift of light from the sun and stars, the advance in the perihelion of Mercury, and the deflection of light in a gravitational field) can be regarded as inconclusive or at least as not absolutely conclusive.

Personally, I find it hard not to believe in the gravitational frequency shift described in Section VI of my paper, because of the simple (though perhaps fallible) arguments which lead to it. However, I do look forward to the results of satellite clock experiments.

Of course I have no direct experience with human travel at velocities near that of light. I cannot assert that I have seen twin B age one year while twin A aged 10 years. However, a consistent interpretation of various experimental results leads me to believe that this would happen. What am I to say, however, if someone states that he finds this impossible to believe, even in the absence of experimental contradiction? I can only assume that he has some firm and final direct insight into the laws of nature which has been denied to me.

With regard to the comments concerning the words near the bottom of column 1, page 1057, I did not propose to get the right answer at that point, and as I had not brought distance in, I could scarcely refer to it.

The various correspondents cite a number of references, many of them unfamiliar to me. I will note that Coupling⁴¹ pointed out the unconscionable energy required to approach the speed of light two years before McMillan did.

A truly excellent paper⁴² treating the "clock paradox" in special relativity in terms of proper time has come to my attention since my paper was published.

I wish to thank R. S. Fuller for pointing out that in my paper, lines 10 and 11, page 1053, column 2, should read "traveling ship R , and the other from the nose of ship R to the tail of ship L ," and in the last term of (24), v_e should be replaced by v_v in the numerator.

J. R. PIERCE
Bell Telephone Labs., Inc.
Murray Hill, N. J.

⁴⁰ H. E. Ives and G. R. Stilwell, "Experimental study of the rate of a moving clock," *J. Opt. Soc. Amer.*, vol. 28, pp. 215-226, July, 1938; Part II, vol. 31, pp. 369-374, May, 1941.

⁴¹ J. J. Coupling, "On atomic jets," *Astounding Science Fiction*, vol. 54, pp. 115-127; January, 1955.

⁴² A. Schild, "The clock paradox in relativity theory," *Amer. Math. Monthly*, vol. 66, pp. 1-18; January, 1959.

³⁹ Received by the IRE, July 16, 1959.

Correspondence

Hall Effect in High Electric Fields*

In a recent communication¹ Gibbons has pointed out some advantages which one has in using the Hall effect in high electric fields, where the drift velocity becomes almost independent of the applied electric field. He goes on to compare the materials germanium, silicon and indium antimonide used in this way, and, on the basis of the curves shown in his Fig. 2, recommends silicon as the material with the largest drift velocity, above fields of 10⁴ v/cm.

It is the purpose of this note to point out that some of the curves shown in Fig. 2 are not in agreement with the most recent published data. Table I summarizes this

TABLE I

Semi-conductor	"Saturation" drift velocity at room temperature (cm/sec)	"Saturation" drift velocity at 77° K (cm/sec)
Ge ^{2,3}	7 × 10 ⁶	9 × 10 ⁶
Si ⁴	8.2 × 10 ⁶	—
InSb ^{4,5}	> 3.4 × 10 ⁷	> 5.4 × 10 ⁷

situation. In the case of indium antimonide at room temperature, Prior's observations show that the drift velocity is still rising at least as fast as the electric field (no sign of "saturation") at 800 v/cm; if it "saturates" it should then do so at some value well above the velocity of 3.4 × 10⁷ cm/sec estimated at this field strength. In the observations at lower temperature,⁵ the drift velocity was obtained from Hall effect measurements. At 1050 gauss, this velocity was 5.4 × 10⁷ cm/sec (and still rising) at 350 v/cm. It was found that the drift velocity showed "saturation" in larger magnetic fields of 3500 and 7000 gauss, for electric fields of 300 and 150 v/cm, respectively.

Using these data, one would conclude that the semiconductor indium antimonide offers appreciable advantages over silicon and germanium, both in the output voltage (proportional to the drift velocity) and in the possible applicability at much lower electric fields of the "saturated" condition.

M. GLICKSMAN
M. C. STEELE
RCA Laboratories
Princeton, N. J.

* Received by the IRE, February 18, 1959.
¹ J. F. Gibbons, "Hall effect in high electric fields," *Proc. IRE*, vol. 47, p. 102; January, 1959.
² J. B. Gunn, "The field-dependence of electron mobility in germanium," *J. Electronics*, vol. 2, pp. 87-94; July, 1956.
³ E. J. Ryder, "Mobility of holes and electrons in high electron fields," *Phys. Rev.*, vol. 90, pp. 766-769; June 1, 1953.
⁴ A. C. Prior, "Avalanche multiplication and electron mobility in indium antimonide at high electric fields," *J. Electronics and Control*, vol. 4, pp. 165-169; February, 1958.
⁵ M. C. Steele and M. Glicksman, "High electric field effects in n-indium antimonide," *J. Phys. Chem. Solids*, vol. 8, pp. 242-244; January, 1959. For earlier data, see *Phys. Rev.*, vol. 110, pp. 1204-1205; June 1, 1958.

The Manley-Rowe Relations*

Parametric amplifiers can be regarded as linear circuits, in which some element is varied periodically by external means, or as nonlinear circuits, in which the action of the nonlinear element is not an explicit function of time but only a function of the instantaneous value of the voltage (or current) affecting it. In the second interpretation, the pump is a secondary signal source and the parametric amplifier mixes the pump-wave with the signal.

For such nonlinear circuits, when the nonlinear element is reactive, Manley and Rowe¹ have derived two general equations:

$$\sum_{n,m} \frac{nW_{n,m}}{(nf_0 + mf_1)} = 0 \quad (1)$$

$$\sum_{n,m} \frac{mW_{n,m}}{(mf_0 + nf_1)} = 0 \quad (2)$$

where $W_{n,m}$ is the average energy of the product-harmonic of frequency $nf_0 + mf_1$ and f_0 and f_1 are the frequencies of the two mixing signals (the two fundamental frequencies). The two equations are energy relations for a completely closed system and there cannot be any exchange of energy with an external source. The system must include all signal sources and loads.

Manley and Rowe derived the equations from the properties of Fourier series in a two-dimensional space. One can also derive them from the conservation of energy.

The conservation of energy yields:

$$\sum_{n,m} W_{n,m} = 0 \quad (3)$$

Eq. (3) is identical to:

$$W_{00} + f_0 \sum_{n,m} \frac{nW_{n,m}}{(nf_0 + mf_1)} + f_1 \sum_{n,m} \frac{mW_{n,m}}{(mf_0 + nf_1)} = 0 \quad (4)$$

The dc term is necessary in order not to multiply and divide by zero.

One should note that:

$$\frac{W_{n,m}}{nf_0 + mf_1} \quad (5)$$

is the average work exchanged by a given product-harmonic within one of its periods.

To deduce the Manley-Rowe equations from (4), it is only necessary to assume the dc energy zero and to prove that the work of each product harmonic averaged over its own period is independent of the values of the fundamental frequencies. To prove that the work per period for each product harmonic is independent of the fundamental frequencies, one has only to find two circuits such that the work per period of the corresponding product harmonics in both circuits is the same, although the fundamental fre-

quencies are chosen different. Such a proof has been given elsewhere.² The proof is, of course, only valid when all nonlinear elements are reactive.

The derivation can be extended to the case when more than two fundamental frequencies exist. One obtains:

$$\sum_{\nu} f_{\nu} \frac{\sum_{n_0, n_1, \dots, n_{\nu}, \dots}}{n_{\nu} W_{n_0, n_1, \dots, n_{\nu}, \dots}} = -W_{0,0} \quad (6)$$

or, when the dc energy is zero:

$$\sum_{n_0, n_1, \dots, n_{\nu}, \dots} \frac{W_{n_0, n_1, \dots, n_{\nu}, \dots}}{n_{\nu} (n_0 f_0 + n_1 f_1 + \dots + n_{\nu} f_{\nu} + \dots)} = 0 \quad (7)$$

The sign of the average energy exchanged by each product-harmonic must be considered. Energy can be generated by a source or absorbed by a load. Because there are only two possibilities, it does not matter which sign is chosen for the generation or correspondingly for the absorption.

Let one assume generation positive, absorption negative. Eq. (4) for a common linear amplifier, yields:

$$W_{00} + W_{1,0} = 0 \quad (8)$$

The dc energy is generated and positive, the ac energy is absorbed and negative. The sum of the two is naturally zero. In the case of an oscillator, $W_{1,0}$ is purely absorbed. In the case of an amplifier, $W_{1,0}$ is made of the sum of the negative ac energy absorbed by the load and the positive ac energy generated by the signal generator. There is not any difference in the form of (8) for the oscillator and for the amplifier. Eq. (8) does not tell *per se* if a device is an oscillator or an amplifier, is stable or unstable. The dc energy is also a sum, the sum of the positive dc energy supplied by the power supplies and the negative dc energy absorbed by the resistances.

The same fundamental reasoning applies to the Manley-Rowe relations in the case of the parametric amplifier with idler and the up-converter.

For the parametric amplifier:

$$\frac{W_{1,0}}{f_0} - \frac{W_{-1,1}}{f_1 - f_0} = 0 \quad (9)$$

$$\frac{W_{0,1}}{f_1} + \frac{W_{-1,1}}{f_1 - f_0} = 0 \quad (10)$$

For f_1 larger than f_0 , signal power $W_{1,0}$ and idler power $W_{-1,1}$ are negative. The pump power $W_{0,1}$ is positive. The signal power is the sum of the signal power absorbed in the load and of the signal power generated by the signal generator. The idler power is only absorbed power. The two equations prove that not only signal power but also idler

* Received by the IRE, March 2, 1959.
¹ J. M. Manley and H. E. Rowe, "Some general properties of nonlinear elements—part I," *Proc. IRE*, vol. 44, pp. 904-913; July, 1956.

² P. A. Clavier, "Parametric Amplifiers," published notes on lectures given at Cornell University, Ithaca, N. Y.; October, 1958.

power must be absorbed by adequate loads. The sign of $W_{1,0}$ is not proof *per se* of the instability of most parametric amplifiers. Indeed, electronic parametric amplifiers are stable.

In the case of the up-converter, the Manley-Rowe equations yield:

$$\frac{W_{1,0}}{f_0} + \frac{W_{1,1}}{f_1 + f_0} = 0 \quad (11)$$

$$\frac{W_{0,1}}{f_1} + \frac{W_{1,1}}{f_1 + f_0} = 0. \quad (12)$$

The output energy $W_{1,1}$ is absorbed by the load. Both signal energy $W_{1,0}$ and pump energy $W_{0,1}$ are generated by power sources. The sign of $W_{1,0}$ tells that the output is at a different frequency from the input. It also tells that an input signal generator is necessary. Eqs. (11) and (12) are proof *per se* of the stability of the up-converter.

P. A. CLAVIER
Westinghouse Elec. Corp.
Electronic Tube Div.
Elmira, N. Y.

Short-Time Stability of a Quartz-Crystal Oscillator as Measured with an Ammonia Maser*

There are many applications, such as that required with atomic standards, where the very short time (second-to-second) stability of a quartz oscillator is important. Work at the National Bureau of Standards Boulder Laboratories on a high-precision oscillator, operated with the quartz crystal immersed in liquid helium, gave the results shown in Fig. 2. This may be compared with the short-time stability (Fig. 1) of another quartz oscillator with the crystal at about 40°C.

Temperature variations of the quartz crystal immersed in the liquid helium are reduced by controlling the pressure of the helium gas above the liquid. Apparently—compare Figs. 2 and 3—the regulator is adversely affecting the short-time stability of the oscillator. The pressure regulator, however, does provide satisfactory long-time stability.

About one hour trace was taken like that of Fig. 2, and about four hours like that of Fig. 3. The results were very consistent. The first run was made with the pressure regulator in operation for a period of over two hours and showed a drift of less than ~ 2 parts in 10^{11} . The following day, a trace was made without the pressure regulator. After about one hour of this recording, the pressure regulator was activated and the transition from the stability illustrated by Fig. 2 to that in Fig. 3 was observed.

The larger frequency fluctuations when the pressure regulator is used may be attributed to either the temperature change associated with pressure fluctuations or to

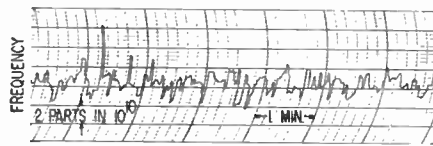


Fig. 1—Oscillator vs maser (approx. 40°C).

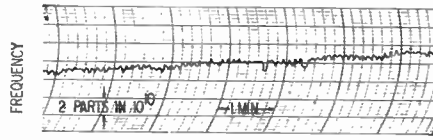


Fig. 2—Helium oscillator vs maser (no pressure control).

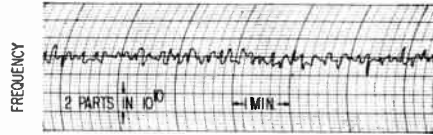


Fig. 3—Helium oscillator vs maser (pressure control).

vals—to 0.001 second¹—could be observed with this maser apparatus with a somewhat different scheme of comparison. The minimum time interval in the above experiment was limited to one second by the electronic counter.

The authors wish to acknowledge the contribution of Dr. R. C. Mockler, who supervised the development of the maser, and also the helpful assistance of P. A. Simpson and J. B. Milton, who were responsible for the cryostat development and the construction and operation of the oscillator.

A. H. MORGAN
J. A. BARNES
National Bureau of Standards
Boulder, Colo.

¹ 0.001 second is the time constant of the maser servo-system.

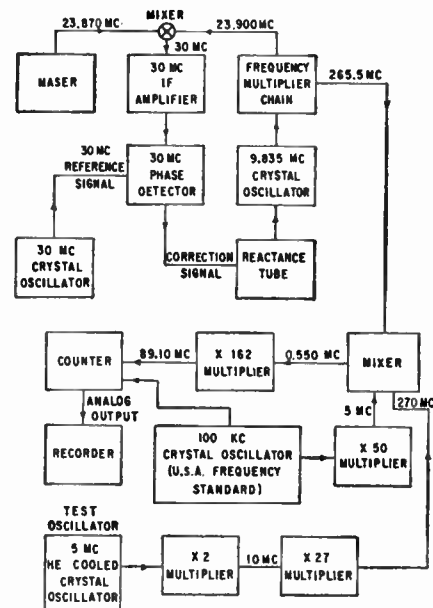


Fig. 4—Maser stabilized frequency-multiplier chain (all frequencies are nominal).

mechanical vibrations introduced by the regulator—crystals at very low temperatures are rather microphonic.

The quartz crystal was enclosed in an evacuated glass bulb and this was placed inside a brass cylinder. Liquid helium was in direct contact with the outside of the cylinder. A double dewar was used, with liquid nitrogen in the outer jacket and the helium in the inner container. In this system the pressure was regulated at about 650 mm of mercury.

The scheme used in comparing the helium-cooled oscillator with a maser-stabilized multiplier chain is shown in Fig. 4. The traces, of which Figs. 2 and 3 are samples, were derived from the analog output of the counter. The counter was set to count for one second and display for one second. Fluctuations at shorter time inter-

Phase Considerations in Degenerate Parametric Amplifier Circuits*

A previous paper¹ has given an expression for the negative resistance introduced into the signaling circuit of a degenerate parametric amplifier employing a quadratic nonlinearity of the magnetic type. It is the purpose of my paper to examine this resistance as a function of the phase angle between the pump and signal voltages. Bloom and Chang consider only signal voltages which pass through zero at alternate zeros of the pump.

We will write the signal and pump voltages as

$$V_1 \cos \omega t$$

and

$$V_2 \cos (2\omega t + \theta),$$

respectively. Their analysis¹ is for the special case $\theta = 0$. The inductance is assumed to have its flux ϕ and its current i related by

$$\phi = L_0 i - \mathcal{L} i^2.$$

The inductance, the series resonant signal circuit, and the series resonant pump circuit are all connected in parallel as in Bloom and Chang. Small signal analysis gives the ratio of the resistance, R , inserted into the signal circuit by the action of the pump, to the resistance R_T of the signal circuit as

$$\frac{R}{R_T} = \beta \left[\frac{(1 + \beta^2) \sin \theta - 2\beta}{1 + \beta^2 - 2\beta \sin \theta} \right] \quad (1)$$

where β is defined by

$$\beta = \frac{\omega_1 \mathcal{L} V_2}{R_T R_3}.$$

R_3 is the resistance in the pump circuit.

For a nonlinear capacitance, having charge q and voltage v related by

$$v = S_0 q - S q^2$$

connected in parallel with the series resonant

* Received by the IRE, March 18, 1959.
¹ S. Bloom and K. K. N. Chang, "Theory of parametric amplification using non-linear reactances," *RCA Rev.*, vol. 18, pp. 578-593; December, 1957.

signal and pump circuits, the resistance ratio is

$$\frac{R}{R_T} = \frac{-\alpha[\cos \theta + 2\alpha + \alpha^2 \cos \theta]}{(1 + \alpha \cos \theta)^2} \quad (2)$$

where

$$\alpha = \frac{SV_3}{2\omega_1^2 R_T R_3}$$

Eqs. (1) and (2) are plotted in Figs. 1 and 2 respectively. As the figures show, the

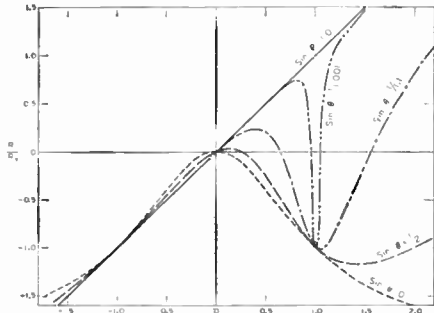


Fig. 1— R/R_T vs β for a degenerate parametric amplifier using a nonlinear inductance.

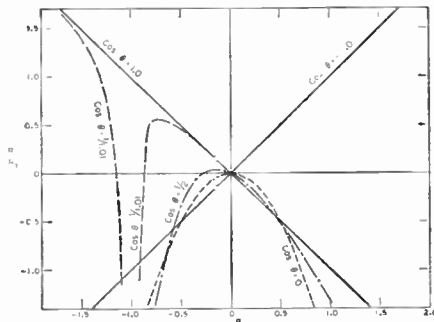


Fig. 2— R/R_T vs α for a degenerate parametric amplifier using a nonlinear capacitance.

oscillation point, $R/R_T = -1.0$, may or may not be sensitive to changes in θ , depending upon the signs of α and β . Actually, as R/R_T approaches -1.0 , the analysis breaks down, since the small signal approximation no longer holds.

As would be expected, the phase θ does not appear in the expression for R in non-degenerate cases.

GEORGE A. KLOTZBAUGH
Westinghouse Res. Labs.
Pittsburgh 35, Pa.

An Iterative Method for Determining Ladder Network Functions*

Practical network designers almost never resort to the classical mesh or node equations to find the driving-point or transfer functions of ladder networks. Of the various "short-

cuts" available, topological methods, such as signal-flow graphs¹ or Kirchhoff's rules² are most generally used. However, even these methods do not yield all the network functions simultaneously. For example, the Kirchhoff rule (or topological formula) used to determine, say, the driving-point admittance of a ladder is not applicable for the voltage-ratio transfer function. We would like to propose a simple construction method whereby it is possible to obtain every pertinent function simultaneously. The method is based upon certain well-known relationships that exist between the branch currents and the node voltages of a ladder network.³

To illustrate the simplicity of the method, consider the general ladder structure in Fig. 1. In this representation, the series arms of the ladder are given as impedances while the shunt arms are represented as admittances. $V_a(s)$ is a node voltage,

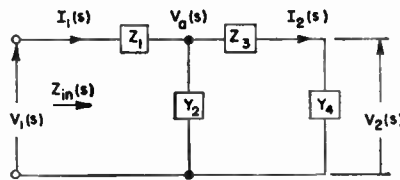


Fig. 1.

while $I_1(s)$, $I_2(s)$ are branch currents. For this network, the following relationships apply

$$V_2(s) = V_2(s) \quad (1)$$

$$I_2(s) = Y_4(s)V_2(s) \quad (2)$$

$$V_a(s) = I_2(s)Z_3(s) + V_2(s) = [1 + Z_3(s)Y_4(s)]V_2(s) \quad (3)$$

$$I_1(s) = Y_2(s)V_a(s) + I_2(s) = [Y_2(s)((1 + Z_3(s)Y_4(s)) + Y_4(s))]V_2(s) \quad (4)$$

$$V_1(s) = I_1(s)Z_1(s) + V_a(s) = [Z_1(s)[Y_2(s)((1 + Z_3(s)Y_4(s)) + Y_4(s)) + [1 + Z_3(s)Y_4(s)]]V_2(s) \quad (5)$$

As we start from the end of the ladder and work towards the front, we see that each equation is obtained by multiplying the preceding equation by an immittance, and then adding to this result the equation twice preceding it. For example, (2) is derived from (1) by multiplying $V_2(s)$ by the immittance $Y_4(s)$. Eq. (3) is then obtained by multiplying (2) by the next immittance down the line, $Z_3(s)$, and then adding to this result, $V_2(s)$, from (1).

From this set of equations, we immediately obtain the network functions by taking ratios of the various equations. For example, the driving-point impedance, $Z_{in}(s)$, is obtained by dividing (5) by (4). The current-

ratio transfer function $I_2(s)/I_1(s)$ is given as the ratio of (2) to (4). Moreover, if $V_2(s) = 1$, the equations are normalized. Eq. (5) is then simply the inverse of the voltage-ratio transfer function, $V_2(s)/V_1(s)$, while (4) is the inverse of the transfer impedance, $Z_{21}(s)$.

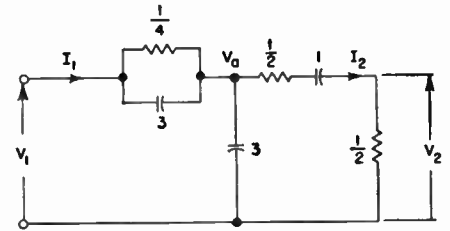


Fig. 2.

Consider the ladder network in Fig. 2. Here we see that

$$Y_4(s) = 2$$

$$Z_3(s) = \frac{1}{2} + \frac{1}{s} = \frac{s + 2}{2s}$$

$$Y_2(s) = 3s$$

$$Z_1(s) = \frac{\left(\frac{1}{4}\right)\left(\frac{1}{3s}\right)}{\frac{1}{4} + \frac{1}{3s}} = \frac{1}{3\left(s + \frac{4}{3}\right)}$$

The right-hand side of the equations can be written in the following triangular form:

$$\begin{array}{r|l} 1 & V_2(s) \\ 2 & I_2(s) \\ 2\left[\frac{(s+2)}{2s}\right] + 1 = \frac{2(s+1)}{s} & V_a(s) \\ 3s\left[\frac{2(s+1)}{s}\right] + 2 = 6\left(s + \frac{4}{3}\right) & I_1(s) \\ \frac{1}{3\left(s + \frac{4}{3}\right)}\left[6\left(s + \frac{4}{3}\right)\right] & \\ + \frac{2(s+1)}{s} = \frac{4\left(s + \frac{1}{2}\right)}{s} & V_1(s) \end{array}$$

Then the following network functions are obtained by inspection:

$$Z_{in}(s) = \frac{4\left(s + \frac{1}{2}\right)}{6s\left(s + \frac{4}{3}\right)}$$

$$\frac{I_2(s)}{I_1(s)} = \frac{1}{3\left(s + \frac{4}{3}\right)}$$

$$\frac{V_2(s)}{V_1(s)} = \frac{s}{4\left(s + \frac{1}{2}\right)}$$

$$Z_{21}(s) = \frac{1}{6\left(s + \frac{4}{3}\right)}$$

One obvious advantage of this method is that it enables a teacher to create compli-

¹ S. J. Mason, "Feedback theory—some properties of signal flow graphs," PROC. IRE, vol. 41, pp. 1144-1156; September, 1953.

² W. Mayeda and S. Seshu, "Topological Formulas for Network Functions," Bulletin 446, Engrg. Experiment Station, University of Illinois, Urbana, Ill.; 1956.

³ M. E. Van Valkenburg, "Network Analysis," Prentice-Hall Inc., Englewood Cliffs, N. J., pp. 233-234; 1955.

* Received by the IRE, April 7, 1959.

cated networks with simple driving-point impedances (by pole-zero cancellation in each line) for examination purposes.

F. F. KUO
Microwave Research Inst.
Polytechnic Inst. of Brooklyn
Brooklyn, N. Y.

G. H. LEICHSER
Dept. of Electrical Engineering
University of Illinois
Urbana, Ill.

Another Approximation for the Alpha of a Junction Transistor*

Several approximations¹⁻⁴ have been put forward for the frequency variation of α , the common-base short-circuit current gain of a junction transistor. In the present author's opinion these are either too crude, and so misleading, or else too ingenious for general use. A useful approximation combines accuracy with simplicity, and the larger the product "accuracy \times simplicity" the better. On this rating, it is felt that the approximation described below scores rather higher than any so far suggested.

We first state the expression to be approximated, then deduce the approximation, list its properties, and comment on them. Finally three other results of interest are appended.

The one-dimensional theory⁵ provides us with the relations (assuming the collector multiplication factor is unity):

$$\alpha(\omega) = \gamma\beta(\omega) \tag{1}$$

$$\beta(\omega) = \operatorname{sech} [\eta(1 + j\omega\tau)^{1/2}], \tag{2}$$

where γ is the emitter efficiency, β the base transport factor; η equals $W/(D\tau)^{1/2}$, where W is the "electrical" base width, and D , τ are the "effective diffusion constant" and "effective lifetime"; $j\omega$ is the complex frequency variable.

It is known⁶ that γ varies with frequency much less than does β , and so we assume that it remains constant at its low frequency value. This gives:

$$\frac{\alpha(\omega)}{\alpha_0} \sim \frac{\beta(\omega)}{\beta_0} = \frac{\operatorname{sech} [\eta(1 + j\omega\tau)^{1/2}]}{\operatorname{sech} \eta}, \tag{3}$$

where α_0 , β_0 are the low frequency values of α , β . Expanding gives

$$\frac{\beta(\omega)}{\beta_0} = 1 / \left[1 + \frac{j\omega\tau\eta^2\beta_0}{2!} \left(1 + \frac{\eta^2}{6} + \dots \right) - \frac{\omega^2\tau^2\eta^4\beta_0}{4!} \left(1 + \frac{\eta^2}{10} + \dots \right) + \dots \right]. \tag{4}$$

This is the expression we want to approximate.

Eq. (3) plotted on the complex plane gives the well-known spiral,⁷ and intuition suggested that a semicircle coinciding with the low frequency end of the spiral might provide the required approximation. The general form of a semicircle passing through the point (1,0) with center on the real axis is $z = (1 - jcm)/(1 + jm)$, where c is constant and m a parameter varying from 0 to $+\infty$. This may be expanded to give:

$$z = 1 / [1 + jm(1 + c) - m^2c(1 + c) + \dots]. \tag{5}$$

A direct comparison of (5) with (4) yields values for c and m , and if we assume $\beta_0 \approx 1$, we obtain

$$\frac{\beta(\omega)}{\beta_0} \sim \frac{1 - j\omega/5\beta_0\omega_s}{1 + j\omega/\omega_s}, \tag{6}$$

where

$$\omega_s = \frac{6}{5} \left(\frac{2D/W^2}{\beta_0} \right). \tag{7}$$

If we now put $\beta_0 = 1$ in the numerator of (6), we obtain, with small error, the following approximation⁸ for α

$$\frac{\alpha(\omega)}{\alpha_0} \sim \frac{1 - j\omega/5\omega_s}{1 + j\omega/\omega_s}. \tag{8}$$

The properties of this approximation are now briefly noted.

1) It has been shown⁹ that for normal values of β_0 ,

$$\frac{\omega_s}{1.216} = \frac{2D/W^2}{\beta_0},$$

where ω_s is the 3-db cutoff frequency. Hence $\omega_s = 0.987\omega_a$, and for all practical purposes ω_s may be substituted for ω_a in the approximation. The original form (8) is retained here for the sake of clarity.

2) The magnitude error at the cutoff frequency ω_a is 2 per cent; the error in phase angle is 2°. The errors rapidly become quite insignificant as the frequency is reduced.

3) The common emitter cutoff frequency deduced from the approximation is $\omega_s(1 - \alpha_0)/(1 + \alpha_0/5)$, compared with the true value¹⁰ $\omega_{\alpha'} = \omega_s(1 - \alpha_0)/1.2$.

4) The frequency at which the common emitter current gain $\alpha' = \alpha/(1 - \alpha)$ is unity is $\omega_s/1.183$, compared with the true value¹⁰ $\omega_1 = \omega_s/1.203$, i.e., an error of 2 per cent.

5) The 3-db frequency of the approximation (8) is $1.043\omega_s$, compared with the true value $\omega_a = 1.013\omega_s$, i.e., an error of 3 per cent.

It is clear from 1)-4) above that only negligible errors are encountered for fre-

quencies up to cutoff, whether or not ω_s is replaced by ω_a . Only if the approximation is used in reverse, 5), are discrepancies greater than 2 per cent. From 5) it appears that the 3-db frequency of the approximation is not exactly the 3-db frequency of the transistor, —and if ω_a replaces ω_s the situation seems paradoxical, if not intolerable. However, the paradox is easily resolved. The approximation is designed to be accurate at low frequencies, and so in this context ω_a is a constant characterizing the low frequency behavior, which itself happens to be defined by the high frequency behavior. For drift transistors ω_s and ω_a can differ considerably,¹¹ and the situation does not arise.

SWITCHING

The applications of the approximation in the field of switching are of interest. The switching theory given by Moll¹² is based on the approximation $\alpha = \alpha_0/(1 + j\omega/\omega_a)$ and if we replace this by the approximation (8), then we find e.g., for the 0 to 90 per cent turn-on time, under the same conditions,

$$T_0 = \frac{1}{\omega_s} \ln \frac{1.2I_E}{I_E - 0.9I_C/\alpha_0} \sim \frac{1}{5\omega_s} + \frac{1}{\omega_s} \ln \frac{I_E}{I_E - 0.9I_C/\alpha_0}, \tag{9}$$

(common base)

$$T_0 = \frac{1}{5\omega_s} + \frac{(1 + \alpha_0/5)}{\omega_s(1 - \alpha_0)} \ln \frac{I_B}{I_B - 0.9I_C/\alpha_0'} \sim \frac{1}{5\omega_s} + \frac{1.216}{\omega_s(1 - \alpha_0)} \ln \frac{I_B}{I_B - 0.9I_C/\alpha_0'}, \tag{10}$$

(common emitter)

and similarly for common collector; here I_E and I_B are emitter and base currents after the input step is applied, and I_C is the collector current at the edge of Region III. These expressions differ from Moll's by including the "delay time,"¹³ $1/5\omega_s$, the same (roughly) for all three connections, and the factor¹⁴ 1.216 in the common emitter and common collector connections.

CONCLUSION

It is suggested that the approximation described above gives an adequate description of the intrinsic frequency effects in a junction transistor, either in the original form (8), or in the form

$$\frac{\alpha(\omega)}{\alpha_0} = \frac{1 - j\omega/5\omega_s}{1 + j\omega/\omega_s}. \tag{11}$$

It is sufficiently accurate for practical purposes, and sufficiently simple to be easy to use.

APPENDIX

1) If we retain only the first two terms of (4) we have the simplest approximation

* Received by the IRE, April 3, 1959.
¹ D. E. Thomas, "Transistor amplifier—cutoff frequency," *Proc. IRE*, vol. 40, pp. 1481-1483; November, 1952.
² R. D. Middlebrook and R. M. Scarlett, "An approximation to alpha of a junction transistor," *IRE TRANS. ON ELECTRON DEVICES*, vol. ED-3, pp. 25-29; January, 1956.
³ K. L. Pritchard, "Electric-network representation of transistors—a survey," *IRE TRANS. ON CIRCUIT THEORY*, vol. CT-3, pp. 5-21; March, 1956. See (8) and footnote 45.
⁴ A. B. Macnee, "Approximating the alpha of a junction transistor," *Proc. IRE*, vol. 45, p. 91; January, 1957.
⁵ W. Shockley, M. Sparks, and G. K. Teal, "P-N junction transistors," *Phys. Rev.*, vol. 83, pp. 151-162; July, 1951.
⁶ K. L. Pritchard, "Frequency variations of junction-transistor parameters," *Proc. IRE*, vol. 42, pp. 786-799; May, 1954.
⁷ For example, see "Principles of Transistor Circuits," R. F. Shea, Ed., John Wiley and Sons, Inc., New York, N. Y., p. 347; 1953.
⁸ This approximation is similar to that put forward by Middlebrook and Scarlett, *op. cit.* However, the aim, derivation and result are all different; moreover the method used here can be applied to the drift transistor (see footnote 11).
⁹ J. M. Rollett, "The characteristic frequencies of a junction transistor," *J. Electronics and Control*, vol. 5, p. 347; October, 1958.
¹⁰ From (7) and footnote 9.

¹¹ J. M. Rollett, to be published.
¹² J. L. Moll, "Large-signal transient response of junction transistors," *Proc. IRE*, vol. 42, pp. 1773-1784; December, 1954.
¹³ N. H. Enenstein, "A transient equivalent circuit for junction transistors," *IRE TRANS. ON ELECTRON DEVICES*, vol. ED-4, pp. 37-54; December, 1953.
¹⁴ This factor is also found by R. Beaufoy and J. J. Sparkes, "The junction transistor as a charge controlled device," *A.T.E.J.*, vol. 13, pp. 310-327; October, 1957.

for both phase and magnitude of α , i.e.,

$$\frac{\alpha(\omega)}{\alpha_0} \approx \frac{1}{1 + j\beta_0\omega/(2D/W^2)} = \frac{1}{1 + 1.216j\omega/\omega_\alpha}$$

$$= \frac{1}{1 + j\alpha_0\omega/\omega_1} \quad (12)$$

This is only useful for frequencies less than about $\omega_1/3$.

2) Taking the magnitude of (4), we find an approximation for the magnitude of α , i.e.,

$$\left| \frac{\alpha(\omega)}{\alpha_0} \right|^2 \approx \frac{1}{1 + \beta_0^2\omega^2/6(D/W^2)^2}$$

$$\approx \frac{1}{1 - (\omega/\omega_\alpha)^2} \quad (13)$$

This is useful for frequencies up to about $5\omega_\alpha$ and provides a justification for use of the expression $\alpha(\omega) = \alpha_0/(1 + j\omega/\omega_\alpha)$.

3) If it is assumed that the only dissipative elements important at high frequencies are base resistance r_b and collector capacitance C_c , then the maximum frequency of oscillation ω_m is given by¹⁵

$$\omega_m = \frac{|\alpha|^2}{|\text{Im}(\alpha)|} \frac{1}{4r_bC_c} \quad (14)$$

where $\text{Im}(\alpha)$ is the imaginary part of α . Substituting for $|\alpha|$ from (13) (since this gives the magnitude accurately at high frequencies), and for $\text{Im}(\alpha)$ from (8), we obtain

$$\omega_m^2 = \frac{\alpha_0\omega_\alpha}{4.8r_bC_c} \quad (15)$$

which can be written

$$\omega_m^2 = \frac{\alpha_0'\omega_\alpha'}{4r_bC_c} = \frac{\omega_1}{4r_bC_c} \quad (16)$$

This result can also be obtained by using the approximation $\alpha' = \alpha_0'/(1 + j\omega/\omega_\alpha')$ since $|\alpha|^2/\text{Im}(\alpha) = |\alpha'|^2/\text{Im}(\alpha')$, or by working directly from (4). In the second form, (16), it may be applied to drift transistors, since the approximation for α' still holds.^{11,16}

J. M. ROLLETT
British Dielectric Res. Ltd.
London, W. 12, Eng.

¹⁵ This is found by putting the unilateral power gain equal to unity. See S. J. Mason, "Power gain in feedback amplifiers," IRE TRANS. ON CIRCUIT THEORY, vol. CT-1, pp. 20-25; June, 1954.

¹⁶ R. C. Johnston, "Transient response of drift transistors," Proc. IRE, vol. 46, pp. 830-838; May, 1958.

The Significance of Transients and Steady-State Behavior in Nonlinear Systems*

INTRODUCTION

An often misused and apparently not well-understood concept concerns what is meant by transients and steady-state behavior in nonlinear systems. The notion of

these terms seems vague to some even for linear systems. With the advent of systematic methods of analysis of nonlinear systems¹⁻⁶ recently published, it seems quite important to sharply define what is meant by transient and steady-state phenomena arising in nonlinear systems.

SIGNIFICANCE IN LINEAR SYSTEMS

The concept of transient phenomena arises naturally in linear systems and is therefore easily defined for such systems. Consider a linear system depicted by Fig. 1.

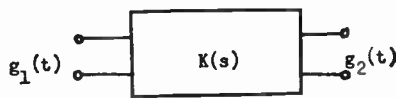


Fig. 1—A linear lumped parameter system.

The instantaneous response⁷ of this system is given by (1)

$$g_2(t) = \int_0^t k(\tau)g_1(t - \tau)d\tau, \quad (1)$$

where

$g_2(t)$ denotes the instantaneous time response,

$k(t)$ denotes the impulse response of the linear system.

$g_1(t)$ denotes the instantaneous forcing function.

s denotes the complex frequency variable.

t, τ denote time variables.

The function $g_1(t)$ satisfies the condition

$$g_1(t) \begin{cases} = 0 & \text{for } t < 0 \\ \neq 0 & \text{for } t > 0. \end{cases}$$

We may regard (1) as the total response of the linear system. Now we note that the integral of (1) may be written as the difference of two integrals, namely

$$\int_0^t k(\tau)g_1(t - \tau)d\tau$$

$$= \int_0^\infty k(\tau)g_1(t - \tau)d\tau - \int_t^\infty k(\tau)g_1(t - \tau)d\tau. \quad (2)$$

Eq. (2) follows from the definition of the integral.⁸ The first term of the right member is recognized as the steady-state term since

¹ A. A. Wolf, "A Mathematical Theory for the Analysis of a Class of Nonlinear Systems," Ph.D. dissertation, University of Pennsylvania, Philadelphia, Pa.; June, 1958.

² A. A. Wolf, "Recurrence relations in the solution of a class of nonlinear systems," AIEE Summer Meeting, paper no. 57-864, June, 1957, To be published in *Trans. AIEE*; 1959.

³ A. A. Wolf, "Generalized relations in the solution of physical nonlinear systems," AIEE Winter Meeting, paper no. 58-437; February, 1958.

⁴ A. A. Wolf, "Analysis of transcendental nonlinear systems," AIEE Summer Meeting, paper no. 58-995; June, 1958.

⁵ Y. H. Ku and A. A. Wolf, "A stability criterion for nonlinear systems," AIEE Winter Meeting, paper no. 59-23; February, 1959. To be published in *Trans. AIEE*; 1959.

⁶ Y. H. Ku, A. A. Wolf, and J. H. Dietz, "Taylor-Cauchy transforms for the analysis of a certain class of nonlinear systems," 1959 IRE NATIONAL CONVENTION RECORD, pt. 2, pp. 49-61.

⁷ Eq. (1) can be written as

$$g_2(t) = \int_0^t g_1(\tau)k(t - \tau)d\tau.$$

⁸ E. T. Whittaker and G. N. Watson, "A Course of Modern Analysis," Cambridge University Press, Cambridge, Eng.; 1927.

(3) is the response in the Fourier convolution sense.

$$\int_{-\infty}^\infty k(\tau)g_1(t - \tau)d\tau = \int_0^\infty k(\tau)g_1(t - \tau)d\tau \quad (3)$$

in which we note $g_1(t) = 0$ for $t < 0$.

The second term of the right member of (2) is therefore the transient term. This result follows from the notion that the total response of a linear system is composed of transient and steady-state terms only.

If we let $g_{2T}(t)$ denote the transient term and $g_{2S}(t)$ denote the steady-state term, then

$$g_{2T}(t) = \int_t^\infty k(\tau)g_1(t - \tau)d\tau \quad (4)$$

and

$$g_{2S}(t) = \int_0^\infty k(\tau)g_1(t - \tau)d\tau. \quad (5)$$

Eq. (2) written in terms of (4) and (5) is

$$g_2(t) = g_{2S}(t) - g_{2T}(t). \quad (6)$$

FOR NONLINEAR SYSTEMS

It is evident therefore that the transient and steady-state behavior is defined for linear systems. The question now arises as to what these mean in a nonlinear system. To begin with we must recognize that a linear system is a special case of a class of nonlinear systems. Thus any definition of transient and steady-state phenomena must be consistent with (4) and (5) and indeed reduce to (6) in the limiting case.

Consider Fig. 2. The transmission char-

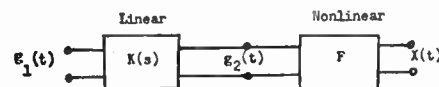


Fig. 2—A nonlinear system with F belonging to the functional class.

acteristics of the nonlinear components are assumed to belong to the functional class.^{1,2} Wolf² shows that the polynomial belongs to this class under certain conditions. Therefore

$$X(t) = \sum_{k=0}^M a_k t^k \quad (7)$$

is a possible form of $F\{g_2\}$. Other forms of $F\{g_2\}$ may involve polynomials of derivatives of $g_2(t)$ and products of derivatives and the various degrees of the function. The degree of (7) is denoted by M . We suppose without loss of generality that F does not load $K(s)$. Under these conditions the output $X(t)$ can be written as (8) in terms of (4) and (5) as follows with the aid of the binomial theorem.

$$X(t) = \sum_{k=0}^M \sum_{n=0}^k a_k (-1)^n \binom{k}{n} g_{2S}^{k-n} g_{2T}^n;$$

$$\binom{k}{n} = \frac{k!}{n!(k-n)!} \quad (8)$$

To display the transient and steady-state terms as defined for linear systems $X(t)$ is expanded as follows

$$X(t) = \sum_{k=0}^M \left\{ a_k g_{2S}^k + (-1)^k a_k g_{2T}^k \right.$$

$$\left. + \sum_{n=1}^{k-1} a_k (-1)^n \binom{k}{n} g_{2S}^{k-n} g_{2T}^n \right\}, \quad (9)$$

* Received by the IRE, March 31, 1959.

or

$$X(t) = \sum_{k=0}^M a_k g_{2S}^k + \sum_{k=0}^M a_k g_{2T}^k + \sum_{k=0}^M \sum_{n=1}^{k-1} a_k (-1)^n \binom{k}{n} g_{2S}^{k-n} g_{2T}^n. \quad (9a)$$

It is clear therefore that the first term of the right member is the steady-state term and the second term of the right member is the transient term. We see in addition that some new terms appear in the nonlinear system which did not appear in the linear system. These new terms will be denoted as the "Cross-Product" terms. We further note that (9a) is consistent with (6) in the limiting case when $M \leq 1$.

CONCLUSIONS AND DISCUSSION

The total instantaneous response of a linear system is defined by a transient and steady-state behavior only while a non-linear system cannot be described by these alone. Another behavior must be considered, namely that arising from the cross-product terms. If one is tempted to call the cross-product terms either steady-state or transient, he immediately is inconsistent with the well-defined concept of these terms in linear systems. It is therefore not enough to think of transients as phenomena which either die out or grow with time.

From the previous development we note the following relations:

Linear System:

Total Instantaneous Response = Steady-State Response - Transient Response. (10)
 Nonlinear System:

Total Instantaneous Response = Steady-State Response - Transient Response + Cross Product Response. (11)

It is easy to show that (11) is true of all nonlinear systems.

ALFRED A. WOLF

The Moore School of Elec. Engrg.
 University of Pennsylvania
 Philadelphia, Pa.

graph and also was presented at the IRE Convention in 1949 [1]:

A new terminology for multi-port networks. In the present discussion, the writer is introducing a new terminology to fill a long-felt need. It is found especially helpful in the treatment of converters.

It has been customary to designate each entrance or exit of a network as a pair of terminals, based on the circuit concept of wires and conduction. The result was cumbersome terms such as "four-terminal networks." The ultimate confusion was caused by the term "two-terminal-pair" with the unobvious meaning of a network with two pairs of terminals. Furthermore, the terminal-pair concept becomes artificial in the case of electromagnetic fields transmitting power within boundaries, through holes, and from one region to another in space.

After considering many alternatives, the writer has adopted the term "portal" or simply "port" as the general designation of an entrance or exit of a network. A self-impedance becomes a "one-port." The usual transducer becomes a "two-port" with one "in-port" and one "out-port." The general network is designated a "multi-port." This plan has received a favorable reaction from the several engineers to whom it has been presented, and is first put to use in this monograph.

In the short space of one decade, this terminology has been accorded increasing acceptance, largely through its adoption by the active theoretical group in the Microwave Research Institute of the Polytechnic Institute of Brooklyn. Two years ago, the term "port" was formally defined in IRE Standards [3]. Just recently, it has first appeared in a complete textbook [4]. Considering the long usage of the previous terminology, it is gratifying that the transition to "ports" has progressed so far in so short a time.

HAROLD A. WHEELER
 Wheeler Laboratories
 Great Neck, N. Y.

BIBLIOGRAPHY

- [1] D. Dettinger and H. A. Wheeler, "Measuring the Conversion Efficiency of a Superheterodyne Converter by the Input Impedance Circle Diagram," Wheeler Monographs, No. 9, March, 1949. Presented at the 1949 IRE Convention, New York, N. Y.; abstract, Proc. IRE, vol. 37, p. 162; February, 1949.
- [2] "Reference Data for Radio Engineers," 4th ed., IT&T Corp., p. 646; 1956.
- [3] "IRE Standards on Electron Tubes: Definition of Terms, 1957," Proc. IRE, vol. 45, pp. 983-1010; July, 1957. Also, "IRE Standards on Antennas and Waveguides: Waveguide and Waveguide Component Measurements," Proc. IRE, vol. 47, pp. 568-582; April, 1959.
- [4] N. Balabanian, "Network Synthesis," Prentice-Hall, Inc., New York, N. Y., 1958.

Ten Years of a "Multi-Port" Terminology for Networks*

Recently I have received some inquiries as to the origin of the term "port" in the field of networks. Some of our readers may be interested in my original approach to this topic. This is best reviewed by quoting from a paper by David Dettinger and the writer, which was printed in the form of a mono-

WWV Standard Frequency Transmissions*

Since October 9, 1957, the National Bureau of Standards radio stations WWV and WWVH have been maintained as constant as possible with respect to atomic frequency standards maintained and operated by the

Boulder Laboratories, National Bureau of Standards. On October 9, 1957, the USA Frequency Standard was 1.4 parts in 10⁹ high with respect to the frequency derived from the UT2 second (provisional value) as determined by the U. S. Naval Observatory. The atomic frequency standards remain constant and are known to be constant to 1 part in 10⁹ or better. The broadcast frequency can be further corrected with respect to the USA Frequency Standard, as indicated in the table; values are given as parts in 10¹⁰. This correction is not with respect to the current value of frequency based on UT2. A minus sign indicates that the broadcast frequency was low.

The WWV and WWVH time signals are synchronized; however, they may gradually depart from UT2 (mean solar time corrected for polar variation and annual fluctuation in the rotation of the earth). Corrections are determined and published by the U. S. Naval Observatory.

WWV and WWVH time signals are maintained in close agreement with UT2 by making step adjustments in time of precisely plus or minus twenty milliseconds on Wednesdays at 1900 UT when necessary; no time adjustment was made during this month at WWV and WWVH.

WWV Frequency†				
1950	#1	#2	#3	
July	1	-31	-33	-29
	2	-32	-35	-31
	3	-32	-32	
	4	-31	-32	
	5	-30	-32	
	6	-30	-32	-28
	7	-30	-32	-29
	8	-30	-32	-28
	9	-30	-32	-29
	10	-30	-32	-29
	11	-30	-32	
	12	-30	-32	
	13	-30	-32	-29
	14	-30	-32	-27
	15	-30	-32	-28
	16	-30	-32	-27
	17	-30	-32	-27
	18	-30	-32	
	19	-30		
	20	-30	-32	-29
	21	-30	-32	-29
	22	-30	-32	-29
	23	-30	-32	-29
	24	-30	-32	-27
	25	-30	-32	
	26	-30	-32	
	27	-29	-32	-28
	28	-29	-32	-28
	29	-29	-32	-29
	30	-29	-31	-28
	31	-29	-32	-28

† WWVH frequency is synchronized with that of WWV.

Column #1 Vs NBS‡ atomic standards, Boulder, Colo., 30-day moving average seconds pulses at 15 mc.

Column #2 Vs atomichron at WWV, measuring time one hour at 2.5 mc.

Column #3 Vs atomichron at the U. S. Naval Research Laboratory, Washington, D. C., measuring time 56 minutes at 2.5 mc.

‡ Method of averaging is such that an adjustment of frequency of the control oscillator appears on the day it is made. No adjustment was made during July.

NATIONAL BUREAU OF STANDARDS
 Boulder, Colo.

* Received by the IRE, April 9, 1959.

* Received by the IRE, August 24, 1959.

Contributors

Robert Adler (F'51) was born on December 4, 1913, in Vienna, Austria. He received the Ph.D. degree in physics in 1937 from the University of Vienna.



R. ADLER

He was assistant to a patent attorney in that city in 1938. From 1939 to 1940, he worked in the Laboratory of Scientific Acoustics, Ltd., in London, England. After one year with Associated Research, Inc., in Chicago, Ill., he joined the research group of Zenith Radio Corporation in the same city in 1941. He became Zenith's Associate Director of Research in 1952. His previously published work in the vacuum-tube field includes the development of the phasitron modulator, of receiving tubes such as the 6BN6 and 6AR8, and of transverse field traveling-wave tubes.

Dr. Adler is a member of the American Association for the Advancement of Science.



L. J. Anderson was born in Salt Lake City, Utah, in 1917. He received the A.B. degree in 1939, and the M.A. degree in 1942, both from the University of California, Los Angeles.



L. J. ANDERSON

From 1942 to 1955 he was a physicist at the United States Naval Electronics Laboratory, San Diego, Calif., where he worked on tropospheric propagation problems, particularly the effects of the lower atmosphere on propagation. He was responsible for developing methods of predicting radio-radar propagation from routine meteorological data, and was also engaged in meteorological instrumentation for propagation purposes. Prior to 1955, he directed the Environment Studies Branch at the Naval Electronics Laboratory. Then, in 1955, he joined colleagues in forming Smyth Research Associates, where he is continuing his work on tropospheric propagation and allied studies.

Mr. Anderson is a member of U.S.A. Commission II of URSI, the American Meteorological Society, and the American Chemical Society.



Julian J. Bussgang (A'52-M'55-SM'58) was born in Lwow, Poland, on March 26, 1925. He received the B.Sc. (Eng.) degree

from the University of London, London, Eng., in 1949, after attending Politecnico di Torino, Italy, for one year. He received the



J. J. BUSSGANG

M.S. degree in electrical engineering from the Massachusetts Institute of Technology, Cambridge, in 1951 and the Ph.D. degree in applied physics from Harvard University, Cambridge, Mass., in 1955.

While attending M.I.T., he was with the Research Laboratory of Electronics. From 1952 to 1953 he was connected with the Lincoln Laboratory, Lexington, Mass. In 1954 he was on the research staff of the Gordon McKay Laboratory at Harvard.

He joined the Radio Corporation of America in 1955. He has worked on radar design, statistical detection theory, nonlinear systems analysis, frequency modulation, and coding. He is at present manager of applied research in the RCA Missile Electronics and Controls Department, Burlington, Mass.

Dr. Bussgang is a member of Sigma Xi, the IEE, and the Society for Industrial and Applied Mathematics.



B. G. Firth was born in Kearny, N. J., on January 28, 1902. He graduated from the engineering training course of the Bell Telephone Laboratories, New York, N. Y., in 1924.



B. G. FIRTH

He remained at the Bell Telephone Laboratories for eleven years, where he worked mostly on vacuum tube research and development, and associated problems. In 1935 he joined the Electronic Tube Division of Tung-Sol Electric, Inc., Bloomfield, N. J., where in 1942 he assisted in the formation of the Tung-Sol Research Lab. He has been with Tung-Sol for twenty-four years, working on practically all phases of vacuum tube research and development, including electronic ignition and hot and cold cathode and vacuum and gas filled tubes.



Louis Essen was born in Nottingham, England, in 1908. He received the B.S. degree in physics from London University, England, in 1928. After a short period of post-graduate study at University College,

Nottingham, he joined the National Physical Laboratory, Teddington, England, where he is now a Senior Principal Scientific



L. ESSEN

Officer. While with the Laboratory, he received the Ph.D. and D.Sc. degrees in 1941 and 1948, respectively, from London University. He has worked on quartz clocks, the velocity of electromagnetic waves, the refractive index of gases, and measurements at microwave frequencies.

Dr. Essen is a member of the Order of the British Empire.



Joseph H. Holloway was born in Cleveland, Ohio, on July 31, 1929. He received the B.S. degree from the Massachusetts Institute of Technology, Cambridge, and the



J. H. HOLLOWAY

B.A. degree from Wooster College, Wooster, Ohio, simultaneously in 1952 on a combined study plan, and the Ph.D. degree in physics from the Massachusetts Institute of Technology in 1956.

Since that time, he has been with the National Company, Malden, Mass., where he has been concerned primarily with the development of atomic beam frequency standards.

Dr. Holloway is a member of the American Physical Society.



George W. Hrbek (A'53-M'57) was born on December 27, 1927 in Oak Park, Ill. He received the B.S. degree in electrical engineering from the Illinois Institute of Technology, Chicago, in January, 1953.



G. W. HRBEK

From 1953 to 1954, he was associated with the Electron Tube Division of Sperry Gyroscope Co., where he worked on traveling-wave tubes and related microwave-tube problems. From 1954 to 1956 he served in the U. S. Army Signal

Corps. Since 1956, he has been a research engineer at the Zenith Radio Corporation, Chicago, Ill., working in the field of transverse-field traveling-wave tubes and transverse-field parametric amplifier tubes.

Mr. Hrbek is a member of Eta Kappa Nu.



Daniel Leenov was born in Washington, D. C., on April 10, 1923. He received the B.S. degree in chemistry from George Washington University, Washington, D. C., in 1943. He began graduate work at the University of Chicago, Chicago, Ill., in 1946, receiving the M.S. and Ph.D. degrees in physics in 1948 and 1951.



D. LEENOV

From 1943 to 1945 he was a research associate on a National Defense Research

Committee rocket project at George Washington University. He taught in the Physics Department of Roosevelt College from 1951 to 1952, and in the College of the University of Chicago from 1952 to 1955. From 1955 to 1956 he was an assistant professor in the Department of Physical Science and in the Department of Physics at the University of Florida. He joined the technical staff of the Bell Telephone Laboratories in 1956, where he has been associated with the microwave diode group.

Dr. Leenov is a member of the American Physical Society and Sigma Xi.



Walter A. Mainberger (S'43-A'45-M'51-SM'57) was born in Würzburg, Germany, on June 28, 1922. He received the B.E.E. degree from the College of the City of New York, N. Y., in 1943.

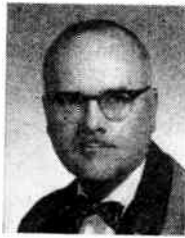


W. A. MAINBERGER

After serving two years in the U. S. Navy as a radio technician, he was employed for five years by the Federal Telecommunications Laboratories, where he worked on instrument landing and omnirange systems and helped develop the prototype TACAN system. He received the M.E.E. degree from New York University, N. Y., in 1951, and that same year joined the W. L. Maxson Company where he helped develop a radar map-matching navigational computer. In 1955, he joined the National Company, Malden, Mass., where he has since been engaged mainly in the development and production of atomic frequency standards and is now manager of the Electronic Systems Department.

Mr. Mainberger is a registered Professional Engineer in Massachusetts.

Donald W. Mayer was born in Philadelphia, Pa., in 1919. He received the B.Sc. degree from the Philadelphia College of Pharmacy and Science in 1941.



D. W. MAYER

He joined the research laboratory of John Wyeth & Company until called to military service in 1942. In 1946 he entered the research laboratory of Merck & Company where he remained until 1950, at which time he became associated with Tung-Sol Electric, Bloomfield, N. J., as a research chemist. His first problems were on the screening of black and white TV tubes. Later he was engaged in work on semiconductor, color television, and finally, the MgO cold cathode project.



Viktor Met was born on September 10, 1928, in Vienna, Austria. He received the Dipl. Ing. from the Technische Hochschule,



V. MET

Vienna, in 1952 and was the recipient of a Fulbright Travel Grant in the same year. He received the M.S. degree in electrical engineering in 1953 from the University of Minnesota, Minneapolis, during which time he was a teaching assistant at the University. Upon his return to Austria, he became a research assistant at the Technische Hochschule and received the Dr. techn. degree in 1955. Since November, 1955, he has been a member of the technical staff at the General Electric Microwave Laboratory in Palo Alto, Calif.



Paul Nesbada was born on June 20, 1921, in Trieste, Italy. He received the Dr. Math. Sciences degree from the University of Pisa,



P. NESBADA

Italy, in 1943. From 1943 to 1952 he was engaged in teaching and research in theory of functions, calculus of variations, and integration theory at the University of Trieste, Italy, the Catholic University of America, Washington, D. C., the University of Paris, Institut H. Poincaré, and the Institute for Advanced Study, Princeton, N. J.

In 1952 he joined RCA Victor Division in Camden, N. J., where he worked in the application of statistical estimation to the

fields of communication and radar detection. Since 1958 he has been leader of the Applied Mathematics Group at the Missile Electronics and Controls Department of RCA in Burlington, Mass.

Dr. Nesbada is a member of the American Mathematical Society, the Mathematical Association of America, the Institute of Mathematical Statistics, the Society for Industrial and Applied Mathematics, and Sigma Xi. He is also listed in "American Men of Science."



J. V. L. Parry was born on September 12, 1923, in Mountain Ash, Wales. He received the B.S. degree, and, in 1942, the M.S. degree from University College, Cardiff, Wales.



J. V. L. PARRY

From 1944 to 1946, he was engaged in radar research at the Royal Radar Establishment. He was at the National Physical Laboratory, Teddington, Middlesex, England, from 1946 to 1958, where he worked on dielectric measurements, microwave measurements, and atomic standards. Mr. Parry is presently the principal physicist at the Diffusion Plant of the Atomic Energy Authority, Capenhurst, Cheshire, England.



Friedrich H. Reder (A'54) was born in Garsten, Upper Austria, on December 9, 1919. He received the cand. ing. degree in technical physics from the Institute of Technology, Graz, Austria, in 1947, and the Ph.D. degree in physics from the University of Graz in 1949.



F. H. REDER

From 1948 to 1950, he was at the University of Graz, where he was engaged in work on microwave cavity methods for determining the dielectric constant of solids and liquids, and in work on interference microscopy. From 1950 to 1951, he was with the Massachusetts Institute of Technology, Cambridge, where he was a research fellow engaged in work on microwave gas discharge phenomena in pure He gas. From 1951 to 1953, he worked on gas discharge projects and high-vacuum techniques at the University of Graz and at the Shell Research Laboratory, Amsterdam, The Netherlands. Since 1953 he has been with the Frequency Control Division of the U. S. Army Signal Research and Development Laboratories, Fort Monmouth, N. J., where he is now in charge of research and development work in atomic and molecular frequency control.

Dr. Reder is a member of the American Physical Society.

Harris Safran was born in Denver, Colo., on April 28, 1923. He received the B.S. degree in physics in 1948, and the M.S. degree



H. SAFRAN

in mathematics in 1949, both at the University of Utah, Salt Lake City. From 1949 to 1952 he continued graduate study in mathematics at Harvard University, Cambridge, Mass.

From 1952 to 1955 he worked in the fields of guided missiles, and guidance and control, at the

Massachusetts Institute of Technology, Cambridge.

Since 1955, Mr. Safran has been at RCA Missile Electronics and Controls Department, Burlington, Mass., working in the fields of systems analysis and radar.



A. Melvin Skellett (M'44-SM'50-F'56) was born in St. Louis, Mo., on July 14, 1901. He received the A.B. and M.S. degrees



A. M. SKELLETT

in physics in 1924 and 1927, respectively, both from Washington University, St. Louis, Mo., and the Ph.D. degree in astronomy from Princeton University, Princeton, N. J., in 1933.

After two years at the University of Florida, Gainesville, where he held the positions

of assistant professor of physics and chief engineer of the state-owned radio station WRUF, he joined the technical staff of Bell Telephone Laboratories. Fifteen years later he left Bell to become director of research and vice-president of National Union Radio Corporation where he also served on the Board of Directors. He holds 80 U. S. patents, and served for a number of years as consultant to the Department of Defense of the U. S. Government. In 1955, he joined Tung-Sol Electric, Inc., Bloomfield, N. J., where he is presently employed as director of research.

Dr. Skellett is a life member of the American Astronomical Society, and a member of the American Physical Society, American Ordnance Association, and Sigma Xi.



Arthur Uhler, Jr. (A'53-SM'58) was born in Chicago, Ill., on February 2, 1926. He received the B.S. and M.S. degrees in chemical

engineering from the Illinois Institute of Technology, Chicago, in 1945 and 1948, respectively, and the S.M. and Ph.D. degrees



A. UHLER, JR.

in physics in 1950 and 1952, respectively, from the University of Chicago, where he was an AEC predoctoral fellow from 1949 to 1951.

He was a process analyst at Douglas Aircraft Co., Chicago, Ill., in 1945. From 1945 to 1948, he was engaged in fluid mechanics research at Armour Research Foundation. In 1951, he joined the Transistor Development Department of Bell Telephone Laboratories. There he worked on point-contact transistor theory, semiconductor surface protection, and electrochemical properties of semiconductors, and developed an electrolytic micromachining technique for metals and semiconductors. He was also engaged in work on microwave semiconductor devices. Since September, 1958, he has been with Microwave Associates, Burlington, Mass.

Dr. Uhler is a member of the American Physical Society, Sigma Xi, Phi Lambda Upsilon, and the American Association for the Advancement of Science.



S. H. Unger (S'47-M'57), for a photograph and biography, please see page 1767 of the October, 1958 issue of PROCEEDINGS.



Glen Wade (S'51-A'54-SM'57) was born in Ogden, Utah, on March 19, 1921. He received the B.S. and M.S. degrees in electrical



G. WADE

engineering from the University of Utah, Salt Lake City, in 1948 and 1949, respectively. He did graduate study at Stanford University, Stanford, Calif., where he was first a Sperry Fellow and then an RCA Fellow in Electronics, receiving the Ph.D. degree in 1954.

He had worked for a year at the Naval Research Laboratory in Washington, D. C., and after receiving the Ph.D., was employed as a research associate by the General Electric Microwave Laboratory at Stanford. At present he is an associate professor of electrical engineering at Stanford and a senior staff member of the Stanford Electronics Laboratories.

Dr. Wade received an Eta Kappa Nu Award in the "Outstanding Young Electrical Engineer" competition in 1955. He is a

member of the American Physical Society, Phi Kappa Phi, Tau Beta Pi, Eta Kappa Nu, and Sigma Xi.



Steven Weisbrod (S'49-A'50-M'55), was born in Warsaw, Poland, on July 30, 1925. He came to the United States in 1939, and



S. WEISBROD

received the B.S. degree in physics in 1949 from the California Institute of Technology, Pasadena, and the M.S. degree in engineering in 1959, from the University of California, Los Angeles.

During World War II, he served with the American expeditionary forces in Europe, and, from 1949 to 1955, was employed as a physicist at the Navy Electronics Laboratories in San Diego, Calif. During that time he specialized in the problems of ionospheric radio propagation, backscatter and diversity systems. In 1953, for his work on the high-frequency backscatter system, he received the Navy Superior Accomplishment Award. In 1955, together with some of his colleagues, he helped form Smyth Research Associates in San Diego, Calif. He is now senior physicist there and, in this capacity, is continuing basic research in the field of ionospheric physics, electromagnetic wave propagation and meteor and field aligned scatter, and has written a number of papers on these subjects.

Mr. Weisbrod is a member of the American Mathematical Society.



Gernot M. R. Winkler was born on October 17, 1922 in Frohnleiten, Austria. He attended the Realgymnasium in Graz, Austria, and received the Ph.D. degree from the University of Graz in 1952.



G. M. R. WINKLER

In 1949, he joined the Solar Observatory, Kanzelhoehe, and later worked at the Astronomical Observatory, Graz, where he became assistant to the director. He came to this country in 1956 and

has been working since at the U. S. Army Signal Research and Development Laboratories, Fort Monmouth, N. J., in the field of precision frequency control. He is presently Consultant of the Atomic Resonance Branch of the Frequency Control Division.

Scanning the Transactions

Experiments with teaching machines are proving them to be dramatically effective. Automated teaching systems have several very important advantages over conventional methods of instruction: 1) They provide every student information feedback that is individually tailored to his particular response. 2) They provide this information immediately. 3) The teaching process is individually geared to the learning pace of each student. Although the experimental machines in use now are simple—even crude—their superiority over standard classroom techniques has been clearly proven. Machines have taught first semester German in 40 hours and a college algebra course in 30 hours. When a college psychology course was recently automated, the standard final exams had to be revised because the median final score was 94 per cent, with no student making less than 85 per cent in the course. The only criticism reported came from college juniors taking an automated physical chemistry course at The Ohio University—they complained that the course was too easy! There is much yet to be learned in this infant field about programming techniques and machine requirements. It is an area that electronics people will be intimately associated with, requiring teachers to experiment and engineers to develop required teaching devices, and last but not least, eventually involving electronics students in their classrooms. (R. F. Mager, "Preliminary studies in automated teaching," IRE TRANS. ON EDUCATION, June, 1959.)

Talking to yourself is not necessarily as easy as you think. Psychoacoustic studies have shown that in order to speak freely and normally the average person has to be able to hear what he is saying. Along these lines, Marvin Camras reports an interesting incident which occurred when a wire recording was being monitored as it was being made, with the pickup head spaced a fraction of a second after the recording head. An announcer accidentally put on the monitoring headphones while he was speaking. He heard his own voice, to be sure, but what he heard was completely out of phase with what he was saying. The effect was so unexpected and overwhelming that he became absolutely speechless. The headphones were tried on others, with the same result—they became powerless to speak. In fact, a few small wagers were won from the uninitiated who thought they could recite a short paragraph while wearing the magic headphones. Dr. Camras adds that later studies by others showed that there are differences among individuals in the degree of confusion generated by delayed listening, with women seeming to be less susceptible than men. This would seem to support the theory that the more voluble talkers among us never listen to themselves. If true, this might explain one of nature's most puzzling and common phenomena—two women talking to each other simultaneously, and yet hearing every word the other said. ("The Editor's Corner," IRE TRANS. ON AUDIO, July-August, 1959.)

Microminiaturization is rapidly becoming an outmoded word as the density of component packaging increases by leaps and bounds. We have now reached the point where we can cram 50,000 parts in one cubic foot of space. How much more "miniature" do we expect to get? Now the experts are talking about densities ten times as great—and in only 3 to 5 years. In fact, a few special units, consisting of resistors, capacitors and transistors, have already been built in the 500,000 to 700,000 parts-per-cubic foot range. Indeed, we are approaching the time when the average volume of a single component will be 10^{-6} ft³, or a *micro*cubic foot, so to speak. Too bad we didn't save the word "*microminiature*" for that day. (S. F. Danko and V. J. Kublin, "Micro-modules: com-

ponent parts and material requirements," IRE TRANS. ON PRODUCTION TECHNIQUES, August, 1959.)

Should we say "monaural?" The term really means "one-eared." Maybe "monophonic" would be more accurate. (P. W. Klipsch, "Wide-stage stereo," IRE TRANS. ON AUDIO, July-August, 1959.)

A new type of ferrite switch has been proposed that operates by reflection rather than absorption. The switching ratio is high (60 db) and the bandwidth is determined mainly by the applied magnetic field. These characteristics differ considerably from those of conventional absorptive ferrite switches. The switch takes the form of a ferrite slab imbedded in a circular waveguide, and among its many interesting applications are tunable cutoff filters, antenna switching, and AGC systems. (R. F. Soohoo, "A ferrite cutoff switch," IRE TRANS. ON MICROWAVE THEORY AND TECHNIQUES, July, 1959.)

A Solid-State issue of TRANSACTIONS has just been published by one of the Professional Groups—not the Electron Devices Group, as one might think, but the PG on Nuclear Science. The field of nuclear science is principally one of instrumentation and control, and thus has become especially fertile ground for exploiting the several and varied capabilities of solid-state devices. These devices have intriguing potentialities for the detection of neutron flux and other forms of radiation, and for use in all types of associated circuits, ranging from direct-current amplifiers of great sensitivity to pulse amplifiers and switching circuits operating at megacycle rates. They can also be used as switches, controlling large amounts of power, and thus are a potential replacement for relays. It is worthy of note that nuclear science is by no means the only field in which the solid state is having a field day. A review of last year's major advances in the microwave field, for example, shows that solid-state developments overshadowed all else, due to progress in solid-state masers and, especially, various forms of parametric amplifiers for generation and low-noise amplification at microwave frequencies. The stream of solid-state advances runs broad and deep indeed. (Solid-State Issue, IRE TRANS. ON NUCLEAR SCIENCE, June, 1959; R. E. Beam and M. E. Brodwin, "Report of advances in microwave theory and techniques in U.S.A.—1958," IRE TRANS. ON MICROWAVE THEORY AND TECHNIQUES, July, 1959.)

The ingenuity of man in simulating conditions he expects to encounter or wants to investigate is admirably illustrated by the variety of simulation devices that have been developed in the military electronics field. A sampling of eight simulation techniques are presented in a recent issue of TRANSACTIONS. Running through the list we find that devices, largely electronic in nature, have been developed to train celestial navigators, helicopter pilots and space crews. Simulated radar displays are described that can train radar operators to identify terrain features from the air and to track targets from the ground. One simulator even prepares a three-dimensional model of the terrain from a topographic map. (IRE TRANS. ON MILITARY ELECTRONICS, July, 1959.)

O-guide and X-guide will now have to be added to G-line and H-guide as a part of the microwave engineer's working vocabulary. The surface-wave transmission line, originally dubbed the G-line, has taken on more sophisticated and electrically efficient forms. The O-guide consists of a hollow cylindrical structure made of a thin dielectric sheet. The X-guide, as might be guessed, is a dielectric structure with an X-shaped cross section. These new surface-wave lines are being proposed for use in the SHF region, where they exhibit

a lower loss than do coaxial lines, G-lines, H-guides and rectangular waveguides. (M. Sugi and T. Nakahara, "O-guide and X-guide: An advanced surface wave transmission concept," IRE TRANS. ON MICROWAVE THEORY AND TECHNIQUES, July, 1959.)

Recent applications of circuits tend to demand more and more knowledge of how to switch effectively between different transmission properties and how to obtain directional selectivity in a network. The first of these problems involves the theory of varying parameter systems, and the second that of nonreciprocal systems. In an important subclass the first problem leads to two-state networks in which the parameters are changed between two sets of values by a bias control, while the second leads to two-port networks with unequal transmittance functions for the two directions of propagation. To define a figure of merit for networks from the point of view of such applications, the scattering matrix notation may be effectively employed. In the switched case, the scattering

matrices before and after switching should show maximum difference between corresponding elements, while in the non-reciprocal case, maximum difference between off-diagonal elements of a single two-by-two scattering matrix is sought. Schaug-Pettersen and Tonning have shown how these differences may be maximized by lossless reciprocal imbedding of the given network and that the best possible result in both cases depends monotonically on a characteristic positive real parameter which is invariant to such transformation. This parameter is related to the invariant found by S. J. Mason in his study of power gain in feedback amplifiers. A figure of merit for state separability and nonreciprocity of devices and materials can thereby be defined and canonical procedures for obtaining the optimum performance in individual cases can be established. (Schaug-Pettersen and A. Tonning, "On the optimum performance of variable and nonreciprocal networks," IRE TRANS. ON CIRCUIT THEORY, June, 1959.)

Books

The Upper Atmosphere, by H. S. W. Massey and R. L. F. Boyd

Published (1959) by the Philosophical Library, Inc., 15 E. 40 St., N. Y. 16, N. Y., 325 pages + 7 index pages + 1 bibliography page + xii pages. Illus. 6 × 9. \$17.50.

It was but twelve years ago that Prof. S. K. Mitra, of the University College of Science in Calcutta, published the first comprehensive treatise on the upper atmosphere.¹ This monumental work which, as he put it, took him a solar cycle to complete, has remained without a peer. Mitra regretted his inability to include the results of the first explorations of the upper atmosphere by American workers using V-2 rockets but felt that he could not delay publication any longer. The book was quickly sold out and within five years (1952) was published in a second edition with much material added.

Now there is an avalanche of research focused on the upper atmosphere and Prof. Massey and Dr. Boyd, of the Physics Department at University College in London, have recorded the great advances made during the International Geophysical Year of 1957-1958 and the years just preceding. Their book, however, is not simply an extension of Mitra's work. In the authors' words, it is neither a text nor a monograph. There are no direct references to the literature, although a selected list of twenty items for correlative reading has been included at the end. In a book which is slightly less than half as long as Mitra's, the authors make a good attempt to touch upon every aspect and known phenomenon of the upper atmosphere, treating the most basic with some degree of completeness and making every effort to include the most recent. The treatment has been kept as nonmathematical as possible although, inevitably, it does

contain some mathematics, or at least concepts, which are more than elementary. Certainly the authors are to be criticized for not using rationalized MKS units and for using English units frequently.

For the new student of the upper atmosphere, the book is a complete and current introduction though he may wish to consult Mitra's more exhaustive treatment of many subjects and his many references to the literature.

For the advanced student of the upper atmosphere, the clear statements of physical interpretation will be edifying and may clear up more than one point that he has never had the perspective to see.

There are twenty-one half-tone plates and four pages of attractive colored illustrations. The latter show an instrumented rocket nose-cone, three photographs of the aurora, a laboratory discharge in nitrogen, and a laboratory demonstration of the fluorescence of sodium vapor when illuminated by yellow light.

The chapter titles are: 1) The Relevant Physics; 2) The Atmosphere; 3) Research by Balloons and Rockets; 4) Probing with Sound Waves; 5) Probing with Radio Waves; 6) The Ozonosphere and the Ionosphere; 7) Lights in the Night Sky; 8) Aerial Tides and Magnetic Effects; 9) Solar, Magnetic, and Ionospheric Disturbances; 10) Meteors; 11) Cosmic Rays; 12) Artificial Satellites; and 13) Future Possibilities.

The first major international scientific conference concerned with rocket exploration of the upper atmosphere was held at Oxford University in 1953. Some forty-five papers which had been presented at the conference were published the next year under the editorship of Dr. Boyd and M. J. Seaton in consultation with Prof. Massey.² Thus

the authors of the present volume have been well informed on this new field from the outset and their book undoubtedly makes its most original contribution in this area.

M. G. MORGAN
Thayer School of Engineering
Dartmouth College
Hanover, N. H.

General Circuit Theory, by Gordon Newstead

Published (1959) by John Wiley and Sons, Inc., 440 Fourth Ave., N. Y. 16, N. Y. 140 pages + 2 index pages + 2 bibliography pages + vii pages. Illus. 4 × 6½. \$3.00.

In this book, the author undertakes to develop "a concise self-contained introduction to the subject of circuit theory from a more or less advanced viewpoint." It is one of the few books available in the area of advanced circuit analysis, and, in general, is well written and contains the latest developments in the theory of linear networks.

The book contains five chapters, and opens with an introduction to the basic definitions of impedance, networks, mesh and node equations, circuit elements, analogy between electrical and mechanical elements, and the concept of transducers. However, it would be desirable to have a proof or physical justification for the number of independent mesh and node equations. Cramer's rule is used in solving mesh and node equations without any comment on the non-singularity of the mesh and node determinants.

In the second chapter, a number of basic theorems and properties of linear networks are developed; the superposition theorem, Tellegen's theorem (principle of conservation of energy in a linear network), reciprocity theorem, gyrator as a nonreciprocal element, Thevenin's theorem, and passivity. Each theorem and definition is concisely stated and well illustrated. Thevenin's theorem, however, needs a more detailed investigation of its validity for a network containing dependent sources.

¹ S. K. Mitra, "The Upper Atmosphere," The Asiatic Society, Calcutta, 1947; 2nd ed., 1952 (713 pages).

² R. L. F. Boyd and M. J. Seaton, editors (in consultation with H. S. W. Massey), "Rocket Exploration of the Upper Atmosphere," Pergamon Press, 1954 (376 pages).

Chapter 3 contains properties of linear passive four-terminal networks, open- and short-circuit parameters, general circuit parameters, interconnection of networks, image parameters, matching problems, reflection and insertion loss, etc.

Chapter 4 is the longest chapter, and it contains Fourier transforms, Heaviside and Dirac functions, the use of the complex frequency plane to develop the impulse response of a network, and properties of network functions for two- and four-terminal networks. The relationship between the real and imaginary parts of a network function, the phase-area theorem, and minimum and nonminimum phase shift networks are illustrated.

Chapter 5 deals with approximation methods in nonlinear problems such as the linearization method, the method of power series or high order approximation, and the switch method.

This reviewer feels that some of the illustrations are too concise, and consequently some of the important mathematical and physical implications are lost. The brevity of presentation may have resulted from the author's noble effort to keep the size of the book small.

WAN H. KIM
Dept. of Elec. Eng.
Columbia Univ.
New York, N. Y.

Experimental Music, by Lejaren A. Hiller, Jr. and Leonard M. Isaacson

Published (1959) by McGraw-Hill Book Co., 330 W. 42 St., N. Y. 36, N. Y. 179 pages +17 appendix pages. Illus. 6 X9 $\frac{1}{2}$. \$6.00.

Most of this book is a description of a sequence of digital computer programs for the composition of music. The programs were developed by the authors and executed on the Illiac computer. A variety of styles was produced, ranging from strict counterpoint to exceedingly dissonant atonal chromatic passages. All works are for string quartet. In some pieces only part of the music, such as pitch or time or dynamics, is specified by the computer; in others all is a computational-result.

The essence of the composition program is a random number generator producing a sequence of independent numbers, a mapping from these numbers onto the musical parameter to be selected, and a set of rules for rejecting numbers or sequences not meeting certain requirements. The rules are furthest developed for strict counterpoint and include sequential specifications over a maximum of three notes and harmonic specifications over a maximum of two successive chords. Additional rules could be used to limit the range of a voice and to terminate with a cadence. The development and use of these rules is probably the authors' greatest advance over existing music composing programs.

Samples of the various compositions were combined into one piece, "The Illiac Suite," which lasts for about 15 minutes. A copy of the score is appended to the book. Perhaps the easiest way to appreciate the great significance of the authors' work is by hearing the music. The most impressive feature is that the various styles for which the programs were intended are indeed achieved. The early counterpoint might well have come from a hymn. The unrestricted chromatic passages are reminiscent of von

Webern, while the chromatic passages with controlled harmonics occupy an intermediate position and can be compared with Bloch's style. Both the range of styles and the control over style is excellent.

The computer music for short times of 5 to 10 seconds compares well with similar sections of a human product. Over longer times, the computer music tends to seem aimless and thus inferior. If the computer is viewed as an aid to a human composer, then the 10 second time is a measure of achievement in that the composer need only specify the music every 10 seconds. Without the computer, he must specify several notes per second. Thus, the computer has achieved a saving in work of perhaps 40 to one, a saving which is quite substantial.

The most apparent limitation to the computational process is the difficulty of introducing long range correlations in the music, such as repeated themes and developments. Generation with independent random numbers tends to produce uncorrelated results. The authors have tried making successive intervals dependent by use of a Markoff chain. However, much more complex statistical structures must be developed which will allow high correlations between widely separated portions of the music.

MAX V. MATHEWS
Bell Telephone Labs.
Murray Hill, N. J.

Radio Engineering Handbook, Fifth Edition, edited by Keith Henney, prepared by a staff of specialists

Published (1959) by McGraw-Hill Book Co., Inc., 330 W. 42 St., N. Y. 36, N. Y. 1748 pages +27 index pages +ix pages. Illus. 6 X9 $\frac{1}{2}$. \$25.00.

Any reference manual that has been serving an industry for more than a quarter of a century as a first source when a quick answer to any general problem is needed, does not need much of an introduction by a reviewer. This Fifth Edition has been almost tripled in size and includes seven chapters on new subjects. It seems that all material in the previous edition, which appeared in 1950, has been competently re-examined, and a vast amount of new information has been added, particularly in the fields of solid state device applications, nonlinear circuits, and new tubes, components, and measurements in high frequency applications. The wealth of formulas, tables, circuits and descriptions of systems that have appeared in earlier editions in each branch of radio is still included, augmented by additional items and updated revisions where necessary. There is no hesitancy in suggesting that this reference will find frequent use if kept at hand by any engineer. This edition will usually prove worthwhile, even if an earlier one is still at hand.

RALPH R. BATCHER
Electronic Consultant
Douglaston, N. Y.

Proceedings of the Fourth Conference on Magnetism and Magnetic Materials, sponsored by the Magnetics Subcommittee of the AIEE Committee on Basic Sciences. Supplement to the Journal of Applied Physics, Vol. 30, 1959

Published for the American Institute of Physics by the McGraw-Hill Book Co., Inc., 330 W. 42 St., N. Y. 36, N. Y. 323 pages +vi pages. Illus. 8 X10 $\frac{1}{2}$. \$10.00.

This book offers, in a single volume, an

excellent compendium of recent research and developmental effort in the broad field indicated by the title above. Over 144 papers are included, covering every area of current interest in magnetism. Of special interest to the IRE member are the papers dealing with amplifiers, microwave applications, instrumentation, computer components, and thin films. Although this book will primarily be of interest to those working in the field of magnetism, it is reviewed here since it is such an excellent collection of important papers in a field which is of increasing technological importance.

JOHN H. ROWEN
Bell Telephone Labs., Inc.
Whippany, N. J.

Basic Electronics, by Bernard Grob

Published (1959) by McGraw-Hill Book Co., Inc., 330 W. 42 St., N. Y. 36, N. Y. 487 pages +10 index pages +3 bibliography pages +21 appendix pages +ix pages. Illus. 6 X9 $\frac{1}{2}$. \$9.25.

This is an excellent book for an introductory course on electronics. It contains enough material to offer the reader an understanding of the basic principles. Books written on this subject frequently contain too many topics for proper comprehension. Covering only the basics reflects good judgment on the part of the author.

The book includes Ohm's law, series and parallel circuits, meters, magnetism, dc and ac, resistance, inductance, capacitance, plus the basic ideas of electron tubes and transistors. Circuitry and applications of these basic ideas are left to a second volume now in preparation. By including only the basics, the author has been able to give fairly comprehensive treatment of each topic. Items such as the practical use of components, care and maintenance, and basic troubles might have suffered had the complete subject been attempted in one volume. This is illustrated in the chapter on batteries where charging and maintenance are included.

Much of the writing seems to anticipate the reader's questions, which no doubt stems from the author's own experience in teaching the subject. The chapter arrangement is extremely logical and the material within the chapters shows much more than just casual organization. The writing itself is clear and concise, and sufficient pictures and diagrams are included to improve the presentation greatly.

Each chapter begins with an introduction, giving the reader some idea of what to expect. A summary at the end of each chapter emphasizes the main points presented. Self-examination questions for each chapter (with answers in the back of the book) are extremely helpful to all students, particularly to those who will read this without the aid of an instructor. A ready source of information is available through the many appendices at the end of the book.

This is the first printing, and this book, too, seems to contain its share of minor discrepancies, for example on page 31 the average cost of electricity is listed as 3¢ per kilowatt hour and on page 352 it is 4¢. In the appendix, the FCC assignments are listed from 30 kc instead of 10 kc.

In general, the book is a valuable addition to the electronics field.

JOSEPH J. GERSON
Devry Tech. Inst.
Chicago, Ill.

Sampled-Data Control Systems, by John R. Ragazzini and Gene F. Franklin

Published (1958) by McGraw-Hill Book Co., Inc., 330 W. 42 St., N. Y. 36, N. Y. 312 pages +5 index pages +5 bibliography pages +8 appendix pages +ix pages. Illus. 6 X 9. \$9.50.

This book presents a lucid and explicit summary of the techniques for analysis and design of sampled-data systems. It opens with an analytical description of the processes of regular sampling of time functions and of the reconstruction of time functions from their samples. The description of the Z transform covers the processes of direct and inverse transformation and the initial and final-value theorems. The concept of the transfer function to describe pulse filters is presented. Next, the application of transfer functions to analyze sampled-data systems is presented and the stability criterion is derived. The next two chapters deal with selection of compensation elements for feedback systems. First, the use of continuous signal compensators is considered; then digital compensators are considered. The fact that the analysis of digital compensators is the more tractable leads to a much simpler and more explicit design procedure for digital compensation than for continuous signal compensation. Several techniques are presented for analysis of the behavior of the continuous output of a sampled-data system between sampling instants. The analysis techniques for sampled data systems with random inputs are presented. Multirate sampled systems are discussed and several applications of sampled-data theory are presented.

The book will be useful both as a text book and as a reference. Its strongest feature is its clear and explicit exposition of various analysis techniques. As a text book, it suffers most from the absence of emphasis on concepts rather than merely on techniques. There is little explicit comparison between the concepts of design of continuous servos and those which would be applicable to sampled-data servos. The reader already familiar with continuous servo design would find little in this book which he could recognize as analogous to what he already knows, beyond the general similarity in techniques.

In many cases, explicit comparisons

would have been illuminating. In conventional servos, the effectiveness of the feedback loop is increased with the increases in loop gain that can be accommodated. Generally, the error coefficients provide an effective measure of the servo following capability and its insensitivity to load disturbances. The relevance of these measures of performance of sampled-data servos was not mentioned. From a practical point of view, it would be very valuable to have a simple measure of how often the error must be sampled to provide adequate suppression of load disturbances. While techniques for making such evaluations are presented, the concepts are not pointed out, and they probably would be missed by the uninitiated student. No doubt the authors intended that such concepts be driven home to the student by problems.

On the whole, the book makes a very useful contribution. Its style is clear and specific, the selection of topics is good, and it does a good job of summarizing the work done in the field.

WILLIAM K. LINVILL
The RAND Corp.
Santa Monica, Calif.

Electron Physics and Technology, by J. Thomson and E. B. Callick

Published (1959) by the MacMillan Co., 60 Fifth Ave., N. Y. 11, N. Y. 515 pages +11 index pages +xiv pages. 5 1/2 X 8 1/2. \$10.00.

This book, written by Professor J. Thomson of the Royal Naval College, Greenwich, and E. B. Callick, Chief Engineer of the English Electric Valve Company, is intended as an undergraduate engineering textbook on electron tubes and their operation. However, about 10 per cent of the text covers semiconductor device principles and technology, so that the authors have chosen to adopt a broad title, even though this may be a little misleading.

The first of the six major sections covers a general introductory treatment of free and bound electrons, including the principles of electron emission, electron optics, vacuum and gaseous conduction, a short chapter on semiconductors, and a chapter on noise. The next section is entitled Electron Devices

Employing Space-Charge Variation, chiefly diodes and grid-controlled tubes; a short chapter on the bipolar transistor is also included, thereby showing that the section title is something less than accurate. The next two sections, on electron inertia effects, and on microwave tubes, comprise about one-third of the book, and they are its best parts. Magnetrons, klystrons, and traveling-wave tubes are explained both in principle and in some detail. The fifth section is on special tubes, and it covers cathode-ray, storage, switching, and photosensitive devices. A final section covers electron tube materials and construction, and includes one short chapter on semiconductor technology.

The shortcoming of the book lies in the cursory and inadequate treatment of solid-state devices. The transistor and many of its offspring are already important devices at low frequencies. Every year new solid-state switching and computing devices are uncovered. At microwaves, one can expect increasing student interest in such things as masers, reactance (parametric) amplification, and ferrite effects. None of these are discussed, and it may be necessary to supplement this text with material on modern solid-state applications to effect better coverage. Unfortunately, suitable references are lacking. In fact, no supplementary references at all are given in the first three sections; those given in the last half of the book are chiefly to books which, since they predate the present volume, are even less likely to provide a desirable breadth of perspective. In defense of the authors, however, this reviewer does not know how a single book could be prepared in reasonable size and yet cover the entire electron device field.

The authors have written their text with a maximum of practical descriptive material and a minimum of complex mathematics, so that it is easily read, even by someone with little mathematical skill. The book is well indexed and will be of help to those who wish to make a quick review of parts of the electron tube field, as well as to the serious student who follows it through from cover to cover.

E. W. HEROLD
RCA Labs.
Princeton, N. J.

Abstracts of IRE Transactions

The following issues of TRANSACTIONS have recently been published, and are now available from the Institute of Radio Engineers, Inc., 1 East 79th Street, New York 21, N. Y. at the following prices. The contents of each issue and, where available, abstracts of technical papers are given below.

Sponsoring Group	Publication	Group Members	IRE Members	Non-Members*
Audio	AU-7, No. 4	\$0.30	\$0.45	\$0.90
Circuit Theory	CT-6, No. 3	1.60	2.40	4.80
Education	E-2, No. 3	1.65	2.50	4.95
Microwave Theory and Techniques	MTT-7, No. 3	1.65	2.45	4.95
Military Electronics	MIL-3, No. 3	1.25	1.90	3.75
Production Techniques	PT-5	2.45	3.70	7.35

* Libraries and colleges may purchase copies at IRE Member rates.

Audio

VOL. AU-7, No. 4, JULY-AUGUST, 1959

The Editor's Corner (p. 89)**PGA News** (p. 91)**Wide-Stage Stereo**—P. W. Klipsch (p. 93)

Stereophonic playback systems are studied to determine the accuracy with which they can reproduce the geometry of the original sound. Sounds were generated in a geometric pattern, recorded, and reproduced over a loudspeaker array. The methods used were similar to those used by Steinberg and Snow in 1933. Using two sound tracks, a derived center playback channel, and corner placement of flanking speakers, geometry plots were made with almost as good accuracy as when observers listened to an actual person speaking at the indicated stations in the geometric array.

Since wide speaker spacing was used, corner placement becomes natural.

An evaluation of corner speaker placement from the tonal standpoint (as contrasted with the geometric) shows that there is a large increase in quality available by taking advantage of the reflections of the floor and walls. It is shown that corner placement of flanking speakers and use of a derived-channel center speaker affords the best reproduction of geometry as well as tonality.

A Study of a Two-Channel Cylindrical Transducer for Use in Stereo Photograph Cartridges—C. P. Germano (p. 96)

An analytical as well as experimental evaluation of the electromechanical equivalent circuit constants of a two-channel flexural-type element is presented. This unit is a hollow cylindrical PZT ceramic structure electroded and polarized to be responsive to two signals perpendicular to each other.

The electromechanical equivalent circuit chosen to represent this element is based on the analogy between mechanical and electrical vibrating systems, and is a modification of the electromechanical circuit proposed by Mason. It is made up of lumped electrical and mechanical parameters in combination with an ideal transformation ratio.

Along with this evaluation, a brief discussion of performance characteristics of an experimental cartridge utilizing this element will be presented.

A Frame Grid Audio Pentode for Stereo Output—J. L. McKain and R. E. Schwab (p. 101)

The development and performance capabilities of a dual pentode using a single cathode, two separate *Framelok* grids and a twin-plate structure contained in one envelope is described. This new pentode, known as Type 6DY7, is a high-performance tube with superior characteristics of uniformity and stability obtained from its unique structure. Such factors as greater uniformity in tube-to-tube characteristics, reduced characteristic spread, and less susceptibility to characteristic deterioration at high dissipations can be obtained.

This dual pentode offers extreme flexibility in application. Three basic configurations are: 1) sections operated separately (single-ended) giving 5 watts of audio power per section; 2) two sections in push-pull, Class AB₁ providing up to 20 watts output at less than 3 per cent distortion; and 3) two tubes in push-pull parallel.

A single tube can be used for two stereo output channels, or two tubes can be operated in push-pull for higher power requirements. The same advantages can be used for monophonic audio systems.

The tube, therefore, offers the circuit designer a choice of usage not possible in presently-available tubes and at cost advantages realizable through a reduction in the number of circuit components.

Circuit Theory

VOL. CT-6, No. 3, JUNE, 1959

Applications of Routh's Algorithm to Network-Theory Problems—W. D. Fryer (p. 144)

The well-known Routh's criterion uses a very efficient computational method, or algorithm, that has been found to reduce greatly calculational labor and chances of error in a number of other important applications to circuit theory. Among these applications are finding common factors of polynomials, computing Sturm's functions, synthesizing RC, RL, or LC ladder networks by means of continued-fraction expansions, determining RC, RL, or LC realizability of a given immittance function, and analysis of ladder networks. Methods of handling the first two problems, both in normal and special cases, are given and illustrated.

On the Optimum Performance of Variable and Nonreciprocal Networks—T. Schaug-Petersen and A. Tonning (p. 150)

Lossless, reciprocal transformations of two-state and nonreciprocal two-ports are discussed. (Two-state networks are networks whose parameters may be switched simultaneously between two different values.) The minimum loss of such networks for various applications are shown to depend upon a single characteristic number which is invariant under the transformations studied. When a two-state or non-reciprocal material is used to realize such a network, there is an upper limit for the value of the characteristic number, and this is defined as a figure of merit for the material.

A Power Theorem on Absolutely Stable Two-Ports—G. E. Sharpe, J. L. Smith, and J. R. W. Smith (p. 159)

The stability criteria of two-ports are briefly reviewed, and the activity of two-ports is then discussed at some length. It is found that the real power available from an absolutely stable two-port for a fixed input excitation and passive load cannot exceed a maximum value. This maximum value is only obtained when the two-port is *unilateral* and has its parameters on the *stability boundary*.

A "figure of merit" for active two-ports can now be defined in terms of "maximum absolutely stable power gain."

Time-Response Characteristics of a System as Determined by its Transfer Function—J. D. Brule (p. 163)

In this paper a study is made of the step and impulse responses of systems whose transfer functions have all their poles on the negative real axis. The effects that real zeros of the transfer function have on the system response are evaluated. One result shows that if the transfer function has n finite zeros, all on the positive real axis, then the step response of the system has exactly n zero crossings. These step-response characteristics are studied further to establish upper and lower bounds on the position of the zero crossing for the case $n=1$, and other bounds on the time functions for the cases $n=0$ and $n=2$.

Flow-Graph Solutions of Linear Algebraic Equations—C. L. Coates, (p. 170)

A weighted, oriented topological structure, denoted by G and called a flow graph, is associated with a set of m equations in n variables, denoted by $KX=0$, such that K is a connection matrix and X a vertex weight matrix of the associated graph. This same set of equations can be written as $A^-X=0$ where A^- and A^+ are negative and positive incidence matrices and where C and X are respectively branch and vertex weight matrices of the graph.

By familiar algebraic procedures, an expression for the weight x_p of a nonreference vertex of G is obtained as a linear combination of the weights of the reference vertices (vertices with zero negative order) and can be written

as $x_p = \sum_{j=1}^n \zeta_{p,r_j} x_{r_j}$. To these algebraic results there correspond topological expressions in terms of subgraphs of G for the coefficients, ζ_{p,r_j} . A similar correspondence is obtained between the topological operation of deleting a vertex from the flow graph and the algebraic operation of eliminating a variable from the set of equations. These results are derived from the algebraic equations written in terms of the incidence and weight matrices of the graph. They are similar to those given for the familiar Signal-Flow-Graph, although they are more convenient to use, since the topological properties of the flow graph depend only upon the algebraic properties of the set of equations.

A flow graph can be drawn directly from an electric network diagram, and the flow-graph properties, used to obtain a solution of the network equations. Examples of this for two types of feedback networks are shown.

Triode Network Topology—A. W. Keen, (p. 188)

The 0- and 1-cell elements of topology are identified with a single terminal-pair and a two-terminal-pair transmission network, rather than with a single-terminal (or node) and a one-terminal-pair (or branch), respectively, in order to facilitate topological consideration of unilateral transmission networks, as typified by the triode valve. It is shown that even the simplest triode network has a feedback interpretation; in more general networks, several signal transmission loops may be distinguished, including both inverting and noninverting unilateral paths.

Application of Mellin and Hankel Transforms to Networks with Time-Varying Parameters—F. R. Gerardi (p. 197)

Integral transform techniques for solving linear integro-differential equations can provide insight and flexibility in solving physical problems, especially network problems. The type of differential equation which describes the physical system will dictate the transform that should be applied to simplify the solution and this paper deals with two transforms, namely, the Mellin transform and the Hankel transform. The Laplace transform can be used to solve linear constant coefficient differential equations or networks which are represented by this type of equation. A familiarity with this transform is assumed and is not covered in this paper.

Mellin transforms may be applied to networks which yield the Euler-Cauchy differential equation. This transform will simplify the solution of such an equation. A transform table, similar to that type used in Laplace transform theory, is developed and applied to network problems.

Hankel transforms may be applied to networks which yield the Bessel differential equation or variations of this equation. Unlike the Laplace and Mellin transforms, the Hankel transform is symmetric and the transformed variable is a real, rather than a complex variable.

A transform table of both operations and functions is developed and applied to network problems as before. Three methods can be used to establish the table of transform pairs. They can be described as: performing the integral operation, applying the table of operations on known transform pairs, and deriving the Hankel transform from the Laplace transform. With both transforms, the applications are made to problems in analysis, instrumentation, and synthesis.

Image Parameter Square-Frequency Filter Design—D. B. Pike (p. 208)

By homographic or bilinear transformations of the square frequency plane, it is shown that the image propagation behavior of filters of reactive impedances can, on normalization to the bandwidth, be described independently of the relative bandwidth.

A graphical filter design method, similar to the Kosowsky approximation method for filters of narrow relative bandwidth, is hence made available as an accurate method for any relative bandwidth. For relating critical frequencies of lattice impedances to the peaks of infinite attenuation, results combine the simplicity of the Kosowsky (approximate) formulas with complete accuracy for all relative bandwidths. Methods of treating reflection loss are given.

In terms of the transformed square frequency variable, the image propagation behavior of any filter represents a whole class of filters from which, by homographic transformations, individual members may be formed as band-pass, high-pass, low-pass, or all-pass filters.

Maximally-Flat Time Delay Ladders—S. Deutsch (p. 214)

The driving-point impedance for a maximally-flat time delay response is derived. The impedance is synthesized as an infinite low-pass LC ladder that starts with an $\epsilon G/\omega_0$ -farad shunt capacitor. The ladder elements rapidly taper toward a capacitance of $2G/\omega_0$ farads and an inductance of $2R/\omega_0$ henries. The impulse and step responses of the impedance are derived as a series of Bessel functions.

A three-terminal maximally-flat time delay transfer impedance is also considered. The conditions for a smoothly-tapering ladder structure are given. The transfer impedance is synthesized as an infinite low-pass LC ladder whose first two shunt capacitors are $32G/(9\omega_0)$ and $\epsilon^2 G/(9\omega_0)$ farads, respectively. The impulse and step responses of the transfer impedance are also derived.

On Realizability of a Circuit Matrix—R. B. Ash and W. H. Kim (p. 219)

Methods of testing the realizability of a matrix as the circuit matrix of a linear connected graph are presented. Several theorems pertaining to realizability are derived. A systematic synthesis procedure is illustrated for a restricted class of matrices.

Theoretical Limitations on the Gain-Bandwidth Product of Three-Terminal Networks—J. J. Spilker, Jr. (p. 224)

Wherever parasitic impedances are found shunting the terminals of a network, certain limitations on the electrical behavior of this network can be found. Typically, these parasitic impedances might represent a transistor, vacuum tube, or some other loading effect. In this paper, theoretical limitations are derived for the gain-bandwidth product of passive linear three-terminal networks (not necessarily lossless) used as low-pass filters. An important use of these limitations is in determining the upper bounds on the performance of video amplifiers.

Bode has considered limitations of this type for an important but restricted class of networks where the parasitic elements are purely capacitive, whereas in this paper, limitations are shown for arbitrary parasitic impedances. One important application of this new generality is that limitations can now be established for transistor amplifiers. This development has required the use of a general resistance integral theorem, the derivation of which is given in this paper. Different limitations are indicated for RLC networks and those allowing mutual inductance. Examples are given.

Book Reviews (p. 229)

Correspondence (p. 232)

PGCT News (p. 236)

Education

VOL. E-2, NO. 3, JUNE, 1959

An Experiment in IRE-Secondary School Cooperation—J. W. Kearney and M. T. Lebenbaum (p. 67)

The Long Island Section of the IRE has attempted to attack the problem of cooperation with the secondary schools in its region in

two ways. The first is to supply technical support to the high-school science teacher by direct contact with the student in areas where rapid scientific advances have made specialist knowledge a requirement. The second is towards the provision of a lecture series specifically for the teachers themselves. This paper describes the approach and the results of the first two years of operation of the program.

Advanced Education in Industry—J. D. Cassidy (p. 73)

With few exceptions, companies in the electronics industry sponsor advanced education. They derive many benefits from the sponsorship of these programs, such as keeping their engineering staffs up to date on new technical advances, increasing the staff prestige, and attracting outstanding engineering graduates.

Industry and Education must provide better advanced education in industry if we are to meet the challenges of tomorrow. Certain problems now present will be overcome in the future with better coordination and planning.

Undergraduate Laboratories—Some Comments on Efficient Use of Student's Time—W. J. Fahey (p. 75)

Some sort of reportorial process is necessary for evaluation of undergraduate laboratory work. A variety of methods currently employed are not entirely satisfactory. Ideally, such a process should accomplish its purpose with a minimum expenditure of time and effort and, wherever possible, enhance the educational efficiency of the laboratory. Under certain conditions, verbal communication may be employed to these ends. In addition to more efficient use of time, other results include: more accurate evaluation, increased effectiveness of laboratory problems as teaching devices, and useful training in the use of verbal communication. In other terms, the communication channel between instructor and student may be given greater capacity, less noise, and changed more nearly into a closed loop.

Criteria for the Selection of Engineers for Employment—L. H. Noggle (p. 78)

The demand for greater numbers of technically-trained personnel, along with the scientific sophistication needed to meet tomorrow's need for new technologies, indicate that we must take a new look at our present criteria for the selection of engineers for employment.

Criteria must be more basic than the mere evaluation of personality, grades and interests. This fact suggests the necessity to re-define the present industrial concept of engineering.

1200 Case Studies of Engineering Motivation—G. E. Moore (p. 82)

Ability, motivation, work challenges, and environment—these things set the pattern for a successful engineering career. One company, through a personal approach, is endeavoring to develop a better understanding of these factors in order to assist its young engineers in fulfilling their true potential.

It is expected that this "Personal Follow" program will result, ultimately, in more effective utilization of engineering personnel, furtherance of professional growth and development, and greater technical contributions from these young members of the profession.

Understanding, Mathematics, and Scientific Education—W. L. Kilmer (p. 85)

The purpose of this paper is to state what the author believes is a good way to develop the powers of understanding of talented college science students. After making a careful and somewhat novel distinction between knowledge and understanding, the paper closely defines the main problem in terms of the new interpretation of "understanding." A short discussion follows which concludes that what is needed is more and better schooling in the central ideas of mathematics. At this point, the tenor of the paper is changed and a semi-popular discussion is given on the fundamental type of mathematics the author has in mind.

Finally, a proposal is made which is general enough to be adapted to a wide variety of situations.

Dynamics of Engineering Education—Uniformity or Quality—E. Weber (p. 89)

A number of internal and external pressures bear down on engineering colleges today. These include the shortage of experienced manpower, the rapid rate of scientific discoveries requiring absorption in curricula, the increasing college population, competition by industry for faculty members, and the need for additional income for plant expansion and faculty salaries.

Within the body of engineering schools, one faction presses for the scientific reorientation of curricula while another holds to the professional art of design as the principal requirement in engineering colleges.

Despite the traditional assumption that education is distinguished by large moments of inertia and that the time scale is measured in terms of generations, we lack sufficient time in a world of latent chaos. Positive and exciting internal forces must be injected into our dynamic system.

Success in Science or Engineering—A. G. Grashberg (p. 94)

This study tests several hypotheses concerning the effects that family structure has on an individual's personality development and its influence on his success in a science or engineering curriculum. One of the principal ideas tested is that success in college in science or engineering requires that the student develop strong feelings of independence and consequently be free from over-concern with interpersonal relations. Data were gathered on sixty undergraduates at the Massachusetts Institute of Technology. Two groups of thirty students each were selected: one a "successful" group and the other an "unsuccessful" group. Success and lack of success were defined in terms of academic performance. In general, the successful students come from homes in which the power structure and the roles of the parents are more clearly defined, thus allowing these boys to have a stronger identification with their fathers. The successful students are also found to be less concerned with interpersonal relations. The low achievers showed a stronger preference to work with people than did the high achievers.

To explore further the origins of concern with interpersonal relations, two deviate sub-groups, one from each sample, were studied in depth: the high achievers who preferred to work with people, and the low achievers who preferred *not* to work with people. In the case of the six low achievers who disdained working with people, there is evidence that strong conflict existed within the family during their childhood and that these students probably reacted to these painful experiences by resisting further interactions with people. This gave rise in later life to a preference to work with things. Unfortunately, however, these students are not successful in working in abstract areas. The four high achievers who preferred to work with people are shown to have an adequate identification with their fathers, who, however, are perceived as having considerable "expressive" or feminine-role behavior. It appears that the father who is successful in meeting the demands of an occupation, but who also has time to concern himself with the internal workings of the family, is the one that produces sons who have strong achievement drives and also have a desire to work with people. It is curious, however, that although these students are skillful in interpersonal situations and turn out to be the campus leaders, they do not have a warm regard for people.

Preliminary Studies in Automated Teaching—R. F. Mager (p. 104)

Known learning principles cannot be efficiently applied in the traditional classroom environment. To achieve efficient learning it is

necessary to remold the teaching-learning configuration to one in which the state of the art can be applied. Teaching machines provide such a configuration, and have proved to be dramatically effective in teaching a wide variety of subject matters. There is a need for more sophisticated machines with which to research possibilities of automating instruction in the maintenance of complex electronic systems. Engineers can contribute to teaching machine technology through programming of technical content, through design of appropriate hardware, and through support of teaching-automation research.

Industry's Contribution and Needs in Graduate Education—D. F. Kline (p. 108)

The reduction in time between the discovery of new knowledge and its application to fill human needs has demanded rapid sophistication of engineering and science graduates employed by industry. In a very short time an integrated work-graduate study program provides these graduates with education in depth, an introduction to industry and a realistic base upon which to make a career decision. Industry's need is graduate-study opportunity for its employees; its contribution is the integrated work-graduate study program.

Contributors (p. 110)

Microwave Theory and Techniques

VOL. MTT-7, No. 3, JULY, 1959

Frontispiece (p. 306)

Guest Editorial—H. J. Riblet (p. 307)

Report of Advances in Microwave Theory and Techniques in U.S.A.—1958—R. E. Beam and M. E. Brodwin (p. 308)

Report of Advances in Microwave Theory and Techniques in Great Britain—1958—J. Brown (p. 325)

Report of Advances in Microwave Theory and Techniques in Western Europe—1958—G. Goudet (p. 327)

Report of Advances in Microwave Theory and Techniques in Japan—1958—I. Someya (p. 331)

A Ferrite Cutoff Switch—R. F. Soohoo (p. 332)

The theory and operating characteristics of a new type of high performance reflective switch is given. It utilizes the cutoff phenomenon in transversely-magnetized ferrites. The insertion loss of the device is 0.4 db and over 60 db within the 8.8 to 9.5 kmc band when the ferrite is demagnetized and magnetized respectively. The reflection coefficient of the switch in the "off" state is more than 90 per cent over this same band. In contrast to most other ferrite devices, it is of the reflective rather than the absorptive type. Furthermore, it has the unique property that its operating bandwidth is determined mainly by the magnitude of the applied field. Possible applications of the device in antenna switching and as a tunable cutoff filter will be discussed.

Propagation of Constants of Circular Cylindrical Waveguides Containing Ferrites—H. K. F. Severin (p. 337)

The paper describes some results of a theoretical and experimental investigation of the propagation behavior of circular cylindrical waveguides containing longitudinally magnetized ferrite rods. As long as no concentration of the RF-magnetic field in the ferrite occurs, theoretical expressions for the propagation constants can be given by applying first-order perturbation method. Faraday rotation measurements have been made between 5000 and 7600 mc using commercially available ferrites. Reasonable agreement between theoretical and experimental results has been found for a thin axial ferrite rod in an air-filled guide in both cases of saturated and nonsaturated ferrites. Energy concentration in the ferrite determines the propagation behavior in the partially

filled waveguide. This effect can be enhanced by surrounding the ferrite rod with a dielectric tube. For a given rod diameter and permittivity of the tube there is an optimum outer diameter of the tube for which the Faraday-rotation becomes maximum.

Magnified and Squared VSWR Responses for Microwave Reflection Coefficient Measurements—R. W. Beatty (p. 346)

In conventional microwave impedance measuring instruments, the measured ratio of maximum to minimum detector signal level is ideally equal to the voltage standing-wave ratio (VSWR) of the termination. In this paper, it is shown how radically different types of response are obtainable in which the observed ratio may approximately equal the square of the VSWR or may be magnified any desired amount. Theory is given enabling accurate measurements by interesting techniques. Accuracies of 0.1 per cent in VSWR to 2.0 have been achieved using magnified response techniques.

Microwave Reflectometer Techniques—G. F. Engen and R. W. Beatty (p. 351)

A rigorous analysis of the microwave reflectometer is presented for what is believed to be the first time. By means of this analysis, the correct adjustment of auxiliary tuners is described, and the errors resulting from incorrect adjustments are treated in a quantitative manner.

It is shown how the reflectometer technique may be further simplified while preserving the accuracy of measurement. A convenient method of adjusting the auxiliary tuners is described, sources of error are discussed, and an example is given of the calculation of error limits.

Application of a Backward-Wave Amplifier to Microwave Autodyne Reception—J. K. Puifer (p. 356)

A microwave receiver using a single-circuit backward-wave amplifier as a combination radio-frequency amplifier and homodyne local oscillator is described. The amplifier tube is operated at a value of beam current just above that required to maintain oscillation. It is shown that in this way, the high gain and narrow bandwidth of the single-circuit backward-wave amplifier may be utilized in an electronically tunable microwave receiver. The resultant sensitivity is 10 to 15 db worse than that obtainable from a good superheterodyne. The loss in sensitivity is due entirely to the high noise figure of the backward-wave amplifier, which can theoretically be reduced to a value comparable with that of a superheterodyne. The advantages of the receiver are its simplicity and its lack of image difficulties. Rejection of off-frequency signals is such that they are attenuated by at least 50 db.

Mode Theory of Lossless Periodically Distributed Parametric Amplifiers—K. Kurokawa and J. Hamasaki (p. 360)

In this paper, an operator $T\theta$ is introduced for the analysis of the periodically distributed parametric amplifier. The operator is the product of a diagonal matrix expressing the pumping phase relation and the T matrix of the basic section of the amplifier. The eigenvectors of $T\theta$ are called the "modes" of the amplifier. The orthogonality properties of the modes are proved in a similar way as for the conventional mode theory. Finally, an expression is derived for the power gain of the amplifier as an application of the theory.

Surface Wave Transmission Line Composed of Dielectric Membrane—M. Sugi and T. Nakahara (p. 366)

This paper describes the O-guide and X-guide which are proposed by the authors and are the advanced surface waveguides composed of thin dielectric sheets. The results of an analysis of the TE fundamental mode in the O-guide are described, and the theoretical characteristics as a transmission line are discussed. The practical guides are suitable espe-

cially for the SHF region and guides can be obtained which have lower attenuation constants than coaxial lines, G-lines, and rectangular waveguides.

The Transmission of TE₀₁ Wave in Helix Waveguides—T. Hosono and S. Kohno (p. 370)

Relations are investigated between the transmission characteristics of a helix waveguide and its surface impedance in regions where any simple approximate formulas are not available because of the magnitude of the surface impedance. The numerical calculations show that, for any given value of the surface impedance and the angular mode index, there exists an infinite number of different modes which are distinguishable from each other by different values of the radial propagation constant.

Selecting a mode with minimum attenuation for each given surface impedance, we can draw the equiattenuation lines, connecting these points of equal attenuation on the complex surface impedance plane. At some point on the complex surface impedance plane, a maximum value of the minimum attenuation is found. For the TM₀ mode supported by a helix waveguide 50 mm in diameter, used at a frequency of 50 kmc, this minimax value of the attenuation constant is about 8 neper per meter, and the corresponding value of the surface impedance is about 57.6 - j28.8 ohms. The attenuation constants of all the TM₀ modes corresponding to this optimum value of the surface impedance cannot be smaller than this minimax value.

The same kind of calculations are also performed for the two lowest hybrid modes. Physical structures giving the best value of the surface impedance are also suggested.

Design of Linear Double Tapers in Rectangular Waveguides—R. C. Johnson (p. 374)

This paper considers the problem of a taper connecting two uniform waveguides of arbitrary dimensions and propagating a single mode; an approximate expression for the reflection coefficient is derived. The special case of a linear double taper in rectangular waveguide is examined in detail for propagation in the TE₁₀ mode. Approximate expressions for the reflection coefficient and voltage standing wave ratio as functions of the taper dimensions and free space wavelength are derived and experimentally verified.

Spurious Mode Generation in Nonuniform Waveguide—L. Sloymar (p. 379)

This paper deals with the problem of a nonuniform waveguide joining two uniform ones and the spurious modes generated by it when a pure mode is incident in one of the uniform waveguides.

The generalised telegraphist's equations are stated and transformed into a set of differential equations for the amplitudes of the forward and backward travelling waves. The expressions for the coupling coefficients between the various modes are given and analysed.

By making certain assumptions, the differential equations are solved and the amplitudes of the modes are given in a closed form.

Subject to these same assumptions, it is proved that the power in the spurious modes may be kept below any predetermined level, provided the nonuniform waveguide is sufficiently gradual.

A High Power Duplexing Filter—L. Young and J. Owen (p. 384)

An L-band duplexing filter has been constructed with an estimated power-carrying capacity of 5 megw at atmospheric pressure (for a power safety factor of nearly four to one) and an insertion loss of less than 0.1 db.

The filter consists of two hybrid junctions and two high pass waveguide sections, which are arranged as in a balanced duplexer, with the "TR-tubes" replaced by the high-pass sections.

In the upper frequency band, the input VSWR is better than 1.10 over a seven and one-half per cent bandwidth, but deteriorates only slightly over a larger bandwidth. In the lower frequency band, the input VSWR is better than 1.32 over a 13 per cent bandwidth. The separation interval between these two bands is approximately 10 per cent between their nearest frequencies.

Correspondence (p. 388)
PGMTT News (p. 396)
Contributors (p. 396)

Military Electronics

VOL. MIL-3, NO. 3, JULY, 1959

Guest Editorial—E. C. Callahan (p. 67)
Design Considerations for a Celestial Navigation Trainer—M. D. Bennett and N. B. Mickelson (p. 69)

This paper gives a short history of the need for navigation training and tells what a navigator should know. It also tells how navigators were trained in the middle ages and of training devices used then as well as explaining the requirements of the modern celestial navigation trainer and how the IA19 meets these requirements. It explains, in general engineering terms, the techniques used for simulation of motion and references and changes in references required for navigating.

Synthetic Representation of Terrain Features on a Simulated Airborne Radar Display—J. T. Slattery and M. Kamenetsky (p. 75)

This paper traces the development of the various techniques used to generate synthetic land mass or terrain radar signals for radar training devices. The survey begins with a description and assessment of the Ultrasonic System and concludes with a discussion of the more flexible Two-Transparency System now under development by the Navy.

Development of the First Helicopter Operational Flight Trainer—E. G. Cairns (p. 82)

This paper describes the design and development problems associated with the construction of the first operational flight trainer to simulate a helicopter. Included is a description of the components comprising the trainer along with a discussion of its capabilities and training value for indoctrinating Army helicopter pilots in the flight characteristics of the H-37A Helicopter. Problems in deriving a complete set of motion equations were encountered in the initial phases of the project. These are described as is the approach used in simulating the rotor aerodynamics. The attachment to the operational flight trainer used by the student for visual flight training is also described in detail.

Simulation of Earth's Topography for Research and Engineering—S. Domeshek (p. 87)

This paper explains the present methods of simulating the earth's topography and their uses, the difficulty and time consumed in making some of these simulations, and the limitations of their uses. It then explains the need for some better method because of the greater volume of topographic information required in greater detail because of the needs of cold war, national defense, industry, road expansion, seaway expansion, airport construction, radar site construction—all to be done in a great hurry. It leads up to the automatic terrain model system. It explains quickly the several systems that were considered and why the printed circuit system was chosen. It mentions the fact that the information is stored on magnetic tape and utilized to carve a three-dimensional terrain model, and then goes into detail as to the greater information that this particular system can provide automatically that cannot be done except through extensive hand calculation with the other systems.

An Integrated Space-Flight Simulator—M. Ackerman (p. 92)

The role of the flight simulator in the space vehicle program is presented in this paper. Application of a simulator as an engineering and development aid is the subject of the discussion. A simulator for training the space crew is anticipated and therefore is mentioned in passing.

A brief review is made of contemporary thinking regarding anticipated physiological and psychological effects on the future crew. A simulator is then defined which will integrate these effects, thus providing a complete environment for experimentation.

Early phasing of the integrated simulator with the space vehicle is suggested as a better foundation for design of the space cabin or capsule than sole dependence on feedback from early flights.

The Human Disorientation Device—A Simulator of Angularly-Accelerated Motion—J. H. Achilich (p. 99)

The Human Disorientation Device has been developed as a research tool in the field of aviation medicine for the generation of angularly accelerated motion to enable the accomplishment of medical research in the field of animal or human responses to angular acceleration.

The device will produce accurately known and controlled values of angular acceleration about two axes of rotation when subject is seated so that his head is located at the point specified by the intersection of the axes.

The Human Disorientation Device will allow medical research in the field of sensory responses to angular acceleration, vertigo, and similar phenomena required for an analysis of human behavior and human performance limitations in the rapid maneuvering (spin and tumbling, etc.) of high-speed aircraft and spacecraft.

A Land-Mass Radar Simulator Incorporating Ground and Contour Mapping and Terrain Avoidance Modes—W. P. Jameson and R. M. Eisenberg (p. 105)

This paper describes a method of simulating the radar displays of an airborne radar system. The simulator employs a scan-programmed vidicon tube and a low-power light source in conjunction with a three-dimensional terrain model to simulate radar return from land-mass formations, cultural areas, and target complexes. All effects of a moving aircraft, including velocity, heading, altitude, position, and attitude, are included in the simulation.

This device will produce the displays for ground mapping, contour mapping and terrain clearance radar systems. It may be employed with an operation flight simulator or as a self-contained radar mission trainer for radar navigation and blind bombing operations.

Thirty-Two Aircraft Radar Track Simulator—L. Packer, M. Raphael, and H. Saks (p. 114)

This paper describes a Radar Track Simulator which generates the track of thirty-two aircraft in x , y , and h coordinates accurate to one-hundredth of a mile and produces video accurate to one-hundredth of a mile in range, one milliradian in azimuth and two milliradians in elevation. The output video signals are modified by the radar beam pattern, aircraft scintillation noise, radar receiver noise, fading of video signal with range, and blip-scan effects to produce a realistic display.

Contributors (p. 123)

Production Techniques

VOL. PT-5, AUGUST, 1959

Message from the Editor (p. 3)
Guest Editorials and Biographies of Guest Editors—C. F. Horne (p. 4); E. G. Uhl (p. 6); J. R. Moore (p. 8)

Scanning the Issue—A. R. Gray (p. 11)
Second National Conference of the PGPT, June 4-6, 1959

Modular Dimensioning of Electronic Component Parts for Mechanized Assembly—R. A. Gerhold and W. V. Lane (p. 12)

It is pointed out that certain basic design disciplines are prerequisite to more effective mechanized use of printed wiring. The 25-mil layout grid is described as one of these basic prerequisites. Specification SCL-6225, "Design Requirements for Auto-Semblem Army Signal Electronic Equipment," is presented as a basis for the present recommendations. The concept of "projected component volumes" is introduced to make component-parts dimensions compatible with printed-wiring requirements and to provide both a design guide, and a convenient assessment, for volumetric efficiency. Effects of hole, terminal pad, and conductor-spacing variations are discussed. Component-part height variation is charged with the major contribution to poor volumetric efficiency, and corrective measures are suggested.

Dimensions of length, height, and width are all recommended in building-block steps, compatible with printed wiring of the present, and micro-modules of the future; and certain preferences are given. Specification SCL-6254, "Modular Dimensioning of Electronic Parts," is announced. It is concluded that these recommendations will form a logical extension of the large equipment module to provide greater ease of automation and higher volumetric efficiencies.

Future Component Parts for Mechanization—E. G. Plessner (p. 17)

The author introduces Philco's TV middle-of-the-road philosophy for component parts. Basic ground rules are laid down, such as: machines must be simple and specialized; parts must be uniform and easy to handle. A considerable Philco experience with component insertion is indicated. It is pointed out that "universal" insertion machines are always more costly than specialized capital equipment.

Component parts with a rectangular form factor and special leads are proposed, and the advantages of these parts are listed. The state-of-the-art is considered in order to assess the specific ease of conversion to such modular parts. Modular dimensions for multiple component parts are also suggested. It is emphasized that 60-40 solder coated—not solder plated—parts have always, in Philco's experience, surpassed all other types to some degree. Higher temperatures and shorter time cycles are recommended. The coordinate grid system is briefly discussed from the TV manufacturer's point of view.

It is concluded that the industry has much to gain from a reliable mechanization program, and it is stressed that even the smallest detail is important when tooling for new parts. The rectangular component part is suggested as one solution to those conditions which have yet failed to yield reliable results to the machine designer.

Design Trends in Tomorrow's Capacitors—A. A. Tiezzi (p. 20)

A realistic appraisal is made of present capacitor-design improvements, and of immediately-foreseeable design trends. Three trends are discussed—those toward reliability, low voltage, and automation.

In the area of reliability, accelerated-life and vibration test results are presented, covering 8950 "Hyrel Q" impregnated-paper capacitors. It is pointed out that as the demand for such capacitors increases, the cost differential relative to the garden-variety of sub-miniatures will become very small. It is emphasized that high-reliability tantalum-electrolytic, metalized-paper, and ceramic capacitors will be available in the near future and that the developed processes will "rub off" on other types.

The low-voltage trend is discussed in its

relation to solid-tantalum and other electrolytic types. The new Sprague 109D liquid-electrolyte porous-anode tantalum capacitor is described, and a 2 or 3-to-1 volume-efficiency advantage is shown over previous low-voltage types. Other performance, environmental, and reliability advantages are cited. Improved metallized-paper capacitors are placed in a new niche of reliability; and complex-film types are announced for replacing mica and ceramic types. Life-test data is presented showing a 44-to-1 improvement for one dielectric-film combination.

The automation trend is pictured as toward the molded-paper capacitor, because of its better handling and tolerance qualities. Presently-available more-common types are listed, and some pending improvements are mentioned. Two molded automation types are described.

A new monolithic multi-layer ceramic capacitor is announced which has approximately 70 times the capacity of previous ceramics using 20-mil disks. It is emphasized that the surface has only been scratched in the development of new materials for capacitors. In conclusion, it is pointed out that greater standardization on the part of the electronics industry toward a reduction of types and in stopping the usage of obsolete types will result in better capacitors, and at lower prices.

Research and Development for Man-Machine Systems—G. W. Hoover (p. 23)

The fallacies of present methods of Research and Development are discussed, and it is explained why these methods are being used today. It is posed that research itself needs researching. Inhibited thinking is charged with the predominant responsibility for limited research productiveness. Lack of imagination, fear of ridicule, desire to invent at the exclusion of facts, schedules and resistance to tool changes, and too much reliance on experience—these are given as the most important causes of inhibited thinking. The author warns: not to justify compromises, not to rely on luck, and to stop modifying modifications. Stating the problem in its fundamental terms is illustrated by an interesting story. An analogy to the story is provided by the present complex design of aircraft instrument panels.

A methodology is suggested for conducting research and development by establishing a program of uninhibited thinking—a long-range effort seeking ultimate solutions. Seven basic aims and accomplishments of the program are outlined. Examples are shown where breakthroughs have occurred by using this approach. (Slides were used in the verbal presentation for emphasizing certain points and to show examples of equipment developed from an exemplary program.) It is also pointed out that an interim program can make use of the "rake-offs" from the long-range program.

The "Tuf-Plate Hole" for Printed Wiring (Abstract)—G. B. Geddy (p. 27)

Designing with Polystrip Flat-Wire Cables (Abstract)—A. L. Pugh, Jr. and S. J. Stein (p. 28)

Impact of Transistors on Military Electronics Design (Abstract)—A. B. Jacobson and J. C. Nicholas (p. 28)

Micro-Modules: Component Parts and Material Requirements—S. F. Danko and V. J. Kublin (p. 29)

The growth of our microminiaturization capabilities to date is cited as having been random and uncoordinated. The Signal Corps' micro-module effort is described as a definite step toward a concept that has depth and scope. A new dimension—a ten-to-one size reduction over the best now realized, is selected as reasonably attainable in 3 to 5 years. Named as providing the background for the present program, are such designs as the Army's Korean "Handy-Talkie," the Navy's "Tinkertoy," the Bell Tele-

phone Laboratories' transistor, and the Army's "solder-dipped printed wiring." Also credited as being a major contributor is the recent trend toward "packaging by function" where standard modular dimensions and a throw-away maintenance philosophy buy us another two-to-one size reduction, to reach a plateau of around 50,000 parts per cubic foot.

It is stressed that a positive approach is now needed toward a completely new plateau in size and packaging density, of at least 500,000 parts per cubic foot. Our present capabilities are assessed, and a ten-to-one size reduction is shown for Sprague's ceramic printed circuit, and two transistor amplifiers by Centralab. The Army's micro-module wafer element (0.3 inch \times 0.3 inch \times 0.01 inch thick) is announced. A model demonstrating feasibility is shown, where a complete 5-transistor superheterodyne radio receiver is built into an ordinary fountain pen. Present capabilities are displayed for fabricating component parts on the 0.09-square-inch micro element. Specific accomplishments are shown, such as: a precision metal-film resistor, a precision glass capacitor, a flat-plate ceramic capacitor, a hermetically-sealed solid-tantalum electrolyte capacitor, and several other special component parts.

Five categories of Army equipments (portable, vehicular, missile, projectile, and satellite), and three plateaus of temperature (+85°C, +125°C, and +200°C, above a cold level of -55°C) are selected as meeting present Army environmental requirements. The guiding philosophy, in setting up the program, is described as providing: first, a meaningful step forward based on immediately attainable tangible techniques, and second, a parallel solid-state research effort to improve and mature the concept. To accomplish the "big step forward" in size reduction and "throw-away" maintenance, RCA is announced as leader-contractor to coordinate industry-wide activities.

A Punched-Card-Controlled Component-Part Insertion Machine—H. K. Hazel (p. 39)

A new high-speed programmed insertion device for axial-lead component parts is described, which produces the "Y" coordinate motion by movement of the printed wiring board and the "X" and "Z" motion by movements of the insertion head. Although the basic idea is not new, it is claimed that its combination with novel mechanisms has resulted in a truly high-speed experimental programmed machine.

Success of the machine is credited to a new small and lightweight inserting tool, which allows high-velocity movement, using low power, and with reduced resonance. A series of pneumatic cylinders are shown, following the binary progression to provide specific strokes by IBM punched-card control, for both lead preparation and insertion.

Salient features of the mechanism are described as follows: a) almost any part under a diameter of 0.250 inch and a length of 0.850 inch can be handled, b) component parts are center-taped on reels after wrap-around terminals have been added, c) torque sleeves and yokes remove component parts from the tape reels, d) cards are stacked and conveyor fed to the insertion head, e) the controller is in console form, and takes binary-coded cards directly without the need for a decoder, and f) 1920 bits of information are available from only two cards.

Factors which have been experienced in connection with the manufacture of Sage Computers at IBM Kingston are mentioned. It is claimed that for over two million insertions, most failures have been eliminated, even though insertion is at the average rate of 60 per minute. Potential of the system is estimated at a maintained speed of at least 120 per minute,

with its future hinted by the insertion speed of less than 0.1 second which has been attained. Possible utilization of the equipment for other purposes is stressed, such as for programmed drilling.

Evolution of a System for the Production of Electronics Equipment—Mechanization of all Lot Sizes—C. P. Cardani (p. 42)

It is reported that as of last year, an estimated 627,000,000 component parts have been mechanically assembled into 26,000,000 printed wiring boards. It is stated that the production equipment requirements and desires of the various assemblers of electronics equipment vary from a single bench-mounted inserting machine (for small lots), to the punched-card-controlled automatic-assembly machine, or even the automatic conveyor. It is pointed out that there is no one piece of equipment that will satisfy the needs of all assemblers, but that the DYNASERT system described can satisfy most.

The paper includes a discussion of: a) factors governing the choice of a system, b) development of the DYNASERT machine system, including machines for component-part preparation, insertion—4 types, and conveying—up to 48 stations, c) varying the system to meet changing production demands, d) considerations affecting design for mechanical assembly, and e) benefits of mechanized assembly.

An account is given of five users, making from 20 to 7000 panels per day, where all showed a considerable saving through mechanization.

Microminiaturization Techniques (Abstract)—J. Finklestein (p. 50)

New Techniques in Plotting, Encapsulating, and Small Parts Molding (Abstract)—J. L. Lull (p. 50)

Automation of Single-Axis Floated-Gyro Drift Measurement—J. G. Nelson (p. 51)

This paper describes the technique and equipment developed for automating measurement of the drift rate of precision single-axis floated gyros. The basic construction principles of single-axis floated gyros are described and illustrated. The sources and components of drift are then discussed and defined. The random component of drift is shown to be a useful measure of gyro quality and is, by reason of its definition, suited to automatic testing techniques.

The equipment used to measure the random component of drift consists basically of a single-axis servo table (in which the gyro to be tested is mounted), the servo table and gyro operating circuitry, and the programming and readout devices. Although adaptable to a variety of situations, the equipment is designed specifically to applying the "cogging" or repositioning type of single-axis gyro-drift test. The servo table is slaved to the gyro output so that the table angular rate is equal to gyro input plus gyro total drift.

Two microsins (rotary differential transformers) are attached to the table shaft with their null positions spaced at an accurately known angle. The unique phase characteristic of the microsins is used to gate a precision frequency to a time-interval meter and a digital recorder. With a component of Earth Rate as input to the gyro, the time required for the servo table (and gyro) to process through the accurately-known angle is measured a number of times. The standard deviations of the average rates through the angle is taken as random drift.

The time data is printed out in digital form for transfer to punched cards and digital processing. The application of the equipment to the development and production testing of precision single-axis floated gyros provides a means of accumulating large quantities of precise data in a relatively short period of time for a reliable statistical measure of gyro-production quality.

Abstracts and References

Compiled by the Radio Research Organization of the Department of Scientific and Industrial Research, London, England, and Published by Arrangement with that Department and the *Electronic and Radio Engineer*, incorporating *Wireless Engineer*, London, England

NOTE: The Institute of Radio Engineers does not have available copies of the publications mentioned in these papers, nor does it have reprints of the articles abstracted. Correspondence regarding these articles and requests for their procurement should be addressed to the individual publications, not to the IRE.

Acoustics and Audio Frequencies.....	1799
Antennas and Transmission Lines.....	1800
Automatic Computers.....	1800
Circuits and Circuit Elements.....	1801
General Physics.....	1802
Geophysical and Extraterrestrial Phenomena.....	1803
Location and Aids to Navigation.....	1805
Materials and Subsidiary Techniques..	1805
Mathematics.....	1807
Measurements and Test Gear.....	1807
Other Applications of Radio and Electronics.....	1808
Propagation of Waves.....	1809
Reception.....	1809
Stations and Communication Systems..	1809
Subsidiary Apparatus.....	1810
Television and Phototelegraphy.....	1810
Transmission.....	1811
Tubes and Thermionics.....	1811
Miscellaneous.....	1812

The number in heavy type at the upper left of each Abstract is its Universal Decimal Classification number. The number in heavy type at the top right is the serial number of the Abstract. DC numbers marked with a dagger (†) must be regarded as provisional.

ACOUSTICS AND AUDIO FREQUENCIES

- 534.001.5(51)** **2808**
Acoustics in China—Ma Da-Yu. (*Akust. Z.*, vol. 4, pp. 373-375; October/December, 1958.) Outline of the development of research in China since 1949, in the fields of ultrasonics, architectural acoustics, electroacoustics, speech, musical acoustics and hearing.
- 534.213.4** **2809**
Attenuation of Plane Sound Waves of Finite Amplitude in Gases—B. F. Podoshevnikov and B. D. Tartakovskii. (*Akust. Z.*, vol. 4, pp. 369-371; October/December, 1958.) Investigation of the dependence of attenuation on sound intensity. A graph shows the distribution of sound pressure in a resonant aluminium tube at a frequency of 13 kc.
- 534.22-8-14** **2810**
The Propagation of Sound in Seawater—A. V. J. Martin. (*Ann. Géophys.*, 1957, vol. 13, pp. 307-309; October/December, 1957.) A brief description of laboratory experiments using an ultrasonic pulse technique to determine the velocity of sound in pure and salt water. See 1 of January.
- 534.22-8-14** **2811**
The Velocity of Ultrasound in Water near the Freezing Point—N. F. Opushchennikov. (*Akust. Z.*, vol. 4, pp. 376-369; October/December, 1958.) Brief description of measurements made in distilled water at a frequency of 0.7 mc in the temperature range +20° to 0°C. Results indicate a velocity minimum at 0.7°C. and a maximum adiabatic compression at +2°C.
- 534.232-8-14:537.228.2** **2812**
Electrostrictive Generation of Ultrasonics in Liquids—E. Gerdes. (*Naturwiss.*, vol. 45,

The Index to the Abstracts and References published in the PROC. IRE from February, 1958 through January, 1959 is published by the PROC. IRE, May, 1959, Part II. It is also published by *Electronic and Radio Engineer*, incorporating *Wireless Engineer*, and included in the March, 1959 issue of that journal. Included with the Index is a selected list of journals scanned for abstracting with publishers' addresses.

pp. 280-281; June, 1958.) Preliminary report on measurements to determine the magnitude of electrode deformation due to Coulomb attraction. See e.g. 310 of 1956 (Goetz).

534.26 **2813**
Diffraction of Sound Waves in Converging Beams—B. D. Tartakovskii. (*Akust. Z.*, vol. 4, pp. 355-360; October/December, 1958.) Approximate formulas are derived for the sound field near the focal point of a converging beam, characterized by a nonuniform amplitude distribution over the wave front and spherical aberration.

534.522.1 **2814**
Measurements of Finite Amplitude Distortion of Progressive Ultrasonic Waves at Moderate Intensities—K. L. Zankel and E. A. Hiedemann. (*Naturwiss.*, vol. 45, pp. 329-330; July, 1958. In English.) Low-amplitude waves were investigated by measurements in water at 2 and 4 mc, and in carbon tetrachloride at 2 and 3 mc over a range of pressures and at various distances from the transducer.

534.614-8 **2815**
Measurement of Ultrasonic Wave Velocities and Elastic Moduli for Small Solid Specimens at High Temperatures.—H. J. McSkimin (*J. Acoust. Soc. Am.*, vol. 31, pp. 287-295; March, 1959.) Data for fused silica and single-crystal Ge are listed for temperatures up to 300°C in illustration of the measurement methods described.

534.614-8-14 **2816**
Modification of Ultrasonic Interferometer Design—A. A. Isaev, I. G. Mikhailov and A. S. Khimunin. (*Akust. Z.*, vol. 4, pp. 363-364; October/December, 1958.) Note on the design of an improved quartz oscillator for use in interferometric measurements of sound velocity in liquids.

534.75 **2817**
Unpleasantness of Distorted Sounds: A Criterion Derived from the Distortion Spectrum—E. R. Wigan. (*Nature, London*, vol. 183, p. 1320; May 9, 1959.) An objective criterion of "unpleasantness" has been computed. Methods for checking its validity are briefly discussed.

534.76:534.85 **2818**
Moving-Magnetic Stereo—H. Horowitz. (*Audio Eng.*, vol. 43, pp. 19-21, 47; May, 1959.) A description of a pickup in which the stylus lever is attached to a magnet pivoted be-

tween the pole faces of two pairs of pickup coils. Characteristics are discussed.

534.78:621.39 **2819**
Intelligibility Evaluation of Voice Communications—H. Schwarzlander. (*Electronics*, vol. 32, pp. 88-91; May 29, 1959.) The integral of a difference voltage due to the pure speech signal and that passed through the system under test is used as a measure of intelligibility.

534.781:621.374.33 **2820**
An Electronic Speech Sampler for Studying the Effect of Sample Duration on Articulation—R. Fatehchand and R. Ahmed. (*J. Inst. Telecommun. Engrs., India*, vol. 5, pp. 86-88; March, 1959.) The start of any word is signalled by a pulse which itself operates the subsequent electronic delay and gate.

534.845 **2821**
Panel Absorbents for Low-Frequency Sound Absorption—N. K. D. Choudhury and M. V. S. S. K. Rao. (*J. Inst. Telecommun. Engrs., India*, vol. 5, pp. 103-108; March, 1959.) Resonant plywood panels show effective absorption in the range 75-300 cps.

534.861:534.84 **2822**
The Acoustic Design of Talks Studios and Listening Rooms—C. L. S. Gilford. (*Proc. IEE, Part B*, vol. 106, pp. 245-256; May, 1959. Discussion, pp. 256-258.)

621.395.623.7.001.4 **2823**
The Impedance and Phase Angle of Loudspeaker Loads—R. E. Cooke. (*Muirhead Tech.*, vol. 13, pp. 11-16; April, 1959.) A description of the basic measurement circuit and a discussion of the impedance and phase angle characteristics obtained for moving-coil and electrostatic loudspeaker systems.

621.395.623.8 **2824**
Column Loudspeakers for Public-Address Systems—M. L. Gayford. (*Electronics*, vol. 32, pp. 64-65; June 12, 1959.) The principles of design are briefly described, with particular reference to polar response.

621.395.625.3 **2825**
A Regulator of Speed and Pitch for Sound Recordings—A. M. Springer. (*Electron. Rundschau*, vol. 12, pp. 275-276; August, 1958.) An adaptor unit for magnetic-tape recorders is described. This has a rotating assembly of four magnetic heads to provide independent changes of speed and pitch in recordings.

ANTENNAS AND TRANSMISSION LINES

- 621.372.8 2826
The Design and Testing of Integrally Constructed Waveguide Assemblies—G. Craven and V. H. Knight. (*Proc. IEE*, Part B, vol. 106, no. 27, pp. 321-334.) A microwave-link repeater is described as an example of an assembly. Testing facilities include a plug-in reflectometer and a swept-frequency reflection display.
- 621.372.8:537.226 2827
Dielectric Image Lines—S. P. Schlesinger and D. D. King. (*IRE TRANS. ON MICROWAVE THEORY AND TECHNIQUES*, vol. MTT-6, pp. 291-299; July, 1958. Abstract, *PROC. IRE*, vol. 46, p. 1777; October, 1958.)
- 621.372.821 2828
Measurement of the Properties of a Strip Line and its Transition Junction—F. Norman. (*Proc. IRE, Australia*, vol. 19, pp. 788-795; December, 1958.) Measurements made in the range 8-11 cmλ indicate that a single modified TEM mode could be excited efficiently by means of a simple transition junction.
- 621.372.823 2829
The Waveguide for Low-Loss Transmission—K. Noda, A. Konose, T. Fujii and K. Miyachi. (*Rep. Elect. Commun. Lab., Japan*, vol. 6, pp. 394-400; October, 1958.) A report of measurements of attenuation in straight circular waveguides, and in serpentine and uniform bends propagating the H_{01} mode in circular and elliptic waveguides.
- 621.372.826 2830
Launching Efficiency of Wires and Slots for a Dielectric Rod Waveguide—R. H. DuHamel and J. W. Duncan. (*IRE TRANS. ON MICROWAVE THEORY AND TECHNIQUES*, vol. MTT-6, pp. 277-284; July, 1958. Abstract, *PROC. IRE*, vol. 46, p. 1777; October, 1958.)
- 621.372.832.43 2831
Centre-Excited $TE_{10}^D - TE_{01}^D$ Mode Transducer—B. Oguchi and K. Yamaguchi. (*Rep. Elect. Commun. Lab., Japan*, vol. 6, pp. 389-393; October, 1958.) Experimental data are given on the design and performance of a new type of mode transducer for use in the 24-kmc band.
- 621.372.832.8 2832
X Circulator—S. Yoshida. (*PROC. IRE*, vol. 47, p. 1150; June, 1959.) A new four-port waveguide circulator; experimental results are given.
- 621.372.837.2 2833
A New Form of High-Power Microwave Duplexer—P. D. Lomer and R. M. O'Brien. (*IRE TRANS. ON MICROWAVE THEORY AND TECHNIQUES*, vol. MTT-6, pp. 264-267; July, 1958. Abstract, *PROC. IRE*, vol. 46, p. 1776; October, 1958.)
- 621.372.837.3:621.318.134 2834
A Fast Ferrite Switch for Use at 70 kmc/s—E. H. Turner. (*IRE TRANS. ON MICROWAVE THEORY AND TECHNIQUES*, vol. MTT-6, pp. 300-303; July, 1958. Abstract, *PROC. IRE*, vol. 46, p. 1777; October, 1958.)
- 621.372.837.3:621.396.65 2835
A Faraday-Rotation Switch for the TH System—J. A. Weiss. (*Bell Lab. Rec.*, vol. 37, pp. 139-143; April, 1959.) Description of a rapid-acting microwave switch based on the Faraday effect, designed for switching standby oscillators into service.
- 621.372.852.22 2836
A Perturbation Method for Circular Wave-
- guides containing Ferrites—P. J. B. Clarricoats. (*Proc. IEE*, Part B, vol. 106, pp. 335-340; May, 1959.) The propagation coefficient of a guide containing a longitudinally magnetized ferrite is derived. Good agreement is obtained with experimental data.
- 621.372.852.22 2837
A Phenomenological Theory of the Reggia-Spencer Phase Shifter—J. A. Weiss. (*PROC. IRE*, vol. 47, pp. 1130-1137; June, 1959.) Explains the essential properties of the device by means of a simplified model. See 387 of 1958 (Reggia and Spencer).
- 621.372.852.22 2838
Theory of the Mode Spectra of Cylindrical Waveguides Containing Gyromagnetic Media—R. A. Waldron. (*J. Brit. IRE*, vol. 19, pp. 347-356; June, 1959.) The cutoff equations are derived and solved for the dielectric-centered case and the normal modes are studied. The relations between this case and that of the ferrite-centered case studied previously (341 of February) are pointed out.
- 621.372.852.323:621.318.134 2839
Theoretical Analysis of the Operation of the Field-Displacement Ferrite Isolator—K. J. Button. (*IRE TRANS. ON MICROWAVE THEORY AND TECHNIQUES*, vol. MTT-6, pp. 303-308; July, 1958. Abstract, *PROC. IRE*, vol. 46, p. 1777; October, 1958.)
- 621.396.67.095 2840
Four-Dimensional Electromagnetic Radiators—H. E. Shanks and R. W. Bickmore. (*Can. J. Phys.*, vol. 37, pp. 263-275; March, 1959.) The effect of modulating one or more parameters of an antenna or antenna array, such as aperture dimensions, frequency or phase distribution, is discussed, and applications to multipattern operation, simultaneous scanning and sidelobe suppression are considered.
- 621.396.67.095:537.311.5 2841
Determination of a Current Distribution over a Cone Surface which will Produce a Prescribed Pattern—H. Unz. (*IRE TRANS. ON ANTENNAS AND PROPAGATION*, vol. AP-6, pp. 182-186; April, 1958. Abstract, *PROC. IRE*, vol. 46, p. 1439; July, 1958.)
- 621.396.674.31 2842
The Effects of the Physical Parameters on the Bandwidth of a Folded Dipole—J. F. German and F. E. Brooks, Jr. (*IRE TRANS. ON ANTENNAS AND PROPAGATION*, vol. AP-6, pp. 186-190; April, 1958. Abstract, *PROC. IRE*, vol. 46, p. 1439; July, 1958.)
- 621.396.674.33 2843
The Characteristic Impedance of Two Infinite Cones of Arbitrarily Cross-Section—R. L. Carrel. (*IRE TRANS. ON ANTENNAS AND PROPAGATION*, vol. AP-6, pp. 197-201; April, 1958. Abstract, *PROC. IRE*, vol. 46, p. 1439; July, 1958.)
- 621.396.677:523.164:621.318.47 2844
A Compact Antenna Switch for Scintillation Measurements—W. D. Ryan. (*PROC. IRE*, vol. 47, p. 1159; June, 1959.) This switch introduces a phase shift of 90° successively into the lines from each of two antennas.
- 621.396.677.029.63 2845
The Performance of Directive Aerials in Complex U.H.F. Fields—J. A. Saxton and B. N. Harden. (*Proc. IEE*, Part B, vol. 106, pp. 315-217; May, 1959.) Apparent gains of directive antennas, relative to a halfwave dipole, were measured at 580 and 904 mc on a number of urban and rural sites. The median gains were similar to the calculated plane-wave gains, but the apparent gain was low, owing to the complexity of the field, on a significant number of sites.
- 621.396.677.3:523.164.32 2846
A New High-Resolution Interferometer for Solar Studies—Kundu. (See 2936.)
- 621.396.677.3:621.396.964 2847
A Note on the Effective Aperture of Electrically Scanned Arrays—R. W. Bickmore. (*IRE TRANS. ON ANTENNAS AND PROPAGATION*, vol. AP-6, pp. 194-196; April, 1958. Abstract, *PROC. IRE*, vol. 46, p. 1439; July, 1958.)
- 621.396.677.32 2848
The Radiation Characteristics of a Zig-Zag Antenna—D. L. Sengupta. (*IRE TRANS. ON ANTENNAS AND PROPAGATION*, vol. AP-6, pp. 191-194; April, 1958. Abstract, *PROC. IRE*, vol. 46, p. 1439; July, 1958.)
- 621.396.677.71 2849
Design Data for Small Annular Slot Antennas—W. A. Cumming and M. Cormier. (*IRE TRANS. ON ANTENNAS AND PROPAGATION*, vol. AP-6, pp. 210-211; April, 1958. Abstract, *PROC. IRE*, vol. 46, p. 1439; July, 1958.)
- 621.396.677.75 2850
Hemi-Isotropic Radiators for the S- or X-Band—E. G. A. Goodall. (*Proc. IEE*, Part B, vol. 106, pp. 318-320; May, 1959.) "An aerial having approximate hemi-isotropic properties has been constructed on the principle that a dielectric rod will act as a guiding medium for electromagnetic energy. Using this principle, a broad-band, shaped dielectric element has been developed, which, when placed at the aperture of an open-ended circular waveguide, radiates with hemi-isotropic cover over a 20 per cent frequency band."
- 621.396.677.81:621.397.7 2851
The Passive TV Relay and its Practical Possibilities—R. Aschden. (*TSF et TV*, vol. 33, pp. 329-330; November, 1957.) Field strength and antenna gain calculations for typical passive relay systems comprising a coupled receiving and transmitting antenna are given. See also 2852 below.
- 621.396.677.83 2852
Passive Relay by Microwave Mirror—R. Aschen. (*TSF et TV*, vol. 33, pp. 5-7; January, 1958.) Formulas are given for calculating the mirror area and reflection losses for a typical relay circuit based on a received field strength of 2 mv/m at a frequency of 200 mc.
- 621.396.677.83 2853
A Log-Periodic Reflector Feed—D. E. Isbell. (*PROC. IRE*; vol. 47, pp. 1152-1153; June, 1959.) An antenna of the log-periodic reflector type has been constructed which has been used over the range 105-430 mc. Its effective aperture is fairly constant below 325 mc.
- 621.396.677.85 2854
Microwave Stepped-Index Luneberg Lenses—G. D. M. Peeler and H. P. Coleman. (*TRANS. ON ANTENNAS AND PROPAGATION*, vol. AP-6, pp. 202-297; April, 1958. Abstract, *PROC. IRE*, vol. 46, p. 1439; July, 1958.)

AUTOMATIC COMPUTERS

- 681.142 2855
The Design of a Standard Block for a Digital Computing System—R. J. Miles. (*Mullard Tech. Commun.*, vol. 4, pp. 222-248; April, 1959.) Logical theory, design considerations and practical circuit of a block based on alloy-junction transistors operating at frequencies up to 1 mc.

681.142 **2856**
Binary Multiplication in Digital Computers—A. Green. (PROC. IRE, vol. 47, pp. 1159-1160; June, 1959.) Shows how many steps can be eliminated from the usual process of multiplication by computer.

681.142 **2857**
Computation of Sin N; Cos N and mN using an Electronic Computer—E. G. Kogbetliantz. (IBM J. Res. & Dev., vol. 3, pp. 147-152; April, 1959.)

681.142 **2858**
Rotating-Disk Function Generator for Analogue Computers—M. E. Young, W. M. Alexander and H. D. Schwetman. (Rev. Sci. Instr., vol. 30, pp. 318-322; May, 1959.) A variable-radius revolving lamina modulates the light incident upon the cathode of a photomultiplier tube to produce a required voltage time function.

681.142:518.4 **2859**
A Design for an Automatic Graph Plotter—M. P. Atkinson, W. T. Bane and D. L. A. Barber. (Proc. IEE, Part B, vol. 106, pp. 299-306; May, 1959.) Transistors and printed circuits are used in equipment based on digital techniques. Points may be plotted at a rate of three per second, with an accuracy within 0.01 inch.

681.142:621.318.042 **2860**
Magnetic-Core Matrices for Logical Functions—A. L. Freedman. (Electronic Engrg., vol. 31, pp. 358-361; June, 1959.) Some applications of cores having a square hysteresis loop.

681.142:621.318.57 **2861**
The Design of Biased-Diode Function Generators—C. C. Ritchie and R. W. Young. (Electronic Engrg., vol. 31, pp. 347-351; June, 1959.) Relations between the number and spacing of diode sections to give minimum error are derived.

CIRCUITS AND CIRCUIT ELEMENTS

621.3.049.7 **2862**
Recent Advances in Potted and Printed Circuits—H. G. Manfield. (J. Brit. IRE, vol. 19, pp. 289-302; May, 1959.) "The various potting resins are described in relation to the variation of properties with different proportions of hardener and the effects on the parameters of the potted components. The causes of failure of potted circuits are discussed. Design problems in the use of printed circuits are examined with particular reference to questions of conductor thickness and spacing. A method of sealing printed circuits by a thin polysulphide rubber layer which is sprayed or brushed on is described."

621.3.049.7:621.385.1 **2863**
Thermionic Integrated-Micromodules—J. E. Beggs, W. Grattidge, P. J. Molenda, A. P. Haase and A. F. Dickerson. (Electronics, vol. 32, pp. 80, 83; May 15, 1959.) The construction and application of microminiature heaterless tubes, resistors and capacitors using titanium and ceramic materials are described.

621.318.57:537.227 **2864**
The Transpolarizer: an Electrostatically Controlled Circuit Impedance with Stored Setting—C. F. Pulvari. (PROC. IRE, vol. 47, pp. 1117-1123; June, 1959.) The device operates by the controlled transfer of polarization through two or more ferroelectric dielectric sections in series.

621.318.57:621-52 **2865**
An Electronic Timer with Voltage Control of Setting—R. Gladstone. (Electronic Engrg.,

vol. 31, pp. 362-363; June, 1959.) A new grid-controlled "bootstrap" circuit with common-cathode trigger provides accurately controlled time delays up to about 100 seconds.

621.318.57:621.314.63 **2866**
Microwave Switching by Crystal Diodes—M. R. Millet. (IRE TRANS. ON MICROWAVE THEORY AND TECHNIQUES, vol. MTT-6, pp. 284-290; July, 1958. Abstract, PROC. IRE, vol. 46, p. 1777; October, 1958.)

621.319.4:621.3.049.75 **2867**
Tantalum Printed Capacitors—R. W. Berry and D. J. Sloan. (PROC. IRE, vol. 47, pp. 1070-1075; June, 1959.) Description of the structural features and characteristics of capacitors using sputtered Ta films as the base for the anodized oxide film, with evaporated metal counter-electrodes.

621.319.45:669.718.5 **2868**
The Surface Enlargement of Aluminum for Electrolytic Capacitors—P. Werner. (Nachrichtentech. Z., vol. 8, pp. 269-277; June, 1958.) Various chemical and electrochemical methods are described and compared, and details are given of a method of measuring the increase in surface area achieved.

621.372.5 **2869**
General Solution of the Symmetric Iterative Analysis of Asymmetric Passive Linear Quadrupoles—S. Mayr. (Arch. Elektrotech., vol. 44, pp. 120-129; December 8, 1958.) The asymmetric quadrupole is divided into two symmetric quadrupole sections which can be treated by iterative matrix methods.

621.372.57:621.3.087.4:551.594.6 **2870**
Investigation of an Apparatus for Recording Atmospheric—R. Benoit and J. Kernevez. (Ann. Géophys., vol. 13, pp. 321-234; October/December, 1957.) An analysis of an integrating circuit with a long time constant and its response to a series of pulses.

621.372.6 **2871**
A Topological Nonreciprocal Network Element—A. W. Keen. (PROC. IRE, vol. 47, pp. 1148-1150; June, 1959.) The element is a three-terminal device which may be used with physical elements (immittances) to model the more complex nonreciprocal devices.

621.372.6 **2872**
Traditors, a New Class of Non-energetic Nonlinear Network Elements—S. Duinker. (Philips Res. Rep., vol. 14, pp. 29-51; February, 1959.) From an analysis based on the Lagrangian dynamical equations, a class of nonlinear multiport elements is defined, which are characterized by the property of neither dissipating nor storing but only transferring energy.

621.372.632:621.314.63 **2873**
Transmitting Frequency Converter in which Gold- or Silver-Bonded Diode is Used—Kita, Sanpei and Okajima. (See 3145.)

621.372.632.029.6 **2874**
One Aspect of Minimum-Noise-Figure Microwave Mixer Design—S. M. Bergman. (IRE TRANS. ON MICROWAVE THEORY AND TECHNIQUES, vol. MTT-6, pp. 424-326; July, 1958. Abstract, PROC. IRE, vol. 46, p. 1777; October, 1958.)

621.373:537.312.62 **2875**
A Cryogenic Oscillator—G. B. Rosenberger. (IBM J. Res. & Dev., vol. 3, pp. 189-190; April, 1959.) A relaxation process based on the transition between the superconducting and conducting phases of a Pb film is described. Oscillations at frequencies around 100 kc have been obtained.

621.373.42.029.422 **2876**
A Sine-Wave Generator with Periods of Hours—G. Klein and J. M. den Hertog. (Electronic Engrg., vol. 31, pp. 320-325; June, 1959.) An "inverse function generator" based on the difference amplifier [see, e.g., 362 of 1956 (Klein)] is examined and examples of its use are considered 1) in a logarithmic voltmeter, and 2) for sine-triangle waveform transformation. Triangle-sine transformation can be achieved by negative feedback; a VLF triangular waveform obtained from a cathode-ray circuit and relay is thus converted to an accurate sine wave without transients.

621.373.43:621.314.7:621.385.1 **2877**
Tube-Transistor Hybrids Provide Design Economy—G. A. Dunn and N. C. Ilekimian. (Electronics, vol. 32, pp. 78-70; June 5, 1959.) A bistable cathode follower and four-stage ring counter are described. The transistors appear in the cathode circuits of the valves.

621.373.52 **2878**
Physical Principles of Avalanche Transistor Pulse Circuits—D. J. Hamilton, J. F. Gibbons and W. Shockley. (PROC. IRE, vol. 47, pp. 1102-1108; June, 1959.) "A model for the transistor is defined in terms of charge variables and the physical parameters of the device. The transient performance of the model is calculated by focusing attention on the minority carrier charge stored in the base region and the influence of basewidth modulation upon this stored charge. In the charge formulation of the problem, the physical details of the avalanche multiplication process need not be considered; multiplication is accounted for by the boundary conditions which it imposes upon the stored charge. Good agreement has been obtained between calculated and experimentally observed data for a simple avalanche transistor relaxation oscillator."

621.374.3:621.387.4 **2879**
Time to Pulse-Height Converter—J. V. Kane. (Rev. Sci. Instr., vol. 30, pp. 374-375; May, 1959.) A circuit is described for deriving pulses, the amplitudes of which decrease linearly with time.

621.374.3:621.387.4 **2880**
Linear Gate of 20- μ sec Duration—E. L. Garwin. (Rev. Sci. Instr., vol. 30, pp. 373-374; May, 1959.) Diodes with a 6- μ sec recovery time are used in a coincidence circuit.

621.374.5:538.652 **2881**
A Torsional Magnetostrictive Delay Line—A. Rothbart. (PROC. IRE, vol. 47, pp. 1153-1154; June, 1959.) An application of the Wiedemann effect, using toroidal coil transducers.

621.375.018.75:537.311.33 **2882**
Pulse Amplification using Impact Ionization in Germanium—M. C. Steele, L. Pensak and R. D. Gold. (PROC. IRE, vol. 47, pp. 1109-1117; June, 1959.) Some aspects of the phenomena of impact ionization in an impurity-doped semiconductor at 4.2°K are described. Control of the breakdown process is used to obtain pulse amplification in the millimicrosecond range, using two- and three-terminal devices.

621.375.2.029.3 **2883**
Reducing Distortion in Class-B Amplifiers—B. Sklar. (Electronics, vol. 32, pp. 54-56; May 22, 1959.) Linearization is accomplished by a nonlinear compensation network containing diodes. The calculations for an AF amplifier with 2.6 per cent distortion are described.

621.375.232.4 **2884**
Grounded-Grid Power Amplifier Design—J. L. Dautremont, Jr. (Electronic Equip. Engrg., vol. 6, pp. 33-36; December, 1958.) A graph-

ical design procedure is described, using a disk-seal valve Type 2C39-A as an example.

621.375.4.029.3 2885
Single-Ended Amplifiers for Class-B Operation—H. C. Lin and B. H. White. (*Electronics*, vol. 32, pp. 86-87; May 29, 1959.) A transistorized 10-w high-fidelity push-pull amplifier is described in detail.

621.375.4.029.3 2886
Designing High-Quality A. F. Transistor Amplifiers—R. Minton. (*Electronics*, vol. 32, pp. 60-61; June 12, 1959.) A seven-stage 25-w amplifier is described.

621.375.4.029.3 2887
One-Transistor 'Push-Pull'—J. A. Worcester. (*Electronics*, vol. 32, p. 74; June 12, 1959.) An AF output stage in which the biasing condition is controlled by the rectified output.

621.375.9:538.569.4 2888
Molecular Oscillators and Amplifiers—N. G. Basov and A. M. Prokhorov. (*Priroda*, pp. 24-32; July, 1958.) The principle and operation of molecular-beam oscillators and amplifiers are described with reference to the ammonia-beam maser. Molecular amplifiers based on paramagnetic crystals give a wider pass band and a higher output power than the molecular-beam type. The frequency stability achieved is within one part in 10^9 .

621.375.9:538.569.4 2889
Zero-Field Masers—G. S. Bogle and H. F. Symmons. (*Aust. J. Phys.*, vol. 12, pp. 1-20; March, 1959.) "Solid state three-level masers operating with zero magnetic field are shown to be feasible and to have advantages over magnetic field masers in many applications. The requirements of the working substance are discussed and it is found that compounds of Cr^{2+} , Fe^{3+} , Ni^{2+} , and Gd^{3+} should be suitable. Diagrams and tables of maser properties of selected compounds are given; on the basis of present knowledge a number of amplifying frequencies between 120 and 75,000 mc should be available. The range of suitable compounds which has been studied is very small, and should be extended."

621.375.9:538.569.4 2890
Role of Double-Quantum Transitions in Masers—S. Yatsiv. (*Phys. Rev.*, vol. 113, pp. 1538-1544; March 15, 1959.) Conditions are found in which the operation of a three-level maser is governed by the double-quantum process and does not require a true "pumping" stage. Such a case, although realizable in practice, may be of doubtful technical applicability.

621.375.9:538.569.4 2891
Travelling-Wave Solid-State Masers—A. E. Siegman, P. N. Butcher, J. C. Cronack and W. S. C. Chang. (*Proc. IEE*, Part B, vol. 105, supplement no. 11, pp. 711-712; 1958. Discussion.)

621.375.9:538.569.4:123.164 2892
A Maser Amplifier for Radio Astronomy at X-Band—J. A. Giordmaine, L. E. Alsop, C. H. Mayer and C. H. Townes. (*Proc. IRE*, vol. 47, pp. 1062-1069; June, 1959.) "The design and operating characteristics of a maser radiometer for use in radio astronomy at 3-cm wavelength are discussed. The operating system which is described has a bandwidth of 5.5 mc and an input noise temperature, including background radiation into the antenna, of about 85°K. An rms fluctuation level of about 0.04°K is attained using an averaging time of 5 seconds. A discussion of the factors determining the sensitivity of such devices is presented."

621.375.9:538.569.4:538.22 2893
Two-Level Maser Materials—Hoskins. (See 3037.)

621.375.9:538.569.4:538.222 2894
Theory of Three-Level Paramagnetic Masers—P. N. Butcher. (*Proc. IEE*, Part B, vol. 105, supplement no. 11, pp. 684-711; 1958.) Part 1—Quantum Theory (pp. 684-690). Part 2—Amplification and Oscillation (pp. 691-698).

Part 3—Output Noise Power Spectrum (pp. 699-704).
 Part 4—Noise Figure (pp. 705-709).
 Discussion (pp. 709-711).

621.375.9:550.389.2:629.19 2895
Parametric Amplifier Receives Space Signals—(*Electronics*, vol. 32, pp. 80-81; June 5, 1959.) Signal amplification was in L-band and pump frequency in X-band giving a noise factor of 1 db and bandwidth 100 kc. Using a 32-db paraboloid (diameter 18 feet) the fraction of a watt radiated by Pioneer IV was received at 410,000 miles.

621.375.9:621.3.011.23 2896
Microwave Parametric Amplifiers and Converters—G. Wade and H. Heffner. (*Proc. IEE*, Part B, vol. 105, supplement no. 11, pp. 677-679; 1958.) The inherent gain, noise and bandwidth characteristics of basic circuits are discussed and a brief description is given of a ladder-network converter in which the output frequency is higher than the pumping frequency.

621.375.9:621.3.011.23 2897
Circuit Conditions for Parametric Amplification—J. E. Pallett. (*J. Electronics Control*, vol. 6, pp. 261-262; March, 1959.) Correction of an error in Valdes' paper (75 of January).

621.376.23 2898
Simplified Product Detector Design—J. L. Ekstrom. (*QST*, vol. 43, p. 43; May, 1959.) A circuit is described for a pentagrid converter which may be self-excited or separately excited and which has an intermodulation balance adjustment to reduce rectification effects.

621.376.4 2899
The Modulator as a Phase Detector—W. Frazer and R. E. Schemel. (*Electronic Engrg.*, vol. 31, pp. 345-346; June, 1959.) A note on the error due to a finite switching voltage applied to a shunt modulator.

GENERAL PHYSICS

535.13 2900
Solution of Maxwell's Equations in Terms of a Spinor Notation: the Direct and Inverse Problem—H. E. Moses. (*Phys. Rev.*, vol. 113, pp. 1670-1679; March 15, 1959.) The use of spinor notation enables the solution to be obtained in more compact form than does vector notation.

537.226 2901
The Quantum Mechanical Theory of the Dielectric Orientation Polarization of Gases: Part 1—The Static Orientation Polarization of a Dipole Gas consisting of Symmetric Spin Molecules—W. Maier and H. K. Wimmel. (*Z. Phys.*, vol. 153, pp. 297-313; December 5, 1958.)

537.311.1:621.396.822 2902
Noise Theory for Hot Electrons—P. J. Price. (*IBM J. Res. & Dev.*, vol. 3, pp. 191-193; April, 1959.) Nyquist's theorem is extended to the case in which the distribution of electrons is disturbed by a steady electric field.

537.311.4 2903
Transient Behaviour of the Ohmic Contact—M. A. Lampert and A. Rose. (*Phys. Rev.*, vol. 113, pp. 1236-1239; March 1, 1959.) The behavior of ohmic injecting contacts is an-

alyzed for transient currents at a fixed voltage. These occur when the free-carrier density in the solid is changed by some exciting agent as in photoconductivity or bombardment-induced conductivity.

537.311.5:538.566 2904
The Calculation of the Field in a Homogeneous Conductor with a Wavy Interface—J. R. Wait. (*Proc. IRE*, vol. 47, pp. 1155-1156; June, 1959.) Analysis showing that the perturbation of an electromagnetic field in the conductor due to the ripples is proportional to their amplitude.

537.311.5:621.3.015.3 2905
Penetration of Transient Electromagnetic Fields into a Conductor—A. Grumet. (*J. Appl. Phys.*, vol. 30, pp. 682-686; May, 1959.) Theory for a uniform electric field abruptly applied to a plane boundary.

537.322.1 2906
On the Theory of the Peltier Heat Pump—E. S. Rittner. (*J. Appl. Phys.*, vol. 30, pp. 702-707; May, 1959.) The figure of merit for a single-stage pump is optimized in the region of partial Fermi degeneracy.

537.527:537.56 2907
The Space-Charge Field-Emission Hypothesis applied to Hayashi Data on Discharges through Gases—H. Ritow. (*J. Electronics Control*, vol. 6, pp. 236-245; March, 1959.)

537.533 2908
Concerning the Nature of the Aberrations in Electron Sheet Beams—W. E. Waters. (*J. Opt. Soc. Am.*, vol. 49, pp. 304-307; March, 1959.) A power-series expansion is used to derive expressions for the aberrations up to the third order in electron sheet beams subject to purely electrostatic focusing. Four purely geometric aberrations and four aberrations due to chromatic effects are found.

537.542 2909
New Hollow-Cathode Glow Discharge—A. D. White. (*J. Appl. Phys.*, vol. 30, pp. 711-719; May, 1959.) Current densities of 0.5 amp/cm² can be obtained with a cathode consisting of a refractory metal with a spherical cavity. In neon, stable characteristics at a few milliamperes are obtained.

537.56:538.56 2910
New Experimental Results for Plasma Electron Oscillations—D. W. Mahaffey. (*J. Electronics Control*, vol. 6, pp. 193-203; March, 1959.) Study of oscillations in low-pressure mercury vapor discharges with plane oxide-coated cathodes.

537.56:538.56 2911
A Lagrangian Formulation of the Boltzmann-Vlasov Equation for Plasmas—F. E. Low. (*Proc. Roy. Soc. A.*, vol. 248, pp. 282-287; November 11, 1958.) A variational principle is found which leads to a new formulation of the problem of small oscillations about equilibrium.

537.581 2912
Wave-Mechanical Correction of the Richardson-Dushman Emission Formula—F. Ollendorff. (*Arch. Elektrotech.*, vol. 44, pp. 177-188; February 12, 1949.) An attempt is made to overcome the discrepancies between the spin-corrected theory of thermionic electron emission and empirical results.

538.1 2913
Bose-Einstein Lattice Gases equivalent to the Heisenberg Model of Ferro-, Antiferro- and Ferri-Magnetism—T. Morita. (*Progr. theoret. Phys.*, Kyoto, vol. 20, pp. 614-624; November, 1958.) A Hamiltonian is presented

that has the form of a finite series of Bose operators and is equivalent to the Heisenberg model. See also *ibid.*, pp. 728-736.

538.3:535.13 2914
Formation of Discontinuities in Classical Nonlinear Electrodynamics—M. Lutzky and J. S. Toll. (*Phys. Rev.*, vol. 113, pp. 1649-1652; March 15, 1959.)

538.566 2915
Polarization and Angle Dependence of the Reflection Factor of Absorbers for Centimetre Electromagnetic Waves—K. Walther. (*Z. angew. Phys.*, vol. 10, pp. 285-295; June, 1958.) The dependence of the reflection factor on the angle of incidence and plane of polarization of electromagnetic waves is investigated for various types of absorbers and results are confirmed experimentally.

538.566 2916
Transients in Conducting Media—P. I. Richards. (*IRE TRANS. ON ANTENNAS AND PROPAGATION*, vol. AP-6, pp. 178-182; April, 1958. Abstract, *Proc. IRE*, vol. 46, p. 1439; July, 1958.)

538.566:535.42]+534.26 2917
The Effects of Incident Wave Fluctuations on the Mean Intensity Distribution near the Focal Point of a Lens—N. N. Kron and L. A. Chernov. (*Akust. Z.*, vol. 4, pp. 341-347; October/December, 1958.) An extension of Chernov's analysis (3772 of 1958) to the case of fluctuations of arbitrary amplitude.

538.566:535.42 2918
The Kirchhoff-Young Theory of the Diffraction of Electromagnetic Waves—O. Laporte and J. Meixner. (*Z. Phys.*, vol. 153, pp. 129-148; November 14, 1959.) A transformation is discussed which facilitates the evaluation of Kirchhoff's double integrals.

538.566:535.43]+534.26 2919
On Propagation of Waves in Slightly Rough Ducts—J. C. Samuels. (*J. Acoust. Soc. Am.*, vol. 31, pp. 319-325; March, 1959.) Mathematical treatment of acoustic and electromagnetic wave propagation assuming that the heights of the roughness peaks are small compared to the average separation of the duct walls.

538.566.2 2920
The Propagation of a Variable Electromagnetic Field in a Stratified Anisotropic Medium—A. N. Tikhonov. (*Dokl. Ak. Nauk SSSR*, vol. 126, pp. 967-970; June 11, 1949.) Computation of the field on the surface of an anisotropic conducting medium due to a dipole lying in the surface. See also 3036 of 1956 (Tikhonov and Shakhsharov.)

538.566.2:548 2921
On the Propagation of Electromagnetic Waves in a Medium with Appreciable Spatial Dispersion—V. M. Agranovich and A. A. Rukhadze. (*Zh. eksp. Teor. Fiz.*, vol. 35, pp. 982-984; October, 1958.) Brief description of a method more detailed than that of Ginsburg (1169 of April), in which expansions are obtained for "direct" and "inverse," dispersion. It is shown that in cubic crystals inclusion of the spatial dispersion leads to a weak anisotropy of the index of refraction.

538.569.4 2922
A General Theory of Magnetic Double Resonance—K. Tomita. (*Prog. Theoret. Phys.*, Kyoto, vol. 20, pp. 743-773; November, 1958.) The theory describes a system consisting of two interacting different species of spin, one being saturated by a strong resonant radiation field and the other being detected by a weak field. See also 95 of January.

538.569.4 2923
Multiple-Quantum Transitions in Nuclear Magnetic Resonance—S. Yatsiv. (*Phys. Rev.*, vol. 113, pp. 1522-1537; March 15, 1959.)

538.569.4 2924
The Application of Magnetic Resonance to Solid-State Electronics—D. J. E. Ingram. (*J. Brit. IRE*, vol. 19, pp. 357-267; June, 1959.) A description of the basic principles and techniques and an outline of some recent applications.

538.569.4 2925
Excitation of Spin Waves in an Antiferromagnet by a Uniform R. F. Field—R. Orbach and P. Pincus. (*Phys. Rev.*, vol. 113, pp. 1213-1215; March 1, 1959.) It is possible to excite spin waves in an antiferromagnet by a uniform RF field provided that spins on the surface of the specimen experience anisotropy interactions different from those acting on spins in the interior.

538.569.4 2926
Exchange Effects in Ferromagnetic Resonance—M. A. Gintsburg. (*Zh. Eksp. Teor. Fiz.*, vol. 35, pp. 1047-1049; October, 1958.) A single dispersion law for transverse em waves and for spin waves is derived which takes account of both relativistic and exchange interactions.

538.569.4:538.222 2927
Paramagnetic Electron-Resonance Induction—E. Lutze and D. Bösnecker. (*Naturwiss.*, vol. 45, p. 332; July, 1958.) Preliminary note on investigations of induced emission at paramagnetic resonance. $\text{CuSO}_4 \cdot 5\text{H}_2\text{O}$ at room temperature and a wavelength of 3.33 cm were used.

538.569.4:621.318.132 2928
Ferrimagnetic Resonance Modes in Spheres—P. C. Fletcher and R. O. Bell. (*J. Appl. Phys.*, vol. 30, pp. 687-698; May, 1959.) The magnetostatic solutions of ferrimagnetic resonance in ferrite spheres are briefly derived. Some experimental results are compared with the theory.

538.569.4:621.375.9 2929
Role of Double-Quantum Transitions in Masers—Yatsiv. (See 2890.)

538.652 2930
Form Effect in Linear Magnetostriction—H. E. Stauss. (*J. Appl. Phys.*, vol. 30, pp. 698-701; May, 1959.)

539.2 2931
Electron Interaction in Solids. Characteristic Energy Loss Spectrum—P. Nozières and D. Pinse. (*Phys. Rev.*, vol. 113, pp. 1254-1267; March 1, 1959.) The characteristic energy loss spectrum is analyzed with the aid of the dielectric formulation of the many-body problem.

GEOPHYSICAL AND EXTRA-TERRESTRIAL PHENOMENA

523.164:621.396.677.8 2932
Improved Measurements of the Positions of 17 Intense Radio Stars—B. Elsmore. (*Mon. Not. R. Astr. Soc.*, vol. 118, no. 6, pp. 603-608; 1958.) Observations have been made at 1.9 m λ , using the Cambridge radio telescope as a crossed-axis interferometer. See also 103 of January (Edge, et al.).

523.164.32 2933
The Extension of Solar Radio Spectroscopy to Decimetre Wavelengths—K. V. Sheridan, G. H. Trent and J. P. Wild. (*Observatory*, vol. 79, pp. 51-53; April, 1959.) Preliminary report on spectrographic investigations in the frequency range 24-40 mc.

523.164.32 2934
On Short Periodic Variations in Solar Storms on 200 mc/s— \emptyset . Hauge. (*Astrophys. Norveg.*, vol. 6, pp. 43-54; January, 1958.) 19 days of enhanced solar radiation on 200 mc in June, July and August, 1955 are investigated by an autocorrelation method in a search for short periodic variations with repetition times between 7.5 and 90 min. Results indicate that some noise storms are characterized by periodic variations with repetition times differing from day to day, while other noise storms exhibit no periodic variations. It is possible that a specific noise storm area retains its characteristics of short periodic variations in radio emission for a solar rotation or longer.

523.164.32 2935
On the Fine Structure of Solar Bursts in the 200 Mc/s Range and their Drift in Frequency— \emptyset . Elgarøy. (*Astrophys. Norveg.*, vol. 6, pp. 55-74; January, 1958.) High-speed records have been obtained simultaneously on 199 mc and 200.5 mc with a twin-channel receiver at the Harestua Solar Observatory during the period February-September, 1957. An analysis of the records shows that 48 per cent of the bursts occur first on the lower frequency, 34 per cent first on the higher frequency and 18 per cent simultaneously. The results are discussed and the receiving equipment is described.

523.164.32:621.396.677.3 2936
A New High-Resolution Interferometer for Solar Studies—M. R. Kundu. (*J. Inst. Telecommun. Engrs. India.*, vol. 5, pp. 77-85; March, 1959.) The device is essentially a two-element interferometer with the two antennas in equatorial mounting, which permits use far from the median plane and gives a resolving power of the order of 1'. See 2733 of 1957 (Alon et al.).

523.164.4 2937
A High-Resolution Survey of the Andromeda Nebula at 408 Mc/s—M. I. Large, D. S. Mathewson and C. G. T. Haslam. (*Nature, London*, vol. 183, pp. 1250-1251; May 2, 1959.) A report of observations made with the Jodrell Bank radio telescope.

523.164.4 2938
A High-Resolution Survey of the Coma Cluster of Galaxies at 408 Mc/s—M. I. Large, D. S. Mathewson and C. G. T. Haslam. (*Nature, London*, vol. 183, pp. 1663-1664; June 13, 1959.)

523.164.4:621.396.11:523.755 2939
The Scattering of Radio Waves in the Solar Corona—A. Hewish. (*Mon. Not. R. Astr. Soc.*, vol. 118, no. 6, pp. 534-546; 1958.) An account is given of measurements carried out each June over the period 1952-1958 of the radio emission from the Crab nebula at wavelengths of 7.9, 3.7 and 1.9 m. Results indicate a pronounced sunspot-cycle variation in certain regions of the corona, a scatter anisotropy, and the presence of refraction effects in addition to scattering. See also 2286 of 1955.

523.5:621.396.11 2940
Theory of the Radio-Echo Meteor Height Distribution in a Non-isothermal Atmosphere—A. A. Weiss. (*Aust. J. Phys.*, vol. 12, pp. 54-64; March, 1959.) The height distribution of echoing points of shower and sporadic meteors belonging to a homogeneous velocity group is calculated for a model atmosphere whose scale height is a linear function of height. Experimental cutoff and the theoretical approximations involved limit the accuracy with which actual scale height and density may be found from observed meteor trails.

523.5:621.396.11 2941
Elevation, Height, and Electron Density of Echoing Points of Meteor Trails—A. A. Weiss.

- (*Aust. J. Phys.*, vol. 12, pp. 65-76; March, 1959.) These parameters may be evaluated by the continuous operation of ew equipment on 27 mc. At least 60 per cent of all echoes are found to be distorted. The electron density distributions are in qualitative agreement with known meteor mass distributions and trail shapes.
- 523.745:523.165** 2942
Solar Activity and Transient Decreases in Cosmic-Ray Intensity—D. Venkatesan. (*J. geophys. Res.*, vol. 64, pp. 505-520; May, 1959.)
- 523.753** 2943
A New Theory of the Solar Corona—P. J. Kellogg and E. P. Ney. (*Nature, London*, vol. 183, pp. 1297-1301; May 9, 1959.) It is proposed that the solar corona consists of trapped charged particles moving in the magnetic fields of the sun. Experimental data are discussed in terms of this model.
- 550.385** 2944
Disturbances of the Earth's Magnetic Field considered as Relaxation Variations—P. Herrinck. (*Ann. Géophys.*, vol. 13, pp. 211-221; July-September, 1957.) Records of the horizontal magnetic component at Elisabethville and elsewhere show relaxation processes analogous to post-disturbances of magnetic storms and subject to the 27-day recurrence tendency.
- 550.385** 2945
Possible Causes of Geomagnetic Fluctuations having a 6-sec Period—H. J. Duffus, J. A. Sland and C. Wright. (*Nature, London*, vol. 183, pp. 1479-1480; May 23, 1959.) Comment on 1532 of May (Daniels). Short- and long-period oscillations, sometimes preceding but more often accompanying a main train of magnetic activity are described. They are considered to be associated, and of electromagnetic origin.
- 550.385.37** 2946
Geographical Variations in Geomagnetic Micropulsations—H. J. Duffus, J. A. Sland, C. S. Wright, P. W. Nasmyth and J. A. Jacobs. (*J. geophys. Res.*, vol. 64, pp. 581-583; May, 1959.) Significant differences consistently occur in simultaneous data obtained at stations 25 miles apart.
- 550.385.37:551.594.5** 2947
On a Possible Auroral Origin of Certain Geomagnetic Pulsations—J. Coulomb. (*Ann. Geophys.*, vol. 13, pp. 91-102; April/June, 1957.)
- 550.385.4:523.745** 2948
The Relation between the Sudden Disappearance of Filaments and Magnetic Storms—M. Dizer. (*Ann. Géophys.*, vol. 13, p. 325; October/December, 1957.) An analysis of records shows a correlation between the sudden disappearance of filaments close to the sun's central meridian and magnetic disturbances.
- 550.386:523.755** 2949
Green Coronal Line Intensity and Geomagnetism—C. Warwick. (*J. geophys. Res.*, vol. 64, pp. 527-531; May, 1959.) Statistical analysis indicates a minimum in geomagnetic activity following the central meridian passage of regions of high green-line intensity.
- 550.389.2:629.19** 2950
Laws of Motion of an Earth Satellite—Yu. A. Pobedonostsev. (*Priroda*, pp. 19-25; January, 1958.) The principles of multistage rocket flight are considered and formulas for rocket velocity are derived. Tables give the satellite velocity and duration of flight for heights up to 6000 km.
- 550.389.2:629.19** 2951
A Discussion on Observations of the Russian Artificial Earth Satellites and their Analysis—(*Proc. Roy. Soc. A.*, vol. 248, pp. 1-87; October 28, 1958.) The text is given of fifteen papers discussed at a meeting in London, November 29, 1957. These include results obtained using radio telescopes and interferometers, Doppler recorders and direction-finding and field-strength measuring equipment. Applications are made to the computation of orbit parameters. See also 1720 of 1958 for a similar discussion.
- 550.389.2:629.19** 2952
Observations on the U.S.S.R. Earth Satellites and the Study of Radio-Wave Propagation—W. C. Bain and E. D. R. Shearman. (*Proc. IEE*, Part B, vol. 106, pp. 259-263; May, 1959.) Measurements of bearing, angle of elevation and Doppler frequency shift were made at 20 and 40 mc. The observed phenomena could be explained in terms of existing knowledge of ionospheric propagation. The derivation of orbital parameters from the observations is discussed.
- 550.389.2:629.19** 2953
A Type of Variation of the Signal Strength from 1958 δ_2 (Sputnik 3)—L. Liszka. (*Nature, London*, vol. 183, pp. 1383-1384; May 16, 1959.) Fluctuations of signal strength relative to the satellite position in orbit indicate that the satellite produces heavily ionized tracks of very long lifetime. Observations have been made to test this hypothesis and results are given.
- 550.389.2:629.19** 2954
Diurnal Lapse of S gnals from Sputnik III—G. H. Munro. (*Nature, London*, vol. 183, p. 1549; May 30, 1959.) A brief note, dated April 28, 1959, states that systematic observations have established that pulse modulation is present only when the satellite 1958 δ_2 is in sunlight. On very close transits the CW signal can be detected with sufficient strength to record the Doppler shift.
- 550.389.2:629.19** 2955
Density of the Atmosphere at Heights between 200 km and 400 km from Analysis of Artificial-Satellite Orbits—D. G. King-Hele. (*Nature, London*, vol. 183, pp. 1224-1227; May 2, 1959.)
- 550.389.2:629.19** 2956
Fluctuations in the Brightness of the Second Artificial Earth Satellite—V. P. Tsevevich. (*Priroda*, pp. 78-79; April, 1958.) These brightness fluctuations are explained by the rotation of the satellite on its axis, its maximum brightness corresponding to its greatest cross section as seen by the observer. A graph shows these brightness variations as recorded by the Odessa Observatory.
- 550.389.2:629.19** 2957
The Antipodal Reception of Sputnik III—E. Woyk (Chvojková). (*Proc. IRE*, vol. 47, p. 1144; June, 1959.) The mechanism of the propagation of waves around the earth within the ionospheric layers is discussed and the best conditions for antipodal reception are deduced. It is concluded that at Stanford, Calif., the best conditions for frequent reception occur from the southeast during summer afternoons. This is in agreement with observations.
- 550.389.2:629.19** 2958
Satellite-Measured Radiation—G. W. Stuart. (*Phys. Rev. Lett.*, vol. 2, pp. 417-418; May 15, 1959.) The relevance of atomic change-processes to the nature of the radiation belt is noted.
- 550.389.2:629.19** 2959
Some Results of Investigations on Cosmic Rays Using Artificial Earth Satellites—L. V. Kurnosova. (*Priroda*, pp. 85-86; June, 1958.) The intensity variations of cosmic rays as recorded during the flight of the second sputnik are shown. There were no appreciable corresponding variations at ground level.
- 550.389.2:629.19** 2960
Corpuscular Radiation and the Acceleration of Artificial Satellites—L. G. Jacchia. (*Nature, London*, vol. 183, pp. 1662-1663; June 13, 1959.) Observations of satellites 1958 β_2 and δ_1 have been re-examined and more accurate values of acceleration have been calculated at twice the original resolution (see 2564 of August). Correlation with 10.7-cm solar radiation is higher for β_2 than δ_1 , probably due to greater observational accuracy. An increased acceleration of δ_1 at the time of two major geomagnetic disturbances following flares indicates the effect of corpuscular radiation on atmospheric density at the 200-km level.
- 550.389.2:629.19:551.510.535** 2961
On the Existence of a Strong Magneto-ionic Effect Topside of the F Maximum of the Kennelly-Heaviside Layer—P. R. Arendt. (*J. Appl. Phys.*, vol. 30, pp. 793-795; May, 1959.) Observations of the Faraday effect in 108-mc signals from artificial satellites showed noticeable magneto-ionic effects at altitudes up to 2000 km.
- 550.389.2:629.19:551.379.5** 2962
Parametric Amplifier Receives Space Signals—(See 2895.)
- 550.389.2:629.19:621.396.11** 2963
Radio Reflections from Satellite-Produced Ionization—C. R. Roberts, P. H. Kirchner and D. W. Bray. (*Proc. IRE*, vol. 47, pp. 1156-1157; June, 1959.) Observations have been made on frequencies of 5, 10, 15 and 20 mc and two very different effects obtained on both 10 and 15 mc are described.
- 550.389.2:629.19:621.398** 2964
Cosmic-Ray Instrumentation in the First U. S. Earth Satellite—G. H. Ludwig. (*Rev. Sci. Instr.*, vol. 30, pp. 223-229; April, 1959.) The instrumentation was designed for conservation of electrical power and for stable and reliable operation over a wide range of temperatures.
- 551.510.535** 2965
Some Results of Investigations of the Upper Atmosphere—V. V. Mikhnevich. (*Priroda*, pp. 71-72; May, 1958.) Vertical rocket investigations carried out in U.S.S.R. between 1949 and 1958 showed that, contrary to established opinion, above the E-layer there is only a very shallow minimum in electron density. The electron density increases up to 250-300 km with a maximum at 300 km and then slowly decreases so that at 470 km the density is 10^6 electrons per cm^3 .
- 551.510.535** 2966
A Theoretical Study of the Dynamical Structure of the Ionosphere—T. Shimazaki. (*J. Radio Res. Labs, Japan*, vol. 6, pp. 109-241; March, 1959.) A comprehensive survey of the modifications to Chapman theory which are necessary to explain the actual behavior of the ionosphere. Both the large F_2 -layer anomalies and the smaller ones for the E and F_1 layers are discussed. Over 100 references.
- 551.510.535** 2967
Conditions in the Outer Ionosphere—Ya. L. Al'pert. (*Priroda*, pp. 86-87; June, 1958.) It is found that the electron concentration in the outer ionosphere decreases with the height considerably less rapidly than it increases at lower levels. The values obtained

show that at 2000-3000 km the concentrations of electrons and neutral particles are of the order of 10^2 - 10^3 and 1 per cm^3 respectively.

551.510.535 2968
Investigation of the Equatorial Electrojet by Rocket Magnetometer—L. J. Cahill, Jr. (*J. Geophys. Res.*, vol. 64, pp. 489-503; May, 1959.) Two layers of electrical current were detected, one existing near an altitude of 100 km and the other about 20-25 km higher.

551.510.535 2969
Geophysical Effects of High-Altitude Nuclear Explosions—T. Obayashi, S. C. Coroniti and E. T. Pierce. (*Nature, London*, vol. 183, pp. 1476-1478; May 23, 1959.) A report of observations made at Miraiso Observatory on August 1 and 12, 1958. Fade-outs on frequencies between 10 and 20 mc and an enhancement of atmospheric noise at 28 kc have been recorded. These effects are attributed to an increase in D-layer ionization extending over much greater distances than had previously been envisaged.

551.510.535 2970
Sporadic E-Region Ionization, "Spread F," and the Twinkling of Radio Stars—D. F. Martyn. (*Nature, London*, vol. 183, pp. 1382-1383; May 16, 1959.) Kinematic instability in the ionization gradient of a medium drifting across a magnetic field is considered to be responsible for the three phenomena.

551.510.535 2971
The Effect of Sudden Ionospheric Disturbances (S.I.D.'s) on 2.28-Mc/s Pulse Reflections from the Lower Ionosphere—F. F. Gardner. (*Aust. J. Phys.*, vol. 12, pp. 42-53; March, 1959.) During a typical large S.I.D., associated with a class 2 or class 3 flare, the increase in ionization might vary from 20/1 at 65 km through 3/1 at 90 km to unity at 110 km. The amplitude recovery of the E-layer echo lagged about 4 minutes behind the recovery of the lower echoes around 85 km. At all heights below 85 km, echo recovery occurred simultaneously.

551.510.535:621.396.11 2972
Rocket Measurements of Absorption in the Lower Ionosphere—H. Mende, K. Rawer and E. Vassy. (*Ann. Geophys.*, vol. 13, pp. 231-233; July-September, 1957.) Results are given of measurements of the field strength of two medium-wave and one long-wave transmitter. The D-layer minimum height is about 70 km and medium-wave observations indicate maximum absorption at 80 km, the attenuation being 1.2 db/km for normal incidence.

551.510.535:621.396.11:523.164 2973
Refraction of Extraterrestrial Radio Waves in the Ionosphere—M. M. Komesaroff and C. A. Shain. (*Nature, London*, vol. 183, pp. 1584-1585; June 6, 1959.) Expressions are derived for estimating ionospheric refraction at low frequencies. Horizontal gradients of electron density are considered. Positions of a discrete source obtained from observation at 19.7 mc after applying corrections for refraction are within a few minutes of arc of the observed position at 85.5 mc.

551.594 2974
Simultaneous Occurrence of Sub-visual Aurorae and Radio Noise Bursts on 4.6 kc/s—R. A. Duncan and G. R. Ellis. (*Nature, London*, vol. 183, pp. 1618-1619; June 6, 1959.) Records show that there is a correlation between aurorae and noise bursts but anomalies exist which cannot be explained satisfactorily.

551.594.5 2975
Auroral Isochasmis—B. Hultqvist. (*Nature, London*, vol. 183, pp. 1478-1479; May 23,

1959.) Observed isochasmis and projections of circles in the equatorial plane along the geomagnetic lines of force are compared.

551.594.6:621.372.57:621.3.087.4 2976
Investigation of an Apparatus for Recording Atmospheric—Benoit and Kernevez. (See 2870.)

551.594.6:621.396.11.029.45/.51:551.510.535 2977
An Experimental Proof of the Mode Theory of V.L.F. Ionospheric Propagation—Obayashi, Fujii and Kidokoro. (See 3094.)

LOCATION AND AIDS TO NAVIGATION

621.396.93 2978
Radio Aids to Navigation—(*Engineering, London*, vol. 186, pp. 313-323; September 5, 1958.) Three papers presented at the British Association meeting in Glasgow, September, 1958.

1) **Position Finding by Radio**—R. L. Smith-Rose (pp. 313-315).

2) **Marine Radio Navigational Aids**—B. G. Pressey (pp. 316-318).

3) **Radio Aids and Aeronautical Navigation**—C. Williams (pp. 318-323).

621.396.96 2979
Doppler Radar Navigation—F. B. Berger. (*Electronics*, vol. 32, pp. 62-63; May 8, 1959.) A table of characteristics of existing airborne systems.

621.396.96:621.314.63 2980
Using Silicon Diodes in Radar Modulators—Gray. (*Electronics*, vol. 32, pp. 70-72; June 12, 1959.) (See 3110.)

621.396.963:621.374.32 2981
Digital-Counter Techniques Increase Doppler Uses—B. E. Keiser. (*Electronics*, vol. 32, pp. 46-50; May 22, 1959.) The frequency of an oscillator is adjusted automatically to the Doppler frequency of the returned signal and is measured using a circuit which counts 100 pulses per 360° cycle.

621.396.969.3 2982
"Ring Angels" over South-East England—E. Eastwood, J. D. Bell and N. R. Phipp. (*Nature, London*, vol. 183, pp. 1759-1760; June 20, 1959.) The unexplained phenomena described have been observed on high-power L-band radar equipment during the sunrise period at heights up to 2000 feet. The rings expand as ripples at a velocity of 25-55 mph, the maximum diameter recorded being 30 miles.

621.396.969.33 2983
"Escort"—a Marine Radar with Unusual Features—(*Beama Jour.*, vol. 66, pp. 57-59; May, 1959.) Four types of PPI display can be selected and provision is made for automatic resetting of the ship's own position on the display and for automatic alignment correction.

621.396.969.34+621.396.934 2984
Anti-aircraft Radiolocation Techniques—K. Trofimov (*Radio, Moscow*, pp. 27-31; February, 1958.) A description of radar techniques for the location of enemy aircraft and their destruction by guided missiles.

MATERIALS AND SUBSIDIARY TECHNIQUES

533.5:621.385.032.22 2985
Measurements of Gas Evolution or Sorption of Anode Materials under Simulated Life Conditions—C. H. Rehkopf. (*Sylvania Technologist*, vol. 11, pp. 114-116; October, 1958.) A brief description of techniques and results of measurements.

538.58 2986
Electrical Absorption of Gases in the High-Vacuum Pressure Range—G. Strotzer. (*Z. angew. Phys.*, vol. 10, pp. 207-216; May, 1958.) Various hypotheses for the "clean-up" effect in low-pressure gases are investigated.

535.215:538.6:546.682.86 2987
Indium Antimonide Photoelectromagnetic Infrared Detector—P. W. Kruse. (*J. Appl. Phys.*, vol. 30, pp. 770-778; May, 1959.) The theory of operation, construction, and performance data are presented.

535.215:539.2 2988
Photoconductor Performance, Space-Charge Currents, and the Steady-State Fermi Level—A. Rose and M. A. Lampert. (*Phys. Rev.*, vol. 113, pp. 1227-1235; March 1, 1959.) "The performance of a photoconductor is analyzed, via the concept of the steady-state Fermi level, and shown to be limited by the injection of space charge. Using the gain-bandwidth product G/τ_0 as a measure of performance, it is found that $G/\tau_0 = M/\tau_r$, where τ_r is the dielectric relaxation time under operating conditions, and $M = \mathcal{N}_A/\mathcal{N}_T$, with $e\mathcal{N}_A$ the total charge on the anode and $e\mathcal{N}_T$ the total volume charge, free plus trapped, effectively in thermal contact with the free charge."

535.215:546.472.21 2989
Anomalous Photovoltaic Effect in ZnS Single Crystals—A. Lempicki. (*Phys. Rev.*, vol. 113, pp. 1204-1209; March 1, 1959.) Photovoltages larger than the band gap have been observed in both cubic and hexagonal crystals free of such faults.

535.215:546.482.21 2990
Lattice Scattering Mobility of Electrons in Cadmium Sulphide—H. Miyazawa, H. Maeda and H. Tomishima. (*J. Phys. Soc. Japan*, vol. 14, pp. 41-47; January, 1959.) The temperature variation of the lattice scattering mobility is found to be given by the expression $\mu_L = A \{ \exp(\Theta/T) - 1 \}^{-1}$ with $A = 92.5 \pm 15 \text{ cm}^2/\text{sec}$ and $\Theta = 370 \pm 30^\circ \text{K}$. The Conwell-Weisskopf formula is used to correct for impurity scattering.

535.215:546.482.21 2991
Polarization of Photoconductivity Excitation Bands in CdS Single Crystals—R. L. Kelly and W. J. Fredericks. (*Phys. Rev. Lett.*, vol. 2, pp. 389-390; May 1, 1959.) The wavelength of incident light exciting maximum photoconductivity was measured as a function of its angle of polarization with respect to crystal orientation. Results are interpreted with an energy-level model.

535.215:546.482.21:538.63 2992
Relaxation-Time Anisotropy in Cadmium Sulphide Studied with Electrical Resistivity and Magneto-resistance Effect—T. Mazumi. (*J. Phys. Soc. Japan*, vol. 14, pp. 47-56; January, 1959.) Experimental results indicate unusual anisotropic temperature dependence of the galvanomagnetic effects in hexagonal CdS single crystal.

535.215:546.482.21:539.23 2993
Electric Breakdown of Vapour-Deposited CdS Films—C. W. Böer, U. Kümmel and W. Misselwitz. (*Naturwiss.*, vol. 45, pp. 331; July, 1958.) Breakdown field strength is plotted as a function of film thickness for both polarities of the applied voltage.

535.215:546.817.221:539.23 2994
Effect of Thickness of Thin Films of Lead Sulphide on the Spectral Response of Photoconductivity—H. E. Spencer. (*Phys. Rev.*, vol. 113, pp. 1417-1420; March 15, 1959.)

- 535.215:548.73 2995
Crystal Structure of Sodium-Potassium Antimonide (Na_2KSb)—J. J. Scheer and P. Zalm. (*Philips Res. Rep.*, vol. 14, pp. 143-150; April, 1959.) The structure of Na_2KSb , a photoemissive material, has been determined by X-ray analysis. It closely resembles that of Cs_2Sb .
- 535.37 2996
Two-Stage Optical Excitation in Sulphide Phosphors—R. E. Halsted, E. F. Apple and J. S. Prener. (*Phys. Rev. Lett.*, vol. 2, pp. 420-421; May 15, 1959.) Optical evidence shows that the same impurities give rise to electron transitions involving energy levels near or in the valence band as well as the conduction band.
- 535.37:061.3 2997
Transactions of the 5th Conference on Luminescence (Crystal Phosphors)—(*Izv. Ak. Nauk SSSR*, vol. 21, pp. 475-784; April and May, 1957.) The text is given of 98 papers presented at the conference held in Tartu, Estonia, June 25-30, 1956. For a list of titles in English, see *Translated Contents Lists of Russian Periodicals*, February and May, 1958, nos. 107 and 110, pp. 43-45 and 47-50.
- 535.37:539.2 2998
Energy-Level Positions of Silver Luminescent Centres in Sulphides—C. C. Klick. (*Phys. Rev. Lett.*, vol. 2, pp. 418-420; May 15, 1959.)
- 535.37:546.472.21 2999
Excitation Spectra and Temperature Dependence of the Luminescence of ZnS Single Crystals—A. Halperin and H. Arbell. (*Phys. Rev.*, vol. 113, pp. 1216-1221; March 1, 1959.) "The luminescence of ZnS:Cl and ZnS:Cu:Cl crystals was measured for the temperature region 80-500°K and for different wavelengths of exciting light. The behavior of the luminescence versus temperature curves differed from similar curves for powders reported in literature."
- 535.376 3000
A.C.-D.C. Electroluminescence—W. A. Thornton. (*Phys. Rev.*, vol. 113, pp. 1187-1191; March 1, 1959.) The addition of a direct voltage to an alternating voltage exciting visible electroluminescence in certain ZnS powders increases the emission by as much as 250 times under conditions where the dc luminescence alone is about equal to the initial ac luminescence.
- 535.376 3001
Rise and Decay of Intensity of Luminescence of Short-Persistence Phosphors—R. Feinberg. (*Nature, London*, vol. 183, pp. 1546-1547; May 30, 1959.) Results of measurements made on three cathode-ray tube phosphors are discussed in relation to theory.
- 535.376:537.533.2 3002
Investigations of Exo-electron Emission and Luminescence of Inorganic Crystals—G. Gourgé. (*Z. Phys.*, vol. 153, pp. 186-206; November 14, 1958.) The investigations discussed were carried out to determine the relation between exo-electron emission and luminescence; measurements were made at temperatures down to -165°C.
- 535.376:546.281.26 3003
Electroluminescence of Silicon Carbide—D. Rucker. (*Z. angew. Phys.*, vol. 10, pp. 254-263; June, 1958.) The external and internal light emission observed on a dc-excited SiC junctions [see, e.g., 3890 of 1957 (Patrick)] is investigated on blue and green single crystals, and an interpretation of the various effects is given.
- 535.376:546.482.21 3004
On the Mechanism for Carrier Excitation in CdS—D. D. Snyder, C. E. Bleil. (*J. Appl. Phys.*, vol. 30, pp. 736-739; May, 1959.) The production and absorption of X-rays in the experimental crystals have been calculated and some confirmatory data presented.
- 535.376:546.561-31 3005
Electroluminescence in Cuprous Oxide—R. Frerichs and R. Handy. (*Phys. Rev.*, vol. 113, pp. 1191-1198; March 1, 1959.) The electroluminescent properties of Cu_2O are not directly analogous to those of a semiconductor such as Ge or an insulating phosphor such as ZnS. A detail study has been made of current creep effects occurring in Cu_2O plate rectifiers with dc excitation.
- 537.226/.228.1 3006
Studies on (Ba-Pb) (Ti-Zr) O_3 System—T. Ikeda. (*J. Phys. Soc. Japan*, vol. 14, pp. 168-174; February, 1959.)
- 537.226/.227:546.431.824-31 3007
Polarization Reversal in Barium Titanate—(*Bell Lab. Rec.*, vol. 37, p. 144; April, 1959.) A note on the polarization reversal in single crystals which occurs by extensive sideways motion of domain walls. See 155 of January (Miller).
- 537.227:547.476.3 3008
Ferroelectric Hysteresis and After-Effect Phenomena in Rochelle Salt—H. E. Müser. (*Z. angew. Phys.*, vol. 10, pp. 249-254; June, 1958.) Investigation of the constriction of ferroelectric hysteresis loops observed in Rochelle salt. For a similar anomaly in BaTiO_3 see, e.g., 2757 of 1958 (Hegenbarth)
- 537.228.1:549.514.51 3009
 β -Quartz as High-Temperature Piezoelectric Material—D. L. White. (*J. Acoust. Soc. Amer.*, vol. 31, pp. 311-341; March, 1959.) Lengthwise extensional, face shear and thickness shear modes can be excited piezoelectrically by suitable rotation of the crystal plate.
- 537.311.33 3010
On a Simple Model for Impurity-Band Conduction—K. Helmers. (*Philips Res. Rep.*, vol. 14, pp. 1-10; February, 1959.) A study of the influence of impurity-center distribution on the resistance of the sample using a stochastic resistance network.
- 537.311.33 3011
Some Optical Characteristics of Semiconductors—O. Simpson. (*Research, London*, vol. 12, pp. 127-132; April, 1959.) A number of optical phenomena are described and related to the electronic structure of semiconductors.
- 537.311.33 3012
Space Charge in Semiconductors resulting from Low-Level Injection—M. Green. (*J. Appl. Phys.*, vol. 30, pp. 744-747; May, 1959.) A solution of the continuity equations is obtained for the space-charge distribution by assuming that 1) deviations from neutrality are small, and 2) the space-charge fields give rise to pure diffusion and pure "drift-wave" terms with time-dependent coefficients.
- 537.311.33 3013
Role of Single Phonon Emission in Low-Field Breakdown of Semiconductors at Low Temperatures—M. A. Lampert, F. Herman and M. C. Steele. (*Phys. Rev. Lett.*, vol. 2, pp. 394-397; May 1, 1959.) Observations of low-field breakdown are correlated with the known energy-band structure and phonon spectra of Ge and Si. A simple, necessary condition for breakdown is suggested.
- 537.311.33:535.34-15 3014
Effect of Pressure on the Infrared Absorption of Semiconductors—L. J. Neuringer. (*Phys. Rev.*, vol. 113, pp. 1495-1503; March 15, 1959.) Measurements were made on Ge, Si, and Te in the pressure range 1-2000 atm. The pressure coefficients were used to calculate the thermal dilation term in the equation for the change of the energy gap with temperature and hence the magnitude of the electron-lattice interaction.
- 537.311.33:537.32 3015
On the Theory of the Thermoelectricity in Two-Band Semiconductors—E. Haga. (*J. Phys. Soc. Japan*, vol. 14, pp. 35-38; January, 1959.) A theory is developed taking account of the temperature dependence of the energy gap. The Thomson relations are shown to be satisfied.
- 537.311.33:537.533 3016
Field Emission from Semiconductors—G. Busch and T. Fischer. (*Brown Boveri Rev.*, vol. 45, pp. 532-539; November/December, 1958.) Theoretical and experimental work on field emission is reviewed. Results are discussed of an investigation carried out on SiC point electrodes, which confirm the exponential relation between current and field which is characteristic of field emission.
- 537.311.33:538.214 3017
The Effect of Concentration on the Magnetic Susceptibility of Trapped Electrons and Holes in Semiconductors—F. T. Hedgcock. (*Can. J. Phys.*, vol. 37, pp. 381-383; March, 1959.) A model proposed to explain the anomalous magnetic susceptibility of certain impurity semiconductors at low temperatures [see 2800 of 1957 and 3513 of 1958 (Sonder and Stevens)] is found to be attractive qualitatively but quite inadequate quantitatively.
- 537.311.33:538.614 3018
The Faraday Effect in Anisotropic Semiconductors—I. G. Austin. (*J. Electronics Control*, vol. 6, pp. 271-274; March, 1959.) "The theory of the Faraday effect in semiconductors is extended to uniaxial crystals with spheroidal energy surfaces, using the classical Drude-Zener theory. Expressions applicable at infrared frequencies are given and used to discuss preliminary measurements on Bi_2Te_3 ."
- 537.311.33:[546.28+546.289] 3019
Semiconductor Surface Phenomena—A. Many. (*Sylvania Technologist*, vol. 11, pp. 117-124; October, 1958.) "Slow" and "fast" surface states have been established for Ge and Si; their characteristics are summarized and discussed.
- 537.311.33:[546.23+546.289] 3020
Metallurgy of Semiconductors, in Particular Germanium and Silicon—A. J. Goss. (*Marconi Rev.*, vol. 22, pp. 3-17; 1st Quarter, 1959.) 54 references.
- 537.311.33:546.28 3021
The Effects of Seed Rotation on Silicon Crystals—A. J. Goss and R. E. Adlington. (*Marconi Rev.*, vol. 22, pp. 18-36; 1st Quarter 1959.) Single crystals pulled in an argon atmosphere at rotation rates up to 200 rpm have been examined. The effect of rotation on crystal pulling, the growth interface, dislocations, etching, resistivity, 9- μ absorption data and heat treatment of the crystal are given. Results are discussed in relation to a mechanical model of stirring in the melt.
- 537.311.33:546.281.26 3022
Some Surface Properties of Silicon-Carbide Crystals—J. A. Dillon, Jr., R. E. Schlier and H. E. Farnsworth. (*J. Appl. Phys.*, vol. 30, pp. 675-679; May, 1959.) Both work-function and

electron-diffraction studies indicated that SiC surfaces obtained by ion bombardment and annealing were nonstoichiometric.

537.311.33:546.289 3023

High-Electric-Field Effects in Germanium p - n Junction—J. Yamaguchi and Y. Hamakawa. (*J. Phys. Soc. Japan*, vol. 14, pp. 15-21; January, 1959.) Increase of ambient temperature caused the critical voltage for avalanche breakdown to increase and the voltage for the onset of negative resistance to decrease. The barrier temperature was independent of the ambient temperature.

537.311.33:546.289 3024

Barrier Temperature at Turnover in Germanium p - n Junction—J. Yamaguchi and Y. Hamakawa. (*J. Phys. Soc. Japan*, vol. 14, pp. 232-233; February, 1959.)

537.311.33:546.289 3025

Injection and Extraction of Minority Carriers at the Surface of a Germanium Electrode as a Result of Electrochemical Processes—Yu. V. Pleskov. (*Dokl. Ak. Nauk SSSR*, vol. 126, pp. 111-1114; May 1, 1959.)

537.311.33:546.289 3026

Sb Distribution in Quenched Ge-Sb Alloys—G. Pröpstl and G. Zielasek. (*Z. angew. Phys.*, vol. 10, pp. 201-204; May, 1958.) The distribution of Sb in alloys prepared for doping Ge single crystals is investigated using a radioactive isotope. A considerable degree of inhomogeneity is observed in spite of rapid quenching. This difficulty can be overcome by zone melting.

537.311.33:546.289:535.215 3027

The Photoconduction of Germanium after Bombardment with Fast Electrons—F. Stöckmann, E. E. Klontz, J. McKay, H. Y. Fan and K. Lark-Horovitz. (*Z. Phys.*, vol. 153, pp. 331-337; December 5, 1958.) The spectral distribution of photoconduction was measured on differently doped specimens of single-crystal Ge after bombardment with 4.5-mev electrons.

537.311.33:546.289:564.4 3028

The Generation of Dislocations by Thermal Stresses—P. Penning. (*Philips Tech. Rev.*, vol. 19, pp. 357-364; August 22, 1958.) A study is made of etch-pit distribution over the cross section of a Ge rod to assess the influence of the cooling rate on its internal perfection. The theoretical dislocation distribution is calculated assuming that stresses are only partially relieved by plastic flow. Results are in good agreement with observations. See also 2459 of 1958.

537.311.33:546.289:548.5 3029

The Pulling of Germanium Single Crystals from "Floating Crucibles"—J. Goorissen and F. Karstensen. (*Z. Metallkde.*, vol. 50, pp. 46-50; January, 1959.) The floating-crucible technique is described and its theoretical yield is compared with that of the Czochralski and zone-refining methods.

537.311.33:546.623.86 3030

The Formation of Barrier Layers in Aluminium Antimonide by the Alloying Method—H. J. Henkel. (*Z. Metallkde.*, vol. 50, pp. 51-53; January, 1959.) A p - n function is produced by alloying n -type AlSb with Zn-doped aluminium foil.

537.311.33:546.681.241 3031

The Change in the Crystal Structure of Gallium Telluride (Ga_2Te_3) Doped with Copper—G. Harbecke and G. Lantz. (*Naturwiss.*, vol. 45, pp. 283-284; June, 1958.)

537.311.33:546.682.19 3032

Effect of Heat Treatment upon the Electric

Properties of Indium Arsenide—J. R. Dixon and D. P. Enright. (*J. Appl. Phys.*, vol. 30, pp. 753-759; May, 1959.) Large reversible variations in carrier concentration, Hall mobility, and carrier lifetime have been produced in InAs by heat treatment. The observed phenomena are consistent with a model involving the segregation and dispersion of donor impurities to and from dislocations.

537.311.33:546.682.86 3033

Properties of the Semiconductor InSb—M. Rodot. (*J. Phys. Radium*, vol. 19, pp. 140-150; February, 1958.) Properties are reviewed with special reference to the value of the effective mass of the electrons and the scattering mechanism. The theory of thermoelectric and thermomagnetic effects is given and experimental results are presented. See 2469 of 1958.

537.311.33:546.824-31 3034

Infrared Absorption of Reduced Rutile TiO_2 Single Crystals—D. C. Cronmeyer. (*Phys. Rev.*, vol. 113, pp. 1222-1226; March 1, 1959.)

538:061.3 3035

Transactions of the 3rd Conference on the Physics of Magnetic Phenomena—(*Izv. Ak. Nauk SSSR*, vol. 61, pp. 787-904, 1038-1212 and 1215-1336; June, August, and September, 1957.) The text is given of 74 papers presented at the conference held in Moscow, May 23-31, 1956. For a list of titles in English, see *Translated Contents Lists of Russian Periodicals*, nos. 110 and 111, pp. 50-51 and 32-34; May and June, 1958.

538.22:538.569.4 3036

Indirect Coupling of Nuclear Spins in Antiferromagnet with Particular Reference to MnF_2 at Very Low Temperatures—T. Nakamura. (*Prog. theoret. Phys., Japan*, vol. 20, pp. 542-552; October, 1958.) The line width (~ 14 oersteds) of the F^{19} nuclear magnetic resonance in MnF_2 at $1.4^\circ K$ observed by Jaccarino and Shulman (527 of 1958) is shown to come mainly from indirect coupling of nuclear spins through hyperfine interaction with spin waves. The line width of the MnS resonance is about 600 oersteds.

538.22:538.569.4:621.375.9 3037

Two-Level Maser Materials—R. H. Hoskins. (*J. Appl. Phys.*, vol. 30, p. 797; May, 1959.) Comment on some advantages of paramagnetic ions in ionic crystals as materials for two-level solid-state masers.

538.221 3038

Distribution of Magnetic Domains between the Two Phases in a Single-Crystal Flat Disk of Iron—K. F. Niessen. (*Philips Res. Rep.*, vol. 14, pp. 101-110; April, 1959.)

538.221:539.23 3039

Magnetic Properties of Very Thin Films of Nickel—G. Goureaux and A. Colombani. (*Compt. Rend. Acad. Sci., Paris*, vol. 248, pp. 543-546; January 26, 1959.)

538.221:539.234:538.63 3040

Determination of the Distribution of Orientation of the Magnetization Vectors in Nickel and Iron Vapour-Deposited Films using the Magnetoresistance Effect—W. Hellenthal. (*Z. Phys.*, vol. 153, pp. 359-371; December 5, 1958.)

538.221:621.134 3041

Temperature Dependence of the Paramagnetic Susceptibility of Nickel-Zinc Ferrites—V. I. Chechernikov and Yu. D. Volkov. (*Zh. eksp. teor. Fiz.*, vol. 35, pp. 875-879; October, 1958.) The reciprocal of molar susceptibility for a range of Ni-Zn ferrites is plotted as a function of temperature in the range 300° - $1500^\circ K$. Near the ferromagnetic Curie point the de-

pendence of specific magnetization σ on magnetic field strength H is expressed in the form $H = a\sigma + b\sigma^3$, where the coefficients a and b depend on temperature and pressure.

538.221:621.318.134:538.569.4 3042

Magnetic Resonance Studies in the Reaction of Nickel Cobalt Ferrite—S. L. Blum and M. H. Sirvetz. (*J. Appl. Phys.*, vol. 30, p. 795; May, 1959.) Use is made of the analysis of ferromagnetic-resonance line shapes to obtain indications of the course of the reaction as a function of the reaction conditions.

538.221:621.318.134:538.569.4:029.64 3043

Microwave Resonance in Gadolinium-Iron Garnet Crystals—W. V. Smith, J. Overmyer and B. A. Calhoun. (*IBM J. Res. & Dev.*, vol. 3, pp. 153-162; April, 1959.) Ferrimagnetic resonance at 9497 and 23725 mc is described in terms of a two-sublattice model.

538.221:621.318.134:621.318.57 3044

Reciprocity Relationships for Gyrotropic Media—R. F. Harrington and A. T. Villeneuve. (*IRE TRANS. ON MICROWAVE THEORY AND TECHNIQUES*, vol. MTT-6, pp. 308-310; July, 1958. Abstract, *PROC. IRE*, vol. 46, p. 1777; October, 1958.)

538.221:621.318.134:621.375.9 3045

Power-Flow Relations in Lossless Non-linear Media—H. A. Haus. (*IRE TRANS. ON MICROWAVE THEORY AND TECHNIQUES*, vol. MTT-6, pp. 317-324; July, 1958. Abstract, *PROC. IRE*, vol. 46, p. 1777; October, 1958.)

621.315.3(083.7) 3046

Wire in the Electronic Industry—(*Electronic Ind.*, vol. 17, pp. 89, 97; December, 1958.) U. S. specifications, wire codes and general information are tabulated.

621.793:621.3.049.75 3047

Electroless Copper Plating in Printed Circuitry—E. B. Saubestre. (*Sylvania Technologist*, vol. 12, pp. 6-11; January, 1959.) The deposition of copper films on plastic printed-circuit boards by chemical reduction is discussed, and a procedure for producing "plated-through" holes is described. An extension of the plating process for unclad laminates is noted.

MATHEMATICS

512:621.318.57:681.142 3048

Classification and Minimization of Switching Functions: Part 1—N. C. de Troye. (*Philips Res. Rep.*, vol. 14, pp. 151-193; April, 1959.) An attempt to find either the minimal sum of products or the minimal product of sums from a given Boolean function.

516.7:621.3 3049

Geometric-Analytic Theory of Transition in Electrical Engineering—E. F. Bolinder. (*PROC. IRE*, vol. 47, pp. 1124-1129; June, 1959.)

517.942.9:517.949.8 3050

Numerical Solution of Laplace's Equation, given Cauchy Conditions—I. Sugai. (*IBM J. Res. & Dev.*, vol. 3, pp. 187-188; April, 1959.) An expression giving the order of magnitude of the propagated errors is obtained for numerical analysis by methods of finite differences. For the practical aspect in the design of electron guns with curved electron trajectories see *PROC. IRE*, vol. 47, pp. 87-88; January, 1959.

MEASUREMENTS AND TEST GEAR

621.3.011.4(083.74) 3051

The Cylindrical Cross-Capacitor as a Calculable Standard—A. M. Thompson. (*Proc. IEE*, Part B, vol. 106, pp. 307-310; May, 1959.) The capacitor consists of a hollow conducting cylin-

der divided into four insulated sections by gaps parallel to the axis. A practical form described consists of four parallel bars of circular cross section. The capacitance can be computed with precision.

621.3.018.41(083.74) 3052

A Portable Frequency Standard—L. F. Koerner. (*Bell Lab. Rec.*, vol. 37, pp. 173-176; May, 1959.) Description of a unit, the size of a miniature camera, which operates at about 15 mc with an accuracy within 1 part in 10^6 .

621.3.018.41(083.74) 3053

Construction of a Mobile Caesium Frequency Standard—A. H. W. Beck and J. Lytollis. (*Proc. IEE*, Part B, vol. 105, supplement no. 11, pp. 712-715; 1958. Discussion.) Practical details of the construction of a sealed-off version are given.

621.3.018.41(083.74):538.569.4 3054

Construction and Application of a Frequency Standard for Microwave Spectrometers—H. G. Fitzky. (*Z. angew. Phys.*, vol. 10, pp. 297-303; July, 1958.) A 10-mc crystal oscillator and frequency multiplication to 1080 mc are used in the equipment described for measurements of frequency up to 25 kmc with an accuracy of better than 1 in 10^7 .

621.317.3:621.396.822 3055

Measurement of Equivalent Noise Resistance of a Noise-Thermometer Amplifier—H. Pursey and E. C. Pyatt. (*J. Sci. Instr.*, vol. 36, pp. 260-264; June, 1959.) Amplifier noise is compared with that of a wire-wound resistance at a standard temperature, using a vibrating switch to connect the sources alternately to a single channel. An accuracy within 1 per cent is obtained.

621.317.4:538.569.4 3056

Measurement of Magnetic Flux Density by Paramagnetic Resonance—C. P. Allen and M. Sherry. (*J. Electronics Control*, vol. 6, pp. 264-270; March, 1959.) The method is based on measurement of the frequency of paramagnetic resonance in an organic compound. It uses a simple coaxial-line probe unit and enables flux densities in the range of a few hundreds up to some thousands of gauss to be measured to an absolute accuracy of ± 0.06 per cent.

621.317.4:621.3.042.1:621.397.62 3057

Magnetic Measurements on Ferrite U-Cores for Horizontal-Deflection Output Transformers—R. Fäilker and E. E. Hücking. (*Elektron. Rundschau*, vol. 12, pp. 270-274; August, 1958.) Methods of measurement are reviewed and a specially designed core tester is described.

621.317.42:550.385 3058

The Influence of the Self-Inductance of Magnetic-Core Windings used for the Recording of Rapid Variations of the Earth's Magnetic Field—G. Grenet. (*Ann. Géophys.*, vol. 13, pp. 249-251; July/September, 1957.)

621.317.61:621.385.1 3059

A Method for the Accurate Measurement of Mutual Conductance of Thermionic Valves—M. R. Child and D. J. Sargent. (*Proc. IEE*, Part B, vol. 106, pp. 311-314; May, 1959.) Absolute errors are estimated to be less than 0.25 per cent, and comparative error less than 0.1 per cent. Adaptations for measurement of anode conductance and screen-grid amplification factor are described.

621.317.7:621.314.7 3060

A Transistor Characteristic Curve Tracer—J. F. Young. (*Electronic Engrg.*, vol. 31, pp. 330-336; June, 1959.) "A Dekatron is used to develop a stepped voltage controlling the base current of the transistor under test. At each

step a half sinusoidal voltage is applied to the transistor and the resulting collector current is plotted against voltage on an external oscilloscope. A series resistor provides the current signal and limits the transistor dissipation. The unit can also be used to plot the characteristics of normal or of Zener diodes."

621.317.733:621.375.2.024 3061

Use of a Direct-Current Amplifier and Recorder to Balance a Mueller Resistance Bridge—G. T. Armstrong, P. K. Wong and L. A. Krieger. (*Rev. Sci. Instr.*, vol. 30, pp. 339-343; May, 1959.) Methods of reducing system noise to give improved sensitivity.

621.317.733.011.4:621.372.54 3062

The Balanced Unsymmetrical Parallel-T Network as a Three-Terminal Frequency-Dependent Bridge for the Measurement of Capacitance and Dissipation Factor—K. Posel. (*Trans. S. Afr. Inst. Elec. Eng.*, vol. 49, Part 8, pp. 287-298; August, 1958.) The theory of operation of the bridge and its design are detailed. See also 2656 of 1958.

621.317.733.029.62 3063

Coaxial Displacement Dielectric Cell for Liquids Usable to 350 Mc/s—S. E. Lovell and R. H. Cole. (*Rev. Sci. Instr.*, vol. 30, pp. 361-362; May, 1959.) Construction details of a bridge element useful in the determination of capacitance, dielectric loss, or conductivity.

621.317.74:534.2-8:621.373.52 3064

Zero-Crossing Technique syncs Wave-Train Outputs—J. A. Wreb, Jr. (*Electronics*, vol. 32, pp. 64-65; May 8, 1959.) A technique for producing a sinusoidal wave-train starting from the zero-crossing point of another sine wave. The generator is used in testing ultrasonic equipment.

621.317.75.087.6 3065

Homodyne Detector for Reproduction of Periodic Waveforms—C. Lagercrantz. (*J. Sci. Instr.*, vol. 36, pp. 257-259; June, 1959.) An AF signal is scanned using 20- μ gating impulses whose phase is shifted slowly and linearly. The gated output is recorded on a pen recorder. The circuit and performance tests are described.

621.317.763.029.64:621.372.413 3066

The Design of Broad-Band Circular Wave-meters—P. Andrews. (*Brit. Commun. Electronics*, vol. 6, pp. 354-357; May, 1959.) The design is considered mainly with cylindrical cavities in the TE₁₁ mode. Mode suppression and the temperature coefficient of wavemeters are treated.

OTHER APPLICATIONS OF RADIO AND ELECTRONICS

531.721:621.397.9 3067

The Video Differential Planimeter—M. Tobin. (*Rev. Sci. Instr.*, vol. 30, pp. 323-327; May, 1959.) Description of an instrument for measuring variations in the projected area of a remote object by means of a television camera system or flying-spot scanner.

538.566.029.6:541.126 3068

Observations of Detonation in Solid Explosives by Microwave Interferometry—G. F. Cawsey, J. L. Farrands and S. Thomas. (*Proc. Roy. Soc. A.*, vol. 248, pp. 499-521; December 9, 1958.) Confined detonation processes have been studied by a method noted earlier [1833 of 1956 (Farrands & Cawsey)], using apparatus developed from that described by Froome (3532 of 1952).

550.340:621.3.087.6 3069

An Electronic Seismic Transducer for Visual Recording—P. Gouin. (*Ann. Geophys.*,

vol. 13, pp. 234-241; July/September, 1957. In English.) A detailed description of the capacitance-type transducer, amplifier and recorder.

551.508.71:621.372.413 3070

Recording Microwave Hygrometer—J. Sargent. (*Rev. Sci. Instr.*, vol. 30, pp. 348-355; May, 1959.) A description is given of a microwave refractometer designed at the National Bureau of Standards for measurement of low water-vapor pressures in a moving air stream.

621.384.6:621.319.3 3071

Electrostatic - Transformer - Type Particle Accelerator using Ceramic BaTiO₃-Ferrostac—T. Shibata, A. Toi and T. Suita. (*J. Phys. Soc. Japan*, vol. 14, p. 227; February, 1959.) A note on the construction of a 150-kv accelerator in which the hv generator has rotating ferroelectric disks which carry electric charges.

621.384.8:621.318.381:621.316.7.078.3 3072

Current and Field Stabilization of the 9-kW Electromagnet of the A.E.I. Magnetic Spectrograph—R. Bailey and E. C. Fellows. (*J. Brit. IRE*, vol. 19, pp. 309-321; May, 1959.) Signals obtained from nuclear resonance are used to control the strength of a magnetic field ± 0.01 per cent.

621.385.833 3073

Numerical Computation of Electrostatic Immersion Objectives—E. Hahn. (*Optik*, vol. 15, pp. 500-515; August, 1958.)

621.385.833 3074

Space-Charge Aberration and Resolving Power in Electron Microscopes—W. E. Meyer. (*Optik*, vol. 15, pp. 398-406; July, 1958.) Space-charge effects may limit the resolving power more than spherical aberration. Methods of reducing the influence of space charge are indicated.

621.385.833 3075

Stigmatic Image in Rotationally Asymmetric Electron Lenses—F. Lenz. (*Optik*, vol. 15, pp. 393-397; July, 1958.)

621.385.833:535.317.3 3076

Compensation of the Chromatic Dependence of Magnification in the Electrostatic Electron Microscope—W. Weitsch. (*Optik*, vol. 15, pp. 492-499; August, 1958.)

621.385.833:621.3.032.21 3077

Some Electron-Optical Properties of Point Cathodes—S. Maruse and Y. Sakaki. (*Optik*, vol. 15, pp. 485-491; August, 1958.) Experimental results show that electron emission of the point cathode is mainly determined by the Schottky effect. The use of the point cathode as a cold cathode in electron microscopes is discussed. See also 245 of 1957 (Sakaki and Möllenstedt).

621.385.833:621.3.032.213.6 3078

Oxide-Cored Cathode—K. Ando, O. Kami-gaito, Y. Kamiya, S. Takahashi and R. Uyeda. (*J. Phys. Soc. Japan*, vol. 14, pp. 180-185; February, 1959.) Description of a cathode for electron microscopy consisting of a drawn platinum wire filled with oxide powder. The method of preparation and performance tests are described.

621.387.424 3079

Improved Design for Halogen-Quenched End-Window Geiger Counters—K. van Duren and J. Hermesen. (*Rev. Sci. Instr.*, vol. 30, pp. 367-368; May, 1959.)

621.387.464 3080

Modern Development of Scintillation Counters—W. Hanle and H. Schneider. (*Z.*

angew. Phys., vol. 10, pp. 228-248; May, 1958.) Detailed review of design, construction and applications. 242 references.

621.387.464:621.383.27 3081
The Resolving Power of Scintillation Multipliers and the Influence on it of Various Parameters—P. Görlich, A. Krohs, H. J. Pohl, R. Reichel and L. Schmidt. (*Z. angew. Phys.*, vol. 10, pp. 303-309; July, 1958.) Results of measurements on a photomultiplier for scintillation counting are discussed.

621.397.9:522.2 3082
Using TV Techniques in Astronomy—J. Borgman. (*Electronics*, vol. 32, pp. 66-68; May 8, 1959.) A variable star is detected by a differential photographic method which eliminates constant features. Television techniques are used to display the difference signals.

621.397.9:522.2 3083
Television Techniques in Astronomy—N. F. Kuprevich. (*Priroda*, pp. 50-54; March, 1958.) Two systems are described based on: 1) a two-stage electron-optical converter consisting of a photocathode emitting electrons which form an image on a 35-mm luminous screen with a possible increase of brightness up to 100-130 times; 2) the use of an orthicon-type 625-line television screen on which an image is obtained with magnification up to 6.5 times.

621.398 3084
Radio Telemetry: Part 1—Systems—A. J. Shimmins. (*Proc. IRE, Aust.*, vol. 19, pp. 775-787; December, 1958.) Factors which determine system performance are analyzed, taking as an example the R.A.E. subminiature FM/AM system.

621.398:616.831-073.97 3085
A Miniature Electroencephalograph Telemeter System—D. C. Gold and W. J. Perkins. (*Electronic Engrg.*, vol. 31, pp. 337-339; June, 1959.) Transmits the electrical activity of the brain of an unrestrained cat on a 6.8-mc AM carrier.

681.61:621.319 3086
High-Speed Read-Out for Data Processing—R. E. West. (*Electronics*, vol. 32, pp. 83-85; May 29, 1959.) Description of an electrostatic teletypewriter which can print more than 3000 words/min. Input pulses to the print heads charge the surface of paper to which powdered ink adheres.

PROPAGATION OF WAVES

621.396.11:550.389.2:629.19 3087
Radio Reflections from Satellite-Produced Ionization—Roberts, Kirchner and Bray. (See 2963.)

621.396.11:551.510.52 3088
The Role of Turbulent Mixing in Scatter Propagation—R. Belgiano, Jr. (*IRE TRANS. ON ANTENNAS AND PROPAGATION*, vol. AP-6, pp. 161-168; April, 1958. Abstract, *PROC. IRE*, vol. 46, p. 1438; July, 1958.)

621.396.11:551.510.52 3089
The Influence of Moisture in the Ground, Temperature and Terrain on Ground Wave Propagation in the V.H.F. Band—B. Josephson and A. Blomquist. (*IRE TRANS. ON ANTENNAS AND PROPAGATION*, vol. AP-6, pp. 169-172; April, 1958. Abstract, *PROC. IRE*, vol. 46, p. 1439; July, 1958.)

621.396.11:551.510.52 3090
Distance Dependence, Fading Characteristics and Pulse Distortion of 3000-Mc/s Transhorizon Signals—B. Josephson and G. Carlson. (*IRE TRANS. ON ANTENNAS AND*

PROPAGATION, vol. AP-6, pp. 173-175; April, 1958. Abstract, *PROC. IRE*, vol. 46, p. 1439; July, 1958.)

621.396.11:551.510.52 3091
Some Microwave Propagation Experiences from a "Just-Below-Horizon" Path—B. Josephson and F. Eklund. (*IRE TRANS. ON ANTENNAS AND PROPAGATION*, vol. AP-6, pp. 176-178; April, 1958. Abstract, *PROC. IRE*, vol. 46, p. 1439; July, 1958.)

621.396.11:551.510.52 3092
The Diffraction of Electromagnetic Waves by the Earth's Curvature—a Theory of Tropospheric Propagation Near and Beyond the Radio Horizon—O. Tukizi. (*Rep. elect. Commun. Lab., Japan*, vol. 11, pp. 421-425; November, 1958.) Classical diffraction theory is modified to account for the slow rate of decrease of field-strength well beyond the horizon. A saddle-point method is used to take into account the contribution of all the terms of the residue series.

621.396.11:551.510.535:523.164 3093
Refraction of Extraterrestrial Radio Waves in the Ionosphere—Komesaroff and Shain. (See 2973.)

621.396.11.029.45/.51:551.510.535:551.594.6 3094
An Experimental Proof of the Mode Theory of V.L.F. Ionospheric Propagation—T. Obayashi, S. Fujii and T. Kidokoro. (*J. Geomag. Geoelect.*, vol. 10, no. 2, pp. 47-55; 1959.) VLF atmospherics are received on a receiver which continuously sweeps over the frequency band 5-70 kc. The output is displayed on an intensity-modulated cathode-ray tube which is photographed on continuously moving film. There is an intensity maximum near 10 kc and selective absorption bands which vary with time of day and may be associated with the cutoff frequencies of the earth-ionosphere waveguide. The effects of solar flares are also discussed.

621.396.11.029.63 3095
A Contribution to the Knowledge of Propagation Conditions at 1.3 Gc/s based on Measurements over a Transmission Path within Optical Range—U. Kühn. (*Tech. Mitt. BRP, Berlin*, vol. 1, pp. 4-10; October, 1957.) Statistical analysis of field-strength recordings taken in one year over an 82-km path, and comparison with meteorological data for the same period.

621.396.11.029.63 3096
Measurements of 1250-Mc/s Scatter Propagation as Function of Meteorology—D. L. Ringwalt, W. S. Ament and F. C. MacDonald. (*IRE TRANS. ON ANTENNAS AND PROPAGATION*, vol. AP-6, pp. 208-209; April, 1958.) Short detailed report and discussion of the results of measurements made over a 262-mile over-water path between Florida and the Bahamas in December 1956. Ground and airborne field-strength measurements, refractometer soundings, radiosonde data and visual observations were recorded.

621.396.11.029.63 3097
Apparent Correlation between Tropopause Height and Long-Distance Transmission Loss at 490 Mc/s—D. R. Hay. (*PROC. IRE*, vol. 47, pp. 1144-1145; June, 1959.) For a 640-mile path in June-July, 1957, signals were low and steady when the tropopause was low, but were higher and fluctuated more when it was high.

621.396.812 3098
Prolonged Signal Fade-Out on a Short Microwave Path—D. R. Hay and G. E. Poaps. (*Can. J. Phys.*, vol. 37, pp. 313-321; March, 1959.) During a period of one year, the incidence of signal fade-out has been observed in

2-kmc transmissions over a 21-mile path near Ottawa. Fade-out durations varied from a few minutes to several hours, with the most frequent occurrence in the summer and during the night. An analysis of the refractivity of the air at the middle of the radio path indicates that fade-out is associated with a shallow horizontal transition zone in vapor pressure at a level near the antenna heights.

RECEPTION

621.376 3099
Correction Devices Detect Weak Signals—H. R. Raemer and A. B. Reich. (*Electronics*, vol. 32, pp. 58-60; May 22, 1959.) Operating principles of autocorrelators, cross-correlators, and radiometers are described.

621.396.621:621.314.7 3100
How to Design Reflexed Transistor Receivers—J. Waring. (*Electronics*, vol. 32, pp. 70-72; May 8, 1959.) Methods for obtaining IF and AF gain in the same stage without motorboating.

621.396.66:621.396.828 3101
Negative-Supply Outboard Codan—R. L. Ives. (*Audio*, vol. 43, pp. 22-23, 73; May, 1959.) Details are given of a circuit which silences the AF stages of a receiver when the carrier amplitude falls below a predetermined level. The circuit does not alter the characteristics of the receiver to which it is connected.

621.396.812.3:621.396.666 3102
Linear Diversity Combining Techniques—D. G. Brennan. (*PROC. IRE*, vol. 47, pp. 1075-1102; June, 1959.) An analysis and results of measurements of the relative performance are given for three types of diversity combining techniques: 1) selection diversity, 2) maximal-ratio diversity, and 3) equal-gain diversity systems. The effects of various departures from the ideal conditions are considered and the relative merits of predetection and postdetection combining and of long-term distributions are discussed.

STATIONS AND COMMUNICATION SYSTEMS

621.391 3103
On Asymmetric Information Channels—R. B. Banerji. (*J. Brit. IRE*, vol. 19, pp. 305-308; May, 1959.) A study of channel capacity in terms of the probability of possible errors, and application to PCM with amplitude keying.

621.396.3:621.391 3104
Some Operational Considerations Affecting the Use of Automatic Error Correcting Equipment on H. F. Telegraph Networks—E. G. Copper. (*Point to Point Telecommun.*, vol. 3, pp. 21-34; February, 1959.) A discussion of some of the problems associated with the radio error-correcting multiplex (REM) system.

621.396.5:534.76 3105
Compatible Stereo Radio using A.M./F.M. Multiplex—H. E. Sweeney. (*Electronics*, vol. 32, pp. 56-58; May 8, 1959.) Transmission of two channels by amplitude and frequency modulation of the same carrier. A circuit is given for the addition of a FM channel to an AM receiver.

621.396.65 3106
The TJ Radio System—S. D. Hathaway and H. H. Haas. (*Bell Lab. Rec.*, vol. 37, pp. 129-133; April, 1959.) Description of a 6-channel 11-kmc relay system using dual frequency-diversity transmission, giving details of arrangement of subcarriers in the spectrum and examples of use for telephony, television and data transmission.

621.396.65:621.396.41 3107
F.M. Multiplexing for Studio-Transmitter Links—D. Harkins. (*Electronics*, vol. 32, pp. 44-45; May 22, 1959.) Three program signals modulate subcarriers at 26, 65 and 175 kc, which are combined to modulate a 946-mc carrier for transmission to the transmitter site 16 miles away.

SUBSIDIARY APPARATUS

621.3.087.45:621.395.625.3 3108
A Multiple-Channel D.C. Recording System—H. D. Scott. (*Electronic Engrg.*, vol. 31, pp. 340-344; June, 1959.) Describes an AM system with tape-noise cancellation enabling up to twelve 0-10-cps channels to be recorded on a conventional single-track recorder together with speech and timing signals.

621.314.63:546.289 3109
The Thermal Behaviour of Semiconductor Rectifiers—O. Jakits. (*Brown Boveri Rev.*, vol. 45, pp. 540-644; November/December, 1958.) Measurements are described which were made on heavy-current Ge diodes to determine the thermal inertia. The effect of cooling on the overload characteristic is discussed.

621.314.63:621.396.96 3110
Using Silicon Diodes in Radar Modulators—M. G. Gray. (*Electronics*, vol. 32, pp. 70-72; June 12, 1959.) A peak power of 250 kw is developed using Si diodes for charging the artificial line and for clipping reverse voltage swings. The diodes dissipate instantaneous powers up to 300 kw.

621.314.634 3111
Selenium Rectifiers with Artificial Layers of Selenides of Cadmium, Tin, Bismuth and Lead—Y. Moriguchi. (*J. Phys. Soc. Japan*, vol. 14, pp. 152-167; February, 1959.) The action of various selenides as barrier layers has been investigated by measurement of the rectifier dc and ac characteristics. CdSe and SnSe layers play an important role in rectification but the selenides of Bi and Pb seem to be unsuitable. In general, the layer material should have a resistivity $< 10^4 \Omega \text{ cm}$.

621.314.64 3112
Current/Time Relationship in the Forward Direction of Electrolytic Rectifiers—W. C. van Geel and C. A. Pistorius. (*Phillips Res. Rep.*, vol. 14, pp. 123-131; April, 1959.) Qualitative explanation of the effects observed on applying alternating rectangular and sinusoidal voltages.

621.316.721.078:621.375.2.024 3113
Use of Operational Amplifiers in Precision Current Regulators—K. Eklynd. (*Rev. Sci. Instr.*, vol. 30, pp. 328-331; May, 1959.) Low-drift high-gain dc amplifiers in a control loop can reduce steady-state error.

TELEVISION AND PHOTOTELEGRAPHY

621.397.24 3114
Carrier Transmission for Closed-Circuit Television—L. G. Schimpf. (*Electronics*, vol. 32, pp. 66-68; June 12, 1959.) A simple and inexpensive coaxial-cable transmission system, using transistors in the terminal and repeater circuits, is described. Dc supplies to the repeaters are applied via the signal cable.

621.397.611.2 3115
Measurement of the Transmission Characteristics of Television-Camera Preamplifiers—W. Eckardt. (*Tech. Mitt. BRF, Berlin*, vol. 1, pp. 27-32; December, 1957.)

621.397.62 3116
Two Realizations of the New Synchrophase—L. Chrétien and R. Aschen. (*TSF et TV*, vol. 33, pp. 71-76, 152-157, 167-168;

March/May, 1957.) A rejector circuit and a variable video-frequency gain control compensate for phase distortion by altering the shape of the video-frequency response curve. Detailed descriptions are given of a medium-range and a long-range television receiver, with a note on the adjustment of the phase-correction circuit.

621.397.62 3117
Television I.F. Amplifiers with Linear Phase Response—A. N. Thiele. (*Proc. IRE Aust.*, vol. 19, pp. 652-668; November, 1958.) This type of response is discussed in relation to ease of tuning and alignment and to phase equalization at the transmitter.

621.397.62:535.623 3118
Automatic Controls for Colour Television—Z. Wiencek. (*Electronics*, vol. 32, pp. 58-59; May 15, 1959.) A method of control of the phase (hue) and amplitude (chroma) of the color signal using a low-frequency diode gate.

621.397.62:535.623:535.88 3119
The Projection of Colour-Television Pictures—T. Poorter and F. W. de Vrijer. (*Phillips Tech. Rev.*, vol. 19, pp. 338-355; August 22, 1958.) Three projection-type cathode-ray tubes are used respectively with red, green and blue fluorescing phosphors. Each is mounted in a Schmidt optical system; the superposition of the three images is effected either by dichroic mirrors [1701 of May (van Alphen)] or by mounting the three tubes side by side. Projectors using these systems are described.

621.397.621.2 3120
Noise-Immune Synchronizing Circuits for Television Timebase Circuits—D. J. Howlett and L. Buduls. (*Proc. IRE, Aust.*, vol. 19, pp. 680-689; November, 1958.) Noise limiting and AGC circuits are discussed and details are given of an improved form of the heptode sync separator described by Marks (252 of 1953).

621.397.621.2 3121
Some Aspects of Synchronization in Television Receivers—J. van der Goot. (*Proc. IRE, Aust.*, vol. 19, pp. 690-706; November, 1958.) A discussion of scanning oscillators and AFC systems.

621.397.621.2 3122
The Synchronization Separator—An Unexpected Observation—J. Goldthorp. (*Proc. IRE, Aust.*, vol. 19, pp. 706-707; November, 1958.) A note describing the improved performance obtained using a remote-cutoff pentode as composite sync separator in place of a valve with sharp cutoff.

621.397.621.2 3123
Improvements in Television Receivers: Part 5—Stabilization of Line and Frame Output Circuits—B. G. Dammers, A. G. W. Uijtens, A. Boekhorst and H. Heyligers. (*Electronic Applic.*, vol. 18, pp. 129-142; November, 1958.) Detailed descriptions are given of circuits suitable for a 110° cathode-ray tube. Line output stages with flyback ratios of 16, 18 or 21 per cent have been stabilized by voltage-dependent resistors (see Part 4: 989 of March). The frame output stage derives its charging voltage from the stabilized boost voltage. A protective circuit to limit beam current is described.

621.397.621.2 3124
Improvements in Television Receivers: Part 6—Design Considerations for Stabilized Line Output Circuits—B. G. Dammers, A. Boekhorst and D. Hoogmoed. (*Electronic Applic.*, vol. 18, pp. 143-157; November, 1958.) Essential formulas and graphs are given for a quantitative investigation of circuits in which

the line output valve operates above the knee of the I_a/Y_a characteristic. For practical circuits see 3123 above.

621.397.621.2:535.623:621.385.832 3125
Errors of Magnetic Deflection: Part 2—J. Haantjes and G. J. Lubben. (*Phillips Res. Rep.*, vol. 14, pp. 65-97; February, 1959.) Approximate formulas for the design of deflection coils have been developed from a theoretical study [Part 1: 2990 of 1957]. Convergence errors in the shadow-mask tube and in an experimental tube with three guns vertically in line are discussed. For the latter tube a deflection coil can be designed which makes dynamic convergence unnecessary.

621.397.621.2:621.373.444.1:621.314.7 3126
Transistor Line Deflection Circuits for Television—P. B. Helsdon. (*Marconi Rev.*, vol. 22, pp. 38-70; 1st Quarter, 1959.) The shunt diode circuit and the retrace-driven circuit due to Guggi (2382 of 1957) are analyzed and their limitations discussed. A flyback-driven circuit is described with automatic phase control, and reverse base current drive to the shunt diode circuit. The output is sufficient for scanning a 70° picture tube.

621.397.621.2:621.385.832 3127
A New Approach to Short Picture-Tube Design—G. A. Burdick. (*Sylvania Technologist*, vol. 12, pp. 2-5; January, 1959.) A brief description of the construction and principle of operation of the tripotential focus (TPF) gun which can be focused by varying the potential to any one of the three elements.

621.397.621.2:621.385.832.032.269.1 3128
A New Electron Gun for Picture Display with Low Drive Signals—K. Schlesinger. (*J. Telev. Soc.*, vol. 9, pp. 15-25; January-March, 1959.) High control sensitivity required for transistor drive is achieved by a new electron-optical approach. Beam focusing and modulation are effected in a cylindrical cavity by two separate electrostatic fields: one of circular symmetry for focusing, and one of transverse-plane geometry for modulation.

621.397.7 3129
ABN Television Transmitter—F. M. Shepherd. (*Proc. IRE, Aust.*, vol. 19, pp. 609-614; November, 1958.) A brief description of main and standby equipment at Gore Hill.

621.397.7 3130
The ATN Television Centre—M. H. Stevenson. (*Proc. IRE, Aust.*, vol. 19, pp. 614-621; November, 1958.) A general description of the center which is near Sidney. Factors which influenced its design and the provisions made for expansion are discussed.

621.397.7:535.623 3131
Holding Video Level while Switching Studios—J. O. Schroeder. (*Electronics*, vol. 32, pp. 96-98; May 29, 1959.) An automatic circuit designed to compensate for wide variations in color or monochrome input signal levels and to maintain a constant output level.

621.397.7:621.396.65 3132
Equalization of Aural and Visual Delay—I. Kerney and W. D. Mischler. (*Bell Lab. Rec.*, vol. 37, pp. 182-186; May, 1959.) The delay of audio signals relayed by coaxial cable relative to video signals relayed by microwave link is reduced by bypassing demodulating equipment at coaxial relay points.

621.397.7:621.396.677.81 3133
The Passive TV Relay and its Practical Possibilities—Aschen. (See 2851.)

- 621.397.8 3134
Echo Phenomena in Television Images—J. Polonsky, L. Amster and G. Melchior. (*J. Telev. Soc.*, vol. 9, pp. 2-14; January/March, 1959.) English version of 283 of 1957.
- 621.397.8 3135
Results of Investigations on the Recognizability of Small Details on a Television Screen—F. Below, W. Kroebel and H. Springer. (*Z. angew. Phys.*, vol. 10, pp. 277-285; June, 1958.) An objective method of measuring detail recognition is described based on the use of Landolt-ring test pictures (see 3321 of 1957). The effects of bandwidth limitation and contrast are investigated.
- 621.397.8 3136
The Perceptibility of Image Details in Television Images—W. Kroebel, F. Arp and H. Baurmeister. (*Z. angew. Phys.*, vol. 10, pp. 320-327; July, 1958.) The test described in 3138 below is applied to television images. Results are closely related to those obtained with optically projected images.
- 621.397.8 3137
Phase Shift Considerations in Television Broadcasting and Reception—M. W. Davies. (*Proc. IRE, Austral.*, vol. 19, pp. 642-651; November, 1958.) A general description of phase distortion and of the effects this distortion can have on the received signal of a vestigial-sideband system. Methods available for compensation are discussed; see, e.g., 3117 above.
- 621.397.8:535.7 3138
The Visual Properties of the Human Eye as a Contribution to the Problem of Assessing the Quality of Projection and Television Images—W. Kroebel, F. Arp and H. Baurmeister. (*Z. angew. Phys.*, vol. 10, pp. 309-317; July, 1958.) A test is described for the quantitative assessment of the perception of small objects by the eye and a mathematical expression is derived relating perception to contrast and object size. For the underlying statistical considerations see *ibid.*, pp. 317-320 (Arp).
- 621.397.811:621.396.822 3139
Effects of Noise in Television Transmission—T. Kilvington. (*J. Telev. Soc.*, vol. 9, pp. 26-31; January-March, 1959.) The nature of random noise and its effect on sound and vision reception are reviewed. The subjective effects on the picture of both random and periodic noise are described and methods of minimizing them are considered.
- 621.397.8:621.396.822 3140
Theoretical and Experimental Characteristics of Random Noise in Television—R. Fatehchand. (*J. Brit. IRE*, vol. 19, pp. 335-344; June, 1959.) The characteristics of noise distributed uniformly over the frequency band and that concentrated at the high frequency end of the pass band are compared. The effects of a nonlinear transfer characteristic on noise alone and on noise plus signal are studied, and the relation between these effects and noise visibility on a picture tube is examined.
- TRANSMISSION**
- 621.396.61:629.19 3141
Minimum Transmitter System Weight for Space Communications—R. S. Davies and C. S. Weaver. (*Proc. IRE*, vol. 47, pp. 1151-1152; June, 1959.) A method is given for calculating optimum transmitter weight and antenna size.
- 621.396.71 3142
New Radio Transmitters at Ongar—(*Engineer, London*, vol. 207, p. 339; February 27, 1959.) Operational data are given on the seven new radio telegraphy transmitters of the British Post Office.
- TUBES AND THERMIONICS**
- 621.314.63 3143
The D.C. and A.C. Characteristics of Point-Contact Diodes—H. Beneking. (*Z. angew. Phys.*, vol. 10, pp. 216-225; May, 1958.) A *p-n* diode of spherical symmetry [see, e.g., 2411 of July (Hofmeister and Groschwitz)] is investigated by analogy with calculations for the plane configuration (1398 of April). An interpretation of the injection mechanism of point contacts is obtained. Good agreement between measured and theoretical diode characteristics is found.
- 621.314.63:621.318.57 3144
Millimicrosecond Switching Diodes—J. Halpern and R. H. Rediker. (*Electronics*, vol. 32, pp. 66-67; June 5, 1959.) Describes briefly the construction of Ge-In-Sb diffusion diodes for switching speeds of 2-3 μ sec (see 2909 of 1958.) A method of measuring the reverse recovery time is outlined.
- 621.314.63:621.372.632 3145
Transmitting Frequency Converter in which Gold- or Silver-Bonded Diode is Used—S. Kita, H. Sanpei and T. Okajima. (*Rep. elect. Commun. Lab., Japan*, vol. 6, pp. 415-420; November, 1958.) More than 8-db conversion gain with output frequency 4130 mc has been obtained using nonlinear-capacitance Ge diodes [see *Proc. IRE*, vol. 46, p. 1307, June, 1958 (Kita)].
- 621.314.63+621.314.7]-71(083.57) 3146
Taking the Heat off Semiconductor Devices—W. Luft. (*Electronics*, vol. 32, pp. 53-56; June 12, 1959.) Charts and nomograms are given for the design of cooling fins.
- 621.314.7+621.314.63 3147
Transistors and Associated Semiconductor Devices—R. G. Hibberd. (*Proc. IEE*, Part B, vol. 106, pp. 264-278; May, 1959.) Progress in the manufacture and application of these devices is reviewed. Characteristics of many available types are tabulated.
- 621.314.7 3148
Diffusion Capacitance in Transistors—K. Böke, J. B. M. Spaapen and N. B. Speyer. (*Philips Res. Rep.*, vol. 14, pp. 111-122; April, 1959.) Calculations taking into account the influence of the second junction are in agreement with the results of capacitance measurements at different temperatures, voltages and frequencies.
- 621.314.7 3149
A Particular Problem of Temperature Distribution concerning the Theory of Junction Transistors—A. Pignedoli. (*R. C. Accad. naz. Lincei*, vol. 23, pp. 257-262; November, 1957.) The temperature distribution as a function of position and time is analyzed for a cylinder of circular or elliptical cross-section; the solution is applicable to the investigation of temperature distribution in a transistor whose junction temperature is raised.
- 621.314.7:546.28:621.317.3 3150
The Measurement of the Temperature Dependence of the Mobility and Effective Lifetime of Minority Carriers in the Base Region of Silicon Transistors—D. M. Evans. (*J. Electronics Control*, vol. 6, pp. 204-208; March, 1959.) The mobility of holes in the base of a fusion-alloy *p-n-p* transistor was found to vary with the absolute temperature T as $T^{-2.1}$; the corresponding result for electrons in the base of a grown-junction *n-p-n* transistor was $T^{-2.5}$. Results for the effective lifetime of minority carriers in the base are also given.
- 621.314.7:621.317.7 3151
A Transistor Characteristic Curve Tracer—Young. (See 3060.)
- 621.314.7:621.385.4 3152
Theory and Use of Field-Effect Tetrodes—H. A. Stone, Jr. (*Electronics*, vol. 32, pp. 66-68; May 15, 1959.) Characteristics and circuit applications of the device are discussed and a description is given of a technique by which laboratory models have been constructed.
- 621.314.7.012.8 3153
Transmission-Line Analogue of a Drift Transistor—J. te Winkel. (*Philips Res. Rep.*, vol. 14, pp. 52-64; February, 1959.) A method based on a constant drift field is described. Its purpose is to derive base transport parameters and the small-signal equivalent circuit without solving the differential equations explicitly.
- 621.314.7.012.8 3154
Three-Dimensional Electric-Circuit Model of the High-Frequency Phenomena in a Junction Transistor—G. Brouwer. (*Philips Res. Rep.*, vol. 14, pp. 132-142; April, 1959.) The linearized problem, corresponding to small-signal operation of a transistor, is solved with the aid of a model.
- 621.383.27 3155
New Photoelectron Multipliers—N. S. Klibebnikov. (*Izv. Ak. Nauk SSSR*, vol. 22, pp. 70-77; January, 1958.) Five types of photomultiplier are briefly described. Typical field distributions and electron paths are illustrated and operating characteristics are tabulated.
- 621.383.27 3156
Manufacture of Photoelectron Multipliers and Their Basic Parameters—A. E. Melamid. (*Izv. Ak. Nauk SSSR*, vol. 22, pp. 78-82; January, 1958.)
- 621.383.42 3157
The Open-Circuit Electromotive Force of a Selenium Photocell at Low Temperatures—G. Blet. (*J. Phys. Radium*, vol. 19, pp. 166-169; February, 1958.) Assumptions concerning the internal mechanism of photocells are checked and a general expression, independent of photocell size, is given.
- 621.383.5 3158
Photovoltaic Effect in Se Photocells having Artificial Intermediate Layers of CdSe, CdTe, ZnSe and ZnTe—H. Tubota and H. Suzuki. (*J. Phys. Soc. Japan*, vol. 14, pp. 38-40; January, 1959.)
- 621.385.029.6 3159
International Convention on Microwave Valves—(*Proc. IEE*, Part B, vol. 105, supplement no. 11, pp. 609-812; 1958.) The text is given of the following papers which were included among those read at the IEE Convention held in London May 19-23, 1958. Others are abstracted separately. For titles of papers included in supplement no. 10 see 2788 and 2800 of August.
Technology:
1) A new Ceramic Waveguide Window for Use on X-Band Valves—W. F. Gibbons and A. V. Whale (pp. 609-613.)
2) Photo-etching Molybdenum Foil—H. A. C. Hogg (pp. 614-616.)
3) High-Power Windows at Microwave Frequencies—J. V. Lebacqz, J. Jasberg, H. J. Shaw and S. Sonkin (pp. 617-622.)
4) Study of the Lives of Dispenser-Type Barium-Tungsten Cathodes—T. Hashimoto (p. 622.)
5) Application of Discharge Machining to Millimetre-Wave Magnetrons—M. Nishimaki and T. Asaba (p. 623.)

Space-Charge Waves:

6) Large-Signal Linear-Beam Tube Theory

—C. C. Wang (pp. 624-632).

7) A Variation Principle for Small-Amplitude Disturbances of Electron Beams—P. A. Sturrock (pp. 632-634).

8) Space-Charge Waves on Annular Beams in Drift Tubes—A. H. W. Beck and P. E. Deering (pp. 635-641).

9) Magnetic Oscillations in Electron Beams—R. H. C. Newton (pp. 642-644).

10) Microwave Amplification using an Unstable Electron Beam in Crossed Electric and Magnetic Fields—D. J. Harris (pp. 645-648).

Semi-conductors and New Methods of Generation:

11) Parametric Amplification of Space-Charge Waves—A. Ashkin, T. J. Bridges, W. H. Lousell and C. F. Quate (pp. 649-651). See 1025 of March.

12) Some Proposals for Generating High-Frequency Electromagnetic Waves using the Doppler Effect—R. B. R. Shersby-Harvie (pp. 652-655).

13) Fast-Wave Interactions with an Electron Film at Cyclotron Resonance—A. Karp (pp. 656-661).

14) Junction Diodes in Microwave Circuits—A. Uhlir (p. 661).

15) Theory of the Microwave Crystal Mixer—C. Baron (pp. 662-664).

16) Microwave Amplification by means of Intrinsic Negative Resistances—E. Rostas and F. Hülster (pp. 665-673).

Resonators and Slow-Wave Structures:

17) Dielectric Loading for U.H.F. Valves—G. B. Walker (pp. 717-718).

18) A Structure, using Resonant Coupling Elements, suitable for a High-Power Travelling-Wave Tube—A. F. Pearce (pp. 719-726).

19) Results on Delay Lines for High-Power Travelling-Wave Tubes—P. Palluel and J. Arnaud (pp. 727-729).

20) Theoretical Investigation of some Closed Delay Structures for High-Power Travelling-Wave Tubes—F. Sellberg (pp. 730-735). Discussion (pp. 735-736).

21) A New Type of Slow-Wave Structure for Millimetre Wavelengths—E. A. Ash (pp. 737-745).

22) Multiple Ladder Circuits for Millimetre Wavelength Tubes—R. M. White, C. K. Birdsell and R. W. Grow (p. 746). Discussion (p. 746).

23) Dispersion Curves for a Helix in a Glass Tube—D. T. Swift-Hook (pp. 747-755).

24) Some Aspects of the Design of a Helical Coupler for a Travelling-Wave Tube Operating in the 2-Gc/s Band—P. A. Lindsay and K. D. Collins (pp. 756-761).

25) Modified Transmission-Line Couplers for Helices—E. A. Ash and J. D. Pattenden (pp. 762-768).

26) The Coupling of Three Coaxial Helices—B. Minakovic (pp. 769-778). Discussion (pp. 778-779).

27) Characteristics of Interdigital Circuits and their Use for Amplifiers—J. Hirano (pp. 780-785).

Noise:

28) Calculations concerning the Noisiness of a Drifting Stream of Electrons—J. R. Pierce (pp. 786-789).

29) Progress in Low-Noise Microwave Tube Design—W. R. Beam. (pp. 790-795).

30) Frequency Noise in Travelling-Wave Tubes—R. Liebscher and R. Müller (pp. 796-799).

31) Noise in Backward-Wave Oscillators—N. W. W. Smith (pp. 800-804).

32) Oxide Cathodes for Low-Noise Travelling-Wave Tubes—E. Windsor (pp. 805-809).

621.385.029.6 3160

Kinetic Theory of Space-Charge: Part 2—Electron Collisional Damping in the Magnetron (and Diode)—L. Gold. (*J. Electronics Control*, vol. 6, pp. 209-235; March, 1959.) A detailed analysis of the part played by scattering in determining the field and charge distribution in a planar diode or magnetron. Various combinations of magnetic field, scattering frequency and transit time are considered. Part 1: 3696 of 1957.

621.385.029.6 3161

A. C. Operation of Continuous-Wave Magnetrons—W. Schmidt. (*Electronic Applic.*, vol. 18, pp. 158-162; November, 1958.) English version of 4013 of 1958.

621.385.029.6 3162

Current Limitation of A.C.-Operated Continuous-Wave Magnetrons by means of Inductance—E. G. Dorgelo. (*Electronic Applic.*, vol. 18, pp. 163-170; November, 1958.) Adjustment of the angle of flow, combined with high efficiency, can be achieved using a supply unit of low resistance incorporating an inductance of suitable value in the form of stray inductance or a choke.

621.385.029.6 3163

A Proposed Ferrite-Tuned Magnetron—A. Singh and R. A. Rao. (*J. Inst. Telecommun. Engrs., India*, vol. 5, pp. 72-76; March, 1959.) The frequency of an inverted interdigital magnetron can be controlled by varying a biasing magnetic field applied to a ferrite cylinder placed near the shorted end of a coaxial line, which is coupled to the interdigital resonator. A tuning range of 5-10 per cent may be expected as shown by a theoretically evaluated tuning curve.

621.385.029.6:621.372.8 3164

Backward-Wave Oscillations in an Unloaded Waveguide—R. H. Pantell. (*PROC. IRE*, vol. 47, pp. 1146; June, 1959.) Using a system in which electrons travel in a helical beam in ordinary S-band waveguide, oscillations have been observed in the range 2.5-4 kmc at a power level of 0.4 watt.

621.385.029.6:621.396.822 3165

An Experimental Study of Interception Noise in Electron Streams at Microwave Frequencies—B. A. McIntosh. (*Can. J. Phys.*, vol. 37, pp. 285-299; March, 1959.) The frequency used was 3 km. An electron beam was produced in a demountable vacuum system by a parallel-flow Pierce gun in a confining magnetic field. A series of circular apertures and mesh grids on a plate capable of being moved within the vacuum chamber intercepted various fractions of the beam current. The excess noise caused by interception was measured at the anode of the electron gun and at various points in a drift region. Interception noise caused by mesh grids was much greater than that caused by circular apertures.

621.385.032.213.13:538.632 3166

Hall Effect in Oxide Cathodes—T. Yabu-

moto. (*J. Phys. Soc. Japan*, vol. 14, pp. 134-139; February, 1959.) The apparent electron mobility in the range 700°K-1200°K was about 10^8 - 10^4 cm²/v sec which is very high as compared with the values obtained for single crystals. The pore conduction hypothesis is discussed.

621.385.1:621.3.049.7 3167

Thermionic Integrated-Micromodules—Beggs, Grattidge, Molenda, Haase and Dickerson. (See 2863.)

621.385.1:621.314.7:621.373.43 3168

Tube-Transistor Hybrids Provide Design Economy—Dunn and Hekimian. (See 2877.)

621.385.1:621.317.61 3169

A Method for the Accurate Measurement of Mutual Conductance of Thermionic Valves—Child and Sargent. (See 3059.)

621.385.1.012.7 3170

The Mu of Ordinary Receiving Tubes—G. D. O'Neill. (*Pennsylvania Technologist*, vol. 11, pp. 125-132; October, 1958.) A distinction is made between the electronic mu and the electrostatic mu. A new formula is given for mu in terms of electrode dimensions; it is simple to evaluate and more accurate than others which are available.

621.385.832:621.397.62 3171

Design of a Flat Rectangular C.R. Tube—W. R. Aitken. (*Electronic Equip. Engrg.* vol. 6, pp. 24-28; December, 1958.) A qualitative description with a note on operating experience. See 977 of 1958 for detailed analysis.

621.385.832:621.397.621.2:535.623 3172

Errors of Magnetic Deflection: Part 2—Haantjes and Lubben. (See 3125.)

621.385.832.032.36 3173

Energy Losses of Cathode Rays at Binder Films of the Phosphor Screens of Cathode-Ray Tubes—G. Gergely and I. Hanges. (*Z. angew. Phys.*, vol. 10, pp. 225-228; May, 1958.) Measurements of light emission were made on a number of phosphor screens with colloidal binder films of differing composition and thickness, to determine the dependence of losses on electron energy and film characteristics.

621.387 3174

The Effect of Trigger Pulse Polarity on the Anode Breakdown Time of the Cold-Cathode-Arc Conduction Tetrode—R. Feinberg. (*J. Electronics Control*, vol. 6, pp. 246-257; March, 1959.) The breakdown time is found to depend on the trigger pulse duration if this pulse is positive, but not if it is negative. The explanation of this result is discussed.

MISCELLANEOUS

621.3.029.6 3175

Report of Advances in Microwave Theory and Techniques—1957—R. E. Beam. (*IRE TRANS. ON MICROWAVE THEORY AND TECHNIQUES*, vol. MTT-6, pp. 251-263; July, 1958.) 320 references.

621.37/.39(81) 3176

Electronics and Communications in Brazil—J. I. Caicoya. (*Brit. Commun. Electronics*, vol. 6, pp. 364-370; May, 1959.) Gives details of manufacturing and research organizations.